

FACILITY FORM 602

N67-24609

(ACCESSION NUMBER)

236

(PAGES)

CR-81769

(NASA CR OR TMX OR AD NUMBER)

(THRU)

(CODE)

(CATEGORY)

VOLUME 6 OF 8

Final Report

ATS - 4

PREPARED BY

FAIRCHILD HILLER
SPACE SYSTEMS DIVISION

FOR

NASA
Goddard Space Flight Center

DECEMBER 1966

ATS-4 STUDY PROGRAM
FINAL REPORT
(Contract NASW-1411)
VOLUME SIX OF EIGHT

prepared by

FAIRCHILD HILLER SPACE SYSTEMS DIVISION

Sherman Fairchild Technology Center

Germantown, Maryland

for

GODDARD SPACE FLIGHT CENTER

NATIONAL AERONAUTICS AND SPACE ADMINISTRATION

December 1966

PRECEDING PAGE BLANK NOT FILMED.

TABLE OF CONTENTS

VOLUME ONE

Section	Title	Page
1.0	Summary	1-1
1.1	Objectives and Justification	1-1
	1.1.1 Utilization	1-2
	1.1.2 Implementation	1-4
1.2	Program Feasibility	1-6
	1.2.1 Parabolic Antenna	1-6
	1.2.2 Stabilization and Control System	1-8
	1.2.3 Phased Array	1-11
	1.2.4 Interferometer	1-12
1.3	Subsystem Summaries	1-13
	1.3.1 Configuration Description	1-13
	1.3.2 Parabolic Reflector	1-19
	1.3.3 Parabolic Antenna Feed	1-22
	1.3.4 Attitude Stabilization and Control System	1-24
	1.3.5 Launch Vehicle - Ascent and Orbit Injection	1-27
	1.3.6 Interferometer System	1-32
	1.3.7 Phased Array	1-33
	1.3.8 In-Orbit Maneuvers and Auxiliary Propulsion System	1-35
	1.3.9 Additional Experiment Capability	1-37

TABLE OF CONTENTS

VOLUME TWO

Section	Title	Page
2.0	Systems Analysis	2-1
2.1	Mission Profile and Operations Plan	2-1
	2.1.1 Mission Profile	2-1
	2.1.2 Operations Plan	2-20
2.2	Experiment Plan	2-20
	2.2.1 Parabolic Antenna Experiment	2-20
	2.2.2 Monopulse System Operation	2-30
	2.2.3 Phased Array Experiment	2-32
	2.2.4 Orientation and Control Experiment	2-45
	2.2.5 Interferometer Experiment	2-49
	2.2.6 Additional Communication Experiments	2-54
2.3	Power Profiles	2-58
	2.3.1 Preorbital Power	2-58
	2.3.2 Experiment Evaluation	2-61
	2.3.3 Experiment Demonstration	2-61
	2.3.4 Power System Margin	2-61
	2.3.5 Experiment Loads	2-64
2.4	Antenna Accuracy Considerations	2-68
	2.4.1 Reflecting Surface Errors	2-68
	2.4.2 Feed Location Errors	2-73
	2.4.3 Frequency Limitations on Gain	2-74
	2.4.4 Summary of Antenna Error Effects	2-76
2.5	Antenna Efficiencies	2-79
	2.5.1 Parabolic Antenna	2-79
	2.5.2 Phased Array Figures of Merit	2-82
2.6	Faisure Modes	2-91
	2.6.1 System Considerations	2-91
	2.6.2 Parabolic Antenna	2-91
	2.6.3 Stabilization and Control System	2-93
	2.6.4 Phased Array	2-98
	2.6.5 Antenna Experiment Electronics	2-100
	2.6.6 Phased Array Monopulse Operation	2-103
2.7	Weight Summaries	2-105

TABLE OF CONTENTS

VOLUME THREE

Section	Title	Page
3.0	Vehicle Engineering	3-1
3.1	Concept Evolution	3-1
	3.1.1 Trade-off Parameters	3-1
	3.1.2 F/D Trade-offs	3-6
	3.1.3 Spacecraft Concepts	3-8
3.2	Concept Evaluation and Reference Concept	3-21
	3.2.1 Launch Vehicle Choice	3-21
	3.2.2 Split Module Concept	3-21
	3.2.3 Reference Concept	3-25
	3.2.4 Concept Comparison	3-29
	3.2.5 Titan IIC Adaptability	3-29
3.3	Reflector Design	3-33
	3.3.1 Design Evolution and Alternate Approaches	3-33
	3.3.2 Petal Hinging Concepts	3-38
	3.3.3 Petal Structural Design	3-40
	3.3.4 Deployment System	3-47
	3.3.5 Tolerance Considerations	3-47
	3.3.6 Reflecting Surface	3-50
	3.3.7 Petal Locking System	3-53
3.4	Reflector Fabrication	3-57
	3.4.1 Fabrication Considerations	3-57
	3.4.2 Aluminum Substructure	3-57
	3.4.3 Wire Mesh Forming	3-59
	3.4.4 Sub-Assemblies	3-60
	3.4.5 Tooling	3-60
	3.4.6 Assembly Procedure	3-64
	3.4.7 Measurement of Surface Deviations	3-65
3.5	Structural and Dynamic Analyses	3-71
	3.5.1 Analytical Methods and Approach	3-71
	3.5.2 Preliminary Analysis	3-77
	3.5.3 Integrated Spacecraft-Launch Configuration	3-104
	3.5.4 Integrated Spacecraft-Orbit Configuration	3-115
	3.5.5 Orbit Maneuvering	3-121

TABLE OF CONTENTS

VOLUME THREE (Continued)

Section	Title	Page
3.6	Thermo/Structural Analysis	3-129
	3.6.1 Thermal Requirements and Approach	3-129
	3.6.2 Design Orbit	3-133
	3.6.3 Petal Thermal Analysis	3-135
	3.6.4 Thermoelastic Analysis of Reflector	3-154
	3.6.5 Feed Mast Thermal Analysis	3-166
	3.6.6 Thermal Deformation of Feed Mast	3-172
	3.6.7 Spacecraft Thermal Control	3-175
3.7	Dimensional Stability	3-178
	3.7.1 Introduction	3-178
	3.7.2 Precision Elastic Limit	3-179
	3.7.3 Residual Stress	3-179
	3.7.4 Design Application	3-180
	3.7.5 References for Dimensional Stability Discussion	3-182
3.8	In-Orbit Measurement of Antenna Surface Accuracy	3-183
	3.8.1 Basic Techniques	3-183
	3.8.2 Operational Considerations	3-183
	3.8.3 Antenna Surface Errors	3-185
	3.8.4 Equipment Location	3-185
	3.8.5 Conceptual Design	3-186
	3.8.6 Error Resolution Requirements	3-189
	3.8.7 Sampling Surface Measurements	3-191
	3.8.8 The Axial Four Camera System	3-192
	3.8.9 Illumination of the Antenna	3-208
	3.8.10 System Operation	3-209
	3.8.11 General Comments	3-209
Appendix		
3A	Expandable Truss Antennas	3-211
3B	Inflatable Antennas	3-225
3C	Rigid Panel Antennas	3-230
3D	Petal Axis of Rotation Determination	3-248

TABLE OF CONTENTS

VOLUME FOUR

Section	Title	Page
4.0	Power Systems	4-1
4.1	Solar Panel Configuration Study	4-2
4.2	Solar Cell Radiation Degradation	4-6
	4.2.1 Radiation Environment	4-6
	4.2.2 Background Flux	4-7
	4.2.3 Power Margin	4-10
4.3	Battery Characteristics	4-10
	4.3.1 Nickel-Cadmium Battery	4-13
	4.3.2 Silver-Cadmium Battery	4-13
	4.3.3 Silver-Zinc Battery	4-15
	4.3.4 Battery Comparison	4-15
4.4	Battery Charging and Control	4-23
	4.4.1 Constant Current Charging	4-23
	4.4.2 Constant Voltage Charging	4-24
	4.4.3 Modified Constant Voltage Charging	4-26
	4.4.4 Tapered Charging	4-26
	4.4.5 Recommendation	4-26
4.5	Concept Power Subsystem	4-28
	4.5.1 Design Approach	4-28
	4.5.2 Battery Complement	4-32
	4.5.3 Solar Array	4-35
	4.5.4 Power Conditioning and Control	4-36
5.0	Orbital Analysis	5-1
5.1	General	5-1
5.2	Apogee Injection Stages	5-2
5.3	Ascent Trajectories	5-4
	5.3.1 Requirements and General Considerations	5-4
	5.3.2 Synchronous Injection - Single Apogee Impulse	5-7
	5.3.3 Subsynchronous Injection - High Altitude Parking Orbit	5-10
	5.3.4 Recommended Centaur Ascent Trajectory	5-18
5.4	Orbit Payloads	5-23
	5.4.1 General	5-23
	5.4.2 SLV3A/Agena and SLV3C/Centaur	5-23

TABLE OF CONTENTS
VOLUME FOUR (Continued)

Section	Title	Page
	5.4.3 Titan IIIC	5-30
	5.4.4 Payload Data Summary	5-30
5.5	Orbit Injection Errors	5-32
	5.5.1 Error Values	5-32
	5.5.2 Associated Latitude-Longitude Deviation	5-33
	5.5.3 Associated Corrective Velocity Impulse Requirements	5-36
5.6	Orbit Perturbations	5-39
	5.6.1 General	5-39
	5.6.2 Earth Oblateness and Extraterrestrial Perturbations	5-39
	5.6.3 Terrestrial Perturbations - Equatorial Ellipticity	5-41
	5.6.4 Associated Corrective Velocity Impulse Requirements	5-45
5.7	Auxiliary Propulsion System	5-48
	5.7.1 Velocity Impulse and Thrust Requirements	5-48
	5.7.2 Initial APS Comparison Study	5-48
5.8	Orbit Guidance	5-57
	5.8.1 General Requirements	5-57
	5.8.2 Orbit Injection Error Correction	5-58
	5.8.3 Station Keeping and Repositioning	5-63
5.9	References and Symbols for Orbital Analysis	5-65
	5.9.1 References	5-65
	5.9.2 List of Symbols	5-67

TABLE OF CONTENTS

VOLUME FIVE

Section	Title	Page
6.0	ATTITUDE STABILIZATION AND CONTROL SYSTEM	6-1
6.1	Attitude Stabilization and Control Requirements	6-1
6.1.1	Mission Requirements	6-1
6.1.2	Pointing Accuracy	6-1
6.1.3	Control Modes	6-1
6.2	Attitude Reference Subsystem	6-2
6.2.1	Alternate Approaches	6-2
6.2.2	Candidate Reference Sensors	6-11
6.2.3	Selected Configuration	6-22
6.2.4	Sensor Performance	6-23
6.3	Disturbance Torque Model	6-25
6.3.1	Meteoroid Impact	6-25
6.3.2	Gravity Gradient	6-34
6.3.3	Magnetic Disturbance	6-35
6.3.4	Internal Rotating Equipment	6-35
6.3.5	Solar Pressure	6-35
6.4	Torquer Subsystem	6-52
6.4.1	Control Impulse Requirements	6-52
6.4.2	Candidate Reaction Jet Types	6-59
6.4.3	Inertia Wheel Subsystem	6-63
6.4.4	Selected Torquer Configuration	6-69
6.5	Computation and Data Handling	6-71
6.5.1	On-Board Computation	6-71
6.5.2	Up-Data Commands	6-71
6.5.3	Down-Data Monitor	6-71
6.6	System Operational Description	6-75
6.6.1	Control Mode Operation	6-75
6.6.2	System Block Diagram	6-85
6.6.3	Sensor Update	6-89
6.7	System Performance	6-90
6.7.1	Pointing Accuracy	6-90
6.7.2	Acquisition	6-93
6.7.3	Control System Dynamics	6-93
6.7.4	Reliability	6-117
6.8	System Physical Description	6-124
Appendix		
6A	Preliminary Control Torque and Impulse Requirements	
6B	Preliminary Reaction Jet Considerations	
6C	Preliminary Inertia Wheel Considerations For Candidate Vehicle Configurations	
6D	Preliminary Combined Wheel/Jet System Considerations	
6E	Preliminary Transfer Orbit Control Mode Analysis	

TABLE OF CONTENTS

VOLUME SIX

Section	Title	Page
7.0	Communications Experiments	7-1
7.1	Parabolic Antenna	7-1
	7.1.1 Beam Scanning	7-1
	7.1.2 Parabolic Antenna Feeds	7-14
	7.1.3 Aperture Blockage	7-32
	7.1.4 Paraboloid Performance	7-42
7.2	Phased Array	7-58
	7.2.1 Transdirective Array	7-59
	7.2.2 The Butler Matrix Array	7-63
	7.2.3 Space Fed (Lens) Array	7-65
	7.2.4 Corporate-Fed Array	7-71
	7.2.5 Corporate-Fed Phased Array Design Considerations	7-79
	7.2.6 Antenna Definition	7-92
	7.2.7 Digital Beam Steering Unit	7-102
	7.2.8 Packaging Configuration	7-108
7.3	Communications Equipment	7-111
	7.3.1 Transmission Parameters	7-111
	7.3.2 Systems Description	7-113
	7.3.3 Weight, Volume and Power Summary	7-134
	7.3.4 System Performance Summary	7-137
Appendix		
7A	Four Paraboloid Off-Set Feed Configuration	7-139
7B	Ionospheric Effects on Wave Polarization	7-147
7C	Separate 100 MHz Antennas	7-159
7D	Communication Components	7-165

TABLE OF CONTENTS

VOLUME SEVEN

Section	Title	Page
8.0	Radio Interferometer Experiment	8-1
8.1	Introduction	8-1
8.2	Study Approach	8-3
8.3	Candidate Interferometer Concepts	8-5
8.4	Candidate Interferometer Systems	8-11
	8.4.1 Selection Criteria	8-11
	8.4.2 System Block Diagrams	8-11
8.5	Selection of Preferred Concept	8-25
	8.5.1 Candidate Evaluation and Selection of Preferred System	8-25
	8.5.2 Phased Array as an Interferometer	8-44
8.6	Design of Preferred Interferometer System	8-48
	8.6.1 General Circuit Description	8-48
	8.6.2 Mechanical and Thermal Design	8-59
	8.6.3 Interferometer Attitude Sensor Interface	8-68
	8.6.4 Physical Characteristics	8-85
8.7	Error Analysis of Preferred Concept	8-86
8.8	Conclusions and Recommendations	8-116
8.9	Bibliography and Glossary	8-117
Appendix		
8A	Interference Reduction by Correlation	8-136
8B	RF Link Calculation	8-138
8C	Interferometer Angular Error Due to Mutual Coupling	8-141
8D	System Polarization	8-146
8E	Derivation of the Received Voltage Phases on an Elliptically Polarized Interferometer Antenna Pair with an Incident Elliptically Polarized Wave	8-165
8F	Alternative Antenna Switching Systems - Direct Phase Reading Interferometer	8-172
8G	Derivation of Counter Equation	8-180
8H	Gating Time Error Analysis	8-182
8I	Conversion of θ_s into Attitude	8-187
8J	Limitation of Range and Range Rate Capability	8-201
Volume 8	Program Budgetary Costs and Schedules	10-1

TABLE OF CONTENTS

VOLUME SEVEN (Continued)

Section	Title	Page
9.0	Summary	9-1
9.1	Data Flow	9-2
	9.1.1 Definition	9-2
	9.1.2 Requirements	9-2
	9.1.3 Model of the Data Flow	9-3
9.2	Telemetry System	9-8
	9.2.1 Data Handling Requirements	9-8
	9.2.2 Data Handling System Design	9-9
	9.2.3 Data Handling System Configuration	9-17
	9.2.4 Data Transmission System Design	9-23
	9.2.5 Data Transmission Link Calculation	9-28
	9.2.6 System Size, Weight and Power Estimates	9-44
	9.2.7 Equipment Implementation	9-44
9.3	Command System	9-47
	9.3.1 Definition	9-47
	9.3.2 Requirements	9-47
	9.3.3 Word Format	9-50
	9.3.4 Description and Operation of the Onboard System	9-53
	9.3.5 Estimates of Physical Characteristics	9-60
	9.3.6 Transmission Link Power Requirements	9-62
	9.3.7 Equipment Implementation	9-64
	9.3.8 Ground Equipment Requirements	9-65
9.4	Range and Range Rate Transponder	9-69
	9.4.1 Accuracy Requirements	9-69
	9.4.2 Transponder Operating Frequency Selection	9-69
	9.4.3 UHF Transponder Characteristics	9-70
	9.4.4 Equipment Implementation	9-71
9.5	Ground Station Requirements	9-72
	9.5.1 Ground Equipment Description	9-72
9.6	References	9-84
	Appendices	
	9A Commutator Channel Assignment	9-85
	9B Modulation Index Calculations (Mode 1)	9-101
	9C Solving for Receiver Noise Power and Channel Bandwidth Ratios (Mode 1)	9-103
	9D Solving for Receiver Noise Power and Channel Bandwidth Ratios (Mode II)	9-105
	9E Command Signal Catalog	9-106
	9F Telemetry Signal Catalog	9-116
	9G Data Questionnaire	9-131

LIST OF ILLUSTRATIONS

VOLUME ONE

Figure	Title	Page
1.3-1	Fairchild Hiller ATS-4 Concept	1-14
1.3-2	Reference Concept	1-15
1.3-3	Spacecraft Module Detail	1-18
1.3-4	Multiband Prime Focus Feed	1-23
1.3-5	SCS Block Diagram	1-29
1.3-6	ATS-4 Ascent Trajectory	1-31

LIST OF ILLUSTRATIONS

VOLUME TWO

Figure	Title	Page
2.1-1	Satellite Ground Track	2-2
2.1-2	Spacecraft/Sun Orientation in Transfer Orbit	2-4
2.1-3	Satellite Ground Track and Ground Station	2-12
2.1-4	Gross Data Flow Concept	2-17
2.2-1	Major Plane Location and Arts for Antenna Measurement	2-22
2.2-2	Ground Terminal Layout for Monopulse Calibration	2-33
2.2-3	Major Planes and Beam Positions for Station Pattern Tests	2-35
2.2-4	Multiple Pattern Arts Using Two Ground Stations	2-41
2.2-5	Crosstalk Measurement	2-41
2.2-6	Major Plane Arts - Interferometer	2-53
2.2-7	Pointing of the Z-Axis for Interferometer Measurement	2-53
2.3-1	Typical Experiment Evaluation Profile	2-62
2.3-2	Power Profile with Additional Experiments	2-62
2.3-3	Experiment Demonstration Maximum Profile	2-63
2.4-1	Classification of Parabolic Antenna Errors	2-69
2.4-2	Reflector Errors	2-71
2.4-3	Feed Location Errors	2-75
2.4-4	Feed Location Errors ($F/D = 0.3$)	2-78
2.4-5	Frequency Limitation on Gain	2-78
2.5-1	X-Band Radiation Pattern	2-81
2.6-1	Failed Reaction Wheel Backup Subsystem	2-94

LIST OF ILLUSTRATIONS

VOLUME THREE

Figure	Title	Page
3.1-1	Antenna Feed Location	3-3
3.1-2	C.G. Location Study	3-5
3.1-3	Concept SK513-10	3-13
3.1-4	Concept SK513-12	3-15
3.1-5	Concept SK513-11	3-16
3.1-6	Concept SK513-13	3-17
3.1-7	Concept SK513-14	3-18
3.1-8	Concept SK513-16	3-19
3.2-1	Concept SK513-18	3-23
3.2-2	Concept SK513-17 (Reference Concept)	3-24
3.2-3	Spacecraft Module Detail	3-27
3.2-4	Concept Comparison Chart	3-31
3.2-5	Reference Concept on Titan IIIC	3-32
3.3-1	Conic Scissors Parabolic Antenna	3-34
3.3-2	Inflatable Parabolic Antenna	3-36
3.3-3	Retentive Memory Petal Concept	3-39
3.3-4	Non-Radial Petals, Sheet One	3-41
3.3-5	Non-Radial Petals, Sheet Two	3-42
3.3-6	Petal Concept Parabolic Antenna	3-43
3.3-7	Skewed Hinge Design	3-45
3.3-8	Petal Structural Assembly and Hinge Details	3-46
3.3-9	Deployment Synchronizer	3-49
3.3-10	Mesh Segment Installation	3-51
3.3-11	Mesh Reflector Characteristics	3-52
3.3-12	Inter-Petal Locks	3-55
3.3-13	Inter-Petal Lock - Preferred Concept	3-56
3.4-1	Shaping of Mesh Reflecting Surface	3-58
3.4-2	Master Tool	3-58
3.4-3	Assembly Bonding Fixture	3-62
3.4-4	Hinge and Latch Alignment Fixture	3-63
3.4-5	Measurement of Surface Deviations	3-67
3.5-1	Truss Feed Mast Weights	3-78
3.5-2	Truss Feed Mast Frequencies	3-79
3.5-3	Single Tube Feed Mast Analysis	3-81
3.5-4	Four Tube Feed Mast Weights	3-82
3.5-5	Four Tube Feed Mast Frequencies	3-83
3.5-6	Analysis of Quadruped Feed Mast Structure	3-84

LIST OF ILLUSTRATIONS

VOLUME THREE (Continued)

Figure	Title	Page
3.5-7	Quadruped Feed Mast Frequencies	3-85
3.5-8	Analysis of Tripod Feed Mast Structure	3-86
3.5-9	Tripod Feed Mast Frequencies	3-87
3.5-10	Reflector Petal Loading	3-94
3.5-11	Spacecraft, Injection, Motor and Adapter Structural Properties	3-94
3.5-12	Launch Integrated S/C - Analytical Model	3-96
3.5-13	Orbit Configuration - Mass Model	3-102
3.5-14	Preferred Configuration and Analytical Model	3-105
3.5-15	Petal Restraint and Stiffness	3-106
3.5-16	Mass Point Locations and Weights	3-107
3.5-17	YY Direction Mode Shapes	3-109
3.5-18	XX Direction Mode Shapes	3-110
3.5-19	Analytical Model - Orbit Configuration	3-116
3.5-20	Frequency and Mode Shapes - Orbit Configuration, Sheet One	3-118
3.5-21	Frequency and Mode Shapes - Orbit Configuration, Sheet Two	3-119
3.5-22	Frequency and Mode Shapes - Orbit Configuration, Sheet Three	3-120
3.5-23	Response to Single Finite Duration Pulse (Roll Correction Maneuver)	3-124
3.5-24	Response to Single Finite Duration Pulse (Yaw Correction Maneuver)	3-125
3.6-1	Yearly Change in Orbit Position Relative to Sun Vector	3-134
3.6-2	Petal Thermal Analysis	3-136
3.6-3	Relation of Thermal Analysis Nodes to Orbit Position	3-136
3.6-4	Feed Module Shadowing	3-137
3.6-5	Reflection Mesh Sunlight Blockage	3-139
3.6-6	Mesh and Antenna Hub Shadowing	3-141
3.6-7	Coordinate System for Thermal Analysis	3-142
3.6-8	Antenna Feed Shadowing	3-144
3.6-9	Beam Temperatures	3-147
3.6-10	Petal Beam Cross-Section	3-151
3.6-11	Mesh Standoff Fittings	3-151

LIST OF ILLUSTRATIONS VOLUME THREE (Continued)

Figure	Title	Page
3.6-12	Beam Geometry	3-153
3.6-13	Petal Thermal Model	3-159
3.6-14	Radial Displacement Geometry	3-159
3.6-15	Deformation of Radial Member	3-159
3.6-16	Reflector Surface Mesh Geometry	3-165
3.6-17	Surface Mesh Chord Position	3-165
3.6-18	Feed Mast Geometry	3-167
3.6-19	Electrical Simulation, Uninsulated Mast	3-168
3.6-20	Electrical Simulation, Insulated Mast	3-168a
3.6-21	Temperature of Node 4, Uninsulated Mast	3-170
3.6-22	Temperature of Node 4, Insulated Mast	3-170a
3.6-23	Feed Mast Shadowing on Support "A"	3-171
3.6-24	Feed Mast Thermal Model	3-171a
3.6-25	Feed Mast Distortions	3-174
3.6-26	Passive Control Areas Average Temperature versus Dissipation	3-176
3.8-1	Volume Available for Measurement Equipment	3-187
3.8-2	Mirror Position above Camera	3-187
3.8-3	Converse Mirror below Camera	3-187
3.8-4	Concave Mirror below Camera	3-188
3.8-5	Sighting Angles	3-188
3.8-6	Effective Mesh Spacing	3-188
3.8-7	Composite Converse Mirror	3-192
3.8-8	Basic Four Camera Axial System	3-192
3.8-9	Full View Camera System	3-194
3.8-10	Normal Deflection Geometry	3-194
3.8-11	Ring Viewing Angles	3-194
3.8-12	Vidicon Image Dimensions	3-196
3.8-13	Central Circle in Vidicon Image	3-196
3.8-14	Radial and Circular Scan Patterns	3-198
3.8-15	Rim Marker Pattern	3-198
3.8-16	Modified Marker Coding	3-198
3.8-17	Reversed Marker Pattern	3-201
3.8-18	Marker Pattern without 1/2 Inch Plates	3-201
3.8-19	Pattern for Third Ring	3-202
3.8-20	Pattern for Second Ring	3-202

LIST OF ILLUSTRATIONS

VOLUME THREE (Continued)

Figure	Title	Page
3.8-21	Pattern for Central Ring	3-202
3.8-22	Pattern of Perfect Match of Image and Standard Negative	3-203
3.8-23	Pattern of Mismatch of Image and Standard Negative	3-203
3.8-24	Marking Pattern from Deformed Mesh Wires	3-207
3.8-25	Deformed Wires Positioned along a Parabola	3-207
3.8-26	Illumination by Columnar Light Sources	3-208
3.8-27	Illumination by Toroidal Light Sources	3-208

LIST OF ILLUSTRATIONS

VOLUME FOUR

Figure	Title	Page
4.1-1	Flat Plate Array, Two Degrees Of Freedom	4-3
4.1-2	Flat Plate Array, One Degree Of Freedom	4-3
4.1-3	Flat Plate Array, Fixed	4-3
4.1-4	Two Flat Plates Array, Fixed	4-4
4.1-5	Three Flat Plates Array, Fixed	4-4
4.1-6	Cylindrical Array, Fixed	4-4
4.1-7	Double Faced Flat Plate Array	4-5
4.1-8	Double Faced Two Flat Plates Array	4-5
4.1-9	Double Faced Three Flat Plates Array	4-5
4.2-1	Solar Cell Radiation Degradation	4-8
4.2-2	Power Loss Due To Radiation Effects	4-11
4.3-1	Nickel-Cadmium Battery Life	4-14
4.3-2	Energy Per Unit Weight For Various Batteries	4-17
4.3-3	Energy Per Unit Volume For Various Batteries	4-18
4.3-4	Capacity vs. Temperature For Various Cells	4-18
4.3-5	Silver-Zinc Battery Cycle Life	4-19
4.3-6	Silver-Cadmium Battery Cycle Life	4-19
4.3-7	Nickel-Cadmium Battery Cycle Life	4-20
4.3-8	Umbra and Penumbra Patterns For A Synchronous Equatorial Satellite	4-22
4.4-1	Recommended % Overcharge is Temperature	4-25
4.4-2	Overcharge Pressure Vs Current	4-25
4.4-3	Maximum Limiting Voltage Vs. Temperature	4-27
4.4-4	Tapered Charge Characteristic	4-27
4.5-1	Typical Experiment Evaluation Power Profile	4-29
4.5-2	Power Profile With Additional Experiments	4-29
4.5-3	Experiment Demonstration Maximum Demand Profile	4-29
4.5-4	Power System Weight Vs. Load Duration	4-29
4.5-5	Power System Block Diagram	4-37

LIST OF ILLUSTRATIONS

VOLUME FOUR (Continued)

Figure	Title	Page
5.3-1	Ascent Trajectories	5-6
5.3-2	Earth Track of Ascent Trajectory	5-11
5.3-3	Injection Station Longitude Variation	5-11
5.3-4	Effect of Launch Azimuth on Required Increase in Characteristic Velocity	5-14
5.3-5	High Altitude, Ellipstic Parking Orbit Characteristics	5-16
5.3-6	Earth Track of High Altitude Parking Orbit Ascent Trajectory	5-17
5.3-7	Ground Track of Ascent Trajectories	5-19
5.3-8	Spacecraft/Sun Orientation in Transfer Orbit	5-21
5.4-1	Payload and AIS Propellant Weight vs i_c (Burner II)	5-28
5.4-2	Payload and AIS Propellant Weight vs i_c (TE364-3)	5-28
5.6-1	Satellite Semimajor Axis Perturbation	5-42
5.6-2	Satellite Inclination Perturbation	5-42
5.6-3	Long Period Oscillation	5-44
5.6-4	Required Velocity Impulse per Year	5-46

LIST OF ILLUSTRATIONS

VOLUME FIVE

Figure	Title	Page
6-1	Reference Coordinate Frame (Nominal)	6-3
6-2a	Cell Orientation	6-13
6-2b	Cell Outputs	6-13
6-2c	Sun Sensor Signals	6-13
6-3	Meteoroid Extrapolations	6-29
6-4	Percent Open Area in Each Mesh Segment as a Function of Solar Incident Angle	6-41
6-5	Antenna Projected Surface Map	6-43
6-6	Projected Antenna Shaded Area Profile	6-44
6-7	Pitch Axis Solar Pressure Disturbance Torque	6-47
6-8	Roll Axis Solar Pressure Disturbance Torque Due to Antenna and Feed System	6-48
6-9	Roll Axis Solar Pressure Disturbance Torque Due to Fixed Solar Panels Only	6-49
6-10	Roll Axis Solar Pressure Disturbance Torque	6-50
6-11	Yaw Axis Solar Pressure Disturbance Torque	6-51
6-12	Hydrazine Thruster Output Efficiency	6-62
6-13	Liquid Hydrazine System Schematic	6-64
6-14	Block Diagram - Ascent Control	6-86
6-15	SCS Block Diagram	6-87
6-16	Phase Plane Plot Sun Acquisition - Pitch Axis	6-94
6-17	Phase Plane Plot Sun Acquisition - Yaw Axis	6-95
6-18	Phase Plane Plot Earth Acquisition Roll Axis	6-96
6-19	Phase Plane Plot Star Acquisition Yaw Axis	6-97
6-20	Open Loop Bode Plot - Roll Axis	6-99
6-21	Open Loop Bode Plot - Pitch Axis	6-100
6-22	Open Loop Bode Plot - Yaw Axis	6-101
6-23	SCS and Vehicle Dynamics Block Diagram	6-102
6-24	Roll Axis - Rigid Body Amplitude Response	6-104
6-25	Roll Axis - Rigid Body Phase Response	6-105
6-26	Pitch Axis - Rigid Body Amplitude Response	6-106
6-27	Pitch Axis - Rigid Body Phase Response	6-107
6-28	Amplitude Response Roll Axis - Flexible (.01)	6-108
6-29	Phase Response Roll Axis - Flexible (.01)	6-109
6-30	Phase Response Pitch Axis - Flexible (.01)	6-110
6-31	Phase Response Pitch Axis - Flexible (.01)	6-111
6-32	Amplitude Response Roll Axis - Flexible (.005)	6-112
6-33	Phase Response Roll Axis - Flexible (.005)	6-113
6-34	Amplitude Response Pitch Axis - Flexible (.005)	6-114

LIST OF ILLUSTRATIONS

VOLUME FIVE (Continued)

Figure	Title	Page
6-35	Phase Response Pitch Axis - Flexible (.005)	6-115
6-36	Phase Plane Plot Attitude Control During Station Keeping	6-118
6-37	Reliability Diagram	6-119
6A-1	Limit Cycle Impulse Requirements	6A-7
6A-2	Disturbance Torque Impulse Requirements	6A-8
6A-3	Maneuver Impulse Requirements	6A-9
6B-1	Micro-Rocket Applicability Thrust and Total Impulse	6B-4
6B-2	Micro-Rocket Applicability Thrust and Duty Cycle	6B-5
6B-3	Estimated System Weight as a Function of On Board Total Impulse	6B-7
6B-4	Reliability Comparison of Bipropellant or Monopropellant System	6B-8
6B-5	Hydrazine Plenum System Schematic	6B-10
6B-6	Liquid Hydrazine System Schematic	6B-11

LIST OF ILLUSTRATIONS

VOLUME SIX

Figure	Title	Page
7.1-1	Prime Focus Paraboloid Scanning Performance	7-3
7.1-2	Paraboloid Gain Loss as a Function of Beamwidths Scanned	7-4
7.1-3	Beam Scanning Capability of a Multi-Element Paraboloid Switching -Feed System	7-7
7.1-4	Beam Cross-Over Level as a Function of the Beam Scanning Increment	7-8
7.1-5	Cassegrain Antenna Gain Loss with Subdish Rotation	7-11
7.1-6	Radiation Characteristics of a Tapered Circular Aperture	7-16
7.1-7	Paraboloid Subtended Angle and Feed Size as a Function of the F/D Ratio	7-18
7.1-8	S-Band Feed-Edge Taper	7-23
7.1-9	800 MHz Prime Focus Feed	7-24
7.1-10	100 MHz Prime Focus Feed	7-27
7.1-11	Spiral Antenna Monopulse Operation	7-29
7.1-12	Parabolic Antenna Gain Loss as a Function of the Blockage Ratio	7-34
7.1-13	X-Band Radiation Pattern	7-35
7.1-14	Antenna Test Range	7-38
7.1-15	Source Tower	7-39
7.1-16	Feed Support Mast	7-44
7.1-17	Paraboloid Assembly	7-45
7.1-18	Back View of Feed Support	7-46
7.1-19	Left Side View of Feed and Feed Support	7-47
7.1-20	Right Side View of Feed and Feed Support	7-48
2.1-21	Right Side View of Feed	7-49
7.1-22	Feeds, End View	7-50
7.1-23	Feeds, Side View	7-51
7.1-24	E-Plane Radiation Patterns, Frequency 4.6 GHz	7-52
7.1-25	E-Plane Radiation Patterns, Frequency 10.5 GHz	7-53
7.1-26	E-Plane Radiation Patterns, Frequency 12.0 GHz	7-54
7.1-27	E-Plane Radiation Pattern, Frequency 18.0 GHz	7-55
7.1-28	E-Plane Radiation Pattern, Frequency 29.6 GHz	7-56

LIST OF ILLUSTRATIONS

VOLUME SIX (Continued)

Figure	Title	Page
7.2-1	Transdirective Array	7-60
7.2-2	Butler Matrix Array - Block Diagram	7-64
7.2-3	Space Fed (Lens) Array - Block Diagram	7-67
7.2-4	Stripline Diplexer	7-69
7.2-5	Stripline Latching Phase Shifter	7-70
7.2-6	Corporate-Fed Array	7-72
7.2-7	Artist Conception of Corporate-Fed Array	7-75
7.2-8	Schematic of Microwave Subsystem	7-80
7.2-9	Detail of Feed Horn Assembly	7-83
7.2-10	Possible Configuration of 4 Channel Diplexer - Circulator Strip Line Module	7-86
7.2-11	Waveguide Latching Phase Shifter	7-89
7.2-12	Array Element Layout	7-94
7.2-13	Phased Array Patterns	7-95
7.2-14	Phased Array Beam Spacing	7-101
7.2-15	Block Diagram for Digital Beam Steering Unit	7-103
7.2-16	Schematic Diagram for Bit Driver	7-105
7.2-17	Plan View of Radiating Elements	7-107
7.2-18	Side View of Corporate-Fed Array	7-108
7.2-19	End View of Corporate-Fed Array	7-109
7.3-1	RF Power vs Ground Antenna Gain	7-116
7.3-2	ATS-4 Communications System	7-119
7.3-3	Frequency Generator	7-120
7.3-4	Monopulse and Phased Array X-Band Transfer Characteristics-Series 100	7-126
7.3-5	100 MHz Relay Transfer Characteristics-Series 200	7-127
7.3-6	X-Band Transponder Output-Reflector and Phased Array Transfer Characteristics-Series 300	7-128
7.3-7	800 MHz Relay Transfer Characteristics-Series 400	7-129
7.3-8	Filter Response	7-130
7.3-9	S-Band Data Link Transfer Characteristics- Series 500	7-131
7.3-10	X-Band Frequency Generator-Representative Transfer Characteristics-Series 600	7-132
7.3-11	Multipliers in Frequency Generator, Represen- tative Transfer Characteristics-Series 700	7-135

LIST OF ILLUSTRATIONS

VOLUME SIX (Continued)

Figure	Title	Page
7A-1	Four Paraboloid Offset Feed Configuration	7-140
7A-2	Radiation Pattern of a 15-Foot Paraboloid 10 db Tapered Distribution	7-141
7A-3	Radiation Pattern Four Paraboloid Array	7-142
7A-4	Monopulse Radiation Pattern of the Four Paraboloid Array	7-144
7A-5	Four Paraboloid Array Scanning Performance	7-145
7B-1	Faraday Rotation as a Function of Frequency	7-152
7B-2	Attenuation between Arbitrarily Polarized Antenna Caused by Faraday Rotation AF - Axial Ratio	7-156
7B-3	Attenuation between Arbitrarily Polarized Antennas Caused by Faraday Rotation AR - Axial Ratio	7-158
7C-1	Helical Antenna Gain as a Function of Antenna Length	7-161
7C-2	Array Element Spacing as a Function of Array Element Gain	7-163

LIST OF ILLUSTRATIONS

VOLUME SEVEN

Figure	Title	Page
8.4-1	LF Phase Reading Interferometer	8-13
8.4-2	RMS Phase Difference Reading Interferometer Technique	8-16
8.4-3	RF Cross Correlation Interferometer Technique	8-19
8.4-4	Spread Spectrum Interferometer Technique	8-22
8.5-1	Resultant Nonambiguous Pattern after Correlation	8-26
8.5-2	Partial System Schematic of Cross Correlator Interferometer	8-30
8.5-3	Monopulse Space Angle RMS Error	8-31
8.5-4	RMS Space Angle Error Direct Phase Reading Interferometer	8-33
8.5-5	Direct Phase Reading Interferometer Relationship, Space Angle Element Separation, Unambiguous Interval vs D/λ	8-36
8.5-6	Interferometer Phase Error Due to Temperature Differential in Transmission Lines	8-37
8.5-7	Layout of Phased Array	8-45
8.6-1	Direct Phase Reading Interferometer	8-48
8.6-2	Interferometer	8-53
8.6-3	Horn Design	8-63
8.6-4	Interferometer Thermal Flow Diagrams	8-66
8.6-5	Interface between the SCS and Interferometer	8-69
8.6-6	Mode Selection and Phase Measurement	8-72
8.6-7	Timing Diagram for Phase Measurement	8-74
8.6-8	Arithmetic Unit for $\epsilon_z' + \epsilon_z''$ and $\epsilon_y' + \epsilon_y''$	8-78
8.6-9	Arithmetic Unit for $\epsilon_x' + \epsilon_x''$	8-79
8.6-10	Timing Diagram for Computational Instruction	8-81
8.6-11	Time Distribution of the Arithmetic Units	8-82
8.7-1	System Model	8-87
8.7-2	Simplified Block Diagram of Direct Phase Reading Electronics	8-88
8.7-3	Basic Interferometer Relationship	8-90
8.7-4	Geometrical Relationship of Spacecraft Position and Ground Station	8-92
8.7-5	Error in Count vs θ_s	8-96
8.7-6	Refraction Effects	8-97
8.7-7	Atmospheric Effect on Elevation Angle	8-98
8.7-8	Atmospheric Effect on the Slant Range Difference	8-99

LIST OF ILLUSTRATIONS

VOLUME SEVEN (Continued)

Figure	Title	Page
8.7-9	Spacecraft Coordinate System	8-105
8.7-10	Pitch Axis 3σ Error vs Pitch Angle, θ	8-107
8.7-11	Yaw Axis 3σ Error vs Pitch Angle, θ	8-108
8.7-12	Vector Diagram of Satellite - Ground Station Geometry	8-109
8.7-13	Orientation of R_s	8-113
8B-1	ERP vs SNR	8-140
8C-1	Space Angular Error ($\Delta\theta_m$) vs Antenna Separation (D/λ) for Different Mutual Couplings (C)	8-142
8C-2	Space Angle Error Due to Mutual Coupling - Coarse Antenna Pair	8-143
8C-3	Comparison of Antenna Elements - Mutual Coupling	8-145
8D-1	Elliptically Polarized Interferometer Antenna Pair with Elliptically Polarized Incoming Wave	8-149
8D-2	Phase Angle Error vs Axial Ratio Inequality	8-152
8D-3	Phase Angle Error vs Ellipse Tilt Angle Inequality	8-155
8D-4	Phase Angle Error vs Roll Angle (δ)	8-160
8D-5	Phase Angle Error vs Pitch Angle (θ)	8-161
8E-1	Elliptically Polarized Plane Wave	8-166
8E-2	Elliptically Polarized Plane Wave Incident at Angles θ, δ	8-167
8E-3	Receive Antenna with Inclined Polarization Ellipse	8-168
8F-1	Switched Signal Lines	8-174
8F-2	Switched Oscillator Lines	8-175
8F-3	Switched IF Lines	8-176
8F-4	Switched Multipliers	8-177
8H-1	Phase Error Distribution at Start of Count	8-186
8H-2	Phase Error Distribution at End of Count	8-186
8H-3	Phase Error Density Function	8-186
8I-1	Interferometer Illumination	8-188
8I-2	Satellite Orientation	8-193
8J-1	Geometry for Range and Range Rate Analysis	8-201

LIST OF ILLUSTRATIONS

VOLUME SEVEN (Continued)

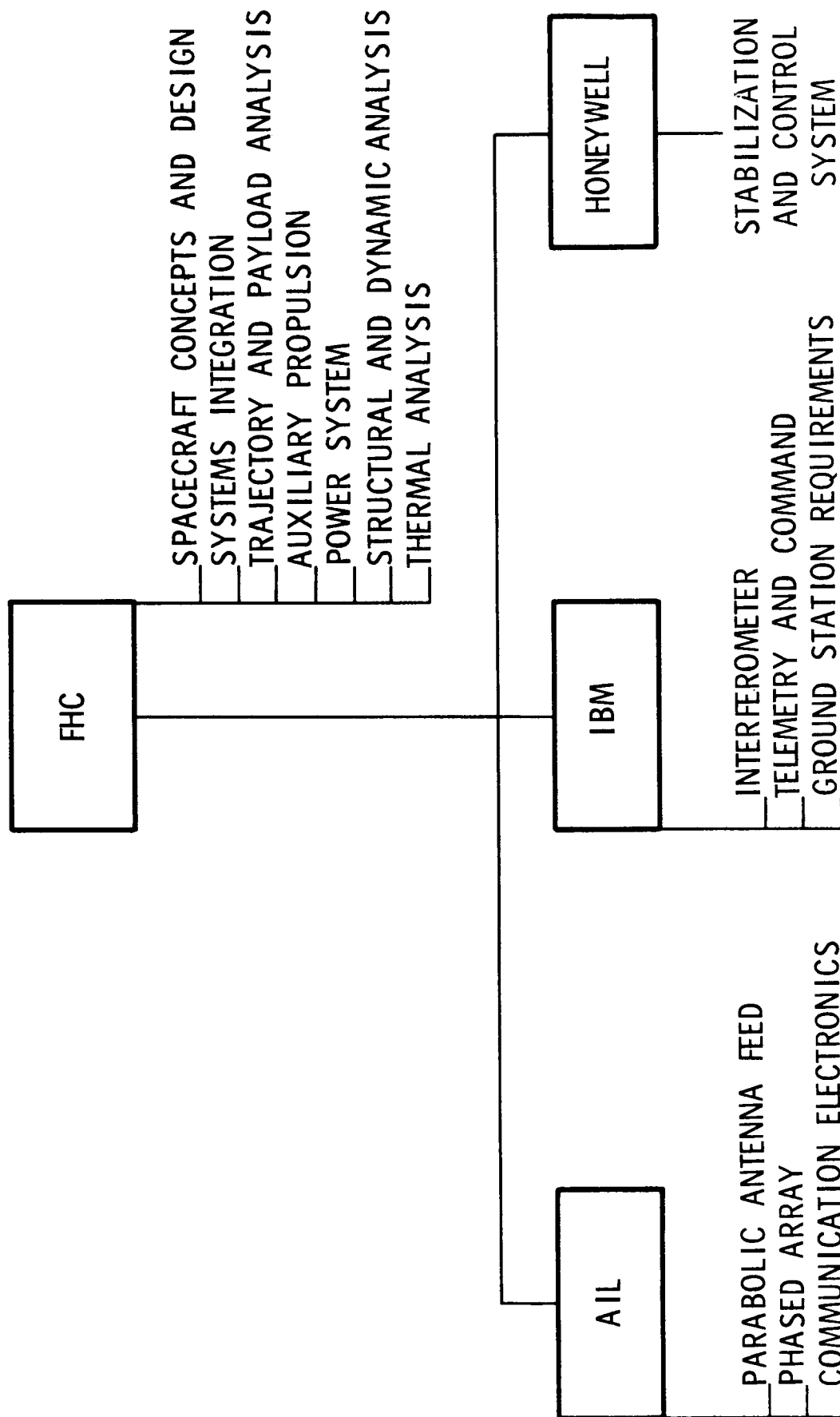
Figure	Title	Page
9.1-1	Onboard System Data Flow, Interfaces to Ground Equipment	9-4
9.1-2	Ground Station Data Flow; Interfaces to Spacecraft and Other Ground Stations	9-5
9.2-2	Basic Commutation Configuration	9-15
9.2-2	Data Handling System Configuration	9-18
9.2-3	Telemetry Data Transmission System	9-25
9.2-4	Telemetry Data Handling and Transmission Configuration	9-33
9.2-5	Block Diagram of Basic Telemetry Receiver	9-38
9.3-1	Command Word Structure	9-51
9.3-2	Command System	9-54
9.3-3	Command Decoder	9-55

PREFACE

This report covers the efforts of Fairchild Hiller Corporation and its team of subcontractors on NASA Contract (NAS-W-1411). The team organization and responsibilities during the study effort are shown on the accompanying chart. The report is divided into eight volumes, as follows:

Volume 1	Summary
Volume 2	Systems Analysis
Volume 3	Vehicle Engineering
Volume 4	Power System
	Orbital Analyses, Propulsion and Guidance
Volume 5	Stabilization and Control
Volume 6	Communication Experiments
Volume 7	Radio Interferometer Experiment
	Telemetry and Command Systems
Volume 8	Program Budgetary Costs and Schedules

ATS-4 TEAM ORGANIZATION



7.0 COMMUNICATIONS EXPERIMENTS

This section describes, in detail, the analysis of the parabolic antenna feed, the phased array and the communications equipment of the ATS-4 spececraft.

7.1 PARABOLIC ANTENNA

7.1.1 Beam Scanning

Scanning of the antenna beam in a prime focus system can be accomplished either by lateral displacement of the feed from the focus of the paraboloid, or by using an electronic cluster feed. The cluster feed can be used to displace the phase center of the feed by either exciting individual elements in the cluster, or by exciting all elements and then varying their phase and amplitudes. The same three techniques are available in Cassegrain systems, along with the possible usage of the subreflector.

Lateral Feed Displacement -- Lateral displacement of the feed consists of a rotation of the feed about the vertex of the paraboloid together with a small amount of axial displacement for refocusing.

As the feed is moved off axis, the antenna beam moves off axis in the opposite direction and in direct proportion to the feed displacement. This proportionality factor is called the beam deviation factor. For flat plates, the deviation factor is unity and for paraboloids, in the useful range of shapes, it is slightly less. As the beam moves off axis, it deteriorates, at first slowly and then more rapidly as the angle increases. As the scan angle continues to increase, the gain decreases further, the beamwidth increases and a series of sidelobes (coma lobes) appear on the axis side of the displaced beam. The sidelobe on the opposite side of the beam decreases, changes sign, and eventually merges with the main beam causing additional beam broadening.

J. Ruze¹ has computed the effects on the antenna beam caused by lateral feed displacement. Several of his curves are shown in Figure 7.1-1 for a paraboloid with an F/D ratio of .325 and an aperture distribution of the form

$$A + B (1 - \rho^2)^p$$

The reduction in gain which occurs when the feed is displaced is significant, the average loss being 3.5 db for a 6 beamwidth scan. At X-band, this is equivalent to a scan range of only ± 1.8 degrees. The more highly tapered aperture distributions have smaller scanning losses because the edge of the dish, where the phase error is greatest, is only slightly illuminated. For the same reason, the coma lobes of the highly tapered distributions are lower. The average coma lobe for a 6 beamwidth scan is about 7 db below the main beam. In systems where sidelobe level is important sidelobe degradation can be the limiting factor. Gain loss as a function of the beamwidths scanned with F/D ratio as a parameter is shown in Figure 7.1-2. For comparison purposes the experimental work of Kelleher² is also presented. Kelleher's measurements, of a paraboloid with F/D = .5 indicate that the theoretical results are slightly optimistic, growing more so as the scan angle increases. Increasing the F/D ratio improves the scanning performance because the comatic phase aberration which is causing the gain loss is inversely proportional to the square of the focal length. The performance curves for the higher F/D ratios are somewhat optimistic because they do not include the effects of astigmatism. Astigmatism is another type of phase aberration which causes a loss of gain. The ratio of astigmatism to coma phase error at the edge of the dish is given by

$$\frac{\text{Astigmatism}}{\text{Coma}} = \frac{2 (F/D) \tan \theta_s}{\left[1 + \left(\frac{D}{4F} \right)^2 \right]^2} \quad (1)$$

where θ_s is the feed tilt angle. For systems employing typical F/D ratios,

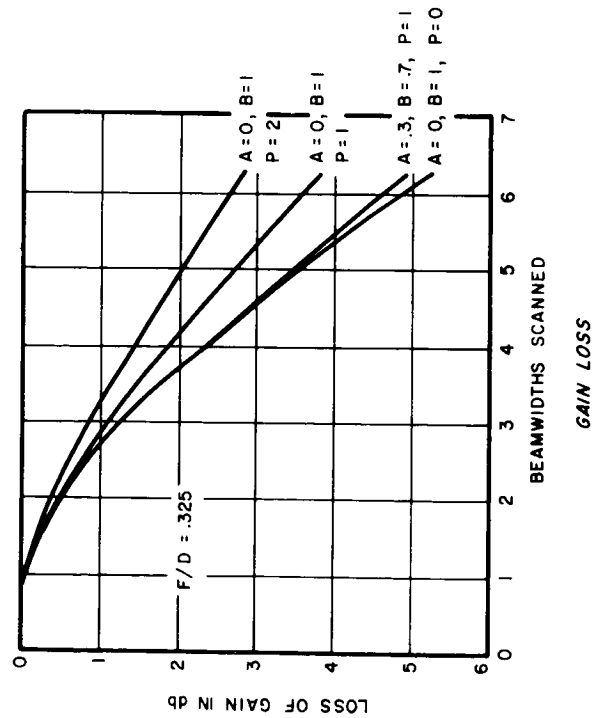
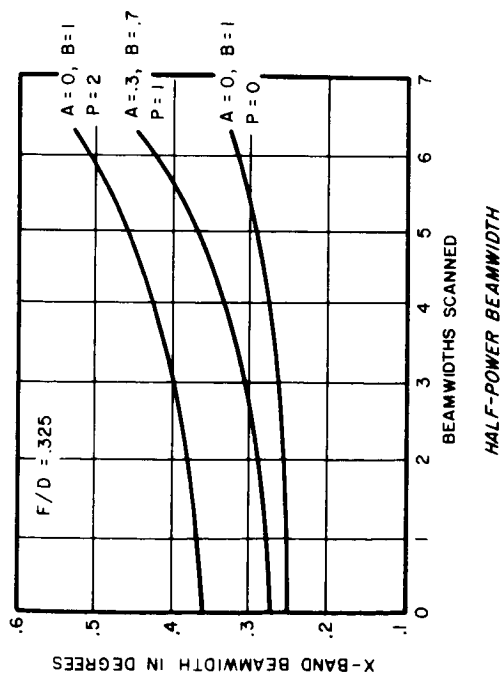
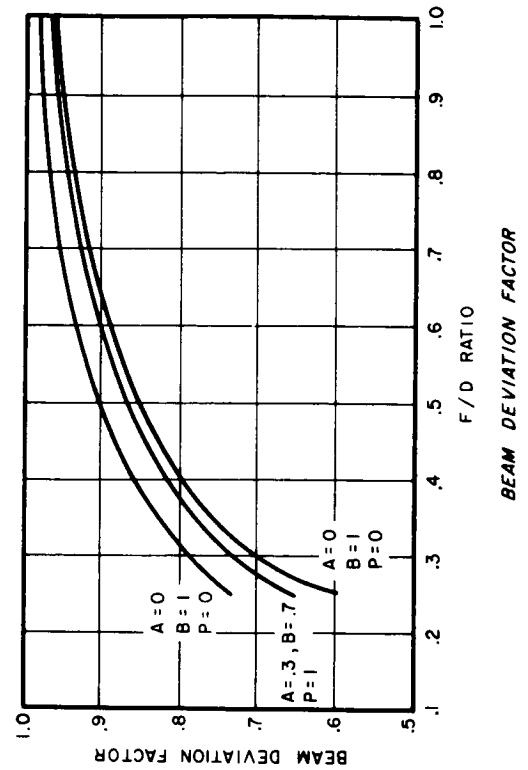
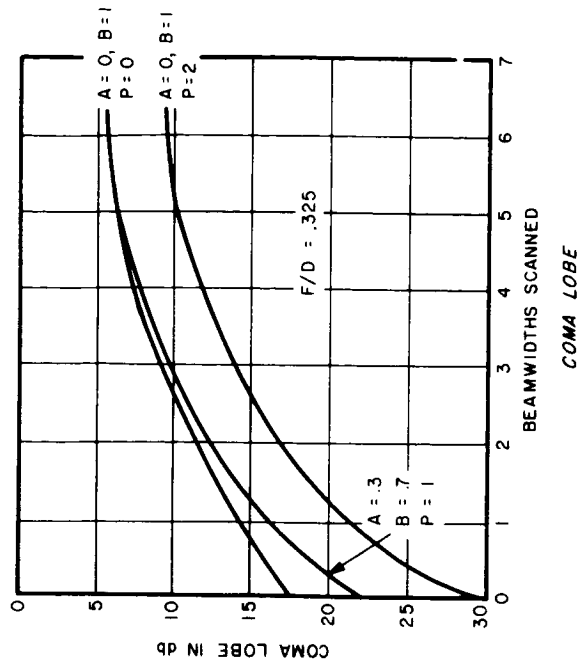


Figure 7.1-1 Prime Focus Paraboloid Scanning Performance

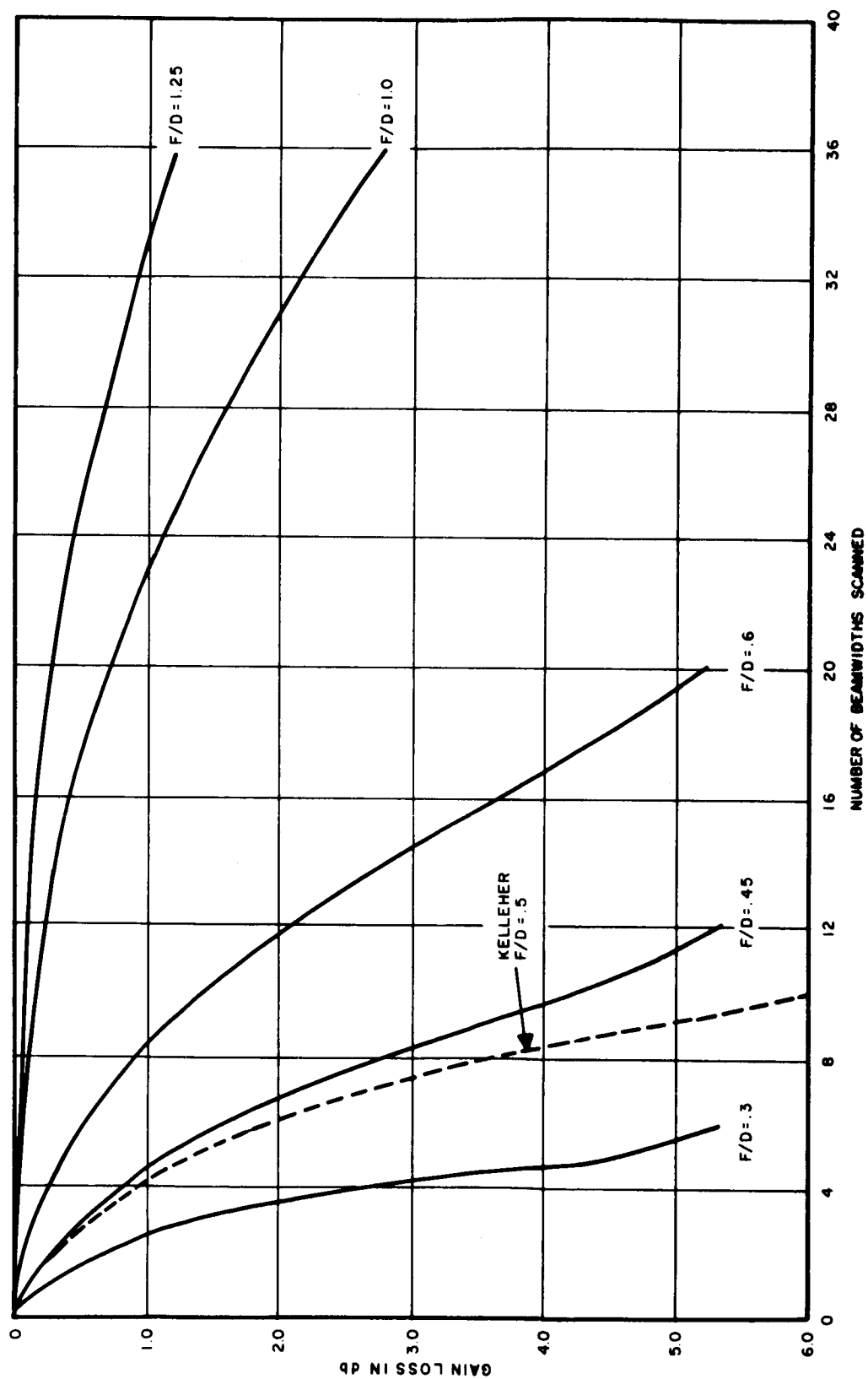


Figure 7.1-2 Parabolid Gain Loss as a Function of Beamwidths Scanned

astigmatism can be neglected; however, for large F/D system, especially Cassegrain systems, its effects must be considered.

At X-band, the amount of scan required for earth disk coverage is about 30 beamwidths. It is clear that no feed scanning paraboloid can give earth coverage without excessive degradation.

Electronic Cluster Feeds -- A coherently excited cluster feed takes the form of a hemispherical array centered on the focus of the parabolic reflector. The phase and amplitude of each element is controlled by the usual techniques employed in array antennas. Control of the amplitude and phase of each element makes it possible to generate a multitude of different aperture distributions which permits "shaping" of the on-axis beam and correcting for surface distortion in the reflector. Beam shaping is an advantageous feature to have should the spacecraft control system fail and a broad antenna beam be required. Since the degree of control of the aperture distribution is a function of the number of elements in the array, the amount of beam scan and reflector compensation are also functions of the number of elements. A rough approximation is that about 1.5 elements are required for each beamwidth of scan. For X-band operation, where the earth disk coverage is about 60 beamwidths, the impractically large number of 8100 elements is required. Low gain elements, such as open ended waveguide clusters, is the form the array would take. The number of elements required for smaller scanning ranges is about 2 per beamwidth so that a 25 element array is required for a $\pm .5$ degree scan. Since the electronically scanned beam will suffer approximately the same degradation as the mechanically scanned beam and is exceedingly complex for large scanning ranges, it should be only applied to systems requiring extremely rapid scanning rates over small angular excursions.

The switched feed method of scanning presents a simpler but less flexible method of beam scanning. Discrete beam steering is accomplished by excitation of a single element in the cluster. An active feed on the antenna

axis results in an on-axis beam, whereas an active feed located off the axis causes a scanned beam. The amount of the scan depends upon the feed displacement and the beam deviation factor. Although axial offset of the outermost elements in the cluster can be used to correct for some beam distortion, individual element design cannot, because the distortion is primarily a phase phenomenon. Since beam steering is discrete, a trade off area exists between beam crossover level and the amount of scan desired from a fixed number of elements. When a high cross-over level is desired the elements must be closely spaced, sometimes taking the form of a subdivided element cluster. Here the area of a single element is divided into two elements which are then coherently excited. The beam scan is now reduced to 1/2 the previous value by exciting the newly created element and the next element in the subdivided array. Subdivision is limited by element complexity, efficiency and coupling problems.

The amount of scan as a function of the F/D ratio, for an X-band cluster in which adjacent feeds are in contact (zero spacing), is shown in Figure 7.1-3. Beam scan is relatively constant with respect to F/D because the element size and hence, the spacing, increases in the same proportion as the focal length. About 0.3 degree of scan per element is obtained yielding the rough rule: switch one element width and move one beamwidth. An approximate formula for the number of elements required for a specified amount of scan is

$$n = \left(\frac{\text{Total scan}}{\text{Beamwidth}} + 1 \right)^2 \quad (2)$$

A one degree scan therefore requires about 16 elements. This is about 1/2 of the number elements required for a completely excited element cluster. The beam cross-over level as a function of the scan increment is shown in Figure 7.1-4. Since a non-subdivided array will provide a minimum scan increment of 0.3 degree, the cross-over level should be between 2 and 3 db.

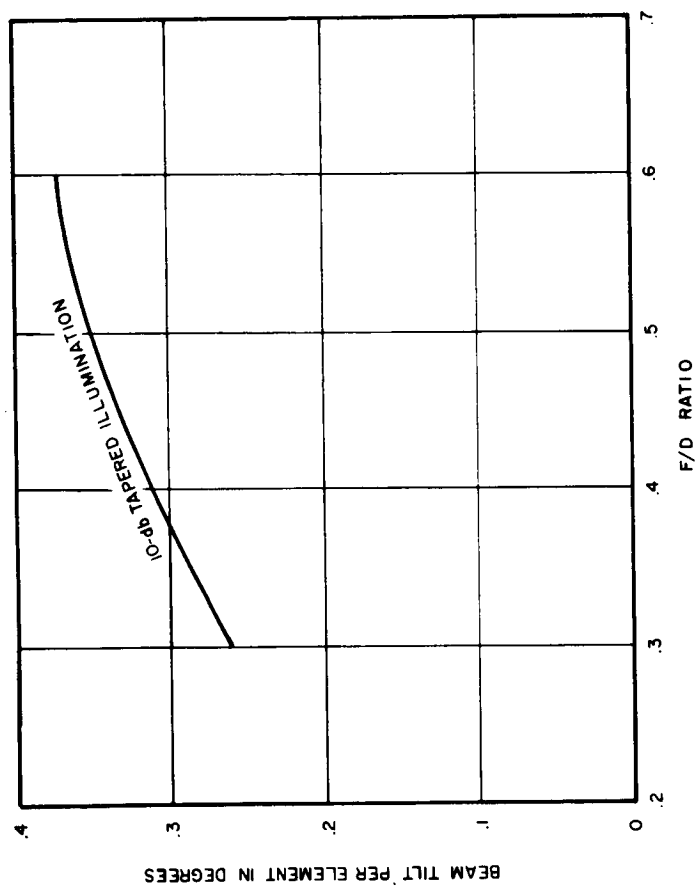


Figure 7.1-3 Beam Scanning Capability of a Multi-Element Paraboloid Switching-Feed System

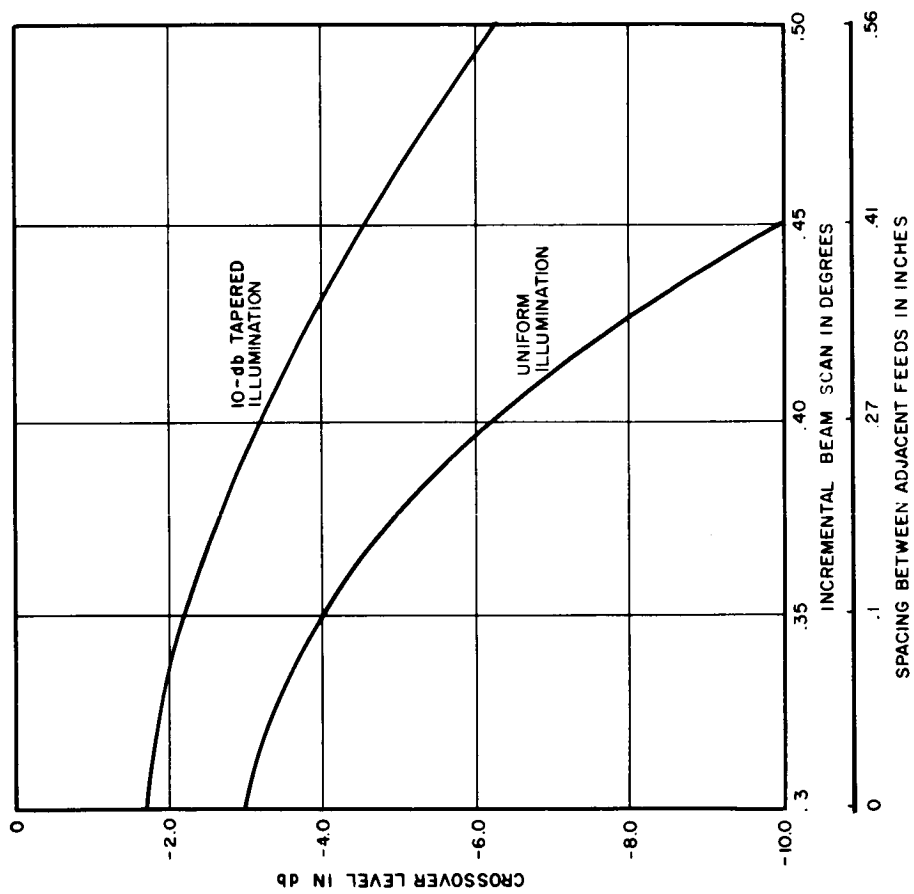


Figure 7.1-4 Beam Crossover Level as a Function of the Beam Scanning Increment

A factor to be considered in either type of feed cluster is its effect on the lower frequency feeds. As the size of the cluster grows, the spacing between the S-band feed elements must also increase. This will result in a more highly tapered S-band aperture distribution. In general, the angular position of the nulls of the S-band array should be outside the included angle of the paraboloid. For an F/D ratio of 0.325 this angle is about 75 degrees. Solving for d in the array factor equation

$$\frac{\pi d}{\lambda} \sin \theta = (2n+1) \frac{\pi}{2} \quad (3)$$

results in a maximum X-band cluster size of 0.52λ , or about 3 inches. In order to achieve larger sizes, a cross polarization technique which intersperses the S-band elements within the X-band cluster must be used.

Cassegrain System Application -- In a Cassegrain system, mechanical scanning can consist of feed rotation, subreflector rotation or a combination of both. Axial displacement of either the feed or the subreflector is required for refocusing of the paraboloid. Rotation of the virtual feed about the vertex of the paraboloid is the result of combined feed and subreflector rotation. This motion is equivalent to feed rotation in a prime focus system. The Cassegrain system is more favorable for scanning applications than a prime focus system because of its ability to scan with the passive subreflector and with somewhat better performance. As discussed earlier, the comatic aberration which causes a loss of gain is inversely proportional to the square of the effective focal length. Since the effective focal length in a Cassegrain system can be made large by using a large magnification factor, its gain degradation is smaller. The magnification properties of Cassegrain systems, however, cannot be extended indefinitely. A large magnification produces increased astigmatism and this results in a loss of gain. Since an increase in magnification requires a smaller subreflector, this also results in an additional gain reduction when the feed or subreflector is rotated. The effect of magnification and subreflector

size on scanning performance is shown in Figure 7.1-5 where gain loss as a function of scan is shown. The curves are the result of a computer-performed ray tracing study by J. F. Nihen and A. F. Kay³. The effect of subreflector blockage has been added to the curves. Since the magnification is a function of both the location of the real focal point and the size of the subreflector, the location of the real focal point is fixed at the vertex of the paraboloid. The prime F/D ratio of the Cassegrain system is 0.5. Figure 7.1-5 indicates that the optimum subreflector diameter is about 20% of the diameter of the reflector; this corresponds to a magnification of about 4.4. For a 3 db loss, the Cassegrain system appears to have about twice the scanning range of prime focus systems with an $F/D = 0.5$. The measurements of DeSize⁴ only partially support this conclusion, however, because his performance is less than 70% of that indicated by the curves. In this regard, it is noted in Nihen's study that for Cassegrain systems, the scan range in beamwidths is not independent of the aperture size as it is for prime focus configurations. If this is true, then DeSize's measurements may not be applicable because the aperture size used in his measurement is only about 1/3 the size of the paraboloid under discussion.

Electronic feed clusters can be used in Cassegrain systems just as they are used in prime focus systems. There are two possibilities, one technique replaces the Cassegrain feed with a cluster of elements and the other technique replaces the subreflector with a space fed reflectarray. Cluster feeds for Cassegrain systems take the same form as those discussed for prime focus systems. The reflectarray, which is fed conventionally, receives, phase shifts, and retransmits to the paraboloid reflector. The advantages and disadvantages of the two systems are similar to those associated with conventional and space fed arrays. The beam degradation in electronic scanning Cassegrain systems will be about the same as that of the mechanically scanning system.

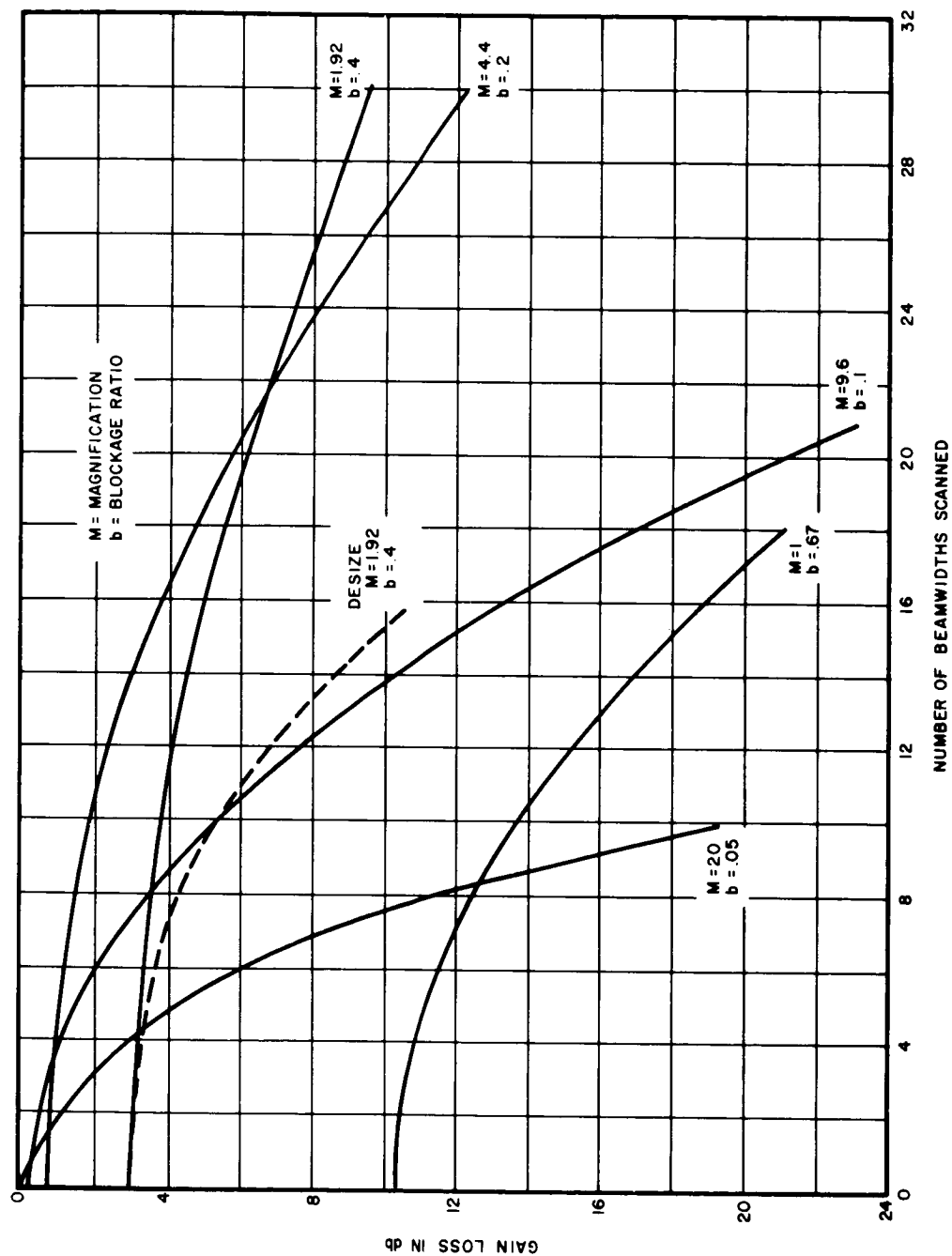


Figure 7.1-5 Cassegrain Antenna Gain Loss with Subdish Retention

Beam Scanning Summary -- Neither the prime focus nor the Cassegrain system offer any possibility of obtaining earth disk scanning coverage. For smaller scanning ranges, the Cassegrain system is preferred because of its superior performance and its ability to be scanned by rotation of the subreflector. Electronic scanning systems are extremely complex and offer no improvement in scanning performance. Application of electronic scanning systems should be limited to situations requiring rapid scanning rates over small angular ranges.

REFERENCES

1. Ruze, J. "Lateral-Feed Displacement in a Paraboloid", IEEE Trans. Vol 1 AP-13, No. 5, Sept. 1965.
2. Kelleher, K. S. "Off Axis Characteristics of the Paraboloid Reflector", NRL Report No. 111099, Dec. 1952.
3. Nihen, J. R., Kay, A. F., "Optimum Dual-Reflector Antenna Design Investigation", TRG Inc. Report, RADC-TDR-63-318, June, 1963.
4. DeSize, L. K., "Investigation of Multibeam Antennas and Wide Angle Optics", AIL Report, No. 7358-1 Jan. 1960.

7.1.2 Parabolic Antenna Feeds

Antenna Configuration -- The configuration of the antenna system can take the form of either a prime-focus fed paraboloid or a two reflector system, such as the Cassegrain antenna.

The prime focus system is a paraboloid fed at its focus with a device radiating a spherical wave. In a comparison with the Cassegrain system, the prime focus antenna has the following advantages for non-scanning applications:

- Simplicity
- Lower cost
- Less weight
- Less aperture blockage
- Lower "close in" sidelobes.

The Cassegrain antenna consists of a parabolic main reflector and a secondary reflector, usually a hyperboloid, located between the feed and the focus. One of the foci of the hyperboloid is located at the focus of the paraboloid and the other is located at the feed point. The magnification effect of the hyperboloid increases the effective F/D ratio of the system. Certain electrical and mechanical advantages accrue when a Cassegrain antenna is used. These advantages are:

- Favorable feed position (in most applications)
- Control of beam scan by rotation of the subreflector
- Control of the primary pattern by modification of the subreflector surface
- Better beam scanning performance
- Larger depth of focus and field of view.

Although the advantage of smaller aperture blockage in the prime focus system is compromised somewhat by the presence of the electronics compartment in

the aperture, an advantage of the Cassegrain system - favorable feed location - is also compromised.

Three of the more important factors affecting the performance of either system are:

- Aperture distribution
- Feed spillover
- Electronics compartment blockage.

Figure 7.1-6 shows the effects of these items on the antenna gain, first sidelobe, and beamwidth. The gain reaches a peak for a taper of about 10 db. This represents a compromise between spillover and distribution losses. The first sidelobe level is lowest for a vanishing edge taper. The effect of the blockage is to decrease the gain and increase the sidelobe level. The sidelobe level, when blockage is considered, is minimized for an edge taper of about 14 db. The gain loss remains minimized for a 10 db taper. The object of the feed design is then to cover the required frequency band with a feed that provides an aperture taper of between 10 and 14 db, and that it also presents the proper impedance to the system. The important effects of the tripod support have not been included because they cannot be calculated. They are not expected, however, to effect the selection of the optimum edge taper. To obtain the 10 to 14 db taper, the feed pattern must have a 6 to 10 db beamwidth of about 155 degrees. This decrease in the edge taper is the result of space attenuation in the prime focus system. For an F/D ratio of 0.325, it is about 4 db. In most Cassegrain systems, free space attenuation is negligible; so that, in general, it is not a consideration.

The feed for either the prime focus or Cassegrain system can take the form of a concentric array of multifrequency radiators, a single broadband feed, or a combination of both types. The feeds for the Cassegrain system will be generally larger than those of the prime focus system. This occurs when the magnification of the Cassegrain system is greater than

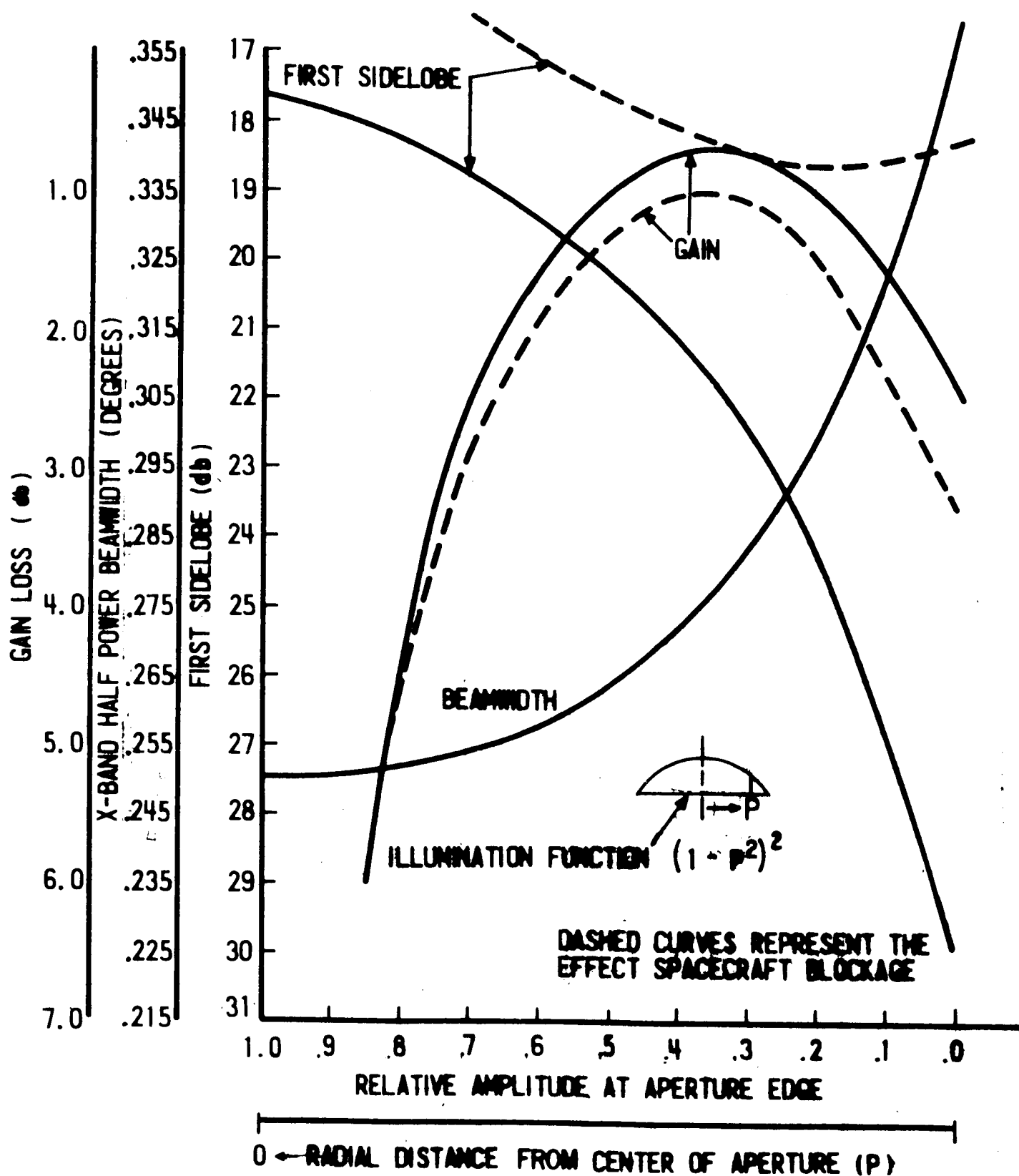


Figure 7.1-6 Radiation Characteristics of a Tapered Circular Aperture

one, which is usually the case. Where one of the feeds in a prime focus system might consist of a four element array, the same feed in a Cassegrain system may consist of as many as 16 elements. This is based on a Cassegrain system of the same F/D ratio, but with a magnification of two. The required aperture of a feed for some of the more common effective F/D ratios is shown in Figure 7.1-7. The effective F/D ratio is the prime value of F/D multiplied by the magnification. In regard to use of single broadband feeds for prime focus and Cassegrain systems, it was found that for high magnification systems the broadband feed was not applicable because of its rather broad pattern.

Multiband Feed -- The concentric array, or multiband feed, consists of an X-band feed located at the center of the array, nearest the focus, surrounded in descending order by the lower frequency feeds. The X-band feed consists of a horn cluster for monopulse operation. The S-band feed is a two-element array of bowtie-type dipole radiators. Dipoles, rather than horns, are used because they permit cross polarization of the S-band feed so that it can be located in front of the X-band feed. In this manner, the proper spacing of the S-band elements is obtained and the feed is closer to the focus. Since circular polarization is required for the 800 MHz feed, its form is restricted to an array of dipole or loop radiators oriented in space and phased in time so as to produce circular polarization. Because of the cross polarization of its elements, the 800 MHz feed must be located outside of the higher frequency feeds. Circular polarization is also required for the 100 MHz feed. Because of its size, this feed is limited to a single turnstile radiator.

X-Band Monopulse Feed -- The X-band monopulse system is used to lock the antenna beam on either a fixed or moving terminal for communication. For optimum performance, it is desirable to control the feed excitation independently in the sum mode and for the azimuth and elevation difference modes. Hannan¹ describes several types of feeds which achieve a measure

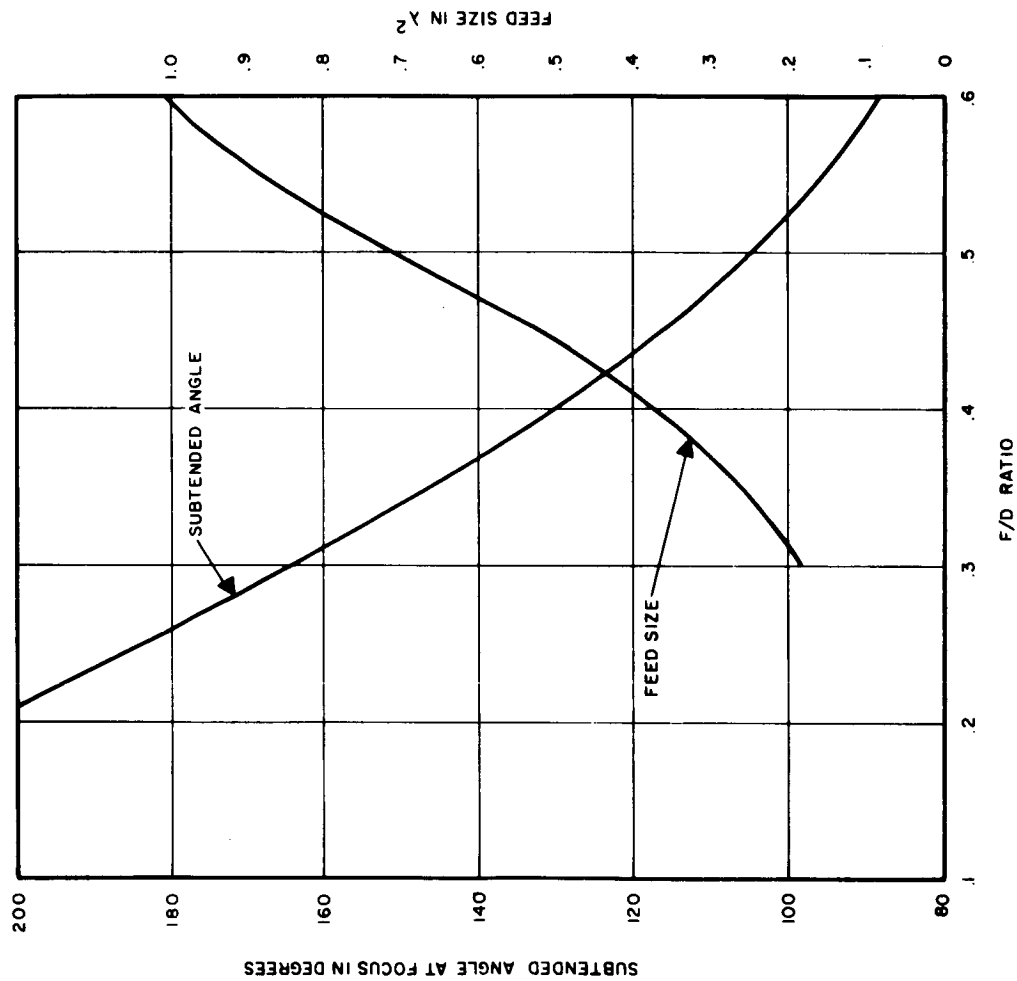


Figure 7.1-7 Paraboloid Subtended Angle and Feed Size as a Function of the F/D Ratio
Assuming a 10 db Illumination Taper

of independent control by using combinations of multihorn and multimode-waveguide feed excitations. These configurations, however, are large and complex.

The most conventional form of monopulse feed is the four-horn cluster. This type of feed has advantages of simplicity and relatively small aperture size. It does not, however, provide independent control of the monopulse modes. This results in an excessively broad difference mode excitation, when the sum mode is optimized, and a poor double-cosine shape for the H-plane even excitation. The sum mode efficiency, including only its distribution loss, is 58%. The broad difference-mode excitation causes a large discontinuity at the edge of the dish and results in high sidelobes in the antenna pattern. Nearly half of the power in the difference modes goes into spillover, so that there is close to a 3 db loss in the difference signal. The high illumination of the edge of the paraboloid also makes the difference mode sensitive to antenna misalignment and edge asymmetries. The large spillover will contribute to additional sidelobes.

A less conventional monopulse system is the five-horn cluster. As in the case of the four-horn cluster, the five-horn system does not provide independent mode control. It does, however, provide the means for improving sum mode efficiency by locating a single horn in the center of a four-horn cluster. This improves the sum mode efficiency to about 75%. This improvement is especially important in a system whose prime purpose is communication, rather than tracking. The price that must be paid for improved sum mode efficiency is a decrease in the difference mode slope. This occurs because the central horn forces a larger-than-optimum separation between the outer horns. Since the tracking angle uncertainty of the antenna is inversely proportional to the difference mode slope, the decrease results in degraded tracking performance. To a certain extent, this degradation can be offset by decreasing the error signal bandwidths, thus providing an improved signal-to-noise ratio. An extremely narrow error

signal bandwidth is possible because of the relatively slow slewing rates required for the antenna.

Prime focus systems with F/D ratios of 0.5 or less usually require loading of the monopulse feed horns. Loading, which consists of either filling the horn with dielectric material or using ridges, is required because the horns must operate below their normal cut off frequency. This is the result of monopulse design requirements. Feed-horn loading problems are eliminated in Cassegrain systems by choosing a magnification factor that results in a horn large enough to transmit at the operating frequency. Everything else about the two systems is the same.

Table 7.1-1 compares the monopulse performance of 4 and 5 horn systems. The table is based on the work of Hannan and R. W. Martin.²

S-Band Feed -- The S-band feed consists of a two-element dipole array. Bowtie dipoles are used because of their large bandwidth. The parameters which are used in control of the pattern are:

- Element spacing (d).
- Height-over-ground plane (D)
- Included angle of the bowtie element (α).
- Element "droop" angle (β).

Assuming an infinite ground plane, the radiation pattern of a two-element array of $\frac{\lambda}{2}$ dipoles is

$$\text{(H-Plane)} \quad E(\phi) = \sin(KD \cos \phi) \cos\left(\frac{Kd}{2} \sin \phi\right) \quad (1)$$

$$\text{(E-Plane)} \quad E(\theta) = \frac{\sin(KD \cos \theta) \cos\left(\frac{\pi}{2} \sin \theta\right)}{\cos \theta} \quad (2)$$

where ϕ and θ are respectively the polar angles in the H- and E-planes. The effect of an increase in the included angle of the bowtie element is to

TABLE 7.1-1 COMPARISON OF 4 AND 5 HORN FEED

System	Sum Gain	Sum 1st Sidelobe	Difference Slope	Difference 1st Sidelobe
4 Horn (Max. Sum Gain Design)	58%	-22 db	.58	-13 db
4 Horn (Max. Sum Gain Difference Slope Product, Design)	47.5%	-25 db	.74	-14 db
5 Horn (Max Sum Design)	75%	-22 db	.48	-22 db

broaden the pattern in the E-plane. This effect has been extensively studied by Brown and Woodward.³ The droop angle of the bowtie will also broaden the E-plane radiation pattern. The ground plane for the S-band feed is provided by the X-band horn cluster which acts as a waveguide operating beyond cut off. Its effect is difficult to assess by any means other than measurement. Figure 7.1-8 summarizes the primary pattern performance of the S-band feed. In order to achieve the favorable 10 db edge taper in the E-plane, the spacing of elements and the height above the ground plane should each be about 0.4λ . The pattern in the horizontal plane must be controlled by experimental adjustments of the droop angle.

The Cassegrain configuration for the S-band feed will be, in principle, the same as the prime focus feed. It will, however, require more elements and a larger aperture area. The size and the number of elements, of course, will depend upon the magnification factor which is selected.

800 MHz Feed -- The 800 MHz feed is a four-element square array of turnstile elements. This type of feed is commonly used for antennas in the UHF range. The radiation pattern of the turnstile element is symmetrical, whereas, its polarization varies from circular along the axis to linear at $\pm 90^\circ$. The horizontal and vertical components of the turnstile array, located over an infinite ground plane, have the following radiation patterns:

$$E_1 = \frac{\sin(KD \cos \theta) \cos\left(\frac{Kd}{2} \sin \theta\right) \cos\left(\frac{\pi}{2} \sin \theta\right)}{\cos \theta} \quad (3)$$

$$E_2 = \sin(KD \cos \theta) \cos\left(\frac{Kd}{2} \sin \theta\right) \quad (4)$$

where θ is the polar angle. Since the complete radiation pattern is symmetrical, E_1 represents either the horizontal component of the horizontal plane pattern or the vertical component of the vertical plane pattern. The opposite is true for E_2 which, in the horizontal plane, represents the vertical component and in the vertical plane represents the horizontal component. Figure 7.1-9

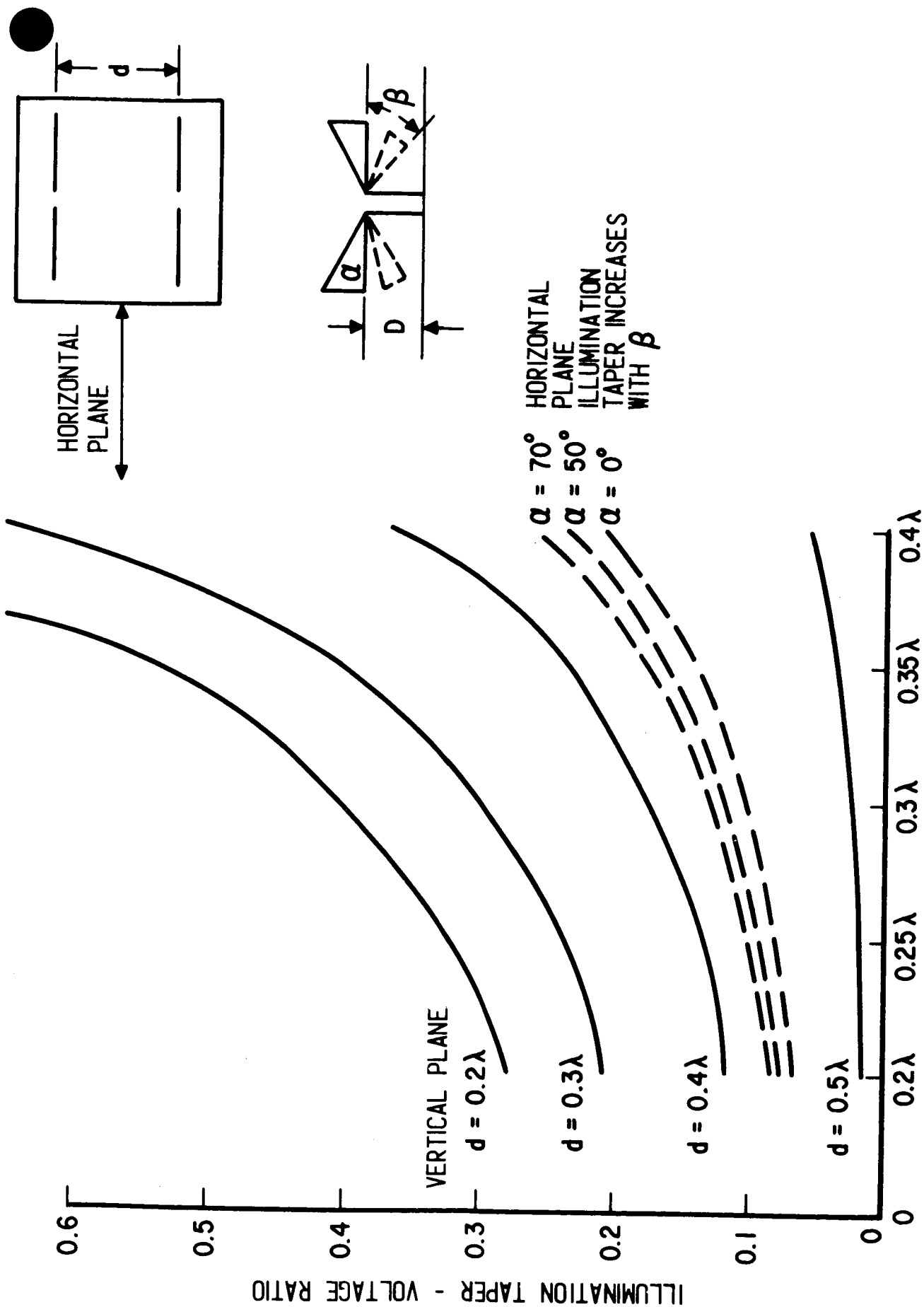
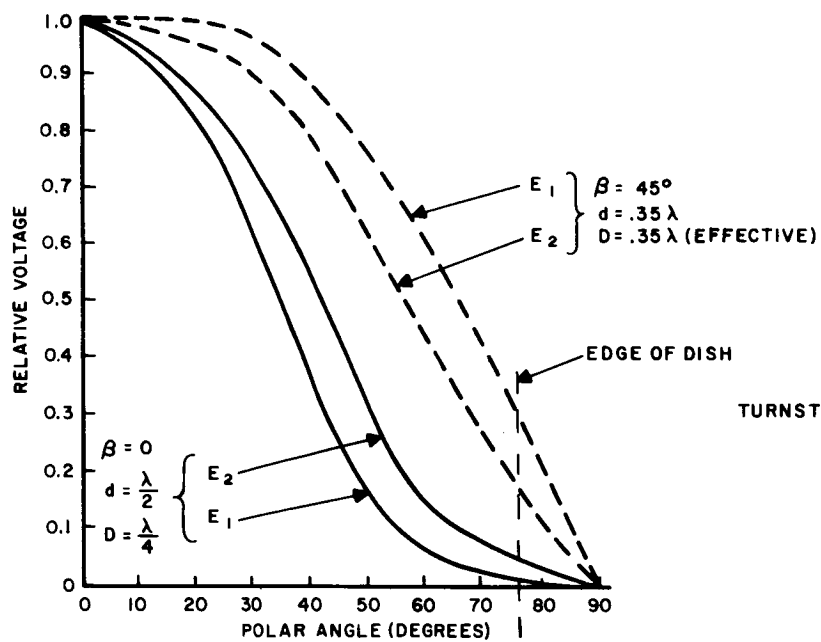


Figure 7.1-8 S-Band Feed-Edge Taper



TURNSTILE ANTENNAS

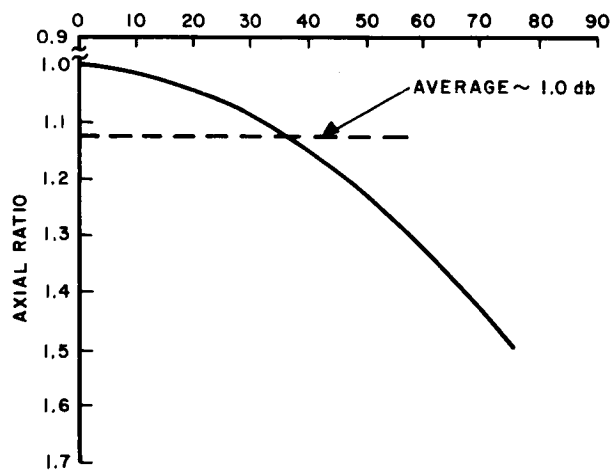
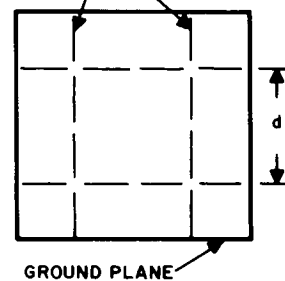


Figure 7.1-9 800 MHz Prime Focus Feed

shows the expected axial ratio of the polarization distribution of the paraboloid.

As in the case of the S-band feed, the 800 MHz Cassegrain feed will be similar, except in size and the number of elements, to the prime focus feed.

100 MHz Feed -- The most suitable 100 MHz feed consists of a single turnstile antenna mounted over the incomplete ground plane provided by the electronics compartment. The efficiency of the paraboloid, however, is expected to be extremely low because of its small electrical size. The STADAN⁴ network currently has in use, at 136.5 MHz, a 40 foot dish with an efficiency of only 30%. E. M. T. Jones⁵ has derived expressions for the gain of a paraboloid fed with magnetic or electric dipoles. The expressions include losses caused by the aperture distribution, spillover, and polarization. The expression for an electric dipole is

$$G = 6 \left(\frac{\pi D}{\lambda} \right)^2 \left[0.49115 \left(\frac{D}{4F} \right) - 0.367 \left(\frac{D}{4F} \right)^3 + 0.3102 \left(\frac{D}{4F} \right)^5 \right]^2 \quad (5)$$

Evaluating G for an F/D ratio of 0.325 and a dish diameter of 30 feet results in a gain of 16.7 db; this is equivalent to a 3 db loss. Adding all of the losses (Table 2.5-1, Section 2.5-1) results in an antenna with an efficiency below 25%.

The idealized turnstile radiation patterns for the vertical and horizontal field components are

$$E_1 = \frac{\sin(KD \cos \theta) \cos\left(\frac{\pi}{2} \sin \theta\right)}{\cos \theta} \quad (6)$$

$$E_2 = \sin(KD \cos \theta) \quad (7)$$

E_1 is either the horizontal field component in the horizontal-plane pattern

or vertical component in the vertical-plane pattern. E_2 is the vertical component in the horizontal plane or the horizontal component in the vertical plane. The radiation patterns are shown in Figure 7.1-10. The considerable difference between the two field components causes the pattern to become elliptically polarized at the edge of the paraboloid. This will be corrected by experimental adjustments of the element droop angles. The estimated axial ratio of the polarization distribution across the aperture is also shown in Figure 7.1-10. Another thing to be considered in the turnstile pattern, is the effect of the gap between dipole elements caused by the presence of the higher frequency feeds. This results in a broader radiation pattern in the E-plane and a modified phase distribution. The magnitude of these effects has not been computed.

It is not practical to operate at 100 MHz in the Cassegrain configuration. This occurs because of the size requirements of the feed and subreflector and their resulting aperture blockage. Hannan's⁶ minimum blockage expression, which equalizes the feed and subreflector size, is

$$D_s = \sqrt{2F\lambda} \quad (8)$$

where D_s is the subreflector diameter and F is the focal length. Numerical substitution in equation 8 results in a subreflector diameter of 14 feet for a 9.75 foot focal length. This results in a quite unacceptable blockage loss of about 4 db.

Broadband Feed -- A prime focus system fed with a single broadband feed is attractive because of its simplicity. A planar cavity-backed Archimedean spiral was therefore investigated for this purpose.

The planar spiral is mechanically advantageous because it is a flat, light weight structure. Electrically, the planar spiral offers the advantages of a relatively broad, frequency insensitive pattern and the capability for monopulse operation. Among its disadvantages are feed network complexity and high losses. It will not be as accurate as the

conventional monopulse system and the control of its pattern will be limited.

A multiple arm spiral of M arms can be operated in M-1 modes. The first radiating band of the zero or sum mode occurs at a radius of $\frac{\lambda}{2\pi}$. Additional sum mode radiation bands occur at $\left[1 + M(C-1)\right]\frac{\lambda}{2\pi}$ where C is the number of the radiation band. The remaining modes take the form of difference patterns. Monopulse operation is obtained by comparing the amplitude and phase of the first sum mode to that of the first difference mode. As described in Figure 7.1-11, the angle θ is obtained from amplitude comparison and the angle ϕ from phase comparison. For good system operation, the purity of both modes must be maintained. In order to achieve this, the spiral must have a sufficient number of arms to suppress the second radiating band of the sum mode. Since the overall size of the spiral is determined by its lowest operating frequency, the number of arms must be selected so that the following inequality will hold

$$\frac{\lambda_L}{2\pi} \geq (1 + M) \geq \frac{\lambda_h}{2\pi} \quad (1)$$

When equation (1) is satisfied, the second band of the sum mode cannot exist. The minimum number of arms, therefore, is

$$M \geq \frac{\lambda_L}{\lambda_h} - 1 \quad (2)$$

In the case where coverage is provided over from 800 MHz to 8 GHz, at least 9 arms are required. The use of this large number of arms requires five wires, which have a rather large dissipation loss. Including the losses in the feed network, the overall spiral loss is expected to be about 3 db at X-band.

Configuration and Feed Selection -- A prime focus feed is selected for the paraboloid rather than the Cassegrain feed because of its simplicity. The two advantages that might accrue by going to a Cassegrain system, namely,

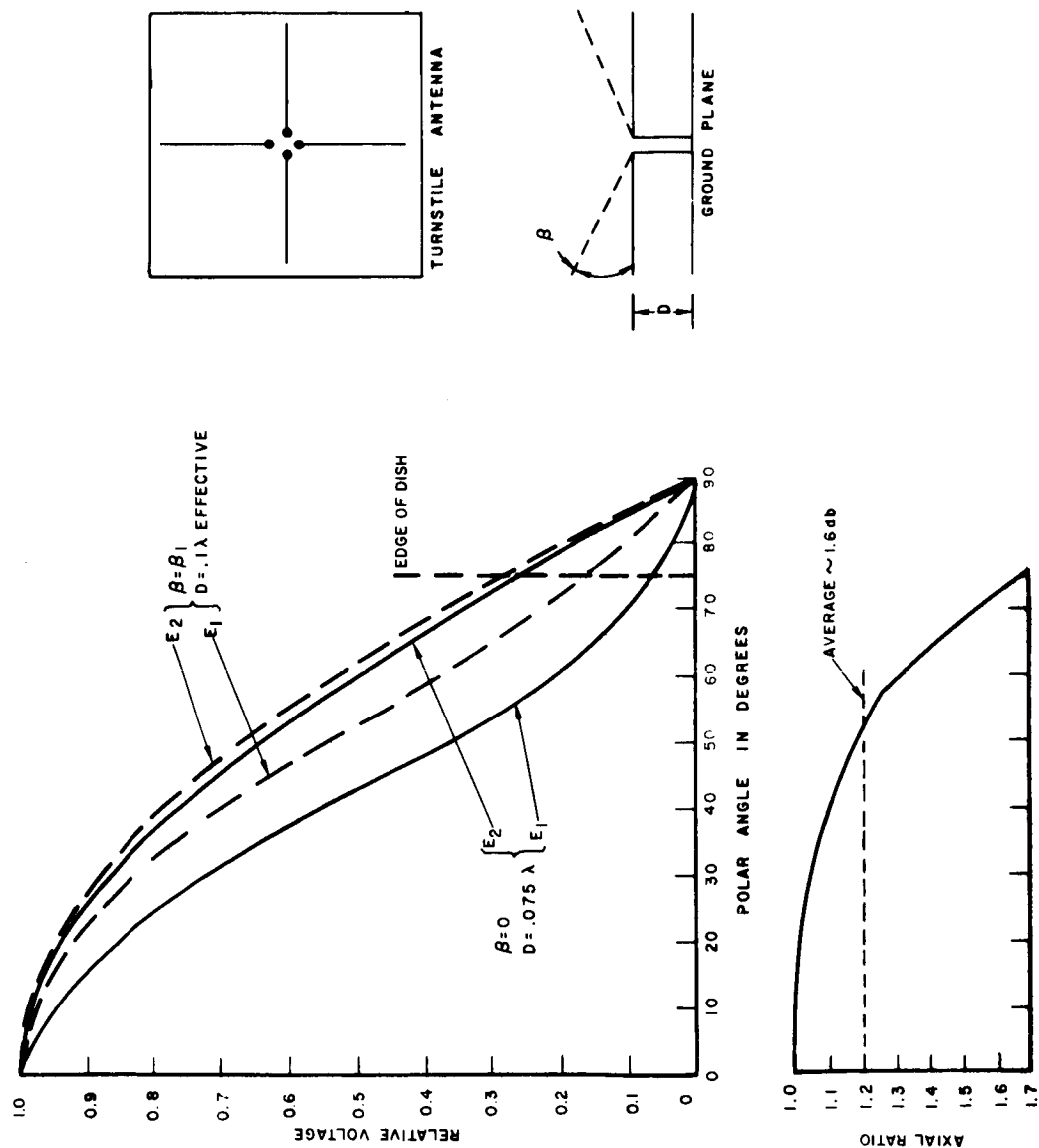
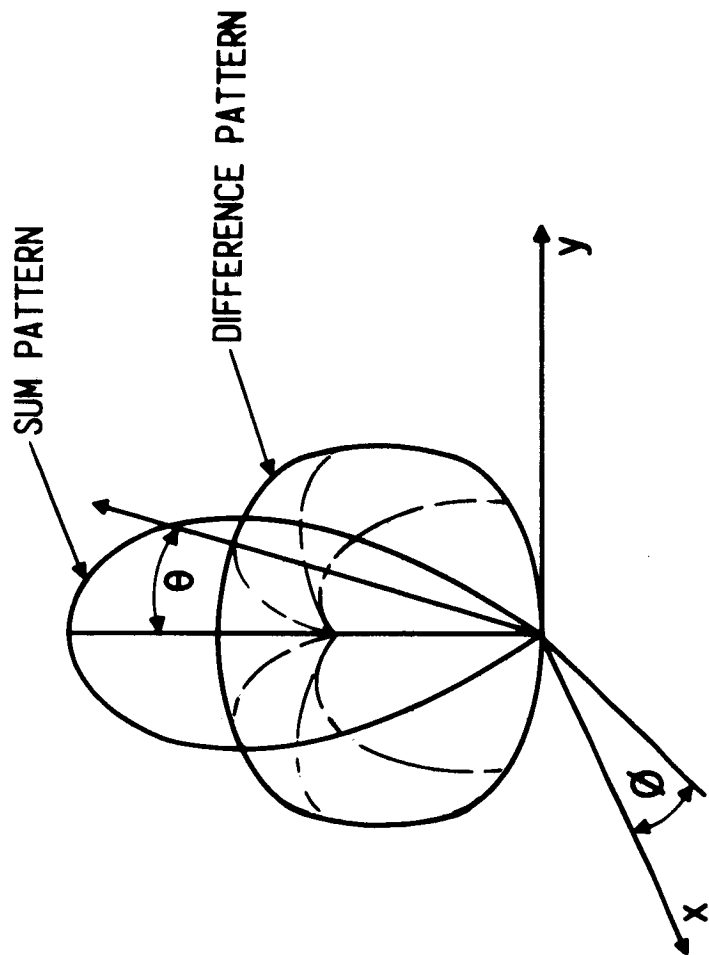


Figure 7.1-10 100 MHz Prime Focus Feed

AMPLITUDE COMPARISON



PHASE COMPARISON

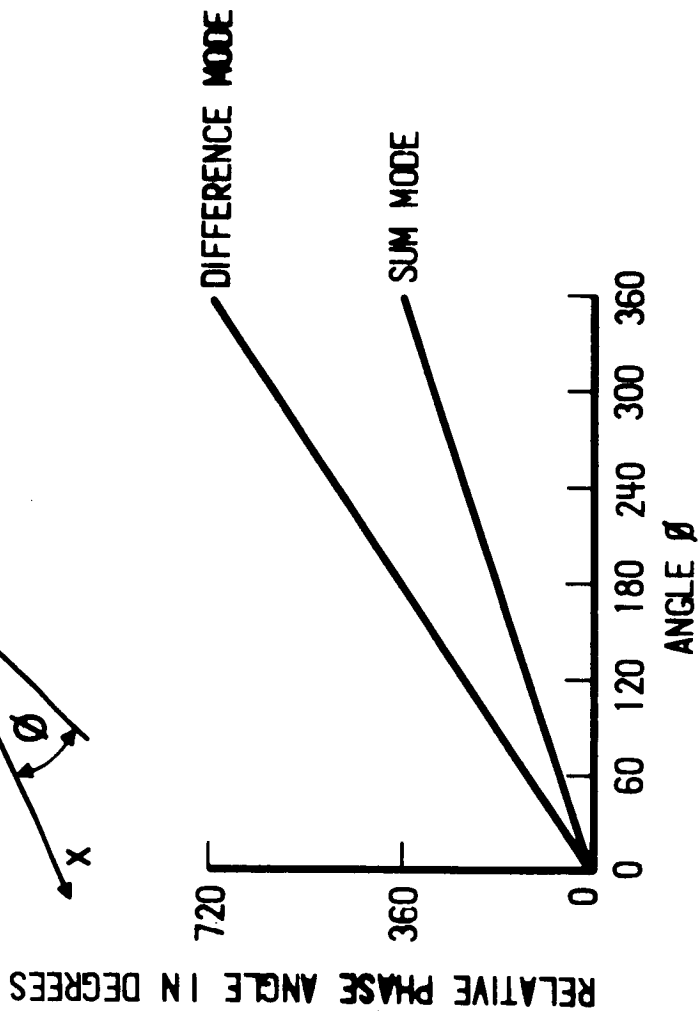


Figure 7.1-11 Spiral Antenna Monopulse Operation

its favorable feed location and its better scan capability are not applicable in the present situation. Beam scan is obtained by rotation of the complete paraboloid, rather than by some feed or subreflector scan technique, because of the large scan range requirement. Packaging together of all electronic equipment eliminates a large wiring problem and results in the electronics equipment compartment being located in the aperture of the paraboloid, rather than behind it.

The conventional multiband feed, rather than the broadband feed is selected for the paraboloid, because of its lower loss, better reliability and better pattern control. The broadband feed sacrifices performance for continuous frequency coverage in the operating bands.

REFERENCES

1. Hannan, P. W., "Optimum Feeds for All Three Modes of a Monopulse Antenna", IRE Trans., Vol. AP-9, No. 5, Sept. 1961.
2. Martin, R. W., Schwartzman, L., 1960, "A Monopulse Cassegrainian Antenna", IRE Con. Rec., Part 1, March, 1960.
3. Brown, G. H., Woodward, O. M., "Experimentally Determined Radiation Characteristics of Conical and Triangular Antennas," RCA Review, Dec. 1952.
4. Lantz, P. A., "Handbook of Antennas at NASA, Satellite Tracking and Space Data Acquisition Network (STADAN) Facilities," Vol. 2, GSFC, N64-27259, pp 6-9, July, 1964.
5. Jones, E. M. T., "Paraboloid Reflector and Hyperboloid Lens Antenna", IRE Trans., Vol. AP-2, No. 3, July 1954.
6. Hannan, P. W., 1961, "Microwave Antennas Derived from the Cassegrain Telescope", IRE Trans., Vol. AP-9, No. 2, March 1960.

7.1.3 Aperture Blockage

Aperture blockage of the paraboloid is contributed by the space-craft electronics compartment and by the feed support tripod. The blockage contribution of the electronics compartment can be computed, while the contribution of the tripod must be measured. Measurements are required because of the complex geometry of the tripod and its effect upon both the primary and secondary patterns.

Electronics Compartment Blockage -- The electronics compartment presents a five foot circular blocking area centrally located in the aperture of the paraboloid. The gain reduction caused by this blockage is easily computed by considering the blocked area to radiate 180 degrees out of phase to the main radiation. This is, of course, equivalent to subtracting the radiation contribution to the on-axis field mode by the blocking area. Mathematically, this is expressed as

$$\text{unblocked signal} = 2\pi \int_0^1 f(\rho) \rho d\rho - 2\pi \int_0^b f(\rho) \rho d\rho \quad (1)$$

where $f(\rho)$ is the aperture distribution, ρ is the normalized aperture radius and b is the ratio of the compartment diameter to the aperture diameter. The loss is given by the ratio of unblocked signal to the total signal. This is expressed as

$$\eta_b = \frac{2\pi \int_0^1 f(\rho) \rho d\rho - 2\pi \int_0^b f(\rho) \rho d\rho}{2\pi \int_0^1 f(\rho) \rho d\rho} \quad (2)$$

or

$$\eta_b = 1 - \frac{\int_0^b f(\rho) \rho d\rho}{\int_0^1 f(\rho) \rho d\rho} \quad (3)$$

The aperture distribution of the paraboloid can be described in the form

$$f(\rho) = A + B(1-\rho^2)^3 \quad (4)$$

where A, B and p are constants. Substitution of equation (4) in equation (3) gives the loss in gain as

$$\eta_b \approx 1 - \frac{24b^2 (A+B) - 12pb^4 + 4p(p-1)b^6 - p(p-1)(p-2)b^8}{24(A+B) - 12p + 4p(p-1) - p(p-1)(p-2)} \quad (5)$$

The constants A, B and p are evaluated by curve fitting to the calculated or measured aperture distribution. Equation (4) is plotted in Figure 7.1-12 for an A=0, B=1, and p=1 distribution.

The negative signal radiated by the equipment compartment will also affect the antenna sidelobe level. Since the compartment is small, it radiates a broad pattern which alternately adds to and subtracts from the sidelobes of the unblocked pattern. The new sidelobe level is therefore given by

$$\text{New Sidelobe Level} = 20 \text{ Log} \left(\frac{\frac{E_s}{E_m} + 1 - \eta_b}{\eta_b} \right) \quad (6)$$

Where E_s/E_m is the unblocked sidelobe level. Equations (5) and (6) are used to compute the gain loss and the new sidelobe level of the X-band radiation pattern shown in Figure 7.1-13.

Tripod-Support Mast Blockage -- The tripod feed-support mast will degrade the pattern of the parabolic antenna by scattering energy in both the primary and secondary patterns. The scattering will manifest itself by causing decreased antenna gain, increased sidelobe levels and a change in the impedance characteristic of the feed. The most pronounced effect will probably occur when the tripod support is electrically resonant. In this case the tripod is electrically coupled to the feed and may have a rather directive reradiation pattern. Depending upon its phase, this reradiation can severely distort the aperture illumination of the paraboloid. In the case where the tripod is non-resonant, reradiation from the tripod

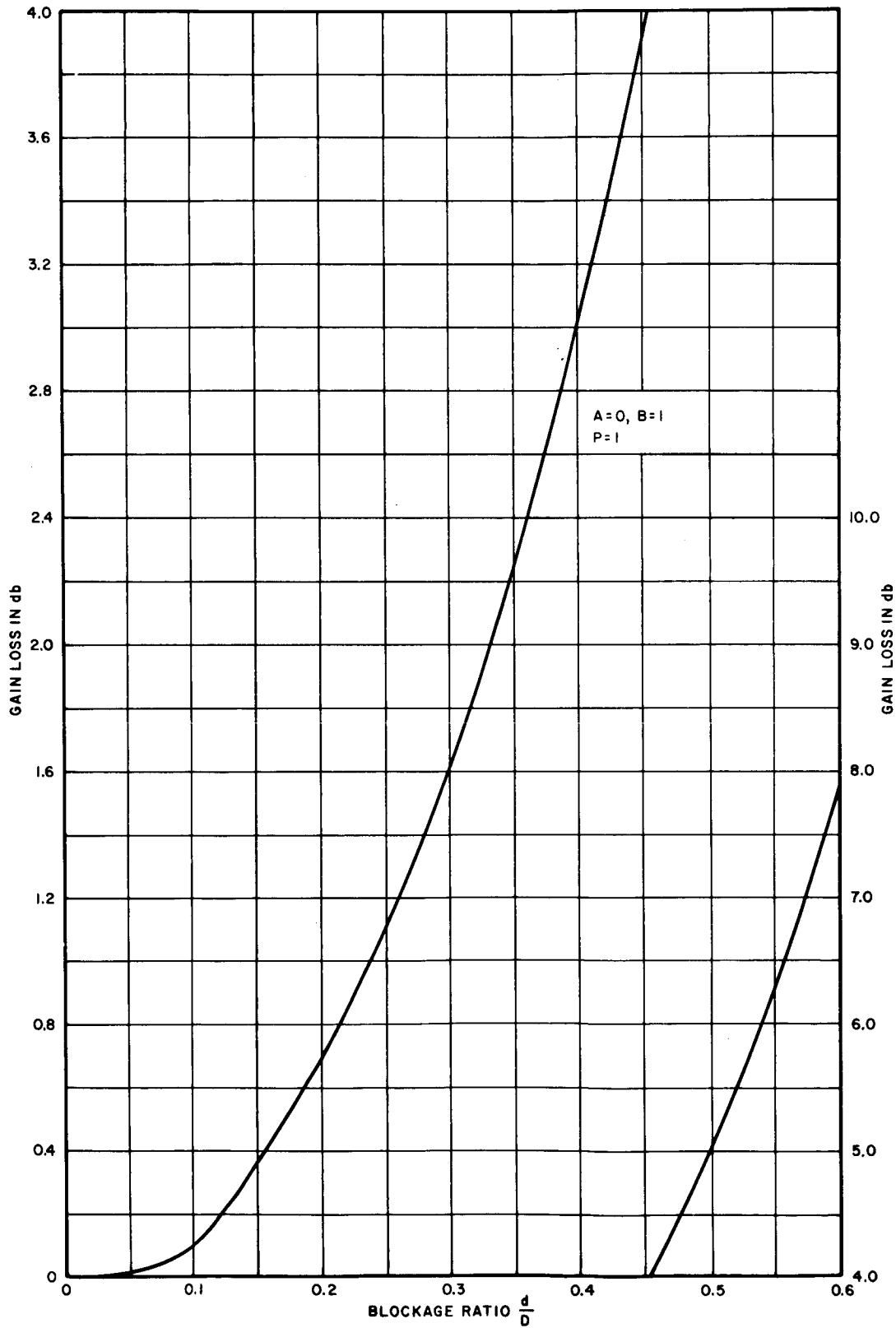


Figure 7.1-12 Parabolic Antenna Gain Loss as a Function of the Blockage Ratio

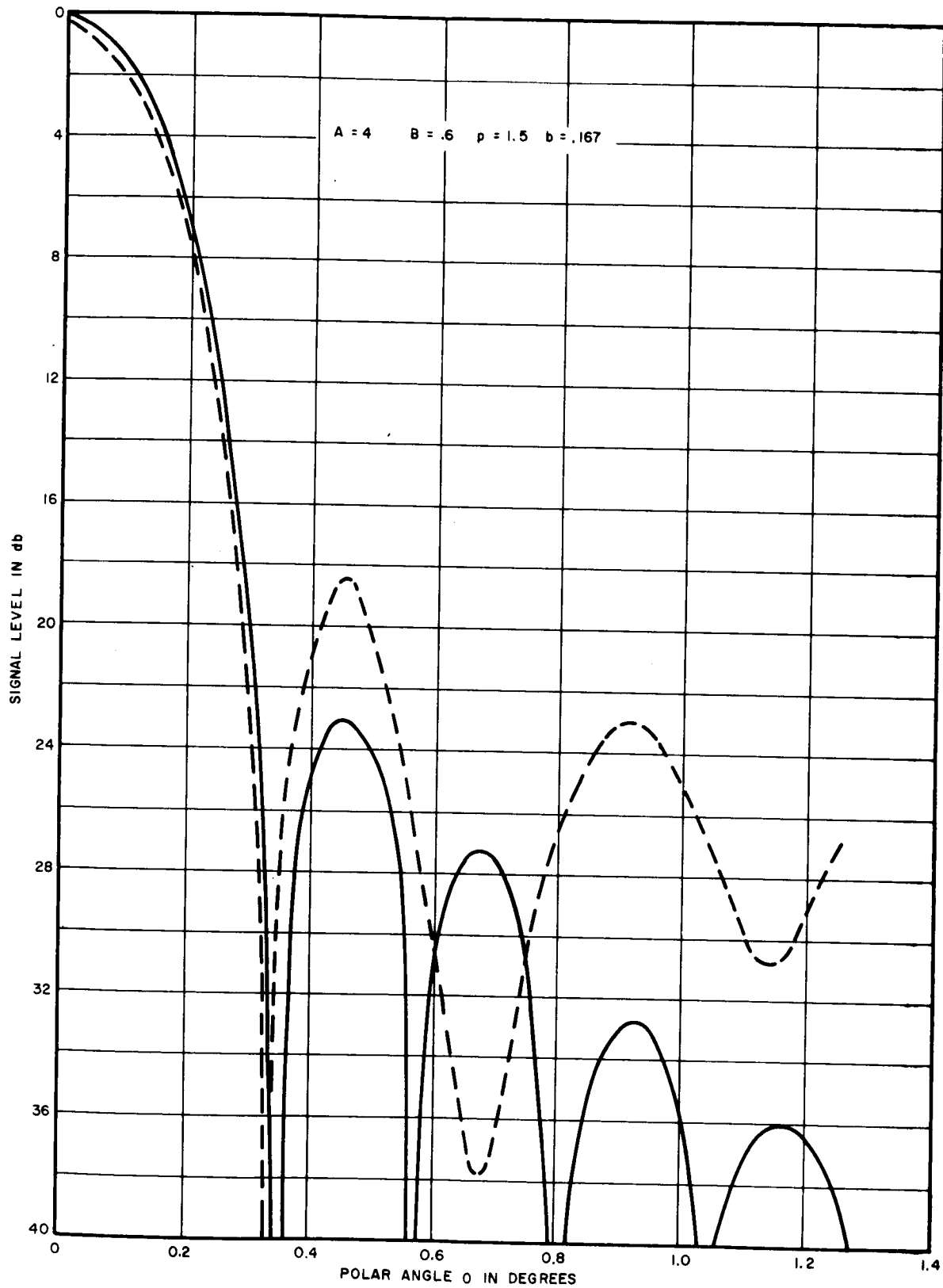


Figure 7.1-13 Attenuation between Arbitrarily Polarized Antennas Caused by Faraday Rotation AF - Axial Ratio

is more omnidirectional in nature and, therefore, will tend to have a smaller overall effect on the performance of the paraboloid. As another possible concept, one may view the tripod support structure as a "leaky" waveguide which, because of its diameter, may "cut-off" TE and TM modes in the 100 MHz region but will propagate waves above this frequency. Since the phase velocity inside the structure is greater than that outside, wave interference will occur between the leaking energy and energy propagating external to the structure. At the upper end of the frequency band, the waves experience scattering rather than waveguide effects because the diameter of the support is large enough to permit almost free-space propagation conditions.

Tests of the tripod support are required because the geometry is such that an analytical evaluation is impractical. The most important quantities to be determined are the changes in the antenna gain and sidelobe level caused by the presence of the tripod support. To obtain this information radiation patterns of a scale model antenna system, excluding the spacecraft electronics package, were measured. A scale factor of 5 was used, based on the availability of a 6 foot dish ($F/d = 0.3$). Table 7.1-2 lists the full scale and model frequencies along with the Fraunhofer and Rayleigh distance of the 6 foot paraboloid. The phase errors at the edge of the paraboloid for the Fraunhofer and Rayleigh distances are respectively 22.5° and 90° . Pattern measurements made at distances less than the Fraunhofer distance require refocussing of the feed in order to obtain the far field patterns. With a measurement range of 150 feet, the amount of refocussing required was of the order of 0.5 inch and consisted of an increase in the distance of the feed from the apex of the paraboloid. The 150 feet test range is shown in Figure 7.1-14 with the transmitting horn in the background. The source horn is adjusted in elevation (see Figure 7.1-15) so that the azimuth cut, which is taken when the turntable is rotated, passes

TABLE 7.1-2 DISTANCES FOR SCALE MODEL TEST

Full Scale Frequency (GHz)	Model Freq- uency (GHz)	Fraunhofer * Distance (ft.)	Rayleigh ** Distance (ft.)
0.1	0.5	25.4	6.4
0.8	4.0	204	51
1.7	8.5	431	108
2.1	10.5	536	134
2.3	11.5	586	147
7.3	36.5	1860	465
8.0	40.0	2040	510

$$* R = \frac{2d^2}{\lambda}$$

$$** R = \frac{d^2}{2 \lambda}$$

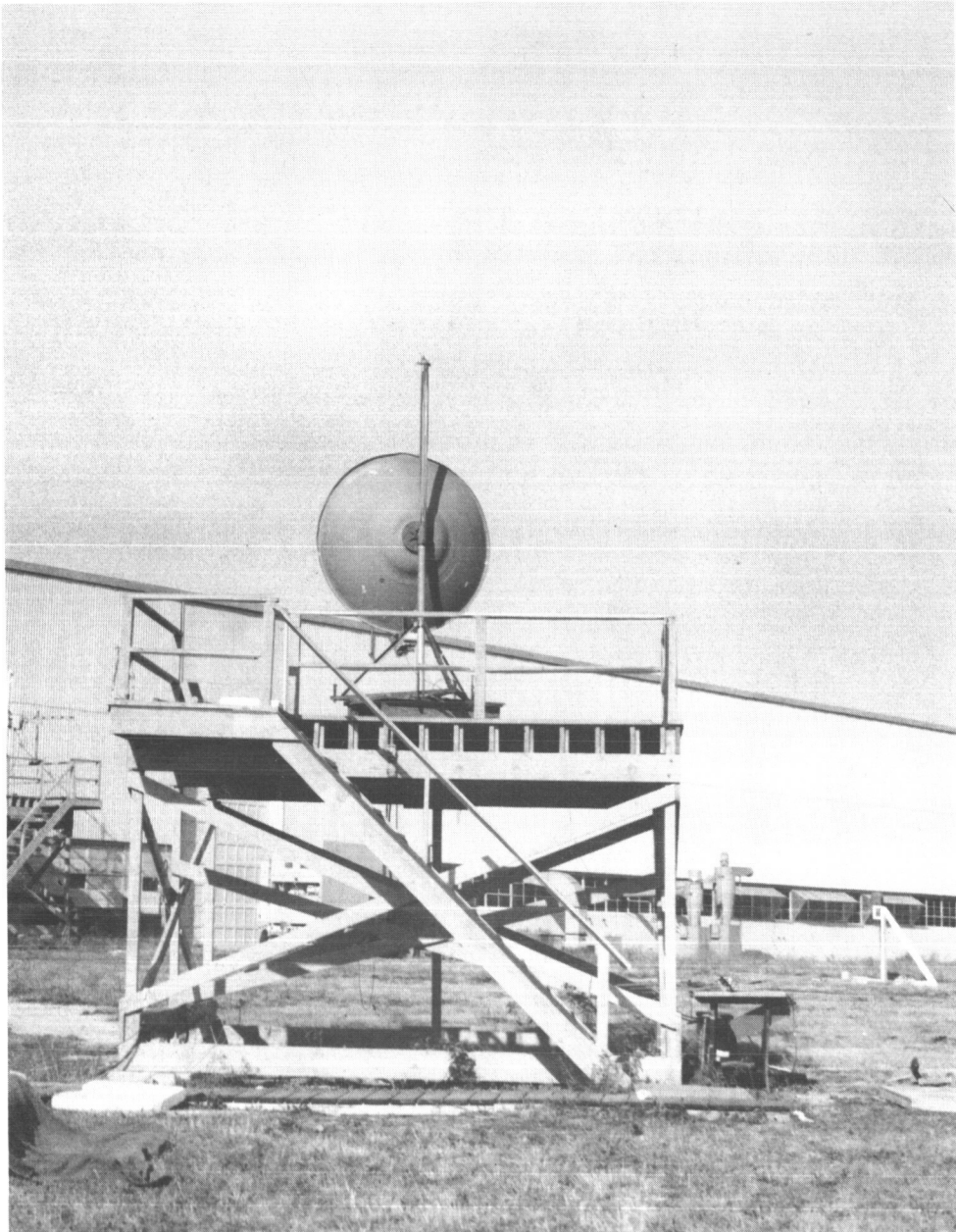


Figure 7.1-14 Antenna Test Range



Figure 7.1-15 Source Tower

through the center of the main beam. Tests consisted of measurements of the radiation pattern with and without the presence of the scale-model tripod support (see Figures 7.1-16 thru 7.1-21). The feed in Figures 7.1-17-20 is an open ended C-band waveguide (RG-48/U) terminated with a round flange. The feed is cross polarized (horizontal) with respect to the waveguide feed support structure in order to minimize obscuration effects. Feeds which were used at the other frequencies are shown in Figures 7.1-22 and 7.1-23. The feed at the left of Figure 7.1-22 is open ended RG-97/U waveguide with a set of E-plane "flaps" and was used at 10.5 and 12 GHz. The right hand feed is WR-51 waveguide and was used at 18.0 GHz. All feeds are shown connected to their respective crystal detector mounts, the outputs of which feed a pattern recorder. Open-ended waveguide feeds were chosen because they provide adequate primary radiation patterns, are readily available, and are simple. Although the scope of this test program did not permit optimization of the feed pattern, an attempt to improve the X-band dish pattern was made by adding the E-plane flaps to the feed. The flaps, however, did not significantly change the pattern.

The results of the radiation pattern measurements are shown in Figures 7.1-24 thru -28. Figure 7.1-24 is the E-plane radiation pattern at 4.0 GHz, with and without the presence of the tripod support. A reduction in gain of about $2\frac{1}{4}$ db, a slight broadening of the main beam and a small increase in the "close in" sidelobe level is noted. Figure 7.1-25 is the radiation pattern at 10.5 GHz. The gain reduction in this case is about $1\frac{1}{4}$ db with a slight increase in the sidelobe level but no measurable change in the beamwidth. The high sidelobes of the 10.5 GHz patterns may be caused by feed defocussing, however, this is not apparent from the shape of the main beam. The presence of high sidelobes should not affect the accuracy of the gain measurement. Figure 7.1-26 is the radiation pattern at 12.0 GHz. The gain reduction is about $2\frac{1}{2}$ db, the sidelobe level is increased, but the beamwidth is unchanged. At 18 GHz, Figure 7.1-27 indicates a loss in gain

of about 1 db, a more substantial increase in sidelobe level than indicated in the previous cases, but no measureable change in the beamwidth. Figure 7.1-28 is the radiation pattern at 39.6 GHz. The reduction in gain is about 1.4 db, the change in the sidelobe level is indeterminate and the beamwidth is unchanged.

Spot checks of the impedance of the feeds was made at 4.0 and 10.5 GHz. In neither case was there a significant change in the VSWR in the presence of the tripod.

The loss in gain caused by the tripod support is larger than that incurred by the common type of feed support structure. For example, P.D. Potter¹ indicates losses of from 0.6 db to 1.0 db for an 85 foot paraboloid employing a truss-type quadripod to support a very small hyperbolic subreflector. On the average therefore, the tripod support might be of the order of 1 db worse than a standard support. This increased loss is, of course, indirectly caused by spacecraft constraints which dictate a cylindrical type of support that tends to enclose the feed. The mechanism of the gain loss is unknown at this point; it is unlikely that geometrical optic considerations can account for it. Further studies must therefore include phase and amplitude pattern measurements of the feed in the presence of the tripod.

Since the object of this limited test program was directed at determining the influence of the tripod, the blocking effect of the spacecraft electronics compartment was not measured. It is expected that, apart from the tripod, the spacecraft will contribute a gain reduction of about 0.5 db. The manner in which the losses due to spacecraft and the losses due to the tripod should be combined is unknown because their relative phases are unknown.

¹ Potter, P. D., "The Design of a Very High Power, Very Low Noise Cassegrain Feed System for a Planetary Radar", JPL Tech. Report No. 32-653, August 24, 1964, p. 12

A study of the performance of the tripod support as a function of frequency may reveal the resonance effects discussed earlier. In this case, construction of the tripod from dielectric material, rather than metal, might be advantageous. Incorporation of RF chokes or damping devices in the construction of a metallic support may also be helpful in changing the frequency of, or eliminating, harmful resonances. A study of resonance behavior, of course, will require a precise simulation of the paraboloid feed system and its environment.

The effect of the tripod support on the monopulse performance of the paraboloid is unknown, especially with regard to the difference mode slope and the antenna boresight. Measurements utilizing models of the feed system are required.

7.1.4 Paraboloid Performance

X-Band Feed -- The X-band monopulse feed is a 5-horn cluster. As described in Table 7.1-3, the sum mode efficiency of the paraboloid is about 38%. This results in a gain of about 53 dbi. The sum mode radiation pattern, including the effect of spacecraft blockage, was shown in Figure 7.1-13. The first sidelobe level is about -18 db. Scale model measurements of the tripod support indicate that perhaps 2 db more should be added to the sidelobe level, to account for support mast blockage. This results in a first sidelobe level of -16 db. The theoretical monopulse performance of the feed was shown in Table 7.1-1. The effect of the tripod on parameters such as the difference slopes can only be assessed by measurement.

S-Band Feed -- The S-band feed is a two element dipole array. The expected efficiency of 43%, as indicated in Table 7.1-3, results in a gain of about 42.2 dbi. Since the aperture taper of the S-band feed is very similar to that of the X-band feed, the first sidelobe level can also be expected to be about -16 db.

800 MHz Feed -- The 800 MHz feed is a four element square array of turnstile elements. The expected efficiency of this feed is 32%. This results in a gain of about 32.7 dbi. As in the other cases its first side-lobe level will be about -16 db. Perfect circular polarization is not produced by the 800 MHz feed. As indicated in the table, the axial ratio of the polarization is expected to be about 1.0 db.

100 MHz Feed -- Because of its electrical size, the performance of the paraboloid at 100 MHz is difficult to assess. However, based on an efficiency of 22%, the gain should be about 13 dbi. Because of this very low gain, the first sidelobe level will be high, probably about -10 db. The axial ratio of the polarization is expected to be about 1.6 db.



Figure 7.1-16 Feed Support Mast

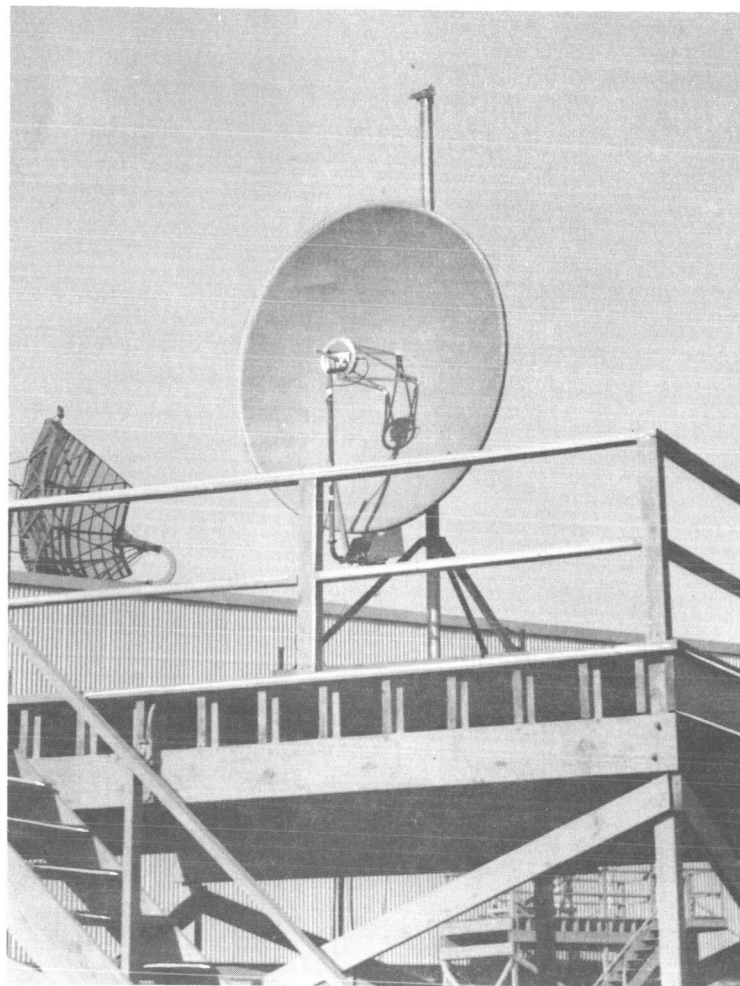


Figure 7.1-17 Parabolic Assembly

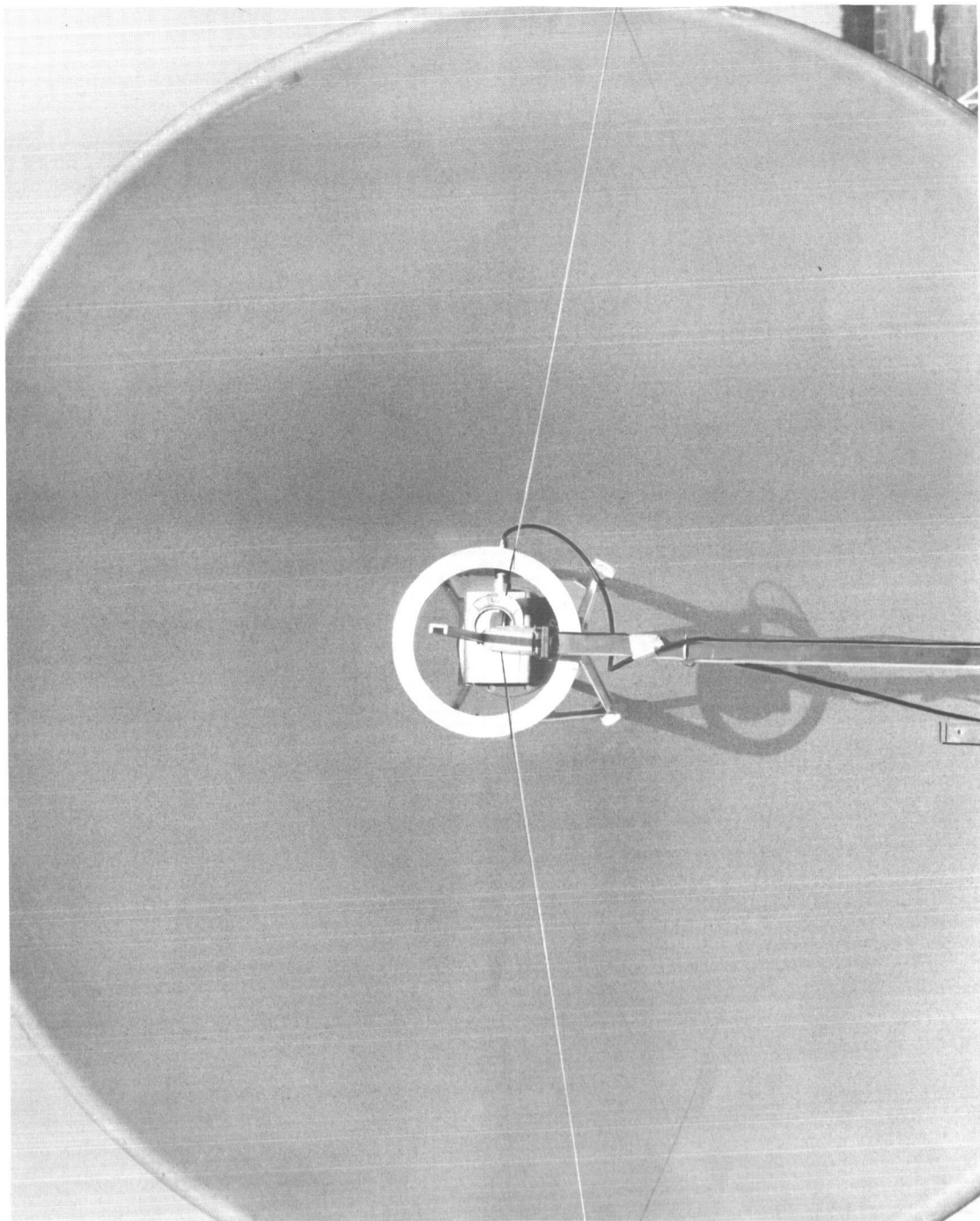


Figure 7.1-18 Back View of Feed Support

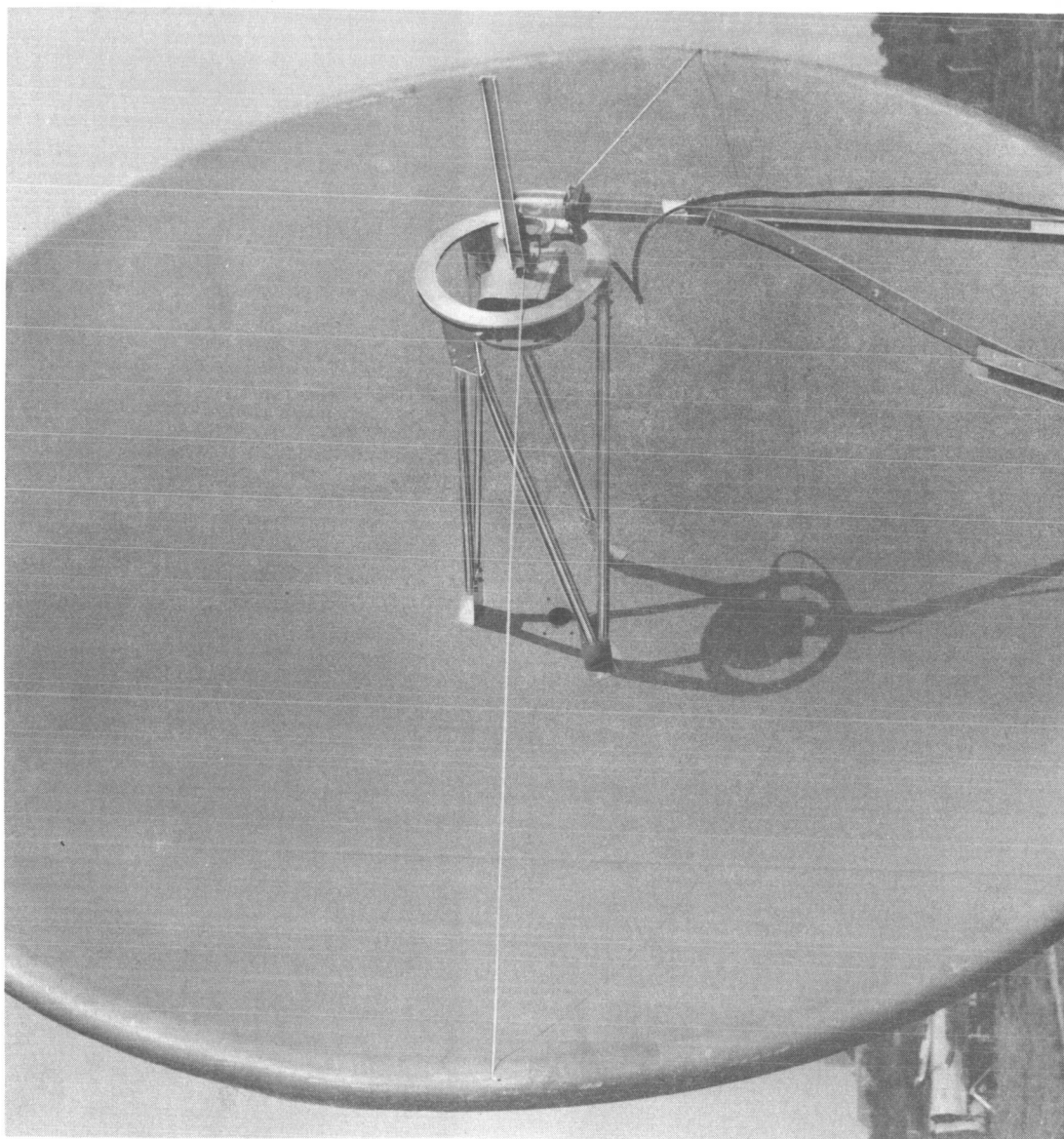


Figure 7.1-19 Left Side View of Feed and Feed Support

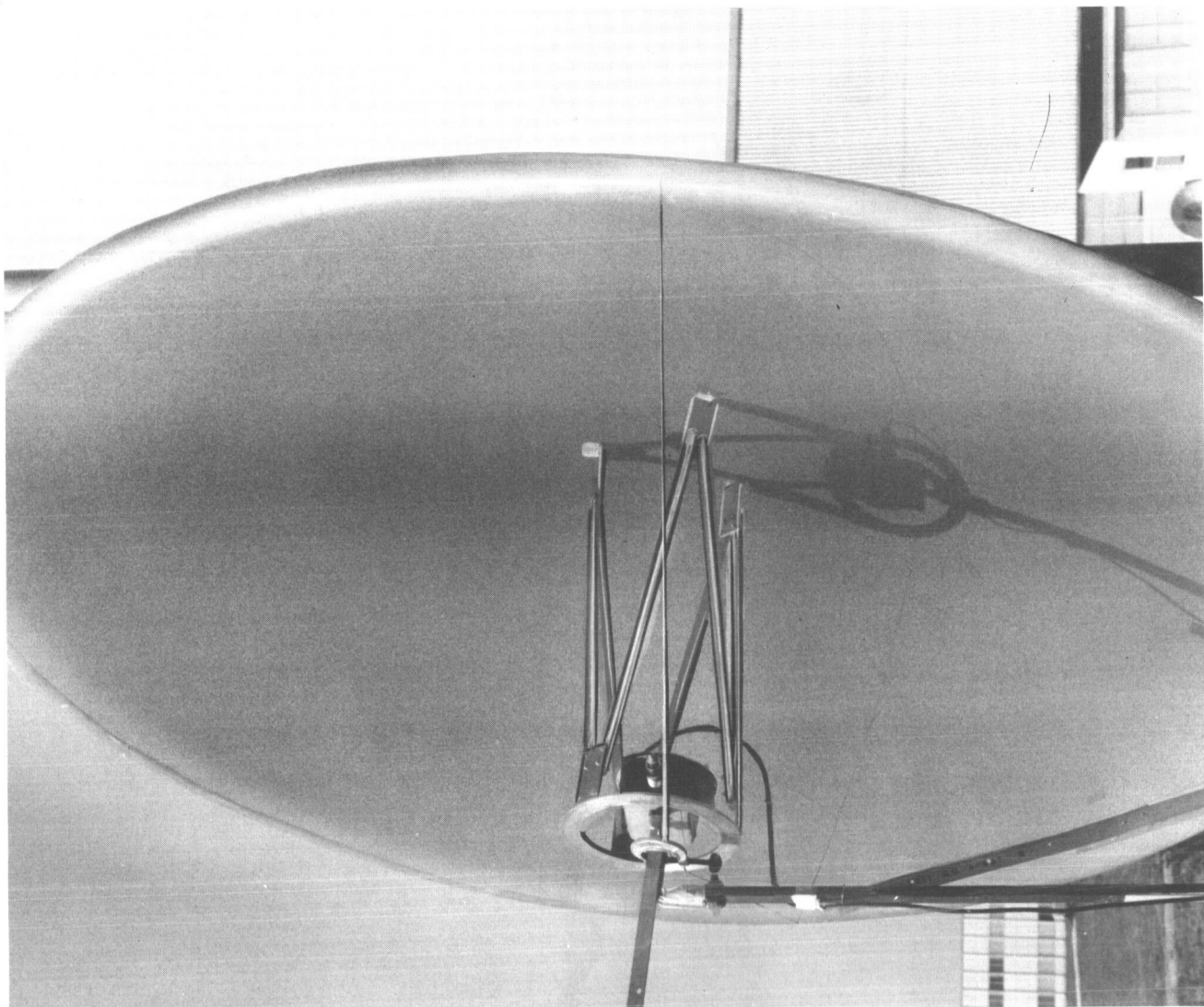


Figure 7.1-20 Right Side View of Feed and Feed Support

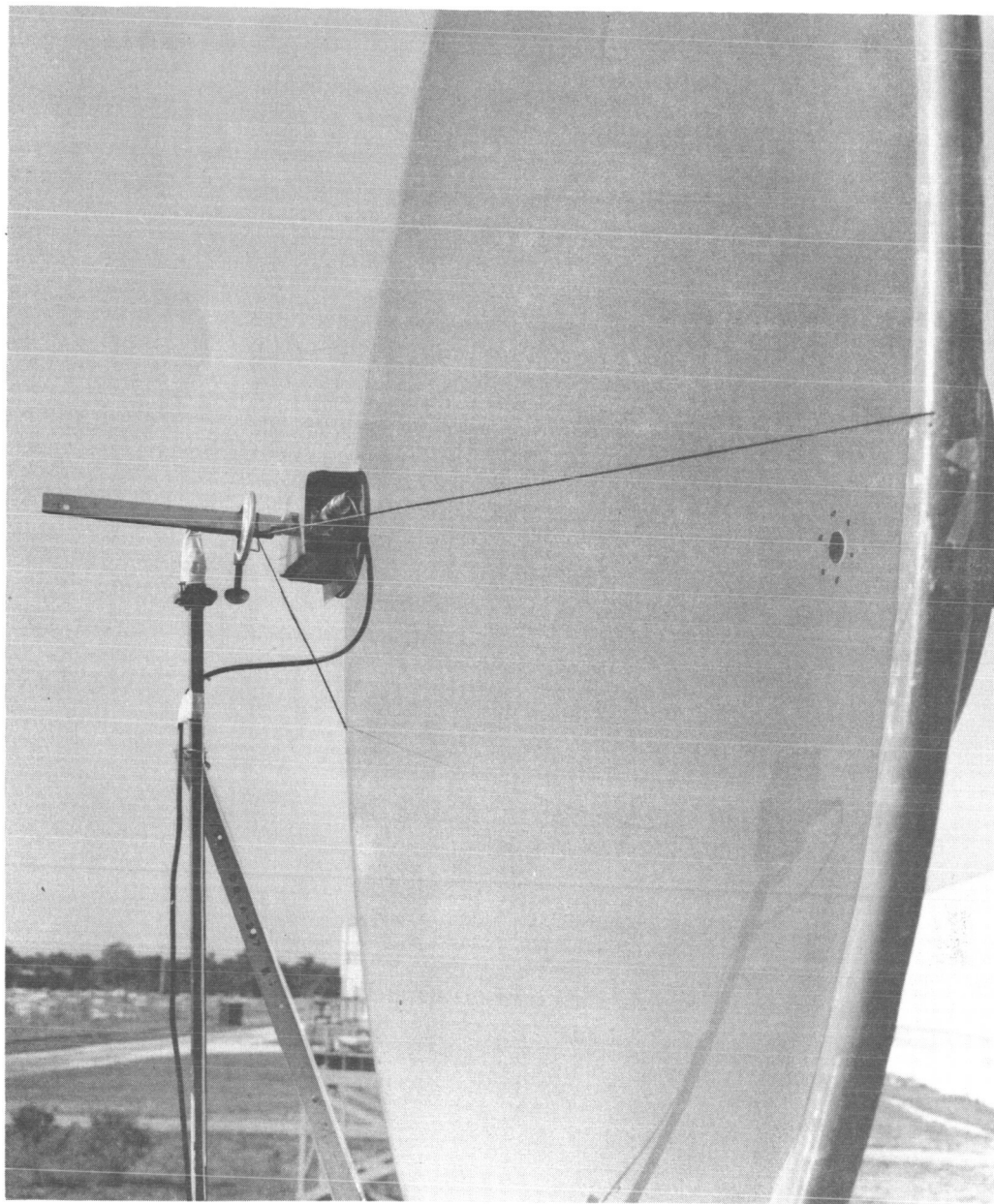


Figure 7.1-21 Right Side View of Feed

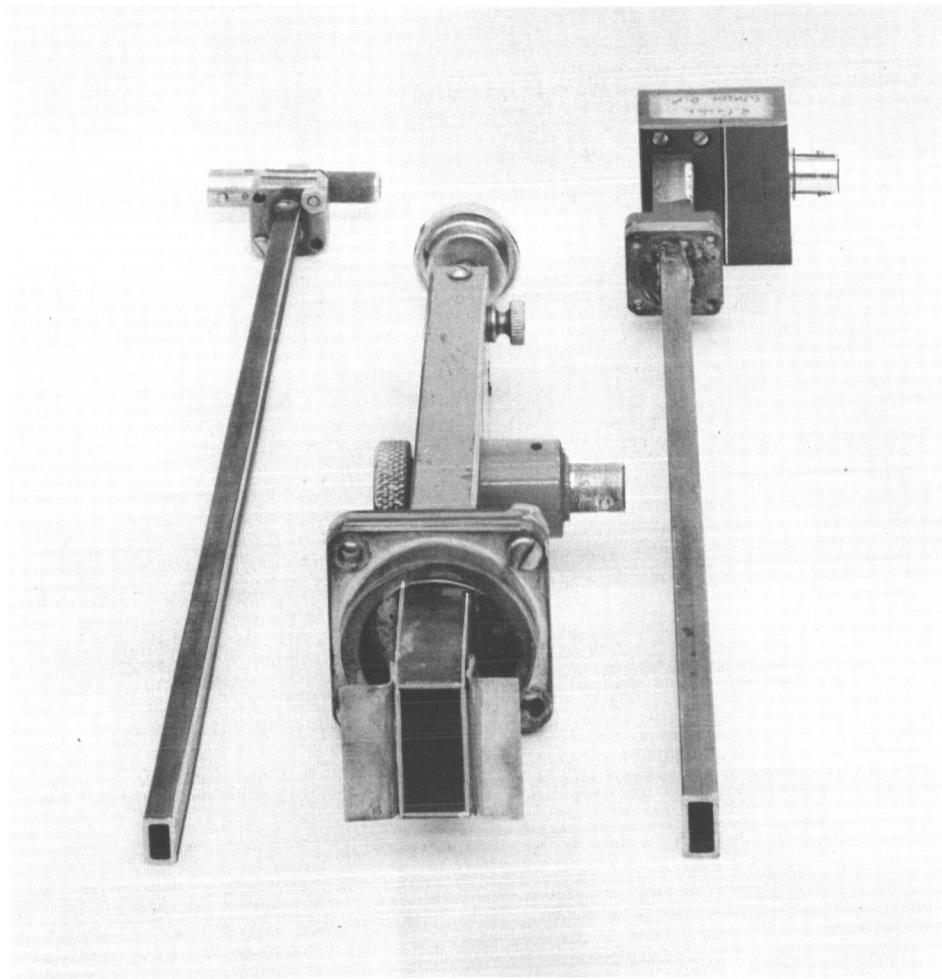


Figure 7.1-22 Feeds, End View

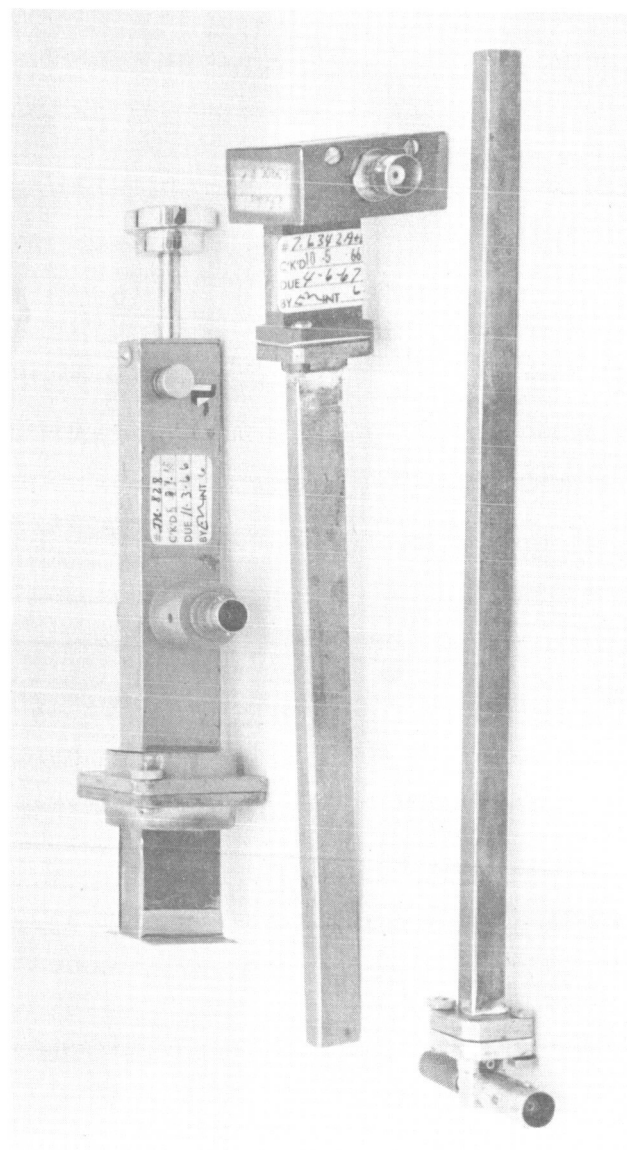


Figure 7.1-23 Feeds, Side View

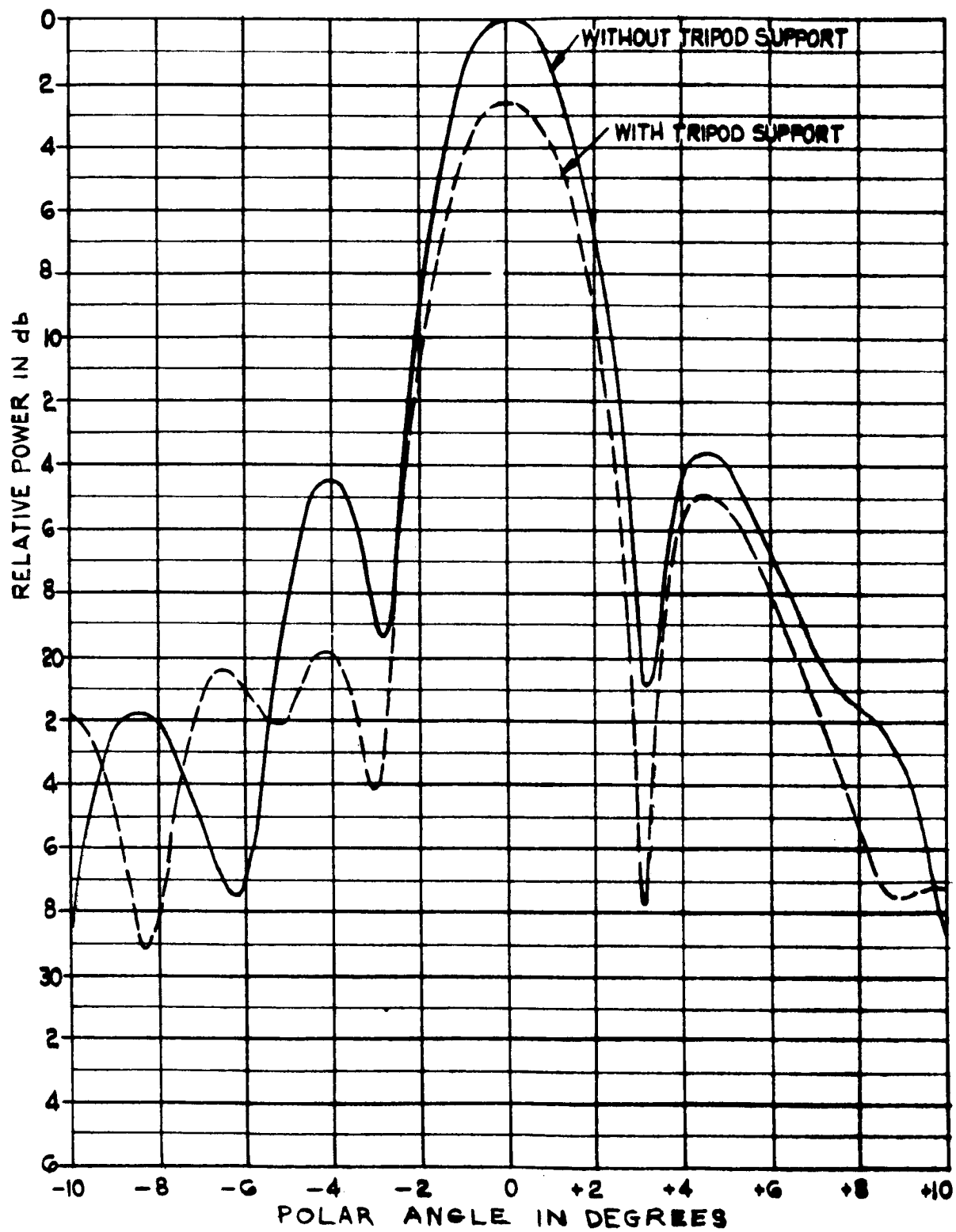


Figure 7.1-24 E-Plane Radiation Patterns Frequency

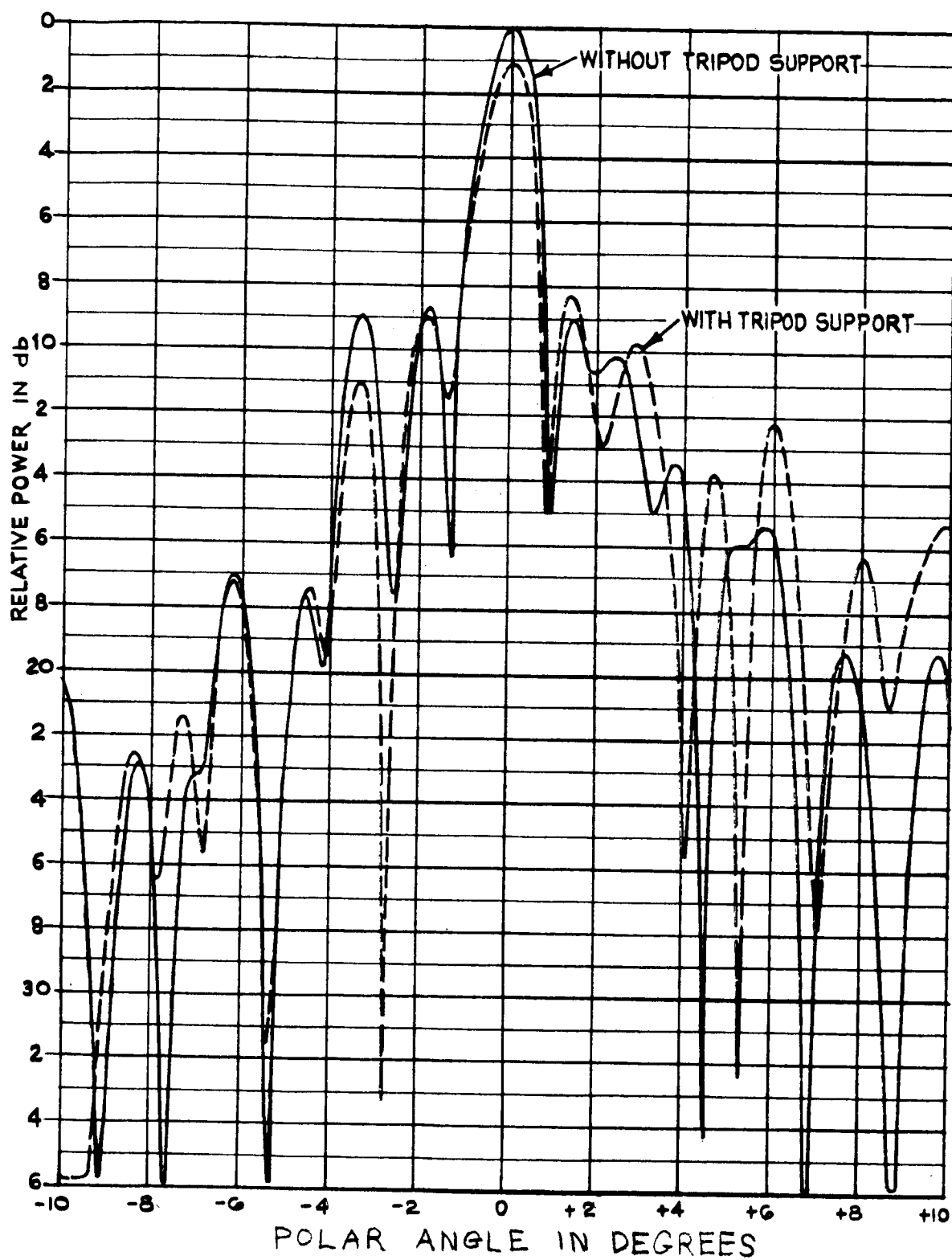


Figure 7.1-25 E-Plane Radiation Patterns Frequency

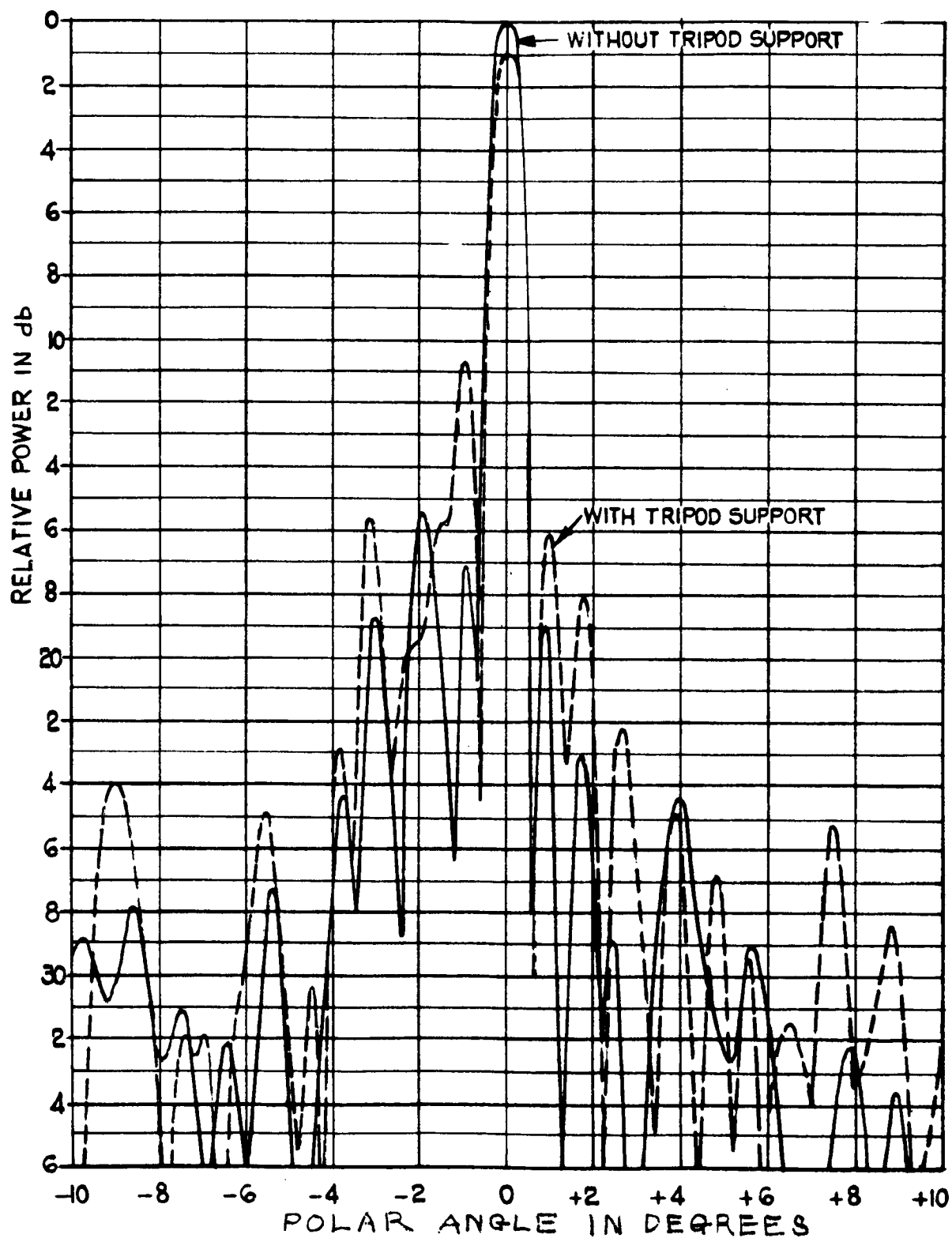
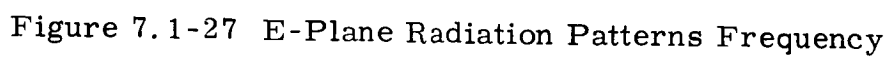


Figure 7.1-26 E-Plane Radiation Patterns Frequency



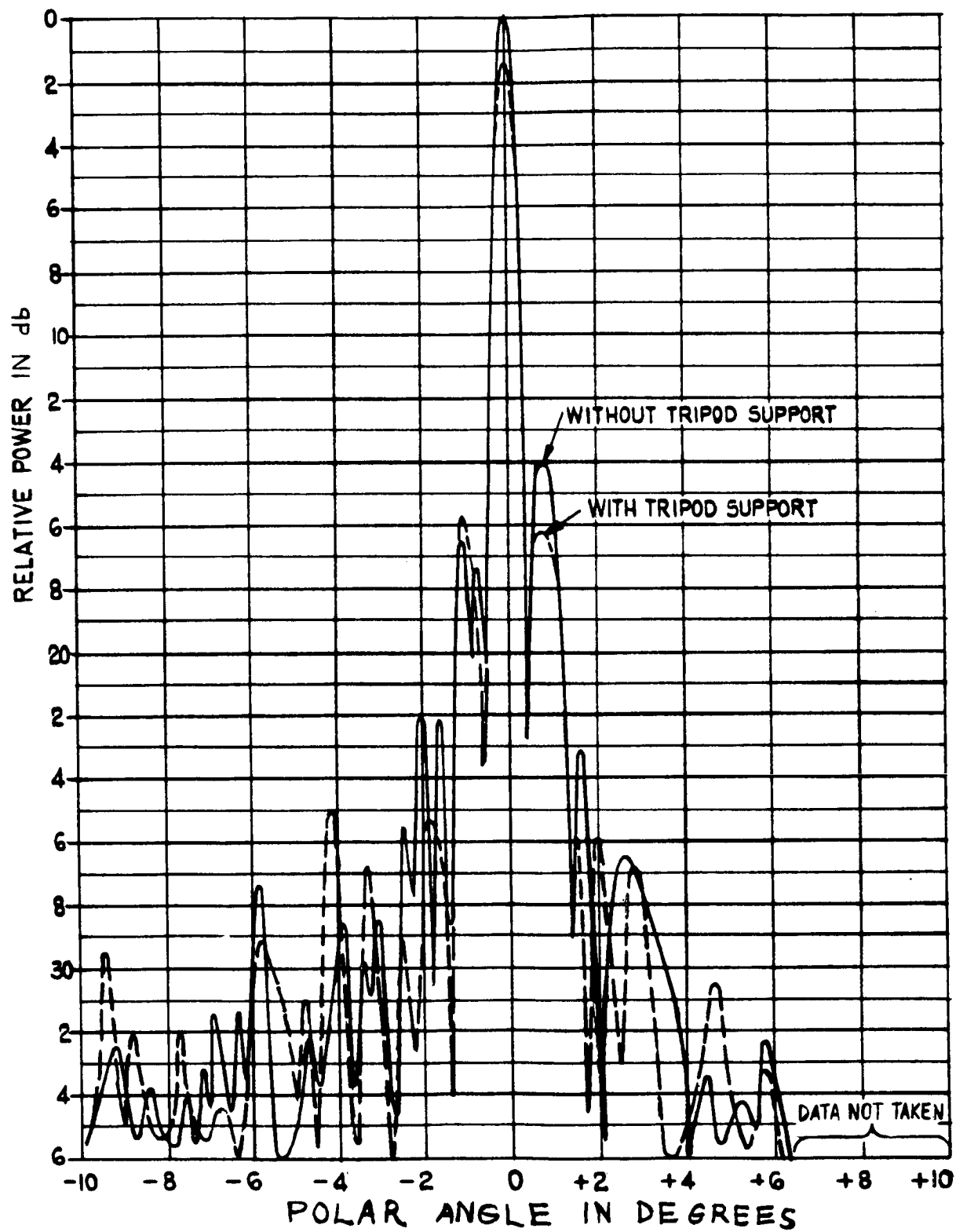


Figure 7.1-28 E-Plane Radiation Patterns Frequency

TABLE 7.1-3 PARABOLIC ANTENNA GAIN

Loss Contributor	X	S	800MHz	100 MHz	
Aperture Taper & Spillover	1.0 db	1.2 db	1.5 db	3.0 db*	
Spacecraft Blockage	.4	.4	.4	.4	
Support Mast Blockage	1.4	1.25	2.25	2.5*	
Systematic Reflector Distortion	.1	0	0	0	
Random Reflector Distortion	.4	.1	0	0	
Feed Lateral** Displacement	.5	.1	0	0	* Estimated
Feed Axial Displacement	.3	0	0	0	
Feed Phase Error	.3*	.3*	.4*	.4*	
Polarization	.05	.05	.05	.05	** Zero loss when monopulse system is in operation.
Dissipation	.1	.1	.1	.1	
Reflection	.2	.2	.2	.2	
TOTAL	4.75 4.25	3.70 db	4.9 db	6.65 db	
Efficiency	33% 38%	43%	32%	22%	

7.2 PHASED ARRAY

This portion of the report is a detailed examination of phased array systems for use in an operational three-axis stabilized communication satellite. These systems include the Transdirective array, the Butler Matrix array, the Space-fed lens array, and the Corporate-fed array. The study concludes that a modified Corporate-fed array is the prime choice by a substantial margin.

The four systems are compared in terms of the whole mission including the ground terminals, air terminals, and the spacecraft itself. This concept must be adhered to since various other systems could be an adequate choice under an incomplete and less demanding set of ground rules.

The following qualifications highlight the major areas of concern, which the mission requirements demand of the array system. The items are listed according to an approximate priority of importance and form the basis of the ground rules.

- High level of reliability.
- Simplicity of concept consistent with high performance.
- Minimum sensitivity to environment.
- Current (or near term) availability of proven hardware.
- Minimum power requirements.
- Flexibility of command, control and evaluation.
- Potential for expanding or improving functions and capability.
- Minimum reliance on ground terminal, air terminal, or other spacecraft to enhance, aid or support its capability.
- Minimum weight and cost.

The Corporate-fed array is found to rate highest in virtually all of the above categories.

7.2.1 The Transdirective Array

The transdirective array is distinct from the other three array configurations in that it is a self-phasing or self-steering system and requires no computer to control the steering angle of either the transmit or receive beams. The steering system can be a closed loop circuit which is an integral part of the relay as shown in Figure 7.2.1. The beam pointing is commanded by a low level CW pilot signal which must be transmitted from a ground or air terminal. The pilot signal illuminates the antenna and each element of the array senses a differential phase shift which automatically programs the receive or transmit phasors (mixers) to collimate a beam in the direction of the pilot signal. Both the transmit and receive beams function in a similar manner. In principle, the system automatically does its own computations using the pilot signal for attitude information. The technique has an advantage in applications where an unstabilized satellite is continuously changing attitude and accurate attitude information is not available. Even in this situation the attitude variation must be less than the scan angle capability of the antenna.

One of the requirements of this satellite mission is for attitude accuracy information in the order of $\pm 0.1^\circ$. This accuracy is needed primarily for use in directing the very narrow beams generated by the parabolic dish antenna. Since the array beam will be about 2.2° , this magnitude of error (0.1°) will have an insignificant effect on the computer generated beam pointing accuracy of more conventional array techniques, and essentially negates the major advantage of the self phasing quality. The requirement of a CW pilot signal to control the transmit and receive beams seriously limits the flexibility of this technique for a ground-to-satellite or air-to-satellite communication link since the system cannot be preprogrammed or commanded to point in an arbitrary direction. It must be limited to use on a prearranged scheduled basis.

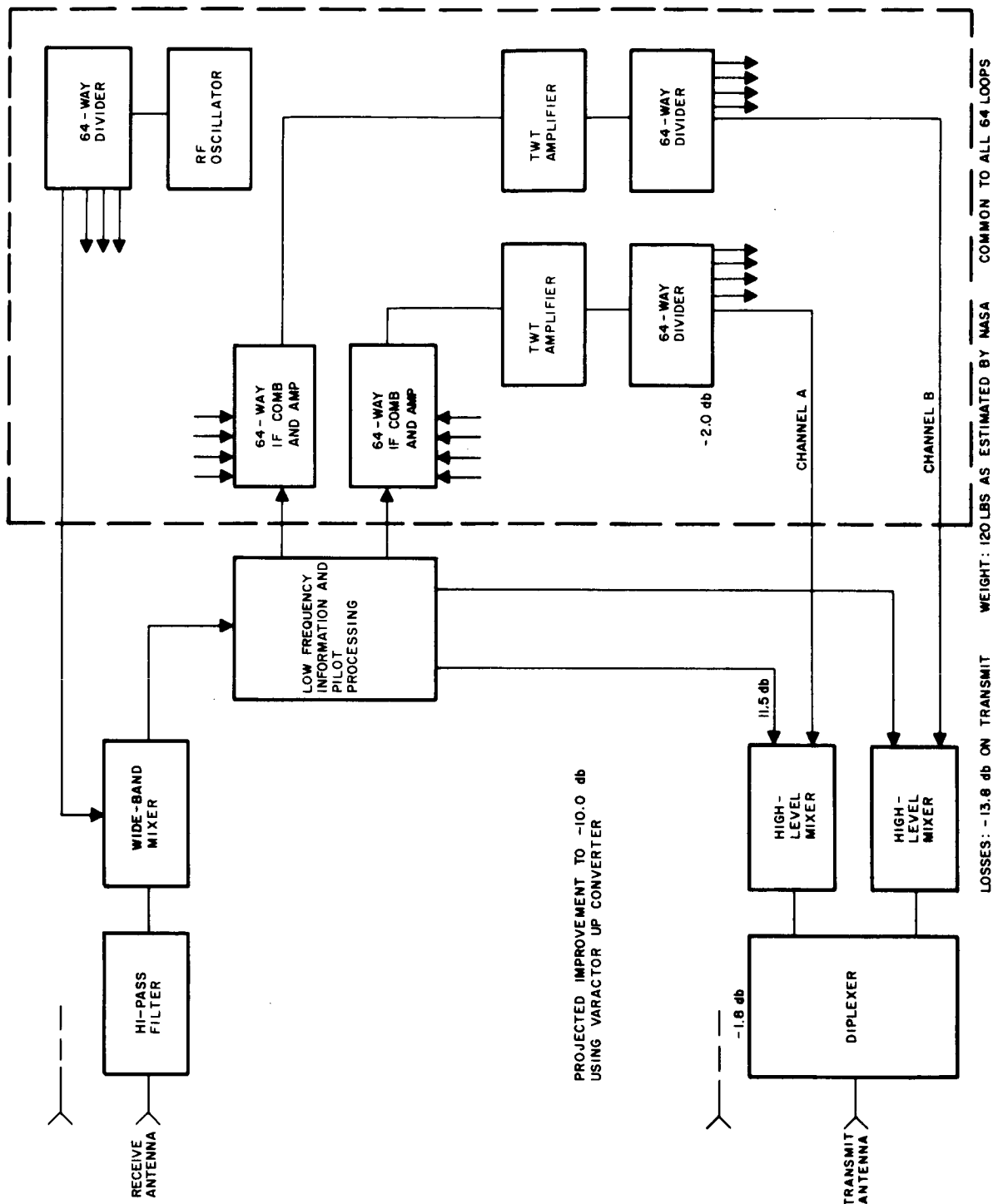


Figure 7.2-1 Transdirective Array Block Diagram

The pilot signals have the advantage that they provide a redundant system for attitude determination. Another advantage rests in the fact that the system is comparatively light weight and compact since a high level of low frequency component integration is possible. Also, the beam is continuously steerable and is not subject to crossover losses as is, for example, the Butler array.

The system is highly inefficient in terms of power output due primarily to the conversion loss of the high level output mixers. Contributing to this system's loss is its inability to make use of rectangular waveguide transmission lines and components. This limitation is imposed by the multiple frequency conversions which take place between the received and final transmitted signal. Thus for this application the heavy RF filtering must be accomplished with the use of lossy coaxial or strip transmission line.

The overall reliability of the transdirective phased array rates lowest of all systems for the following reasons.

- The system is active. The steering mechanism makes use of four to five stages of frequency conversion and amplification. Although the high reliability of low frequency solid state circuitry is well established, this reliability is undermined by the system's dependence on a large number of RF mixer diodes. Each loop, from receiving element to radiating element, is sequentially dependent upon four to five balanced mixers, each of which contains a pair of matched diodes. A deterioration or failure of any one diode in any mixer could knock out the complete loop or result in a sharp reduction in ERP from that radiating element. What is more likely is what results from diode deterioration, viz, a loss of phase tracking which, in some instances, would be worse than a total loss of the radiating element. This comes about since all loops must be

phase balanced on boresight. A 180° tracking error in one radiator would scatter the power radiated or received by essentially two of the elements. There is no way to correct this situation from the ground.

- High premium diodes must be used in balanced mixer circuits to achieve optimum phase tracking between the 64 loops. These diodes will deteriorate with time, especially those diodes used in the high level output mixers where large signal and LO power levels will rapidly deteriorate diode junctions. The use of varactor diodes will improve the reliability of the frequency converters because of their higher power handling capability. Since little work has been done in this area a quantitative evaluation of their phase tracking ability with wide excursions in temperature and RF drive power cannot be made. It would be expected though, with the wide RF bandwidths required for this system (350 MHz, at X-band, which includes both transmit channels plus a guard band), the minimum requirement of $\pm 4^{\circ}$ stability between mixers will not be achievable for some time to come.
- The phase-tracking qualities of I. F. amplifiers also deteriorate as the circuits are subjected to hostile environments. Also, these circuits must inherently operate at low efficiencies of 10-20% in order to achieve phase and amplitude stability. For the present application where hundreds of amplifiers are required, the DC power supply demands would be large.

The transdirective array technique is considered to be the most complex and least reliable of the systems studied under this program. An accurate reliability analysis is beyond the scope of this program, but a qualitative analysis indicates that the MTBF of major subsystems would be down sharply compared to the other systems examined.

Another major disadvantage to this approach for electronic scanning is the need for two antennas, since the transmit and receive frequencies are different. Each antenna requires a different element spacing which is critical for the phase-sensing mechanism that steers the beams. The use of a single antenna would require a small computer and phasors in each line to correct for the frequency differences, thus detracting from the self steering qualities of this system. A common antenna would also complicate the filtering problems (at the expense of further loss and weight) due to the spurious effects which might occur in the frequency converter stages.

In addition, the transdirective antenna system is not easily adaptable to a commanded tracking mode of operation.

7.2.2 The Butler Matrix Array

The Butler Matrix array is similar to the space-fed and Corporate-fed array in many respects. Each of the three systems uses a single antenna. Also, each makes use of two transmit and two receive channels. The four beams are controlled by a beam steering unit which derives its commands from a coded pulse, transmitted to the satellite by a single ground or air terminal. Of these three systems the Butler array is considered least desirable for the following reasons:

- Beam steering occurs in discrete steps with adjacent beam positions being orthogonal. This results in a 7.8 db loss at the diagonal crossover points within the cone of coverage. Although the desirability of communication in these directions is statistically low, a need to do so could result in a serious loss of signal strength.
- The system is somewhat complex and tends to be large in size. It is the heaviest of all the systems examined, having an estimated weight of 190 lbs. Figure 7.2 -2 shows a simplified configuration for this system. Sixteen 8 x 8 Butler

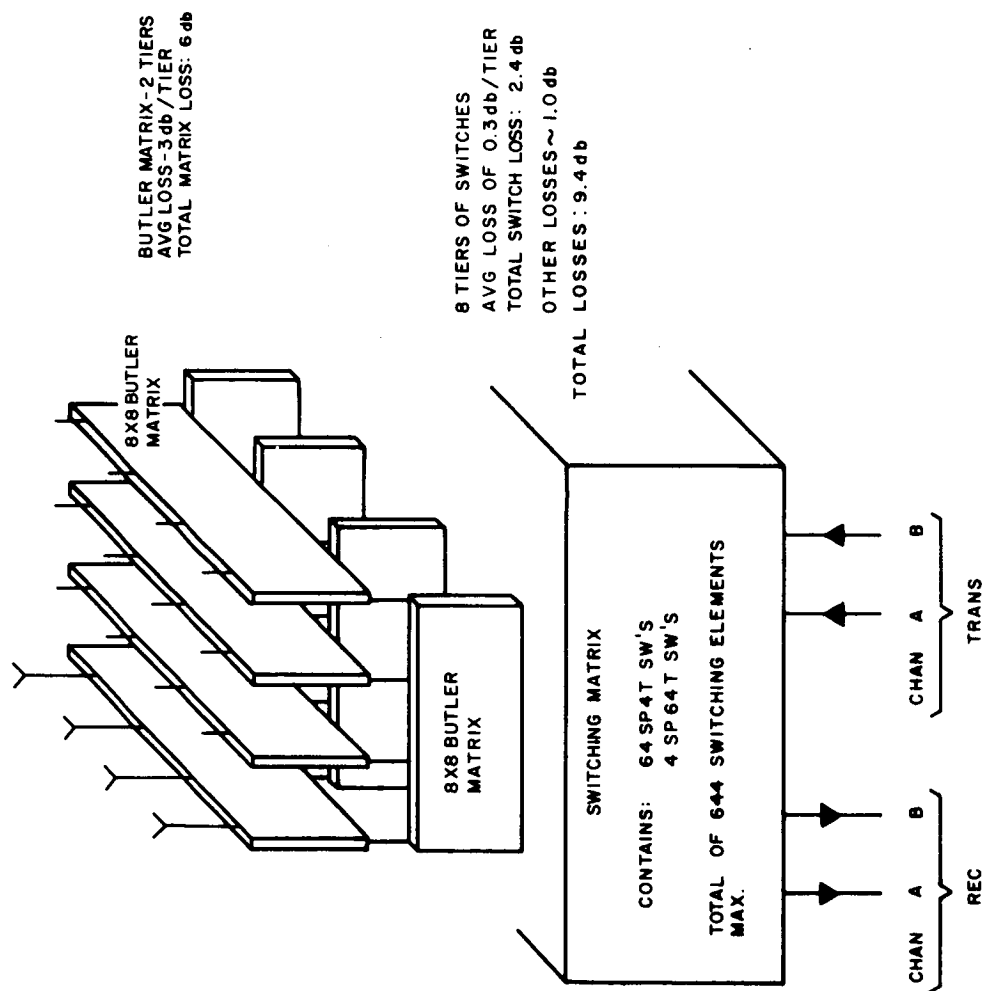


Figure 7.2-2 Butler Matrix Block Diagram

Matrix circuits would be required. In order to package this within reasonable confines, waveguide would have to be abandoned in favor of some multiple layer strip transmission line configuration. This would result in excessive losses at X-band frequencies as indicated in the diagram (approximately -10 db). Although this technique is substantially less lossy than the transdirective array, the large number of ferrite switches (switchable ferrite circulators being more desirable than diodes) make it a few db more lossy than the remaining two systems considered.

- Another disadvantage of the Butler Matrix array is that it requires an element placement which limits flexibility in the design of the antenna.

7.2.3 Space-Fed (Lens) Array

Compared to the transdirective and Butler arrays, the space-fed and Corporate-fed arrays are simpler, have substantially lower system losses, and far fewer components which are subject to failure or malfunction. A comparison between the Corporate-fed and the space-fed arrays requires a careful examination. These systems are quite similar, differing primarily in the way the elements are illuminated (space illumination of lens, direct corporate feeding of elements). They differ also in the way the channel frequencies are separated and the relative flexibility encountered in packaging the components.

The space-fed array suffers a disadvantage in comparison with the Corporate-fed system in terms of size. Although a space illuminated lens appears to have an advantage in not requiring a distribution network, this comes at the expense of requiring three different points of channel separation in the loop. These occur at the input and output to the lens, and at the feed illuminating the lens. This necessarily increases the

severity of the frequency separation problems, at the cost of additional weight and loss. The optical parameters of the lens configuration also impose a minimum depth to the package which, depending upon the choice of radiating elements, could be upwards of 30". Figure 7.2-3 illustrates a configuration which was examined for this application. The 64 elements on the outside of the lens are circularly polarized radiators, such as high gain helical-fed horns. The transmit and receive channels are separated by a circulator providing approximately 20 db of isolation. Each channel is then separated into essentially contiguous bands by a diplexer. The type of diplexer to be used would be a set of singly terminated band pass filters matched to a single input port. Only 20 db of separation is required at this point to prevent phase interference between the two receive or transmit channels. Most of the leakage between the receive channels will be defocused after passing through the phasors. The bulk of the receive channel separation will occur in low-loss waveguide filters after the signals have been combined in the main feed.

As shown in the figure, the horn side of the lens is terminated in separate sets of radiators (dipoles) for the transmit and receive channels. Each set is focused on a separate horn, one for transmitting and one for receiving. The dipoles are cross polarized to one another. The separate fixed focusing is easily achieved by adjusting the lengths of line accordingly in each channel. The separate focal points at the cross polarized horns will provide upwards of 30 db of isolation between transmit and receive channels. The additional 70-80 db of isolation necessary at the front end of the receiver is readily achieved by the proper design of the waveguide filters used to separate the receive bands.

The lens configuration becomes more attractive as additional communication channels are required. Since most of the receiver band separation will be achieved using low loss waveguide filters at the output of the main receive horns, the separation within the lens need only be large

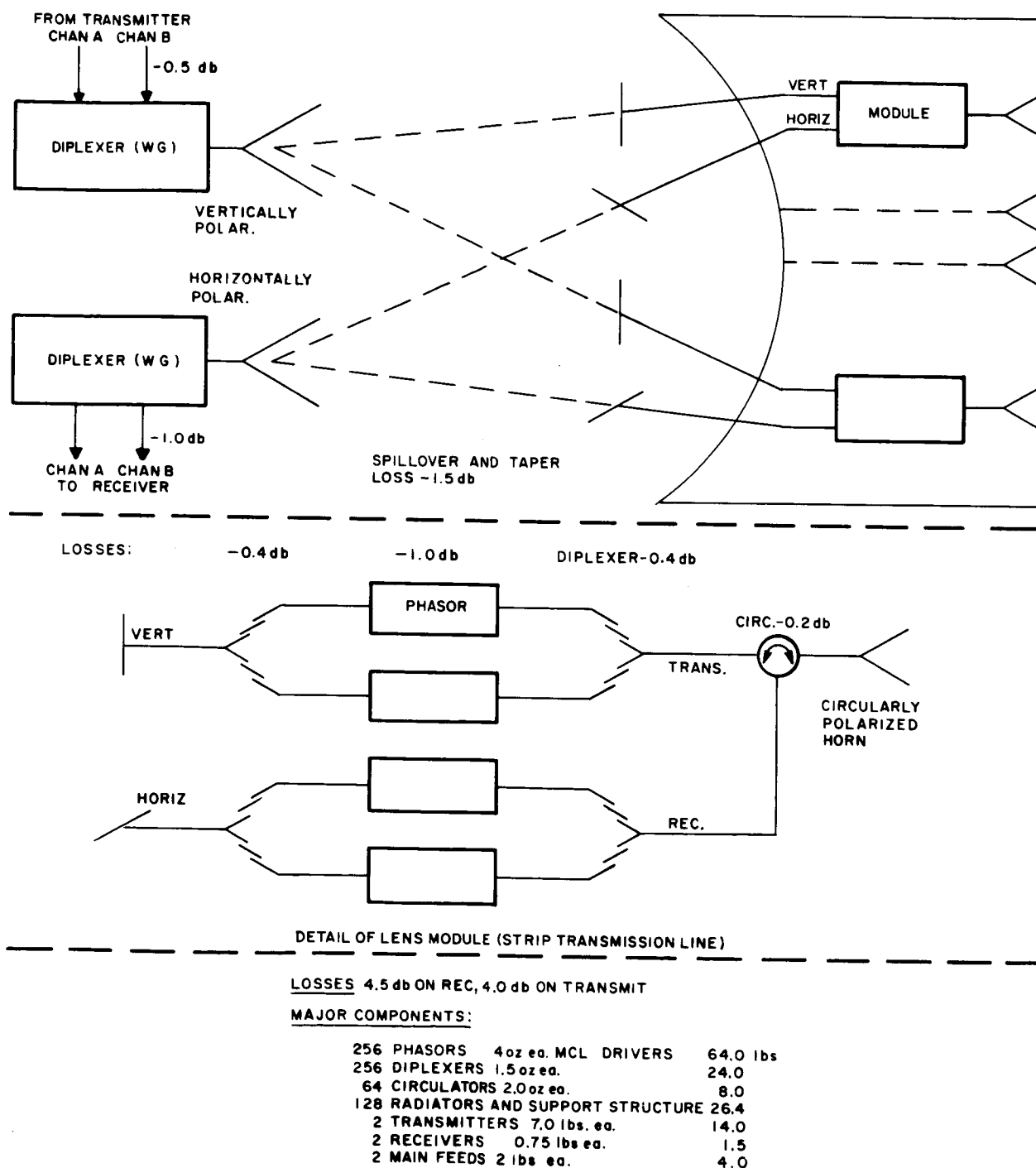


Figure 7.2-3 Space-Fed (Lens) Array Block Diagram

enough to prevent phase interference (20 db). This allows the use of small, lightweight, low loss (two section) stripline filters in the diplexer design of the type shown in Figure 7.2-4. Estimated losses are as low as 1/2 db. The only limitations are the number of phasors that could be packaged within the lens. Figure 7.2-5 is a drawing of a 4 bit stripline ferrite phase shifter for this application. It has approximately 1 db of loss. Each of these units could be readily packaged in a 3" x 3" cross sectional area which is approximately the effective radiating area of the high gain element anticipated for use in this system. This would provide an eight channel simultaneous 2-way system (8 beams) with approximately a 40% increase in weight, a negligible increase in size, and approximately a 1.0 db increase in system loss. A monopulse tracking capability may be incorporated in this system with relative ease.

Some disadvantages of this system are listed below:

- Assuming the desirability of a uniform illumination, the natural taper of the main feed horn would require additional elements to be used to achieve the same gain as the other three systems considered. There is an inefficient use of element gain due to an approximate 10 db edge taper.
- The system is subject to defocusing and disturbance of the beam shape because of feed displacement which may possibly occur during the strain and shock of launch or perhaps due to structural exposure to the wide temperature excursions which occur in the space environment. The nature of the separately focused main feed horns makes them particularly sensitive to mechanical disturbances.
- The body of the lens would house all four sets of phase shifters. Since the lens is somewhat remote from the remainder of the equipment (being located approximately 18-24 inches in front

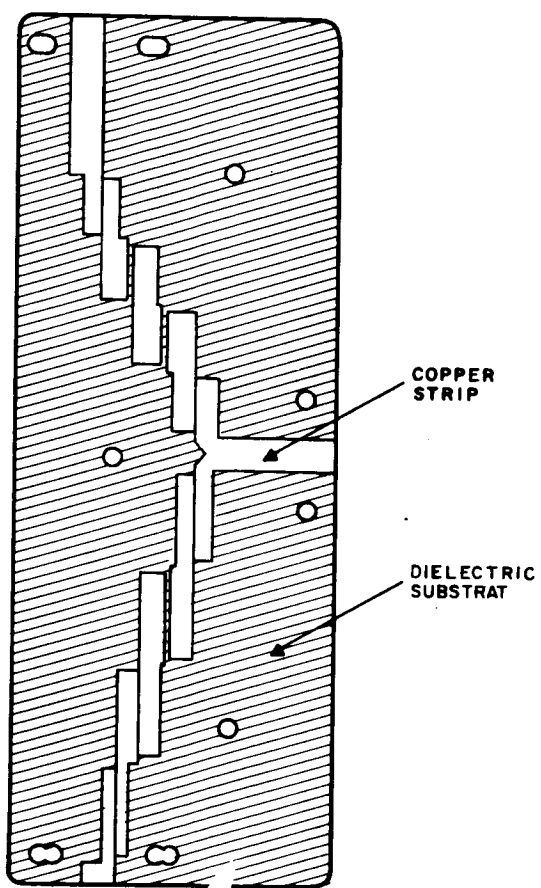
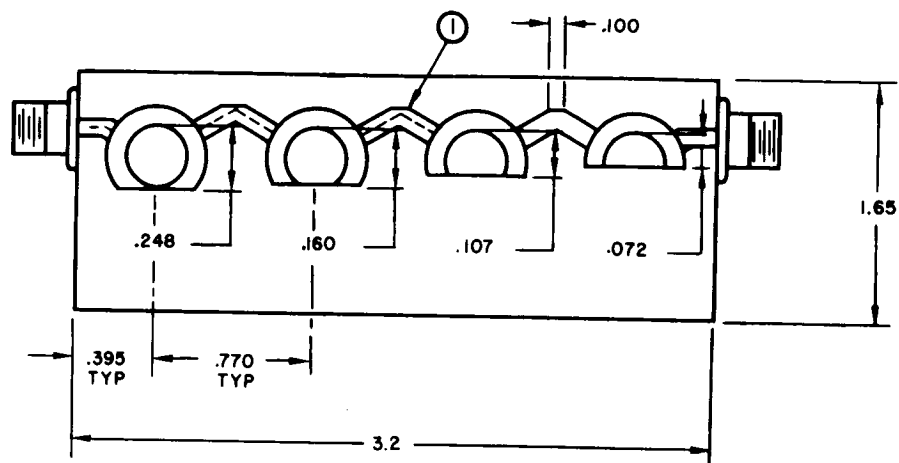
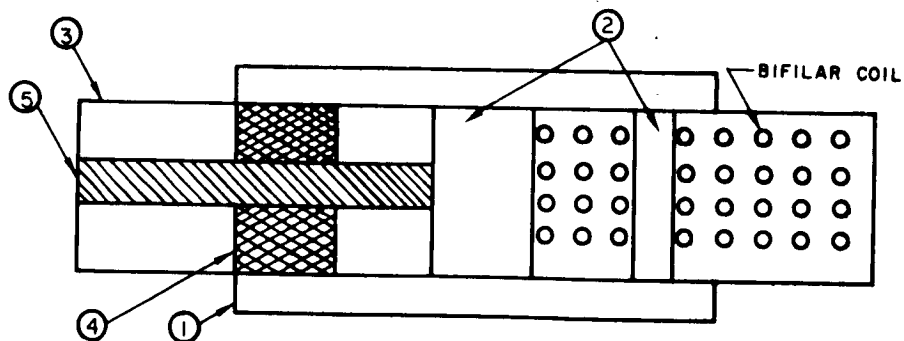


Figure 7.2-4 Strip Line Diplexer



① MITERED BEND

FOUR-BIT PHASE SHIFTER



- 1. FERRITE RETURN PATH
- 2. FERRITE RETURN PATH
- 3. DIELECTRIC, QUARTER-WAVE MATCHING
- 4. FERRITE MICROWAVE
- 5. CENTER CONDUCTOR

CROSS SECTION OF MAGNETIC CIRCUIT

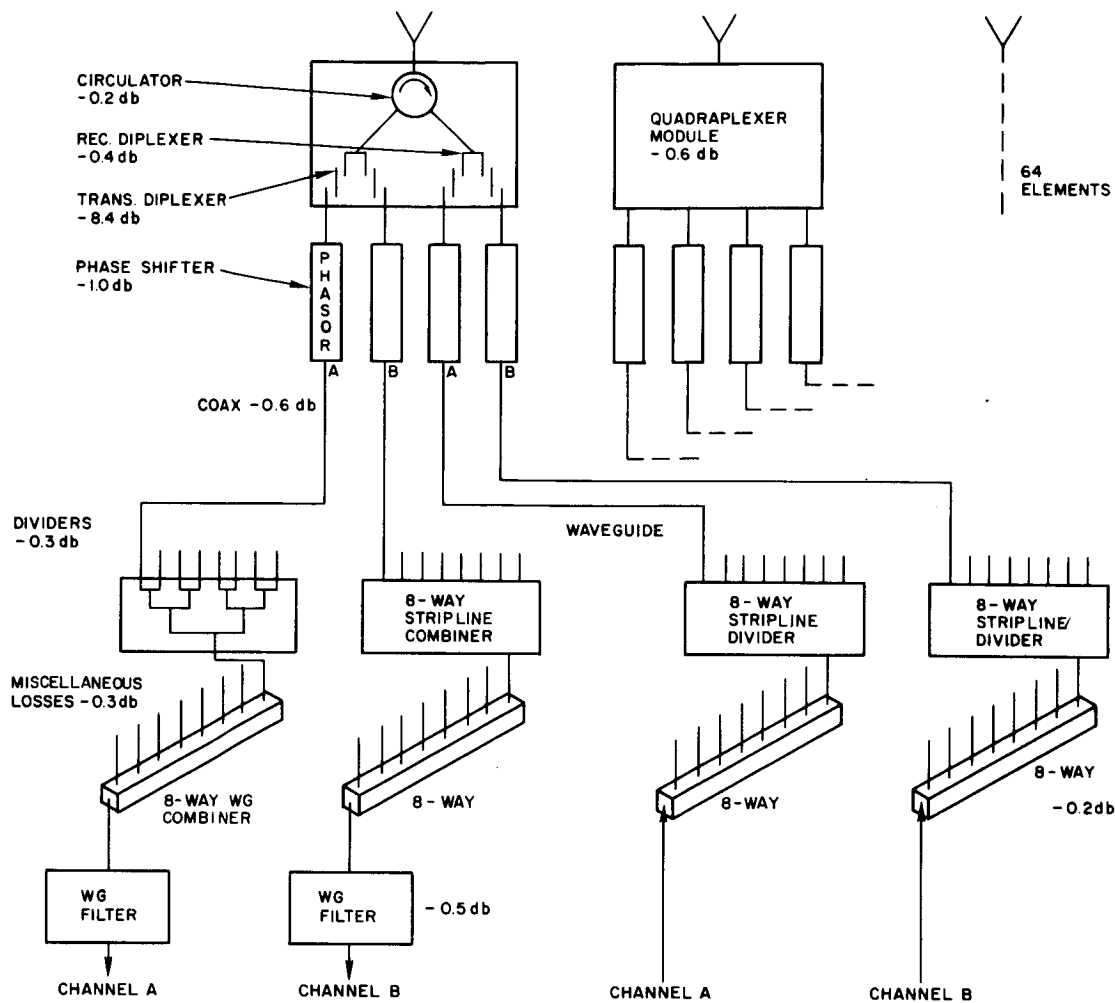
Figure 7.2-5 Strip Line Latching Phase Shifter

of the main feed horns, beam steering units, and heat dissipating equipment), two problems arise. First, operation of the phase shifter drivers becomes complex because of long control wires, and second, temperature control of the phase shifters environment requires additional equipment and power.

7.2.4 Corporate-Fed Array

This array technique provides almost all of the advantages of the other three systems studied and few of the disadvantages. A schematic diagram of the system is shown in Figure 7.2-6.

The fundamental reason for this is that the microwave system is the least complex in concept, requiring the fewest number of component parts without sacrifice in performance. With the exception of the phasor drivers, the two transmitters, two receivers, and simplified beam steering unit (all computations being done on the ground for maximum flexibility) the system is passive. The transdirective array which uses 64 receivers is essentially a completely active system. The latching ferrite phase shifters which are used in the Corporate-fed array are considered passive devices since they are virtually indestructible. The R.F. performance of the ferrite deteriorates when the material is driven beyond the Curie temperature (typical value is 350°C), but it is completely retrievable when the device is brought back to its normal working ambient temperature. The packaging configurations of the Corporate-array as compared to its closest competitor, the space-fed lens array, allows the system to take advantage of heat dissipated by other electronic equipment within its superinsulated environment. The temperature as calculated in sections of this study dealing with thermal characteristics of the spacecraft, predict a 40°F excursion within the superinsulated environment containing the microwave circuit and ferrite phasors. This range, $+50^{\circ}\text{F}$ to $+90^{\circ}\text{F}$, can be held while maintaining a temperature gradient within a few degrees without the use of additional DC power. Sharp temperature transients will have no



LOSSES:

3.0 db ON REC AND 2.5 db ON TRANS.

MAJOR COMPONENTS:

256 PHASERS 2.5 oz EACH, 768 DRIVERS 0.5 oz	640 lbs.
36 8-WAY DIVIDERS AND COMBINERS 14.0 oz ea	31.5
64 CIRCULATOR-DIPLEXER PACKAGES 5.0 oz ea	200
64 HORNS AND SUPPORT STRUCTURE	13.2
2 TRANSMITTERS 7.0 lbs. ea	14.0
2 RECEIVERS 0.75 lbs ea	1.5
BEAM STEERING UNIT	15.0
MISCELLANEOUS	7.0
	<hr/> 166.2 lbs.

Figure 7.2-6 Corporate-Fed Array

permanent effect since the ferrites can be magnetically reset by command when the temperatures return to normal. Fortunately, the minimum temperature sensitivity of many ferrites designed for use at X-band frequencies exists at $72^{\circ}\text{F} \pm 20^{\circ}\text{F}$ which makes the compensation problem even less severe by providing a bit phase tolerance of $\pm 2-3\%$. Additionally, redundant temperature compensation may be provided giving even better control by properly designing the ferrite driving circuits, making use of demonstrated techniques such as the constant flux generator driver.

Another major advantage of the Corporate-fed array's configuration is the wide margin of flexibility allowed in the design and selection of the transmission line and components. At X-band frequencies there is about a 4:1 ratio in loss between coax or stripline and waveguide. Stripline has about a 3:1 advantage in volume over waveguide, whereas a properly designed waveguide package can have a 10-20% advantage in weight over the same circuits build in strip transmission line. This weight advantage depends very much on the type of circuits being built. For example, an 8 x 8 Butler Matrix is considerably larger and heavier in waveguide than in coaxial or strip transmission line, which is why waveguide could not be considered for the Butler array. Furthermore, the nature of the circuit makes treatment of the input and output ports unwieldy in waveguide. As a result stripline was considered for this system and the RF losses became quite high. In the case of the Corporate-fed array where binary power dividers and series fed couplers are used, the less complex nature of the circuits is such that the differences between waveguide and coax or stripline are not nearly so dramatic. Moreover, the input and output ports are a great deal easier to handle. The size of the aperture required for the antenna (32" x 36") has the input ports to the 64 radiating elements uniformly distributed over a wide area. Covering this broad area with lossy coaxial lines from a compactly designed stripline corporate network would have resulted in losses comparable to the Butler array. Also the weight of these flexible cables,

connectors, and associated support straps begins to approach the 2.6 oz per foot of standard aluminum waveguide. It thus becomes apparent that a judicious combination of waveguide and stripline will result in the best overall design. The Corporate-fed array is the only system considered which allows the use of waveguide in this manner. A number of such trade-off configurations were examined during this study program. The resulting configuration shown in Figure 7.2-7 represents a minimum loss system, about 50% larger in volume than an all stripline or coaxial system and comparable in weight. As seen in this illustration the light-weight, self-supporting, low-loss, aluminum waveguide (the use of magnesium or metal-plated plastic will be considered) is used to both split the power into the various channels and carry it the long distances to the different points on the surface of the antenna. All of the heavy RF filtering is done in waveguide which accounts for lower losses over comparable stripline or coaxial circuits. The latching ferrite phase shifter is designed in waveguide as shown. The waveguide phasor, although comparable in size to the equivalent stripline devices, is about 30% lighter and 20% less lossy. The duplexing-duplexing function is done in stripline circuitry. This provides the flexibility needed in the interface between the radiating elements and the remaining circuitry. Although there is a 0.2 db increase in the loss for the stripline filters and circulators, there is about a 200% saving in weight and volume.

The weight of the Corporate-fed array including the antenna, transmitter, receivers, and BSU is conservatively estimated to be less than 170 lbs. A reasonable design goal would be 150 lbs. This is 25% greater than the 120 lbs. estimated for the transdirective array.⁽¹⁾ Even with this additional weight the result is approximately 10 db more ERP per pound for the system. The total ERP for the Corporate-fed array is 22,000 watts. The half power beam width is 2.2° . The transdirective array generates a

(1) See Sec. 1.3.7

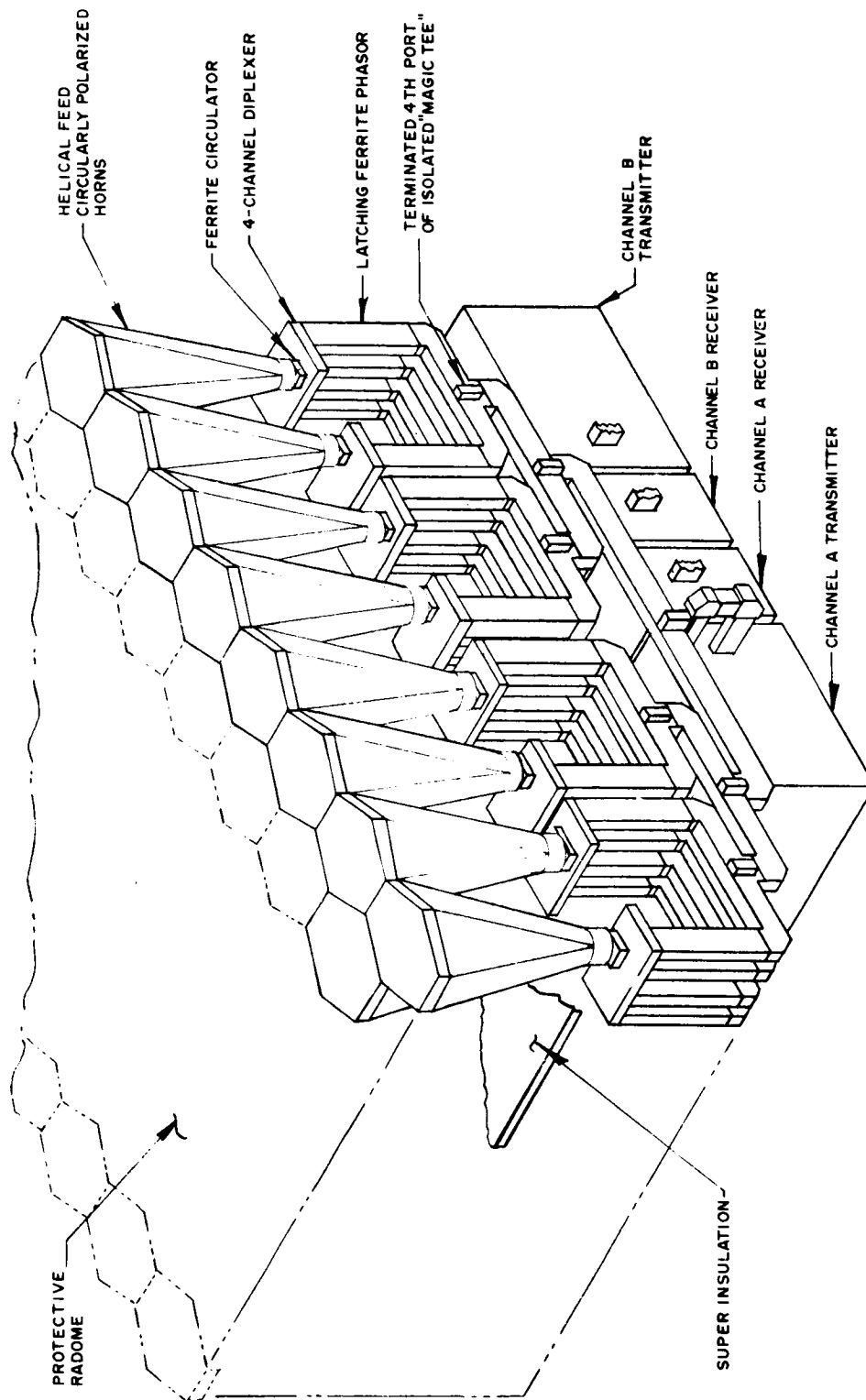


Figure 7.2-7 Artist Conception of Corporate-Fed Array

total ERP of 1700 watts with the same HPBW; both systems use a 10 watt transmitter. The difference is due to the additional 10 db loss in the transdirective's transmit channel. As shown in Section 2.5.2 on the figures of merit, these numbers include a realistic projected improvement for the transdirective system. These numbers are quite significant in view of the fact that availability of DC power aboard the satellite limits its down-link capability.

The Corporate-fed array is adaptable to a beam steering technique which uses a minimum amount of electronics aboard the space craft, yet provides a high degree of versatility in the array's modes of operation. The technique being recommended allows the computations to be performed at a single ground terminal with a maximum command data rate of 35 bits per second to direct all the array's modes of operation. The details of the beam steering unit are discussed in a later section. It will suffice here to point out one of its key advantages. The system may be programmed on the ground to rapidly cycle each phase shifter through its various phase states. Through a direct measurement of the pattern on the ground, a failure or deterioration can be pinpointed to location of element and extent of degradation. The BSU can then be reprogrammed to compensate for this. This enhances the reliability of the system and in a sense provides a redundancy for the phasors. There is no simple technique that may be implemented with the Butler Matrix or transdirective array systems which will detect and compensate for element deterioration or failure.

Conclusions: Table 7.2-1 lists the pertinent system parameters associated with each of the four phased array systems studied. The basis for this data is qualitatively discussed in the above paragraphs and in Section 2.5.2, dealing with phased array figures of merit.

TABLE 7.2-1
SYSTEM COMPARISON

Systems Studied	System Weight	System Estimated ⁽¹⁾ Volume	System Losses	Transmit Figure of Merit (ERP per pound)	Receive Figure of Merit (S/N db per cycle per pound)	Comments
Transdirective Array	120 lbs	11.25 ⁽²⁾ cu. ft.	Trans. -13.8 db Rec. -1.8 db	14.8 ⁽³⁾	0.483 ⁽⁵⁾	Lowest Reliability. Highest power con- sumption.
Butler Matrix Array	188 lbs	7.5 cu. ft.	Trans. -9.4 db Rec. -9.4 db	23.2 ⁽⁴⁾	0.273	High scan- ning losses. Inefficient use of switching elements.
Space-Fed Array	169 lbs	15.00 cu. ft.	Trans. -4.0 db Rec. -4.5 db	91.8 ⁽⁴⁾	0.356	Extremely Sensitive to Mech- anical dis- turbance.
Corporate-Fed Array	166 lbs	11.25 cu. ft.	Trans. -2.5 db Rec. -3.0 db	131.5 ⁽⁴⁾	0.360 ⁽⁶⁾	Highest Reliability Lowest power consumption

NOTES (Table 7.2-1)

- (1) C.P. horns are assumed; array surface is 32" x 36".
- (2) Two antennas are assumed.
- (3) Includes projected +1.5 db improvement in varactor up converter output. Total power out is limited by diode capability.
- (4) Total power out is limited by TWT amplifier availability and DC power available aboard spacecraft.
- (5) System uses 64 wide band receivers; TDA's or non-cooled paramps not considered feasible.
- (6) System uses 2 narrow band receivers; TDA's assumed, non-cooled paramps would enhance S/N.

The essential results of this study are listed in the above table. The Corporate-fed array stands out as the prime choice for this mission requirement. The space-fed (lens) array is the second best choice. The primary disadvantages of the lens are: Amplitude tapering and spillover add an additional 1.5 db of loss, the optical system is susceptible to mechanical disturbances, the remote lens location imposes handicaps on the phasors. The remainder of the report dealing with the phased array will be concerned with design considerations for the Corporate-fed system.

7.2.5 Corporate Fed Phased Array Design Considerations

Introduction - - The following sections describe the operation of the corporate fed array and the design considerations of its component parts. The characteristics of the antenna, receivers, transmitters, and beam steering unit are discussed in detail.

Microwave System - - The 64 element array will be capable of simultaneous reception and transmission of four independently controlled X-band signals, two each on transmit and receive. A schematic of the system and tentative frequency bands are shown in Figure 7.2-8. The separation of the four frequency channels occurs at the base of each of the circularly polarized feed horns. The signals are first separated into the 2 transmit and 2 receive channels by a ferrite Y-junction circulator connected directly to the horn, permitting simultaneous reception and transmission of CW signals. The strip line circulator will provide greater than 20 db of isolation between the transmit and receive channels over the full 10% bandwidth. The contiguous bands at the transmit and receive ports of the circulator are further separated (or combined for transmission) by strip line diplexing filters. For the uplink case the two incoming signals are separated by the narrow band pass filters which provide approximately 20 db of isolation. Additional rejection is not necessary at this point. The primary function of the diplexer is to prevent the signal from entering the wrong feed network where it would be dissipated. The bulk of the isolation between receivers is achieved by high rejection waveguide filters located directly before the receiver front ends. For the downlink case, the two signals are combined in the diplexer prior to transmission from the radiating element. Here an isolation between channels of 15 db is adequate. The circulator and diplexers are combined in an integrated strip line package. Each of the four frequency separated ports are connected to a waveguide ferrite phase shifter via a strip-line-to-waveguide transition.

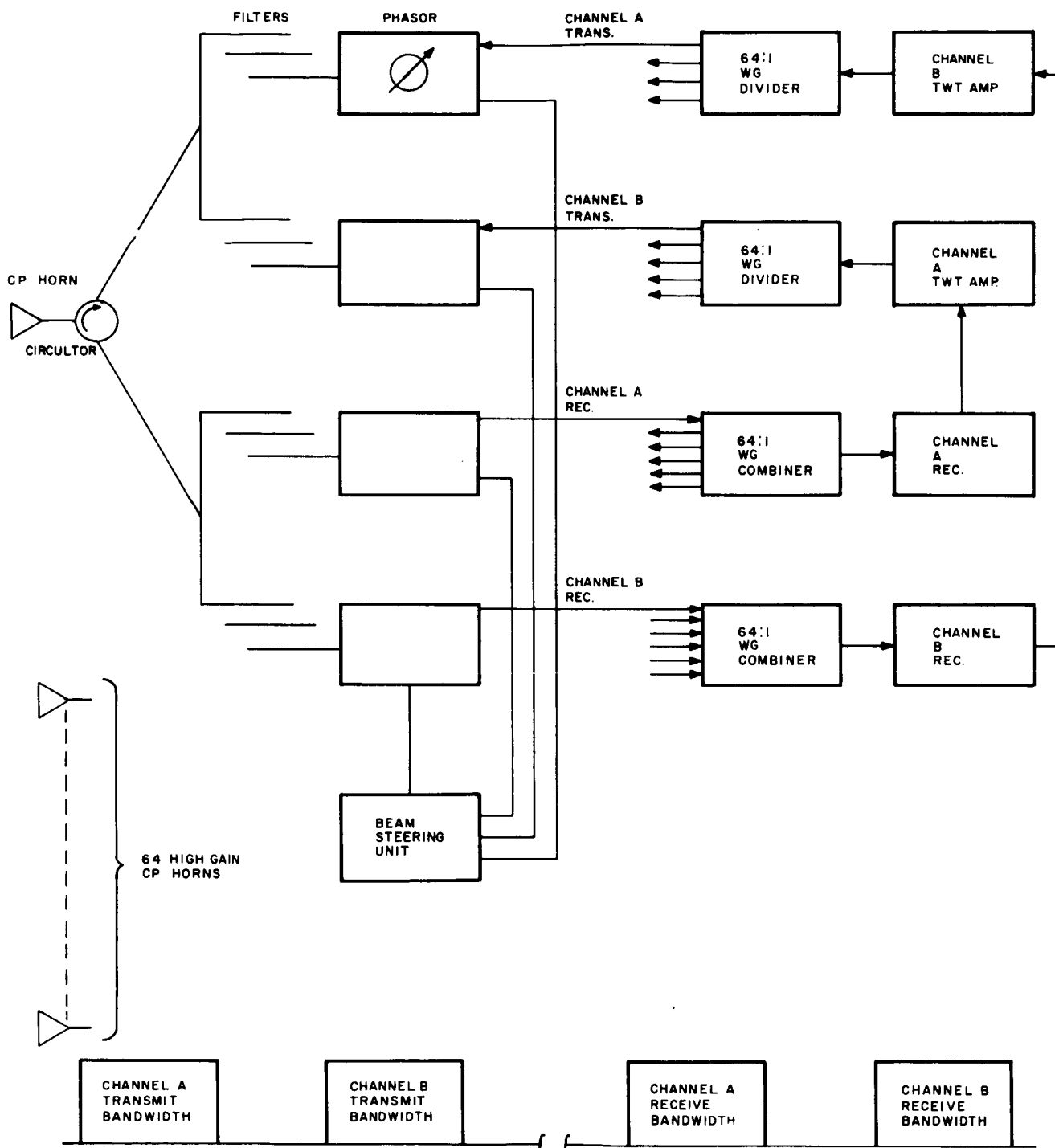


Figure 7.2-8 Schematic of Microwave Subsystem

There are 64 such modules, one for each horn, resulting in 256 phasors, or 4 sets of 64 each. Each set of phasors is then connected to a 64:1 combiner or divider. Upon reception of a signal by the array, the 64 component signals are directed by the diplexing modules to one of the two sets of receive channel phasors. The phasors are programed to allow summing of the signals in accordance with the scan angle of the receive beam at the isolated waveguide combiner. After processing and conversion to the proper downlink frequency the summed signal is boosted to the desired power level for transmission by the TWT amplifier. This signal is equally split by the 64:1 waveguide divider. Each component is phase shifted by the programed set of transmit phasors to direct the beam. The other bands will operate independently in the same manner. The beam pointing directions are controlled independently by the four sets of digital ferrite phasors as directed by the B. S. U. In order to assure adequate signal separation between two relay links sufficient filtering must be implemented. For adequate isolation, at least 100 db isolation between the up link and down link channels is required. The circulator will provide at least 20 db of the rejection, the narrow band pass diplexing filters provide an additional 40 db of rejection. The summing network will contribute a minimum of 15 db of isolation to any leakage signal that enters the circuit with a phase front different than the beam direction in which it is programed to uniformly sum. The remaining separation will be provided by narrow band pass waveguide filters located at the input to each receiver. These filters will easily provide at least 20 db of separation between the two receive channels with at least 40 db of rejection to the transmit link frequencies. Thus the system as described makes provision for as much as 60 db of RF separation between the receive channels and 120 db of rejection to transmitter leakage.

Component Definition - - The following describes the microwave components that would be required for the corporate fed array. Some improvements would be expected in certain areas with modest development effort, but no significant breakthroughs or advances in the state of the art are required to achieve maximum system performance. The components described include:

- Radiating element
- Circulator
- Diplexer
- Waveguide filters
- Waveguide distribution network
- Digital ferrite phase shifters
- Radiating Element - - The requirements of high gain, low loss and circular polarization sharply narrows the available choices for a feed element. The 18 db gain requirement with a 20° HPBW element factor suggests the use of small subarrays of lower gain elements such as crossed dipoles or helices. Unfortunately these subarrays must be fed by uniform power dividers which at X-band frequency tend to be lossy. The limitations of space dictates the use of strip line dividers with as much as 0.5 db additional loss contributed to both the transmit and receive channel. A single helix with 18.5 db gain would be over 9" long presenting element shadowing and coupling problems at the extremes of the desired $\pm 10^\circ$ scanning cone. An array of 64 such elements would use up more than half the available volume.

The element selected for the application is a hexagonal horn energized by a short helix located at the base to provide the circular polarization. The horn shown in Figure 2.7-9 is 6" deep, has a gain slightly better than 18 db and an efficiency of approximately 80%. The horns would be mounted on an equilateral triangular grid. They could be

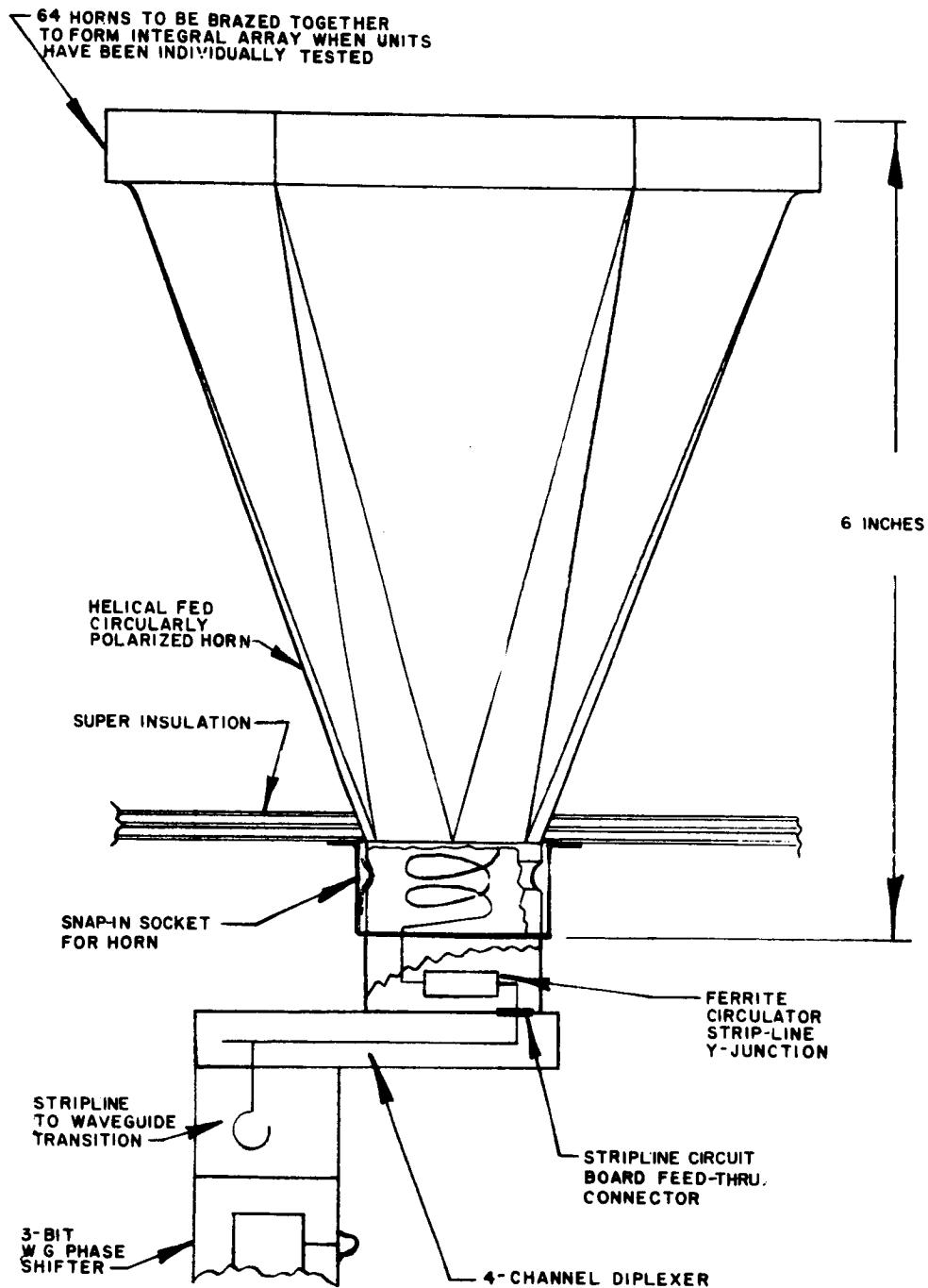


Figure 7.2-9 Detail of Feed Horn Assembly

affixed to the surface of the array with snap-in cups for removal during individual element testing. The pattern performance of this feed is discussed in more detail in the section on antenna performance.

- Circulator - - At X-band frequencies waveguide circulators tend to be heavy and bulky. A more attractive solution makes use of strip transmission line in a three terminal Y-junction configuration which may be readily integrated with other components. Typical performance specifications at X-band would be:

Bandwidth: 10%

Maximum Ins. Loss: 0.1 - 0.2 db

Isolation: 22 db min, 28 db max.

VSWR: 1.15:1

Size: 3/4" x 3/4" x 1/2"

Weight: 2 oz.

Temperature range: -30°F to +130°F

The isolation and insertion loss of a circulator will degrade as the temperature rises above its design range and approaches the Curie point. Temperature drops have a relatively small degrading effect. The predicted temperature excursions within the system's superinsulated environment is well within the normal operating range of the circulator.

- Diplexer - - The interface between the 64 feed horns and 256 waveguide channels makes a compact diplexing network a necessity. The use of strip line is attractive. Narrow band strip line filters tend to be somewhat more lossy at X-band frequencies than the equivalent waveguide network. This loss ratio increases sharply as the required separation is increased. Therefore, the minimum amount of filtering will be used at this point. The object is to provide approximately 20 db of separation between adjacent RF bandwidths primarily to prevent loss

of the signal into the wrong channel. The uplink and down link frequencies are separated by a 500 MHz guard band. The adjacent RF channels within each link are 125 MHz wide and are separated by a 100 MHz guard band. A filter network suitable for this application would consist of a balanced set of singly terminated bandpass filters matched into a common junction as shown in Figure 7.2-4. The common port presents a low VSWR to the two adjacent frequencies while separating and passing each frequency through its proper narrow band network. A 3 section halfwave resonant Tchebyscheff design provides the necessary 20 db of separation while providing at least 40 db of rejection to each of the frequencies in the opposite link. The equal-ripple pass bands introduce approximately 0.3 - 0.4 db of insertion loss into the system. The diplexer performs equally well for both the separating and combining of the signals. The two sets of diplexers can be integrated with the circulator in a single package as shown in Figure 2.7-10.

- Waveguide Filters - - The remaining separation and rejection is provided by a low-loss waveguide filter located at the input to each receiver front end. The additional 20 db of separation between adjacent frequencies in the up-link channel, with at least 40 db of rejection to both channels of the down-link frequencies is easily provided by conventional waveguide filter techniques. Approximately 0.2 to 0.3 db of loss can be expected from a 3 section quarter wave cavity resonant filter.

- Waveguide distribution network - - The networks used for both combining and dividing the RF signals are identical. Each of the 64:1 dividers/combiners splits the power to obtain 64 signals equal in amplitude and phase. In the transmit case the set of 64 phasers connected at each output of the divider will impose a set of phase shifts on the uniform signals to scan the beam. In the receive case the phasors connected at each input port of the combiner will be programmed to remove the

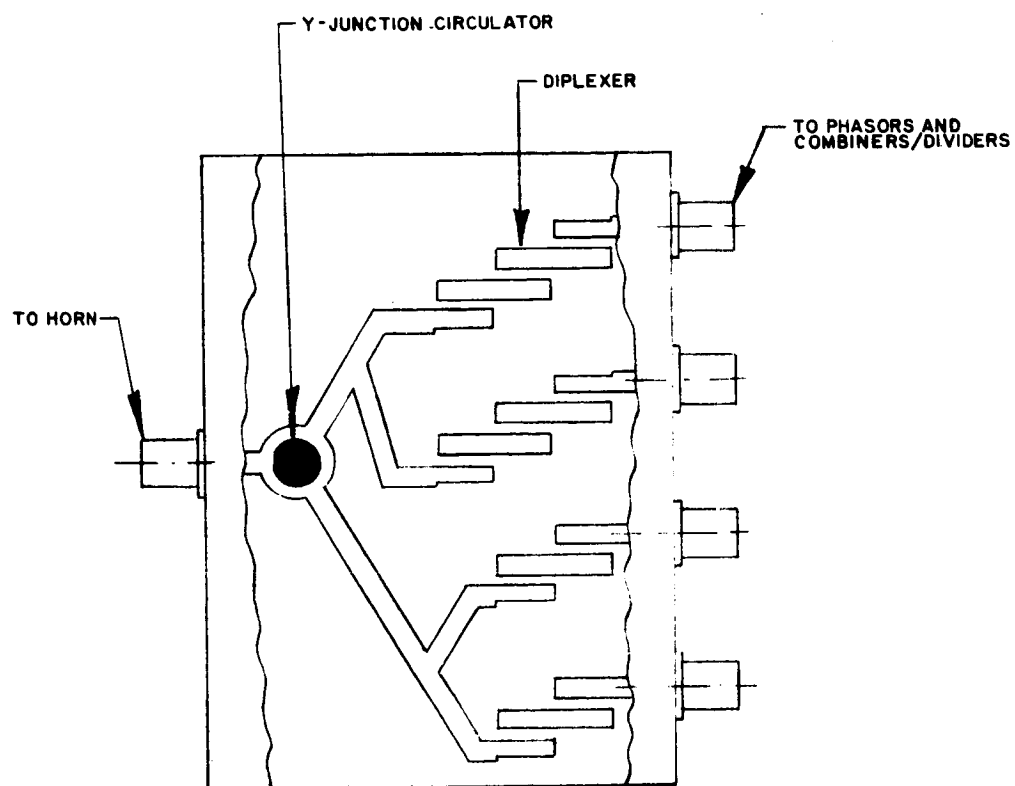


Figure 2.7.10 Possible Configuration of 4 Channel Diplexer - Circulator Strip Line Module

differential set of phase shifts associated with a specific scan angle resulting in perfect summation of the signals at the output of the combiner. A wave front arriving from another direction different than this specific scan angle will be dissipated within the combiner.

Each 64:1 divider will consist of a series-fed terminated coupler, coupling eight uniform signals into identical 8-way binary power dividers resulting in 64 amplitude and phase matched signals arriving at the output ports. Over the narrow RF band of operation (125 MHz=1.6%) the signals can be expected to track each other within 0.3 db of amplitude variation, and 4° of phase variation. Excessive variations in phase tracking may be corrected by properly programing the phasors.

The 8-way dividers feeding from the series fed coupler will be binary combinations of 4 port "magic tees" with the isolated or 4th port being terminated. The use of this tee rather than the less complex reactive 3 port tee permits the dissipation of unwanted signals entering the combiner, and minimizes multiple mismatch problems which tend to produce secondary side lobes and phase aberations which deterioriate the beam pattern. Each 64:1 divider (or combiner) will introduce 0.5 - 0.6 db of loss into the system while providing at least 20 db of internal isolation between channels. The input VSWR's would be in the order of 1.25:1.

- Phase Shifters - - The two principle techniques for phasing arrays involve the use of diode or ferrite devices. Digital operation is the most practical because of the wide margin of tolerance allowable in control circuits. The PIN diode and latching ferrite elements can be designed to operate in a stable manner under these conditions. The diode circuits have proven themselves to work most efficiently at RF frequencies below 4 GHz, whereas ferrite phasors become more attractive at higher frequencies. The high reliability of diodes is well established for low

frequency functions (less than 1 GHz) but little is known of their stability and long term performance at X-band frequencies. In addition the diode device is 10 to 20 percent more lossy than the ferrite phasor and is somewhat larger and more complex. More important is that the diode performance tends to deteriorate with time in a space environment.

Further, a latching ferrite device is preferred to a PIN diode device for satellite application because of lower power consumption. The diode must be continuously biased. A typical diode draws on the order of 0.10 watt of continuous power in its forward bias state (typically +1/2 volt, at 200 ma). In the reversed bias state it draws less than a milliwatt (-200 volts at 1-5 microamps). Statistically half the diodes will be in each state resulting in an average power drain of 0.05 watts. Since there are 6 diodes used in each of 256 phasors the total average power consumption is 76.8 watts ($6 \times 256 \times 0.05$ watts). This is a prohibitive load to place on a satellite power system. The ferrite latching element on the other hand is magnetically self biasing, requiring a 500-1000 microjoule pulse of energy to change states. At the average switching rates required for this system the average power consumption is in milliwatts.

The latching ferrite element is basically a closed circle or toroid of material which can be magnetized by a single pulse of high current. The direction of magnetization is changed by reversing the direction of current on the wire running through the center of the toroid. The device is usually operated between its two stable or saturated states (opposite directions of magnetization). The element may be used in either the waveguide configuration shown in Figure 7.2-11 or the strip line configuration shown in Figure 7.2-5. In the waveguide device all the ferrite actively engages with the RF fields and is switched by a single wire running down the axis of the guide. The differential phase shift between states is a function of ferrite geometry and material but is linearly proportional to the length of the toroid. Thus a 3 bit device ($0-180^\circ$, $0-90^\circ$, $0-45^\circ$) consists of 3 ferrite toroids having lengths pro-

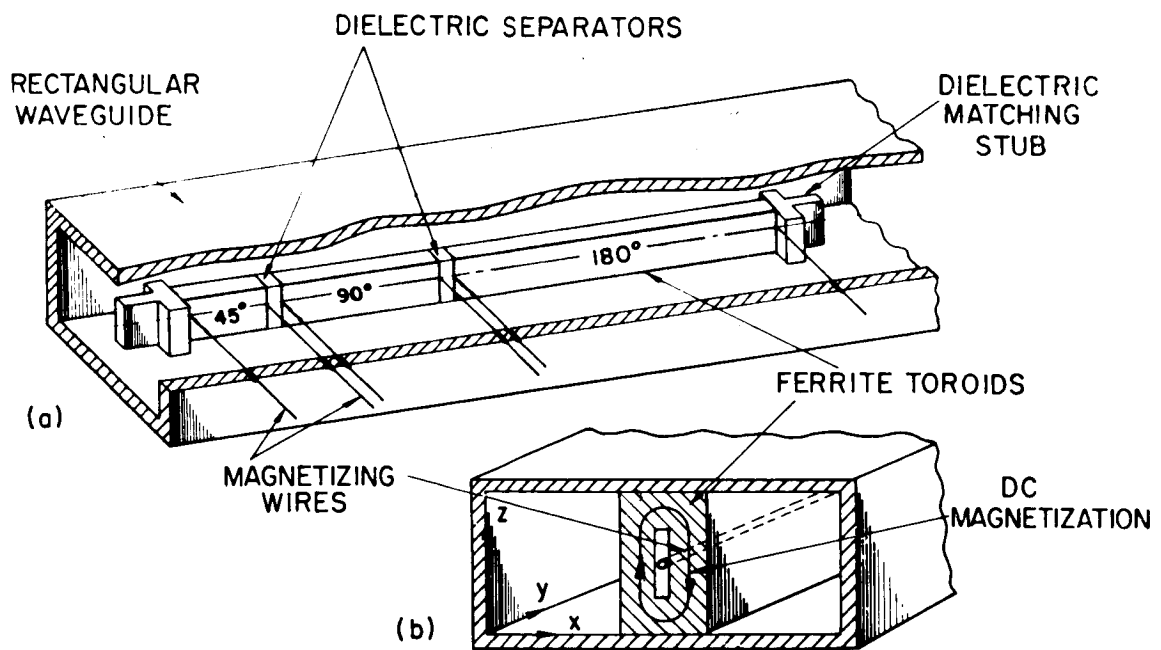


Figure 7.2-11 Wave Guide Latching Phase Shifter

portional to 1, 1/2, 1/4, and separated by small dielectric spacers. The strip line configuration is essentially a series of switchable circulators with the difference port providing differential phase shift dependent upon its electrical length. In this case much of the ferrite is outside the active RF region, requiring additional material and a stronger current pulse through a heavier coil to latch it. Although the strip line phasor has greater packaging flexibility, this additional weight and required driver capacity, coupled with the 10-20% additional insertion loss of the device makes the slightly larger waveguide phasor the better choice.

The insertion loss through the waveguide ferrite phasor will be 0.8-1.0 db. It will weigh 2.5 oz. and be approximately 3.5" long. This performance and size is typical and is readily achievable. Since the device is required to operate over a relatively small RF bandwidth a development effort to optimize each set of phasors for its particular channel frequency will result in an improvement in insertion loss and size. The non-reciprocal nature of this device is of no consequence in this application since all signals pass through only one way.

The temperature characteristics of the ferrite represent the most significant problem to be dealt with. The following conditions tend to ameliorate the problem:

- The performance characteristics of ferrite devices degrade, as temperature excursions approach their Curie point (typically 300°C to 400°C). The RF performance is completely retrievable when the temperature returns to normal by magnetically resetting them.

- Temperature excursions are due to the environment and not dissipation since the devices operate at low power levels. The temperature aboard the space craft will be well below the Curie point where degradation is less severe. The ferrite phasors will be housed in a superinsulated sealed environment where heat dissipated by electronic

elements, the grating lobes scan in the same direction. Those opposite the scan direction move toward broadside. The closer a grating lobe is to the broadside axis the greater is its magnitude. When its magnitude is equal to that of the main beam the gain is degraded by 3 db and the two lobes are indistinguishable.

The initial positions of the grating lobes when the main lobe is at broadside depends upon the element spacing; the further apart the elements, the closer the grating lobes are to broadside. The amount of main beam displacement achievable without serious grating lobe infringement decreases with increased element spacing. The positions of the closest grating lobes in the array pattern are given by:

$$\sin \theta_g = \sin \theta_o \pm \frac{\lambda}{D}$$

θ_g = grating lobe angle

θ_o = main beam angle

D = element spacing

λ = wavelength

When the main beam is at broadside ($\theta_o = 0$) the grating lobes are at $\theta_g = \arcsin (\lambda / D)$.

An 8 by 8 element array has the fewest number of elements which will satisfy the constraints. The elements are placed in a triangular grid layout as shown in Figure 7.2-12. This arrangement allows the maximum scan for a given element size, with the farthest grating lobes. The worst grating lobes occur when scanning in the planes parallel to the altitudes of the triangles. When scanning parallel to the sides of the triangles the lobes are farther from broadside and lower in amplitude, since the effective element spacing is less.

The spacing dimensions shown in Figure 7.2-12 are normalized to the shortest wavelength and have been used to calculate the patterns shown in Figure 7.2-13. These patterns consist of the element factor and

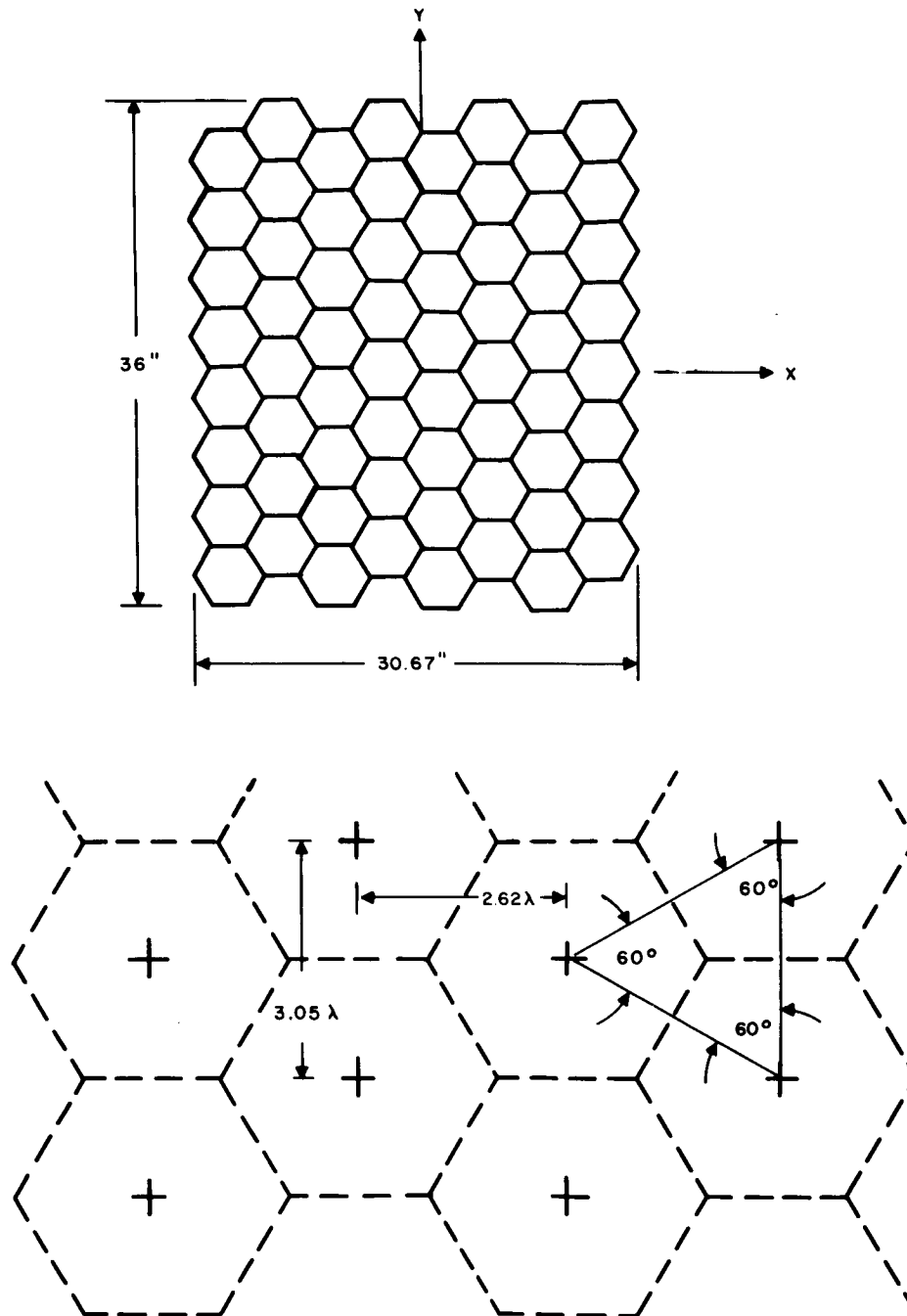


Figure 7.2-12 Array Element Layout

equipment will be used to control temperature excursions. The gradient or differential temperature between phasors will be maintained within a few degrees since the ambient changes slowly.

- Many ferrite materials are available for the design of X-band latching phase shifters with minimum temperature sensitivity in the $72^{\circ}\text{F} \pm 20^{\circ}\text{F}$ range. Most notable among these are the gadolinium-doped garnets. The devices can be designed to operate over a 40 to 50°F temperature range with a phase variation of $\pm 3\%$ and an insertion loss change of less than 0.2 db. Thus the spacecraft controlled environment will maintain the phasors within their best operating range.

- A temperature compensation control can be provided within the control driver design to further increase the allowable temperature excursion by a factor of 4 or 5. The use of the constant flux generator driver to transfer flux from a secondary ferrite coil to the phase shifter toroid to achieve stabilization over wide temperatures ranges has been described in Lincoln Laboratory study reports (1). This hardware is commercially available (2).

- An additional redundant compensation control is provided in the system for use during possible long term temperature excursions or under conditions of unpredictable temperature gradients. The technique for accurately measuring phase shift performance of each individual phasors from the ground within a period of 120 seconds is described in

(1) M.I. T. "Phased Array Studies," March 1965 Technical Report 381

(2) SEDCO Systems Inc., Farmingdale, N. Y.

section 2.6 (Phased Array Failure Mode). This information in addition to temperature information directly telemetered from the space craft may be used to reprogram the command signals to the beam steering unit to correct for aberrations caused by temperature.

7.2.6 Antenna Definition

The array aperture parameters (amplitude illumination, number of elements, element size, and element spacing) have been determined using the following antenna constraints:

- The antenna gain shall be a minimum of 36 db above an isotropic radiator, at broadside (less system losses).
- The beam shall be capable of being scanned up to 10 degrees from the array normal in any direction.
- The antenna shall operate between 7.3 GHz and 8.3 GHz.

The aperture illumination must be approximately uniform in order to achieve the required gain. Uniform illumination is very easily achieved with simple feed networks. Binary branching is the most attractive in a waveguide system because of the ease of design and excellent performance. The fewest elements possible are used in order to simplify the electronics and minimize the cost and weight of the antenna package. As might be expected, design compromises must be made when attempting to achieve a specified gain with the fewest number of elements. The most prominent factor affecting the ultimate design is the magnitude and location of the secondary lobes known as grating lobes, which are an inherent part of array antenna patterns. These lobes can appear in real space for any phased array antenna whose elements are uniformly spaced further than $1/2$ wavelength apart. As the principal lobe is made to scan away from the broadside position by phasing the

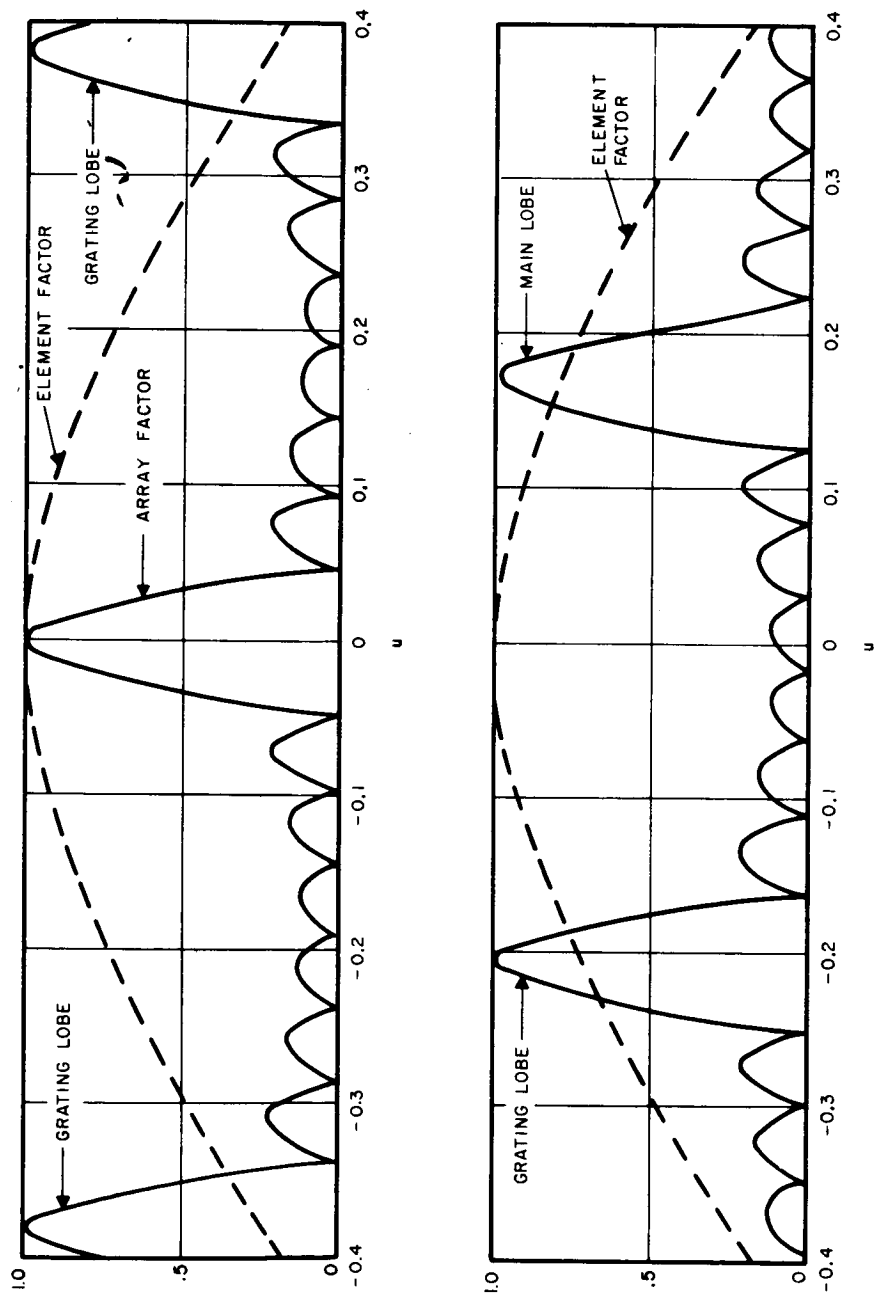


Figure 7.2-13 Phased Array Patterns

the array factor for the X-axis of the antenna. They are plotted against "u" which is the conventional transformation proportional to $\sin \theta$. Note that when the main beam points at 0° , (broadside) grating lobes appears at $u = \pm .280$ corresponding to $\pm 22^\circ$. At the maximum main beam scan angle of 10° , $u = 0.174$, one grating lobe appears at $u = 0.554$ and one appears at -0.206 corresponding to 33.5° and -11.7° respectively. The magnitude of the grating lobes and the main lobe correspond to the magnitude of the element factor at the angle of the particular lobe. The main lobe at 10° , it is noted, is only slightly greater in magnitude than the grating lobe at -11.7° , both about -3 db. This is highly undesirable in most applications because of the interference vulnerability; however, since the earth's disk intercepts only $\pm 10^\circ$ from the satellite, this grating lobe points into space. The only effect then is the degraded main beam gain. To remedy this situation requires a 16 by 16 element array - an unacceptable alternative.

The elements are hexagonal in cross section as shown. This shape leaves no open spaces between elements and simplifies the assembly. The optimum length electromagnetic horns are excited by a small helical feed to produce circular polarization. The size and shape of the horn element is shown in Figure 7.2-9. The calculated gain of the horn is 18.1 db. Multiplied by the number of elements, 64, gives 36.2 db as the array gain at broadside and 33.2 db at the maximum scan angle.

Phase Quantization -- From a geometrical point of view, the antenna meets all the requirements. Some practical aspects, however, must also be considered. The antenna is scanned by varying the phase of the field in each element by means of a ferrite phase shifter. For many reasons which are discussed in another section of this report, the most practical type of phase shifter is of the digital latching variety. This phase shifter is controlled by pulses and consists of a number of toroids of ferrite material,

each of which may be independently pulsed to a saturation state in either of two polarities. The fineness of phase control obtained is determined by the physical size of the smallest toroid. The largest toroid produces 180° of differential phase shift, 90° , 45° and so on, to as small as increment as required. Since the operation of each toroid is binary, the number of toroids may be expressed as bits. A phase shifter with n bits, has $(2^n - 1)$ phase increments, smallest increment being $\frac{2\pi}{2^n}$ radians.

The number of bits, as well as the number of elements, must be minimized to simplify the logic circuitry, reduce insertion loss, and minimize size and weight. The lower limit on the number of bits is determined by the antenna pattern characteristics.

For very large n , the phase of each element can be set to a very close tolerance and the antenna patterns would agree very closely with classical theory. As the number of bits is decreased the possible error in the phase of a given element increases. For three bits the maximum phase error will be $\pm 22.5^\circ$. For two bits it is $\pm 45^\circ$, and for one bit $\pm 90^\circ$. The radiation pattern of an array whose elements are digitally phased may be regarded as the superposition of the pattern of an ideally phased array and the pattern of an array whose elements are phased at the error phase angles. The error pattern contributes to the sidelobe level, and the energy radiated must subtract from the main beam gain. The relationship, therefore, may be summarized as follows: decreasing the number of bits in the phase shifters causes the gain to decrease, and the average sidelobe level to increase.

Another effect of phase quantization upon pattern performance is the pointing accuracy. With lower quantization levels, the pointing accuracy of the array is reduced. For arrays with a very large number of elements, the averaging tends somewhat to compensate for large phase errors. With 64 elements, the boresight accuracy will be limited primarily by phase

quantization. An evaluation of the projected antenna performance for two, three, and four bit quantization was made and is summarized in Table 7.2-2. With gain as a criterion, two bit quantization was found to be unacceptable. The difference between three bit and four bit performance showed that the main difference is in the beam pointing accuracy. The gain of the two can almost be equalized by the insertion loss caused by the additional ferrite.

The sidelobe levels given are limiting values only, so if the illumination sidelobes are higher, these values lose meaning. That is to say, if the amplitude taper were designed for 35 db sidelobes for example, the quantization values would have to be increased. Since this array is uniformly illuminated it therefore has -13.3 db sidelobes. An 18 db or 24 db limitation therefore makes little difference. The choice then is whether a boresight improvement of 50% is worth a component increase of 33%. On this basis, then, three bit accuracy is sufficient for all of the phased array experiments in this program. The extra boresight accuracy, although it would be valuable in the tracking mode of operation, described in the Appendix 7D, does not warrant the extra cost, weight, and decreased reliability.

Phased Array Scanning -- The array is not exactly square because of the triangular element layout, (note Figure 7.2-12). This causes the beam to be slightly broader in one plane than the other. The Y axis beamwidth will be 2.2° and the X axis beamwidth will be 2.45° at the upper frequency, and 2.4° and 2.65° , respectively, at the lower frequency. The beam scanning will be defined in terms of medium beamwidths of 2.3° by 2.55° for simplicity, with the understanding that the crossover points and inter-beam levels will be slightly different at the actual band limits.

The phased array antenna coverage is larger than the earth's disk ($\approx 17.5^{\circ}$), covering a cone of 20° . Because of the digital scanning, this cone must be covered by a finite number of beams. It is proposed that the

TABLE 7.2-2⁽¹⁾ PERFORMANCE CHARACTERISTICS

	No. Bits		
	2	3	4
Gain Decrease (db)	0.90	0.22	.06
Peak Sidelobe Level (-db)	13.00	18.00	24.00
RMS Sidelobe Level (-db)	22.00	27.00	33.00
Pointing Accuracy (B. W.)	.192	.096	.048

(1) Proc. Symp. on Elect. Scanned Array
 Tech. and Applications, Tech. Doc.
 Rpt. RADC-TDR-64-225, July 1964.

individual beams be displaced from each other by 0.25 H.P.B.W. This results in a total of 856 separate beams. The beams will be distributed in a triangular grid layout, similar to the array elements as shown in Figure 7.2-14. If they were not interlaced, but had been placed in a rectangular grid, the level of signal in the darkened space would be lower. In the triangular arrangement the contours shown are the $1/4$ beamwidth contours, which correspond to a signal level of - 0.17 db. The level in the darkened area corresponds to - 0.2 db.

When the antenna is operated in a scanning mode, eg, while maintaining a communications link with a low altitude satellite, the antenna beam position is required to change slowly, of the order of 0.5° per minute. The satellite data link system can supply data up to 35 bits per second or 2100 bits per minute. The number of bits which define a beam setting is 192 (three bits per element times 64 elements). It is therefore planned to direct the beam steering by computing the phase shifter settings on the ground, since the data will be made available 10 times faster than required. The elements will be switched serially when in the scanning mode so that no interruption in communications will result. Since only $1/64$ of the elements are switched at a time the beam will actually move the $1/4$ beamwidth step in 64 finer steps, and an almost continuous type of scan results. When half the elements have been changed, the beam direction will be midway between the two adjacent steps. For this small beam displacement ($1/4$ beamwidth) the effect of half the elements being phased for one beam and half for the next will be similar to having them all phased for the mid-position with a very small distributed phase error. For large beam displacements this serial element switching can cause a shutdown time of approximately six seconds between beam positions (time to transmit 192 bits at 12 bits per second).

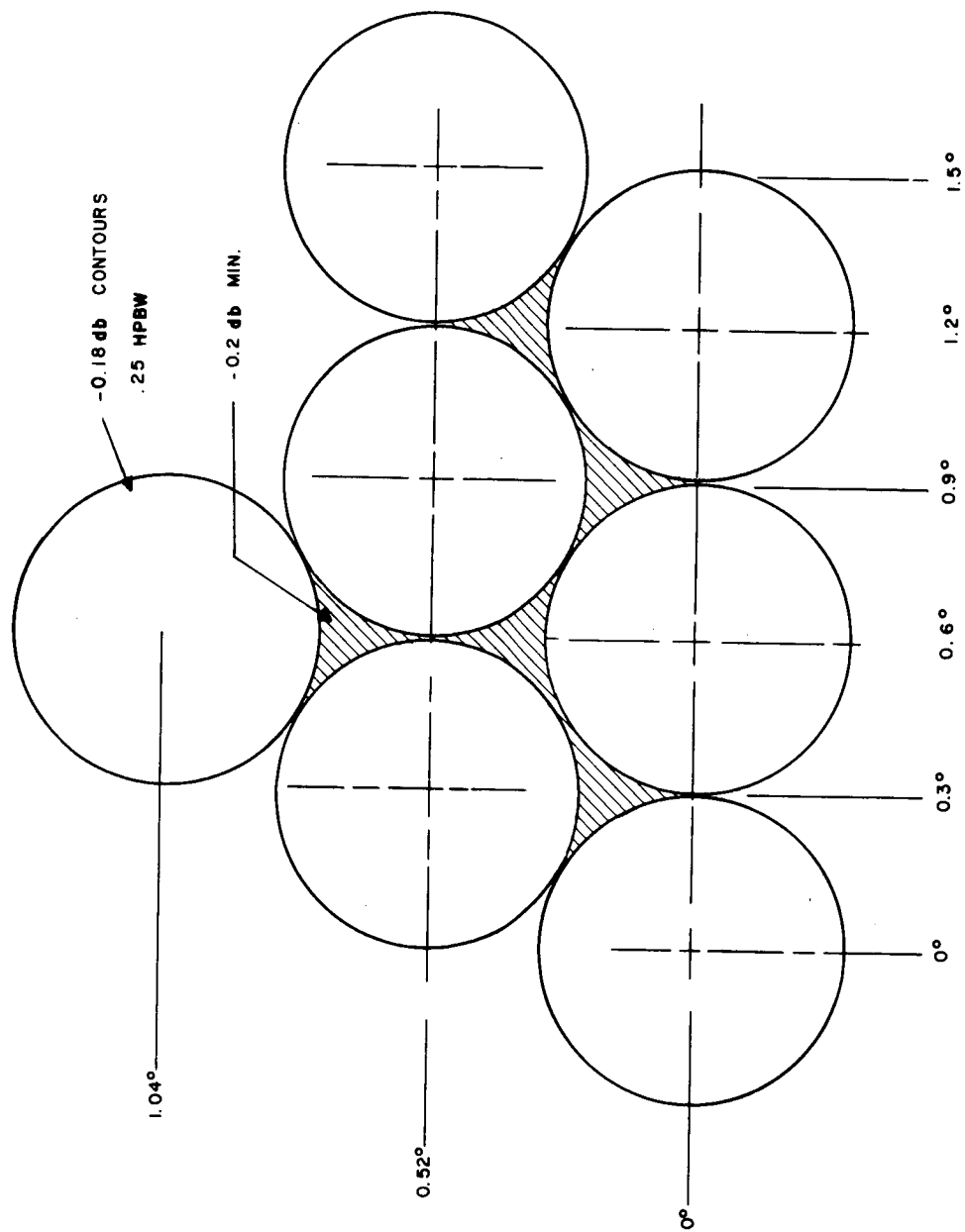


Figure 7.2-14 Phased Array Beam Spacing

7.2.7 Digital Beam Steering Unit

The Digital Beam Steering Unit (BSU) establishes the settings of the digital phase shifters, and hence the patterns for the four array beams. Mode and beam steering commands supplied by the Ground Control Station dictate the operation of the BSU.

Because of the relatively small number of array elements, it is possible to apply simple straight-forward techniques without imposing excessive cost and space requirements on the design of the Unit. The natural advantages of this approach include:

- A high level of flexibility in modifying steering commands.
- A phantom bit resolution equal to the resolution of the ground-based steering computer.
- Increased reliability by paralleling in critical areas.

As shown in Figure 7.2-15 the pre-computed steering commands arrive at the BSU at a rate of 35 bits/sec. Mode commands and frame synchronization signals accompany the steering data and are used to establish signal flow and operating speeds respectively. There are two basic configurations for the BSU, the slow speed configuration for slow beam scanning as used in the dynamic pattern measurement, and the high speed configuration for rapid beam cycling as required in the static pattern measurements or failure mode testing. In the slow speed configuration, steering commands are accepted in-line from the satellite communications receiver and then sequentially commutated to the phase element drivers of the selected array beam (thereby forming a new beam once every six seconds) for the high speed configuration, eight complete beam steering commands (8 x 192 bits) are initially loaded into the read-write memory, in-line with the communications receiver. Once the eight steering commands have been stored, the BSU cycles the antenna beam through the eight beam patterns at a 1 KHz rate.

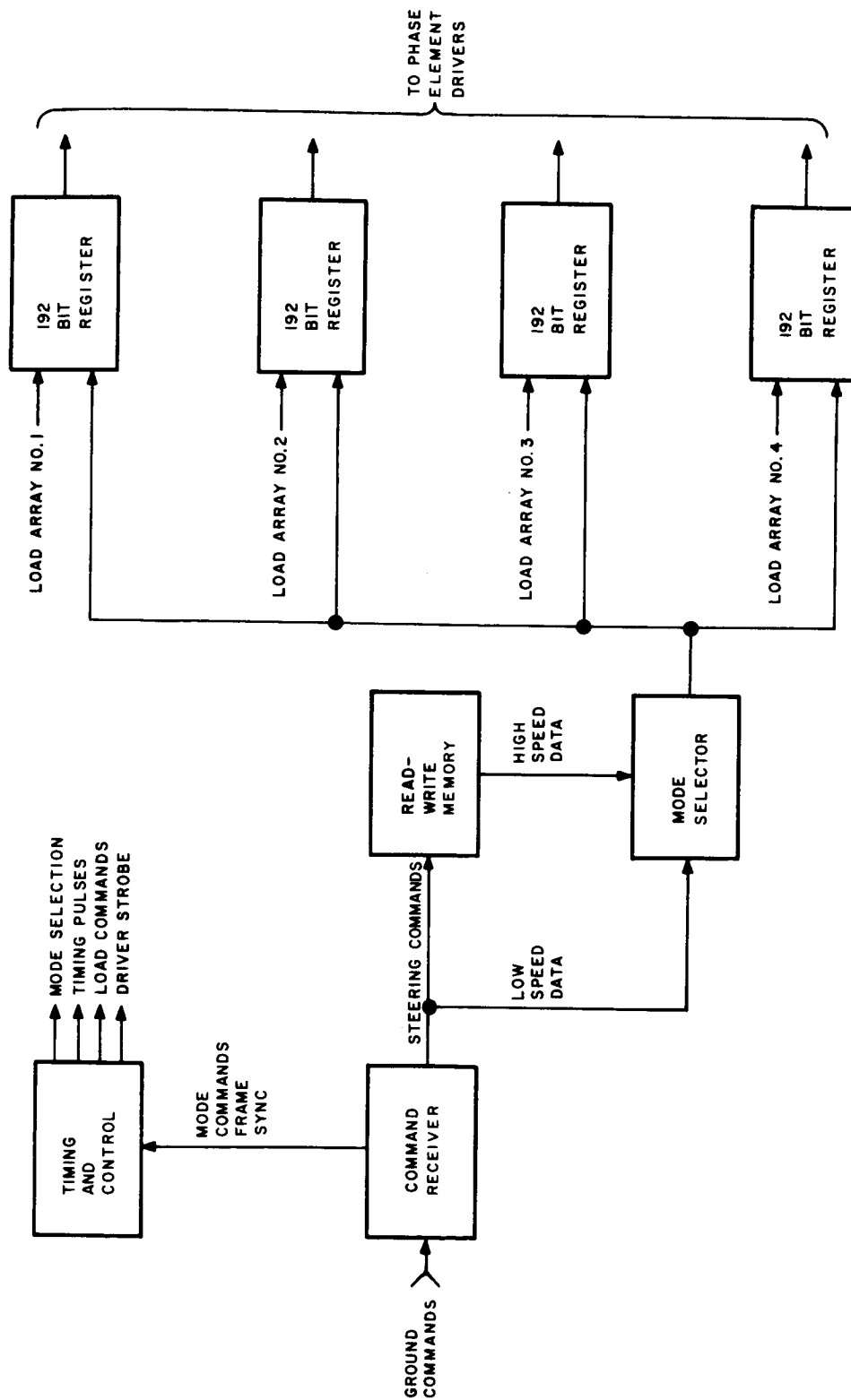


Figure 7.2-15 Block Diagram for Digital Beam Steering Unit

Since the basic function of the antenna arrays is to serve as a communications medium, it is desirable to avoid antenna "dead times", and phase or amplitude modulation when switching the ferrite phase shifters. Therefore, the BSU is designed to sequentially switch the phase elements in a random fashion and thereby minimize the beam shape deterioration that might occur if the phase shifters were switched in an orderly manner.

The logic portion of the BSU consists of standard low-level integrated circuit logic, which provides compact packaging, high reliability, and low power consumption. Phase shifter settings and strobe signals are delivered to the phase element drivers in digital form, with a wide threshold margin between the binary "one" and binary "zero" state to secure against false data transfers. The read-write memory is a small standard magnetic core memory with its associated write and sense amplifiers.

Phase Element Drivers -- Three bit drivers are provided for each of the four sets of 64 phase shifters (256 phasors). These drivers are designed to remain in the "off condition" until a switching command is received from the digital beam steering programmer, thereby minimizing average power consumption. Each bit requires a switching pulse of 500 micro-joules. For a maximum switching speed of 1 KHz, as required in the failure mode switching procedure, an average power of 1/2 watt is required.

Push-pull drivers are employed to permit single line switching on the input and output respectively. Small tantalum capacitors for each bit driver are recommended (see Figure 7.2-16) to provide high level short-term energy which can be replenished from the main power source during the relatively long idle periods for that particular driver. In addition to relieving the peak power load of the primary power supply, these capacitors act as a filtering element for the power supply.

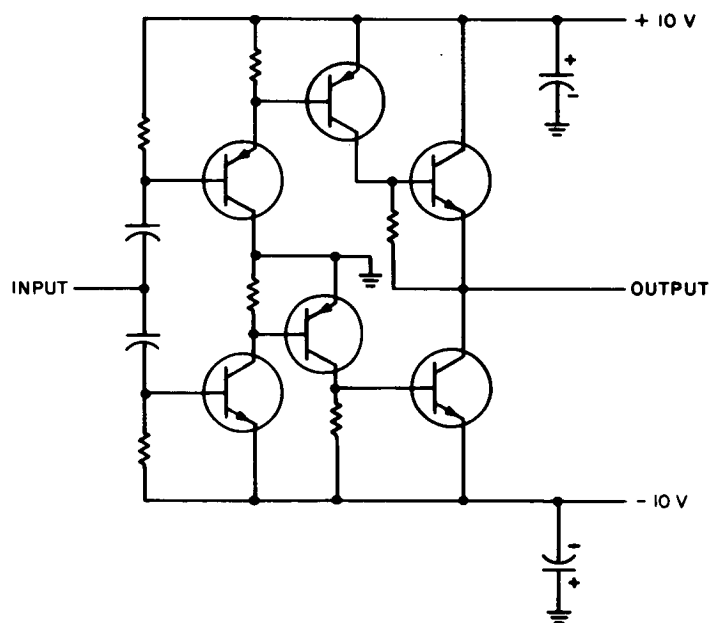


Figure 7.2-16 Schematic Diagram for Bit Driver

7.2.8 Packaging Configuration

Packaging studies were made of the corporate fed system to evaluate the various trade offs available to the system designer. The use of different combinations of waveguide, coaxial and strip transmission line were considered. The characteristics of these tradeoffs have been discussed in the previous sections. The concern has been to achieve minimum system losses consistent with compact packaging within the allotment of volume aboard the spacecraft. The antenna size required for the system gain placed an unavoidable constraint on minimizing this volume. A plan view of the antenna surface is shown in Figure 7.2-17. The wide placement of the 64 feed horns over the 7.5 square foot area (36" x 30-3/4") made the use of wave guide a practical consideration for reducing system losses. Including components the system uses approximately 280 feet of standard 1" x 2" X-band aluminum waveguide (2.5 oz. per foot). The use of waveguide and complete elimination of coaxial lines resulted in a 1.5 db reduction in both transmit and receive losses. Figure 7.2-18 shows a side view of the package with one of the 32-eight way binary combiners visible. The end view shown in Figure 7.2-19 indicates the tight packaging of these devices. The system, including the transmitters, receivers and beam steering unit fits into a rectangular volume 36" long by 30-3/4" wide and 18-1/4" deep occupying a volume of almost 11 cubic feet. At least 1/3 of the volume is not used by the array and will be used for electronic equipment. The support structure is not shown in the layout for the sake of clarity. The rigid waveguide being self-supporting, tends to minimize the need for elaborate structural support. Much of the system will be packed in foam to reduce vibration and shock effects. The system weight including all supports and shock mounts is calculated to be approximately 166 pounds. Table 7.2-3 gives a component breakdown of the weights. A weight goal of 150 lbs. and a 1/3 reduction in volume appears achievable by anticipated improvements in component design.

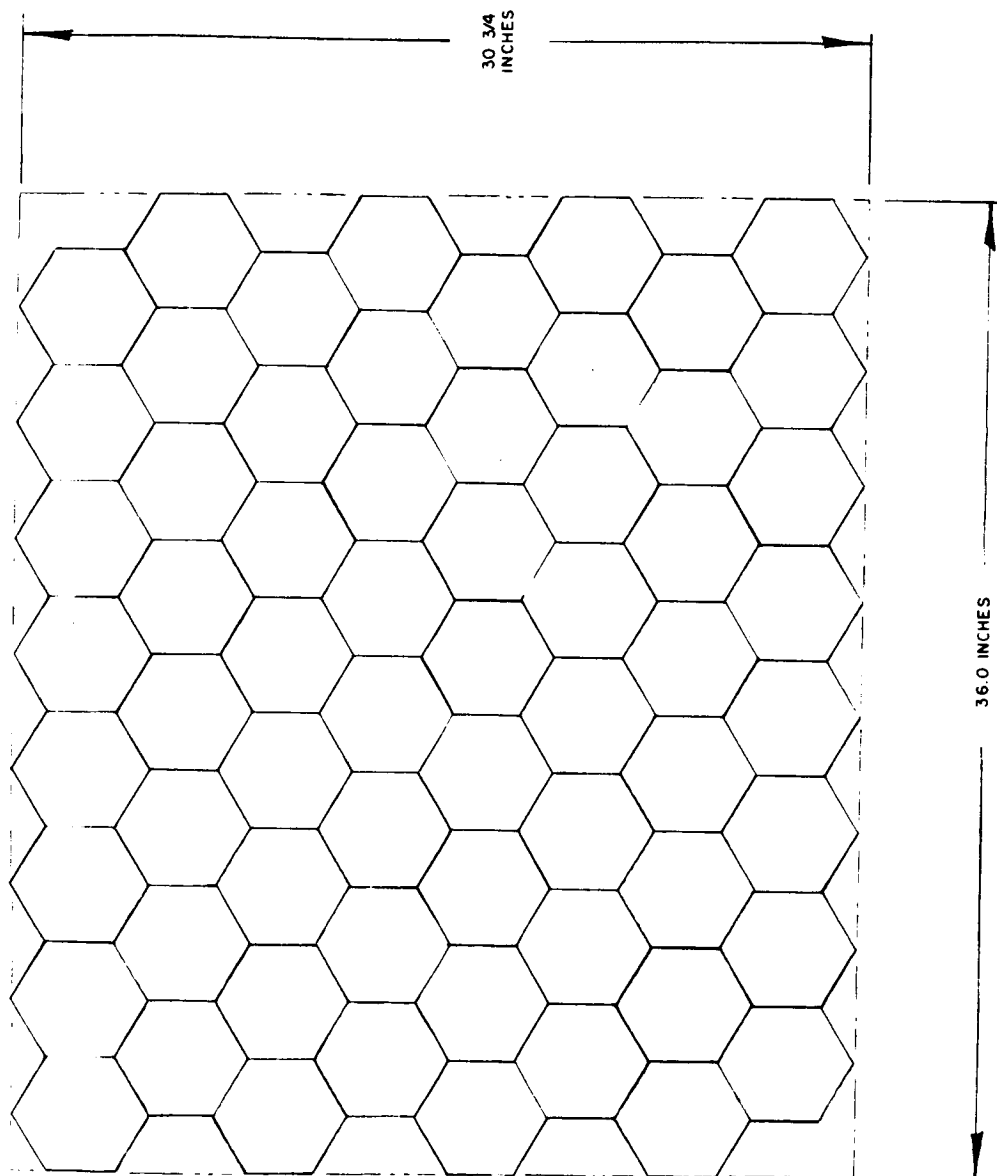


Figure 7.2-17 Plan View of Radiating Elements

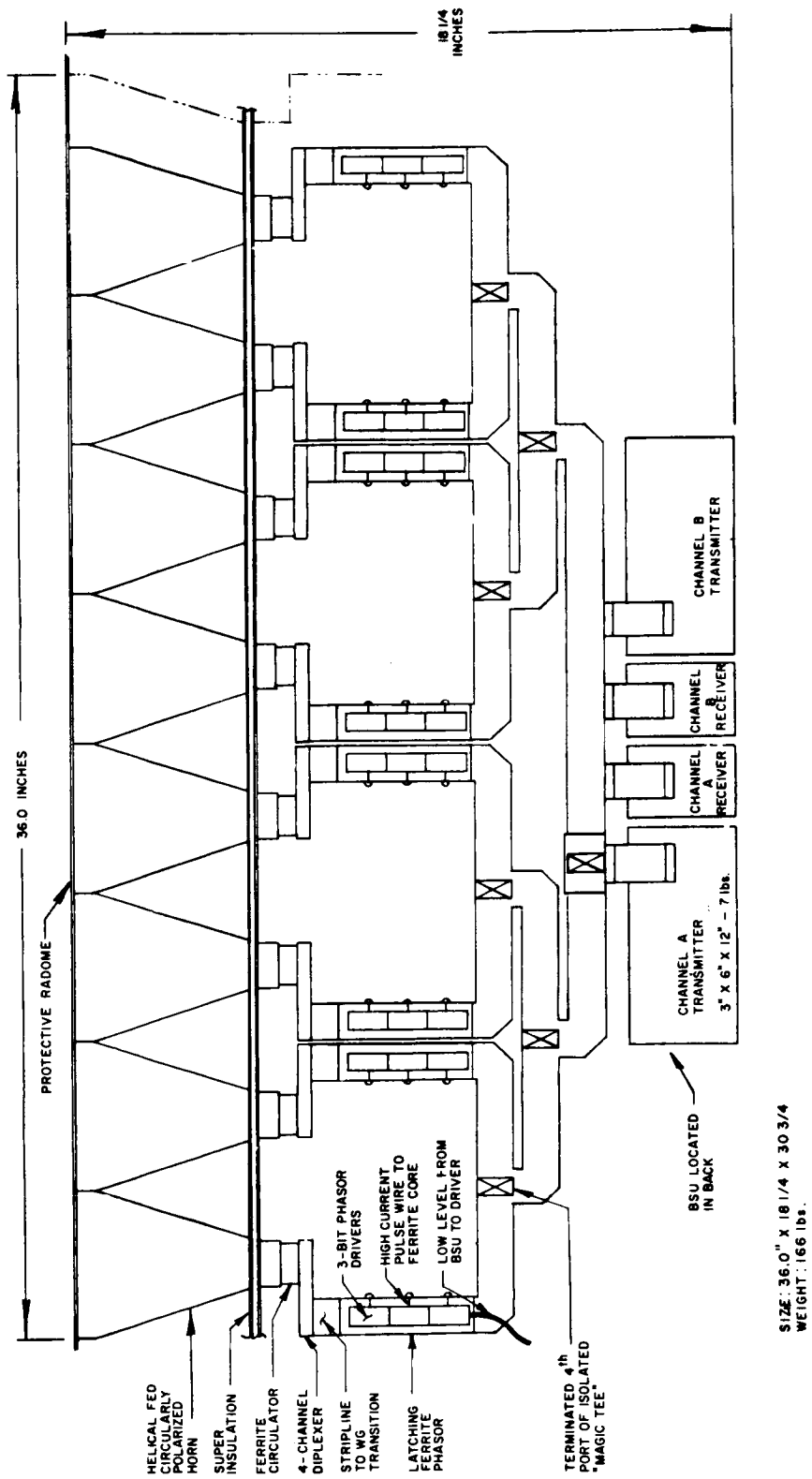


Figure 7.2-18 Side View of Corporate-Fed Array

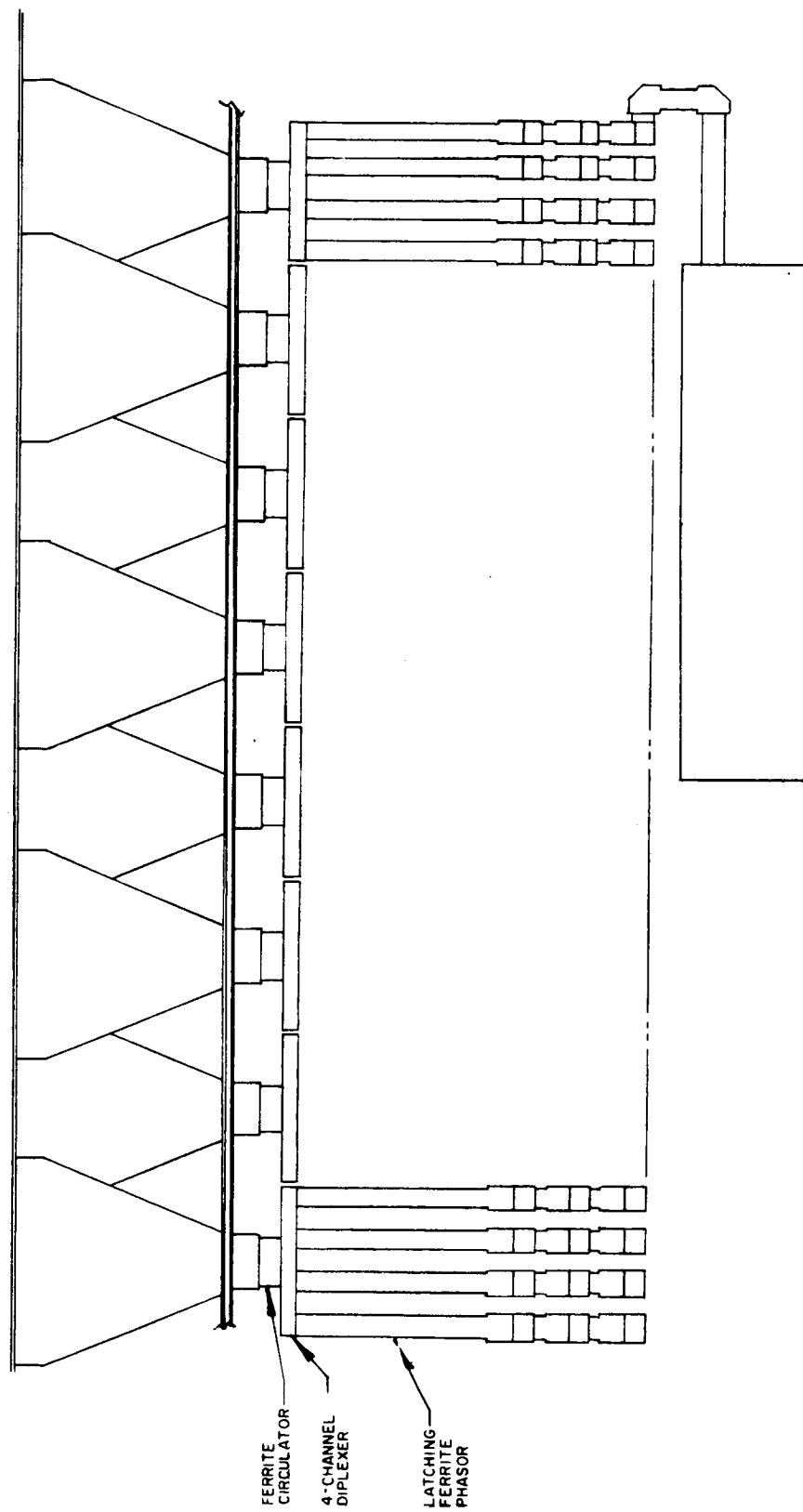


Figure 7. 2-19 End View of Corporate-Fed Array

TABLE 7.2-3 PHASED ARRAY WEIGHTS

	<u>Weight (lbs)</u>
256 Phasors, 64 Quadriplexers	64.0
64 Horns and Support Strut	13.2
64 Diplexer Circulator Package @ 5 oz.	20.0
8 Way Wave Guide Power Dividers	31.5
2 Transmitters (TWT's)	14.0
2 Receivers	1.5
1 Beam Steering Unit and Drivers	15.0
Miscellaneous (Cables, Connectors, Supports)	7.0
	<hr/>
TOTAL	166.2

7.3 COMMUNICATIONS EQUIPMENT

The purposes of the communications equipment are to aid in measuring the antenna performance and to demonstrate the ATS-4 capability to provide advanced communications services. The overall design uses currently available components and proven designs anticipating only improvements in quality and reliability. Since the communications system is complex and inter-related, the discussion to follow is based on the experiments listed in Table 7.3-1.

The transmission parameters indicate that modest satellite receivers, without exotic preamplifiers, will operate with up to 70 db base-band signal-to-noise ratios for measurements of antenna patterns and 40 db signal-to-noise ratios for most of the communications experiments. This performance is repeated on the down link with only 10 watts of RF power from the satellite transmitters and with reasonable ground antennas.

The weight of the satellite equipment is 55 pounds, including 15 pounds which are allocated for redundancy. This is needed for effective performance throughout the life of the satellite. The volume is 1.6 cubic feet maximum, including the redundant elements. The maximum power requirement is about 163 watts and occurs when four of the six transmitters and all of the receivers are operating. With the present plans, this conditions occurs only during the demonstration tests. Standby power is estimated to be 23 watts.

7.3.1 Transmission Parameters

The calculated transmission parameters are based on the assumption that the distance to the satellite is 22,300 statute miles, and that the satellite receivers have a noise figure of 6 db at X-band (4 db at S-band). These parameters, in conjunction with the design values of antenna gains for the 30 foot satellite reflector and phased array, are collectively the basis for the transmission calculations, and are listed by experiment and frequency

TABLE 7.3-1

ENVIRONMENT	UP FREQ.	DOWN FREQ.
1. FM Broadcast relay	8 GHz (R)	100 MHz (R)
2. TV Broadcast relay	8 GHz (A)	800 MHz (R)
3. Teletype link to aircraft one way to aircraft	8 GHz (R)	100 MHz (R)
4. Simplex voice link ground	8 GHz (A)	7.3 GHz (A)
5. Simplex voice link aircraft from ground to aircraft	8 GHz (A)	7.3 GHz (R)
from aircraft to ground	8 GHz (R)	7.3 GHz (A)
6. Satellite Data	2.1 GHz (R)	2.3 GHz (R)
7. Geophysical Data, ground	1.7 GHz (R)	2.3 GHz (R)

(R) - ATS-4 30 ft. reflector

(A) - ATS-4 phased array

in Table 7.3-2. The required bandwidths and signal-to-noise ratios are also listed, as well as the type of modulation used. The performance characteristics are based on standards generated by the FCC for high quality FM and TV broadcast; other parameters are derived from CCIR or MIL Standard 188 for high grade communications links.

The link calculations are indicated in Table 7.3-3 and the results are plotted in Figure 7.3-1, RF Power vs Ground Antenna Gain. The calculations include an 8 - 12db fade margin graded from 100 MHz to 8 GHz.

A complete list, with specific recommendations for RF power and ground antenna gains, is given in Table 7.3-4. The conclusions drawn are that 10 watts of RF power at 7300 MHz, 800 MHz and 100 MHz; and 150 milliwatts at 2300 MHz will perform all measurements and experiments adequately when provided with relatively modest ground antennas.

Table 7.3-4 is a summary of the complete links, including terminal power recommendations, antenna suggestions and received signal levels under the given conditions. For antenna pattern measurements, the AGC of the receivers, both on the ground and in the satellite, is assumed to be a linear AM detector and the source of amplitude data.

7.3.2 Systems Description

General - - The communications system described here is defined as the electronic equipment between antenna parts necessary to perform the experiments discussed previously. There are five basic although inter-related, channels in the ATS-4:

- Monopulse Receiver.
- X-Band, Reflector, Transponder.
- X-Band, Phased Array, Transponders.
- S-Band Transponder.
- Frequency Generator.

TABLE 7.3-2 COMMUNICATION PARAMETERS

Experiment (Direction of Propagation)	Frequency MHz	Reflector Gain DB	Ph. Array Gain DB	Path Attn -DB	Base BW KHz	S/N Des DB	Modulation
TV Broadcast (up)	8000	51	30	202	4500	36	SSB-AM
FM Broadcast (up)					15.0	40	FM
Voice Links (up)					4.0	40	FM
Voice Link (down)	7300	50	29	201	4.0	40	FM
Data (down)	2300	41		191	8.0	15	PSK
Data, Satellite (up)	2100	40		190	0.8	15	PSK
Data, Ground (up)	1700	39		189	0.8	15	PSK
TV Broadcast (down)	800	32		182	4500	36	SSB-AM
FM Broadcast (down)	100	14		164	15.0	40	FM
Teletype (down)					1.0	15	FSK

TABEL 7. 3-3 TRANSMISSION SYSTEMS CALCULATIONS

$$P_t = P_r + L \quad \text{and}$$

$$P_r = P_n + S_n$$

$$L = A + G_s + G_r + L_p \quad \text{and}$$

$$P_n = N_o + N_r \quad \text{then}$$

$$P_t = + N_o + N_r + S_n - A - G_s - G_r - L_p - L_s$$

where

P_t = Transmitter power in dbm

P_r = Receiver input power in dbm

P_n = Receiver noise power in dbm/cycle

S_n = IF signal-to-noise ratio in db

L = System losses in - db

A = Anomolies or fade margin in - db

G_s = Satellite antenna gain in db

G_r = Ground antenna gain in db

L_p = Free space losses in - db

N_o = Noise bandwidth of IF in db over 1 cycle

N_r = Noise power per cycle in dbm

and

$N_r = K T_n$ where T_n is noise temperature

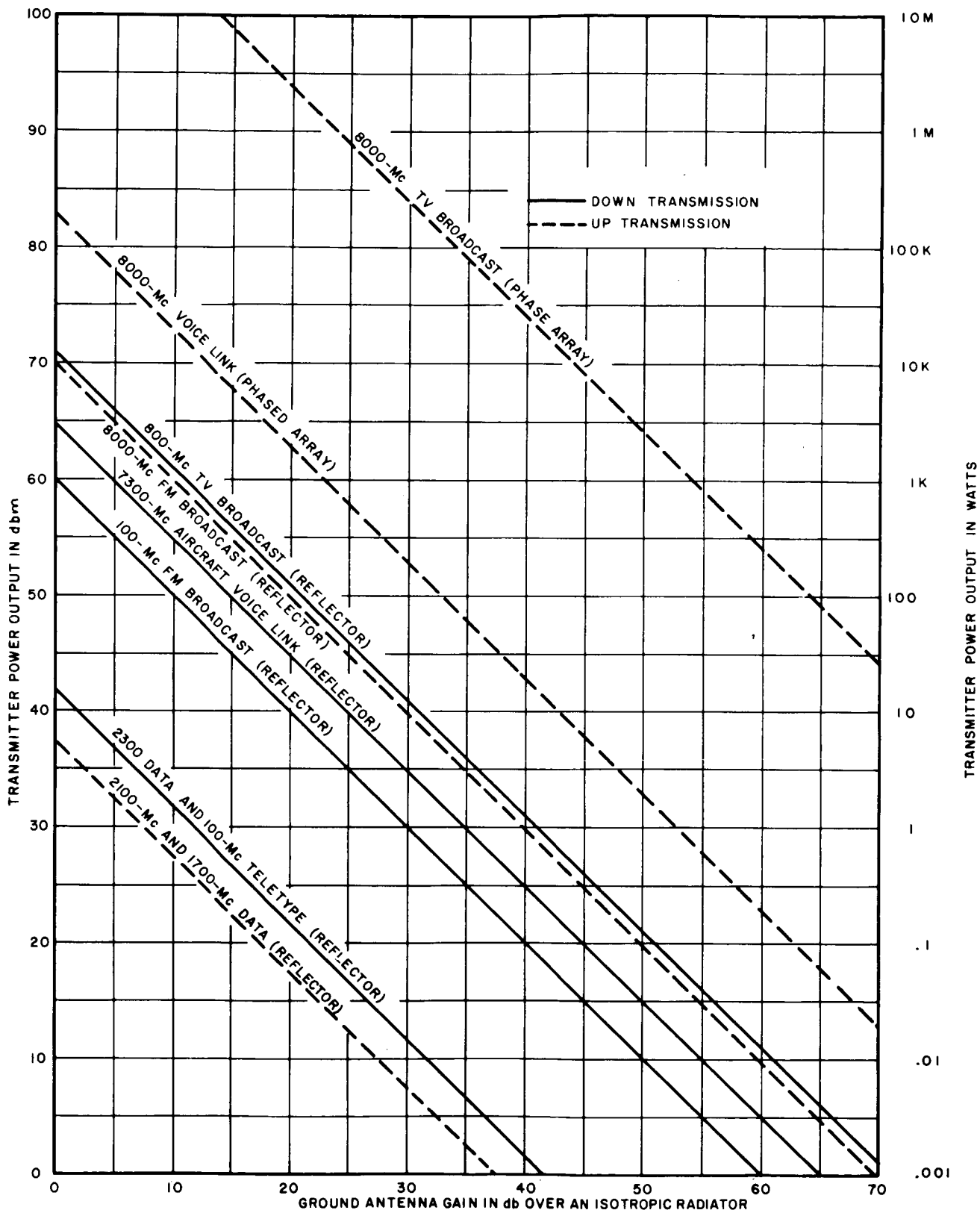


Figure 7.3-1 RF Power vs Ground Antenna Gain

TABLE 7.3-4 SUMMARY OF COMMUNICATIONS SYSTEMS TRANSMISSION PARAMETERS

Use Element	Information Bandwidth (kHz)	Information Signal Noise (db)	Terminal Antenna	Terminal Antenna Gain (db)	Terminal RF Power (dbm)	Satellite Received Power (dbm)	Satellite Transmitter Power (dbm)	Terminal Received Power (dbm)
6000 MHz - Reflector								
Antenna Patterns	0.10	77	2ft. refl.	30	+40	-71.5		
Voice Link (Aircraft to Satellite)	3.5	45.3	1.5ft. array	25	-40	-98.0		
FM Broadcast	15	46.8	2ft. refl.	30	+40	-93.0		
8000 MHz Phased Array								
Antenna Patterns	0.10	54.0	8ft. refl.	43	+40	-100		
Voice Link	3.5	43.3	8ft. refl.	43	-40	-100		
TV Broadcast	4500	38.0	30ft. refl.	54	+60	-70.0		
7300 MHz								
Antenna Pattern (Reflector)	0.10	71.7	8ft. refl.	42			+40	-81
Voice Link to Aircraft (Reflector)	3.5	42.5	1.5ft. array	25			+40	-98
Antenna Pattern (Phased Array)	0.10	41.7	8ft. refl.	42			+40	-101
Voice Link to Ground (Phased Array)	3.5	40.5	8ft. refl.	42			+40	-101
Data Relay								
2300 MHz Antenna Pattern	0.10	46.4	8ft. refl.	32			+21.7	-106.3
Data	8	15.4	2ft. refl.	20			+21.7	-118.3
2100 MHz Antenna Pattern	0.10	47.7	2ft. refl.	19	+36	-105		
Data	0.80	17.6	Dipole	1.6	+36	-122.4		
1700 MHz Antenna Pattern	0.10	47.7	2ft. refl.	17.5	+36	-105		
Data	0.80	17.6	Dipole	1.6	+36	-122.4		
800 MHz								
Antenna Pattern	0.10	74.6	20ft. refl.	31			+40	-87
TV Broadcast	4500	38.4	20ft. refl.	31			+40	-87
100 MHz								
Antenna Pattern	0.10	62.6	3 el. helix	20			+40	-96
FM Broadcast	15	45.5	3 el. helix	20			+40	-96
Radio Teletype	2	15.3	Dipole	1.6			+40	-118.4

Refer to Figure 7.3-2, ATS-4 Communications Systems Block Diagram. The monopulse receiver inputs are the Pitch Error, Roll Error, and the monopulse Sum (Σ) channel. These inputs come from the respective outputs of the monopulse antenna feed. The signals are converted to an IF, amplified and detected in product detectors which are inputs signals to the pitch and error correction controls. Error polarity is derived by referencing the detection process to the sum channel signal. This portion of the block diagram is the monopulse receiver.

The sum channel of the monopulse receiver is also the receiving portion of the X-band reflector transponder. A second output of the sum channel IF is connected to a channel separation filter which will pick out either the FM broadcast signal and retransmit via the 100 MHz channel or the voice link signal for retransmission via the 7.3 GHz channel. The 7.3 GHz channel input can be switched to other X-band transponders, depending on the experiment requirements, eg, for purposes such as receiving signals on one of the phased array beams, or for retransmitting to an aircraft on the reflector beam.

The phased array X-band transponders consist of two identical but operationally independent systems. The inputs are connected to the A and B receive beams of the phased array at 8 GHz and the outputs are connected to the A and B transmit beams of the phased array at 7.3 GHz. The output of the A channel IF amplifier is also connected to the 800 MHz channel for re-transmitting TV broadcast signals.

The S-band signals, received at 1.7 GHz or 2.1 GHz are converted to IF and amplified. The signal processor will accept signals on a first come, first served basis. The detected signal is remodulated on the 2.3 GHz oscillator and sent back down via the transmitter S-band antenna.

The frequency generator, Figure 7.3-3, provides all the local oscillator signals required to convert input signals to IF and then reconvert

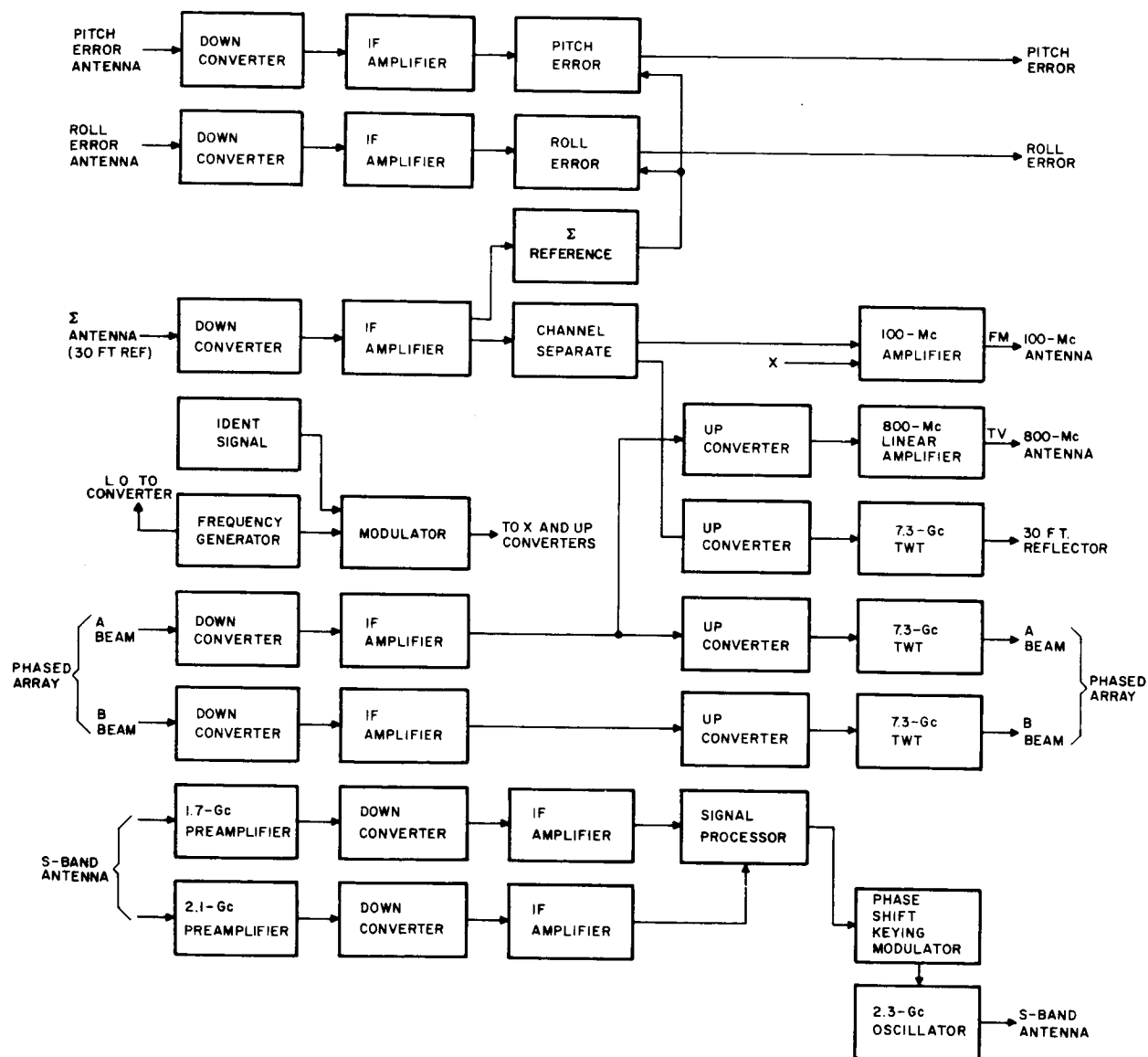


Figure 7.3-2 ATS-4 Communications Systems

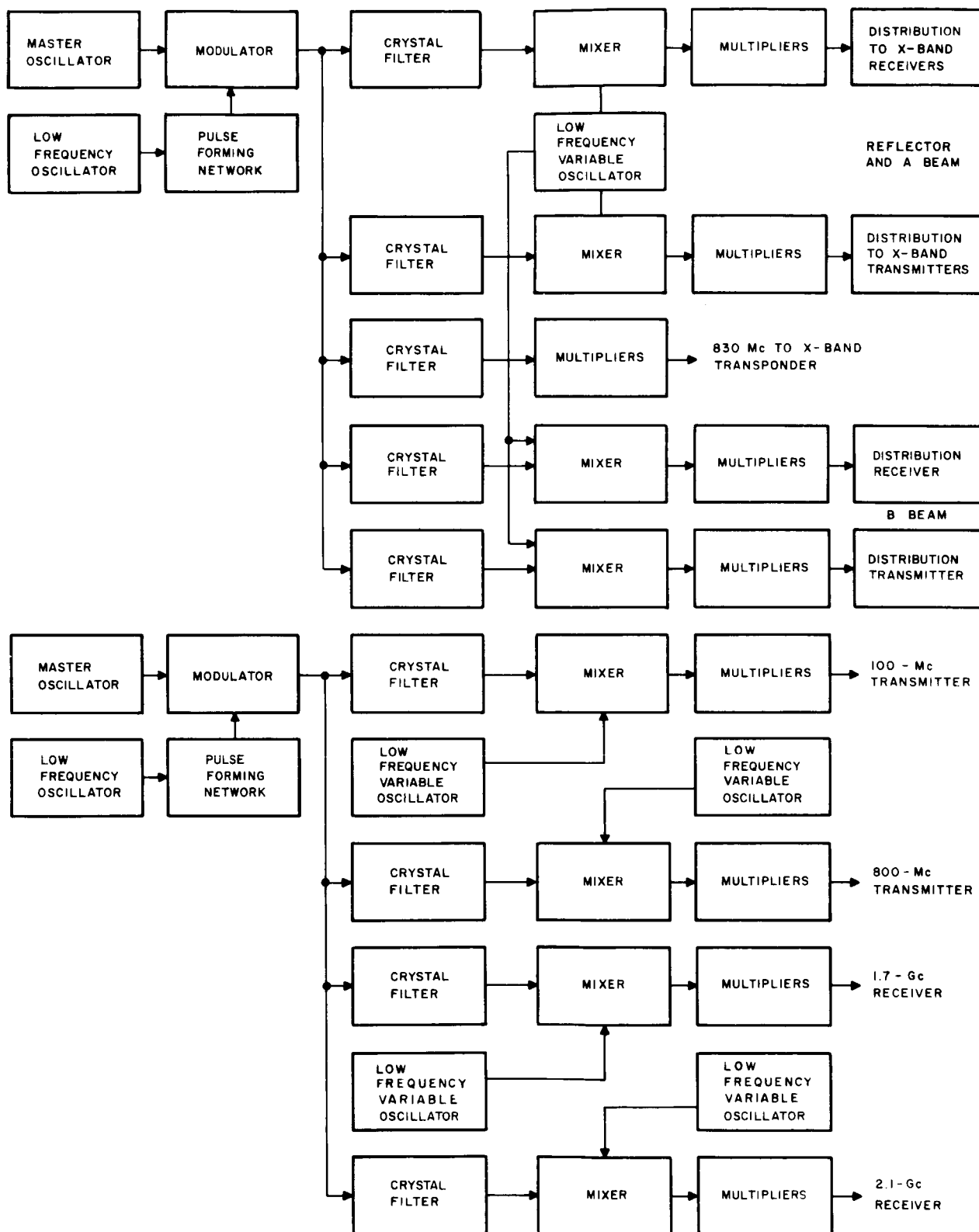


Figure 7.3-3 Frequency Generator

to transmitting frequencies. It also generates a common signal for the transmitting mode of the transponders when antenna pattern measurements are made. When the satellite is in the transmitting mode, there will be a common identifying signal (30% amplitude modulated) on the transmitted carriers.

The communications system has operational constraints both to limit peak power drain and to avoid ambiguity in any of the experiments. The monopulse receiver can be operated independently of any other function in the communications complex.

The frequency generator has two parts, one for X-band operations and another for the remaining functions. Either one can be turned off when not in use. Approximately 10% tuning is shown over the complete receiving and transmitting bands with a frequency offset between A and B beams and with the monopulse receiver tuning with the A beam. This precludes the possibility of tracking on B beam frequency, but also prevents A and B beam from becoming co-channel tuned.

The satellite is constrained to the following combinations:

- TV relay and S-Band.
- FM, voice link, teletype and S-band.
- All receivers on, transmitters off.
- All transmitters on, receivers off.

Preliminary Reliability Study: - - The foregoing general description does not attempt to show redundancy requirements to assure a reliable performance over the expected life of the satellite. While the plan is to use solid-state design to the fullest extent possible, it is necessary to use TWT amplifiers for the 10 watt X-band outputs. Present thinking is to use coaxial-type, high-reliability vacuum tubes for the 800 MHz amplifier.

With the above component stipulations, a preliminary reliability analysis was performed on the communications equipment, with reference to the functions being performed as specified in the system operations. Estimates of the probability of success of the functions required of the communications equipment were made using the following relationship:

$$P_s = \exp \left[- \left(\lambda_o t_o + \lambda_s t_s \right) \right]$$

where

λ_o = Operating hazard rate in failures per million hrs.

λ_s = Non-operating hazard rate in failures per million hrs. (fpmh)

t_o = Operating time in hours

t_s = Non-operating time in hours

For purposes of this analysis, the non-operating hazard rate was determined from the relationship $\lambda_s = \frac{1}{10} \lambda_o$. The operating time (t_o) was estimated to be about 3 hours per day which is cumulatively representative of approximately 1/8 of the total time. The total time (t_r) was assumed to be 2 years. Therefore, the above equation for the probability of success becomes

$$P_s = \exp \left\{ - \left[\left(\lambda_o \frac{t_r}{8} \right) + \left(\frac{\lambda_o}{10} \right) \left(\frac{7}{8} t_r \right) \right] \right\}$$

The parts comprising each of the major subassemblies were estimated and the hazard rates used for the various types of parts are listed in Table 7.3-5. These hazard rates are based on usage of high reliability parts and are considered to be achievable by the 1970 time period. Some of these hazard rates are presently being realized with high reliability Minute-man parts.

Table 7.3-6 indicates the probability of success for the seven major functions. These are independent values based upon equipment hazard rates

TABLE 7.3-5

Part	Basic Failure Rate (fpmh)
Transistor	0.02
Diode	0.01
Resistor	0.001
Capacitor	0.001
Coils	0.005
Mixer Diode	0.10
Recovery Diode	0.10
RF Transformer	0.10
Crystal	0.10
Varactor	25.0

TABLE 7.3-6

Function	MTBF	Reliability
Monopulse Receiver	82,300	0.9734
100 MHz Output	154,500	0.9858
30 ft. Reflector Output	20,100	0.8973 *(0.9798)
800 MHz Antenna	128,000	0.9829
Phased Array (A Beam)	20,100	0.8973 *(0.9798)
Phased Array (B Beam)	20,100	0.8973 *(0.9798)
S-Band	111,300	0.9804

* Using a standby - redundant TWT.

utilized for each function output.

Monopulse Receiver - - The overall block diagram has been expanded to a modular level which is shown in Figures 7.3-4 to 7.3-10, including transfer parameters. The series numbers shown in each block refer to the module specifications provided in Appendix 7D.

In Figure 7.3-4, the monopulse receiver is shown in detail with the gain or loss of each module also indicated. The sum channel is identical in performance and components to the A beam and B beam channels.

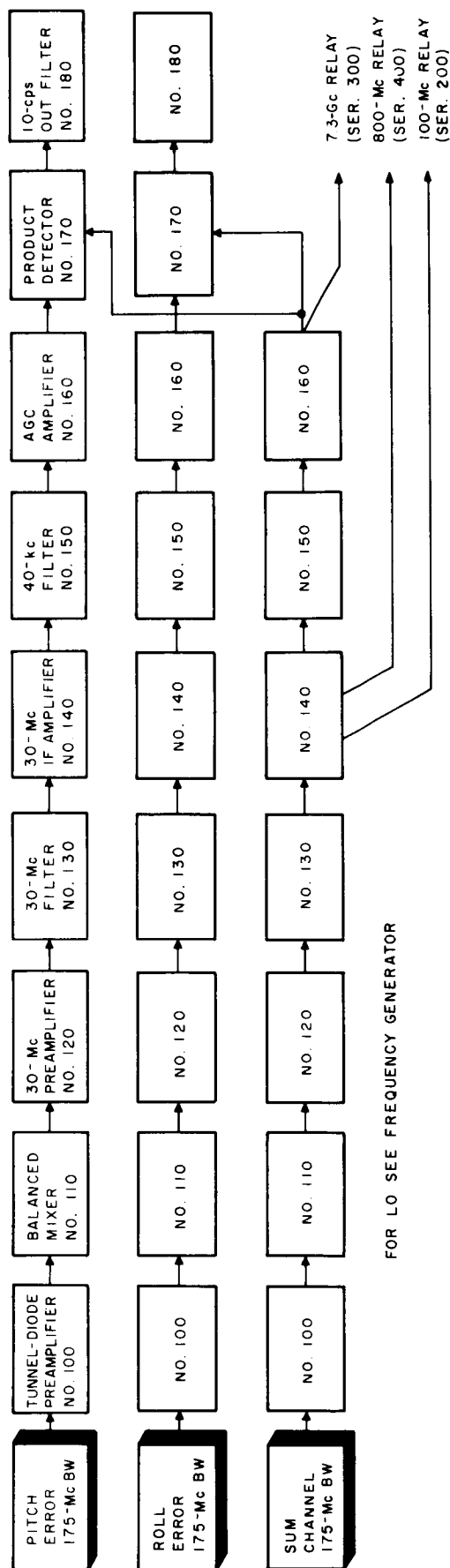
Some of the features to be noted are the tight AGC required for the monopulse receiver operation. These IF amplifiers and the AGC circuits are called out in all the receiving portions of the system.

Another point is the signal-to-noise ratio shown at the output of the error channels. With an input signal level of -120 dbm, the sum channel output is -1 dbm where the noise level and bandwidth are -49.4 dbm and 10 hertz, respectively. This is a satisfactory S/N for 0.003 degree accuracy of the monopulse system.

Phase and amplitude tracking, necessary for the monopulse receiver, is given for each module in the specifications.

X-Band Reflector Transponder - - The X-band reflector transponder has two channels, 100 MHz output and 7.3 GHz output. Referring to Figure 7.3-5, the 165 KHz filter (#210), a part of the channel separation filter, extracts the FM signal and converts it from the 30 MHz IF used here, to the 100 MHz transmitting frequency. The 100 MHz signal is amplified to 10 watts and fed to the antenna.

In Figure 7.3-6, the signal was taken from the 40 KHz voice channel filter (see Figure 7.3-3) and double converted to X-Band. Double conversion is necessary to facilitate filtering all spurious responses of the mixers. The 7.3 MHz signal is amplified to 10 watts by a TWT and fed to the antenna.



Block	Block	Block	Block	Block	Block	Block	Block	Block	Block
GAIN- LOSS IN db	+10	-6	+16	-5 NR-15	+80 AGC 59db	-8 NR-31.4	+32	0	0 NR-36
5 OUT- dbm IN -60dbm IN -120dbm	-50 -110	-56 -116	-40 -100	-45 -105	-24 -25	-32 -33	0 -1	0 -1	0 -1
NOISE dbm NF 6db IN -86 dbm	-76	-82	-66	-86	-65 -6	-104.4 -45.4	-72.4 -13.4	-72.4 -13.4	-108.4 -49.4
ERROR CHANNEL BORESIGHT -160dbm	-150	-156	-140	-145	-65	-73	-41	-41	-41

NR = FILTER NOISE POWER REDUCTION

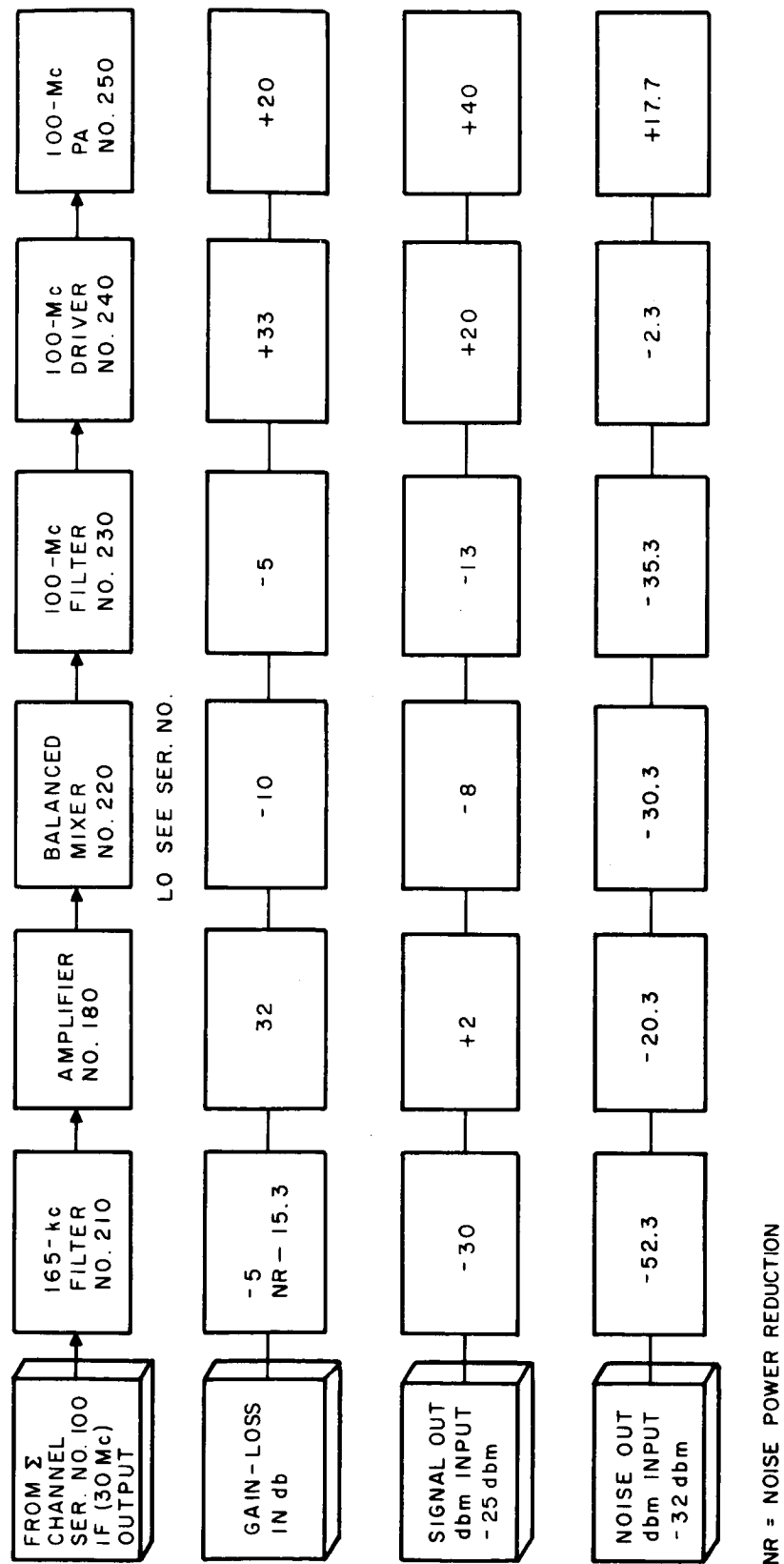


Figure 7.3-5 100 MHz Relay Transfer Characteristics - Series 200

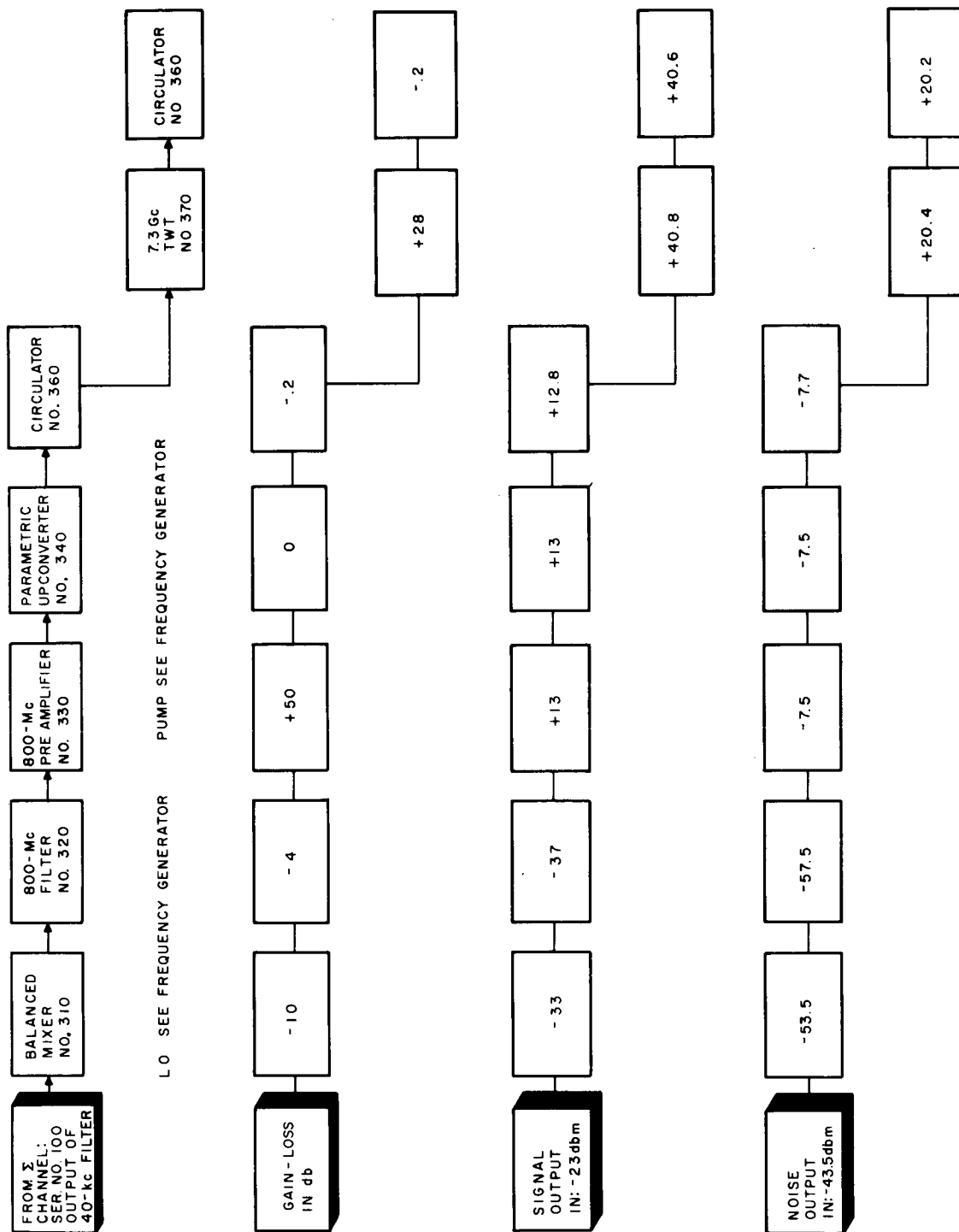


Figure 7.3-6 X-Band Transponder Output, Reflector and Phased Array, Transfer Characteristics - Series 300

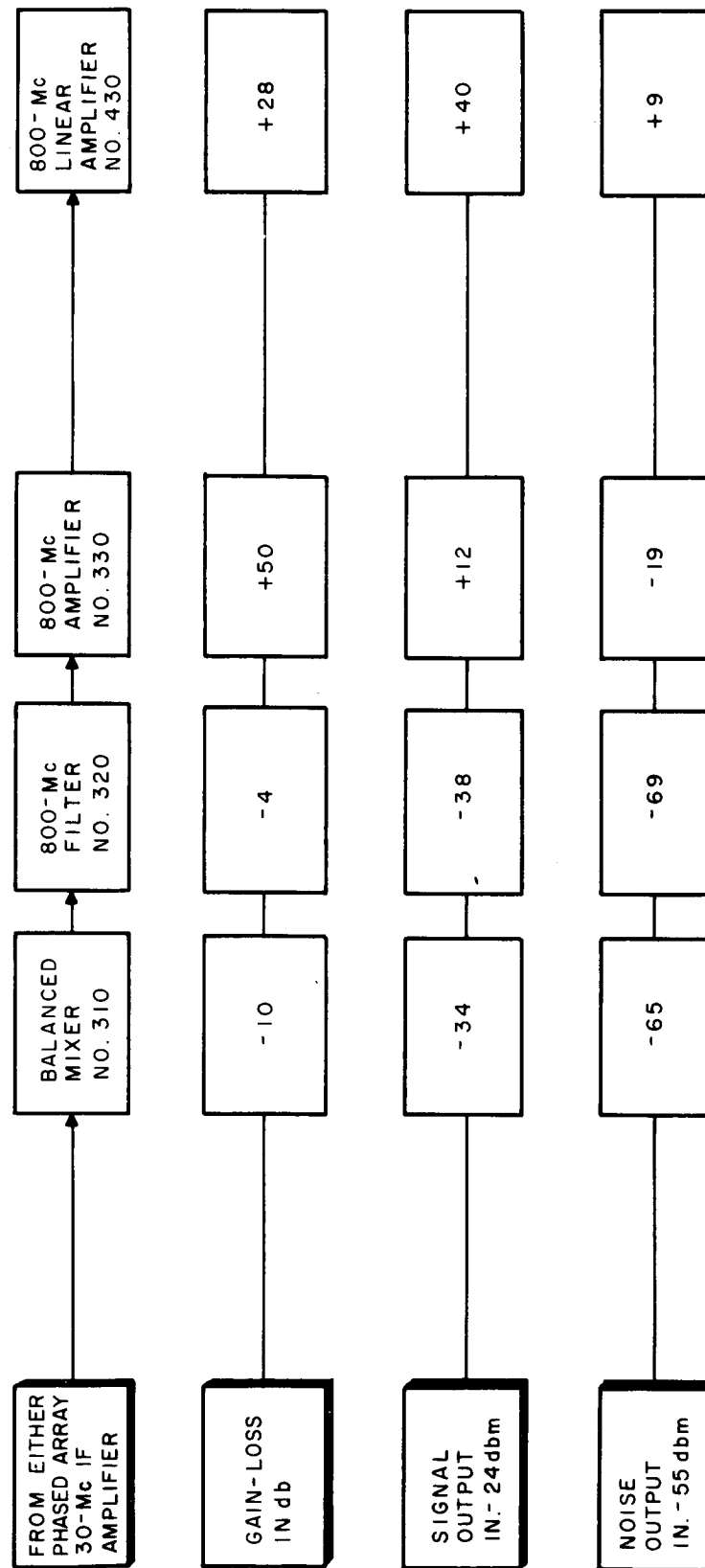


Figure 7.3-7 800 MHz Relay Transfer Characteristics - Series 400

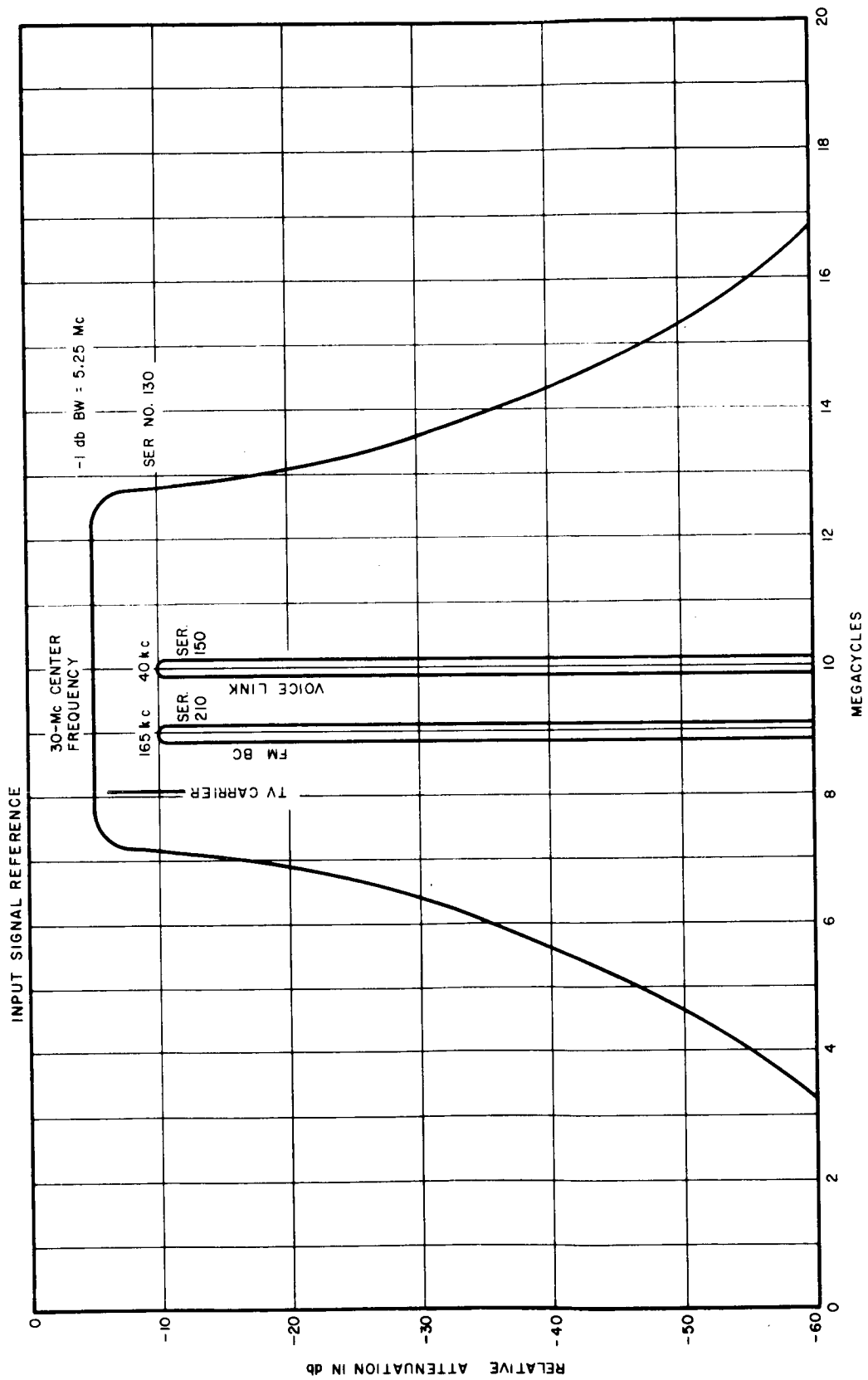


Figure 7.3-8 Filter Response

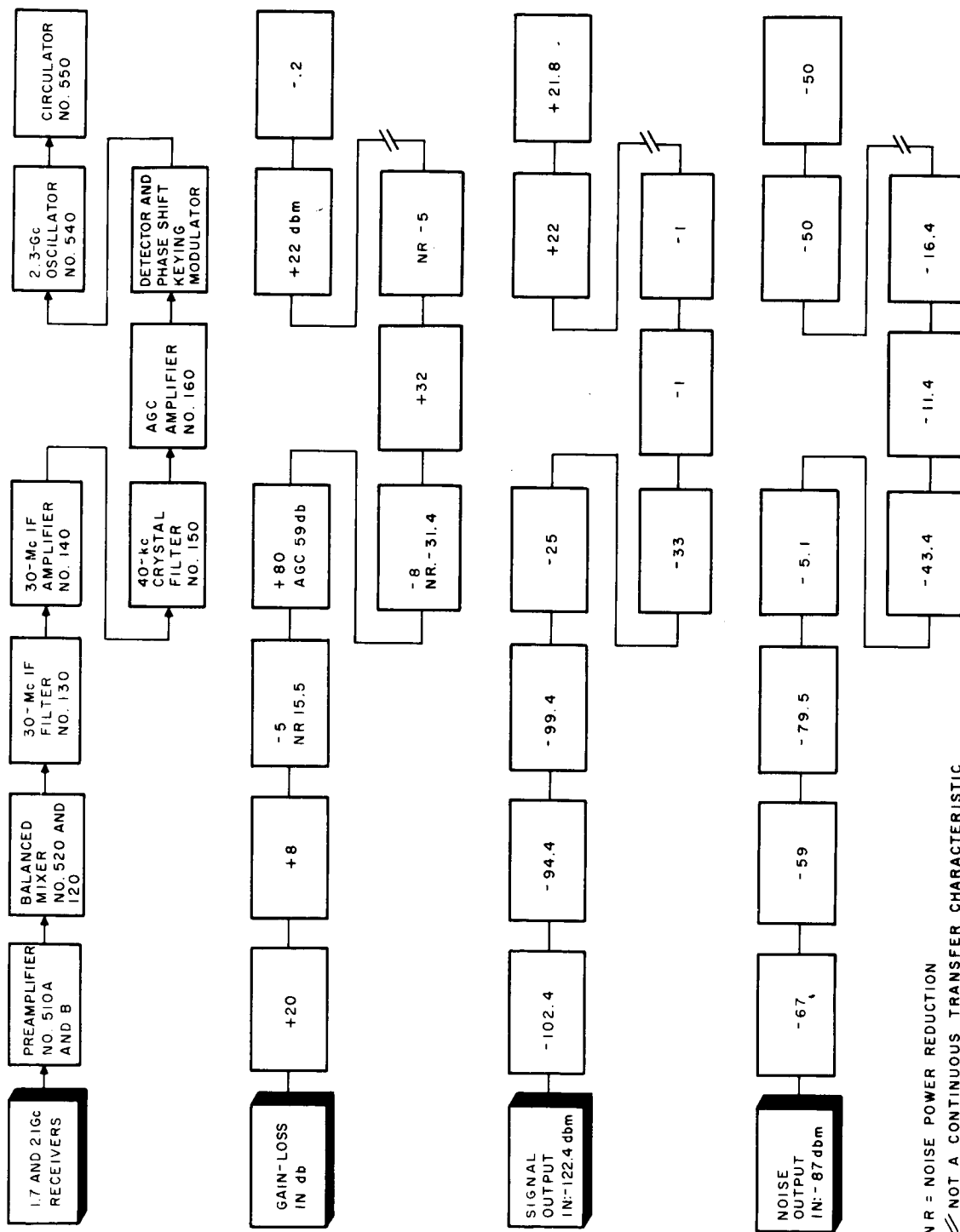


Figure 9 S-Band Data Link Transfer Characteristics - Series 500

X-Band Phased Array Transponder -- Figure 7.3-6 also describes the A and B beam channel transponders for the 7.3 GHz output; the difference between the reflector and phased array being in the antennas used. Figure 7.3-7 shows the conversion of the TV signal to the 800 MHz carrier frequency. The TV signal is picked off at the output of the A beam channel IF amplifier (see Figure 7.3-3). The filter alignment placing the TV carrier and picture, FM broadcast and the voice link into the IF passband is shown in Figure 7.3-8.

S-Band Transponder -- The S-band transponders have basically the same receivers that the X-band transponders have. One half of the receiving system is shown in Figure 7.3-9. The signal is detected in the signal processor (detector-PSK modulator module) which will detect the signal from either receiver while blocking the unused receiver. It then remodulates the data on the 2.3 GHz oscillator signal for transmitting down.

Frequency Generator -- Half of the Frequency Generator is shown in Figure 7.3-10. A spectrum is generated by mixing the output of a high frequency master crystal controlled oscillator which has had its signal converted to a narrow pulse (representative frequencies are shown in Figure 7.3-10). A series of crystal filters (see Figure 7.3-3) selects the spectral frequencies needed. These signals are, in turn, mixed with a low frequency variable frequency oscillator which will allow for approximately a 10% tuning range. In this arrangement, the monopulse receiver and A beam are on the same frequency, while the B beam is offset. Also note that tuning of the receivers and transmitters is performed simultaneously.

The low frequency VFO which provides the tuning, can be removed if it is later decided that a fixed frequency operation is adequate. Removal of these elements does not alter the basic design.

The overall frequency stability is entirely dependent upon the master oscillator since, percentagewise, neither the low frequency crystal oscillators

nor the VFO contribute any appreciable frequency drift to the final signal.

Figure 7.3-11 shows the various multiplier chains that are needed to come up to the required local oscillator frequencies and signal levels for the mixers. The local oscillator signals to the monopulse receiver are derived from a common chain with a constant phase and amplitude, and with 40 db isolation between receiver channels.

A complete set of preliminary modular specifications are given in Appendix 7D. These specifications are key numbered to the block diagrams, Figures 7.3-3 through 7.3-10.

7.3.3 Weight, Volume, and Power Summary

The weight, volume, and power is detailed in the modular specifications. The total weight is 55 pounds, with redundant units. The volume is about 1.6 cubic feet with redundancy. No attempt has been made to specify ultra miniature parts at this time; however, where reliability advantages can be had by the use of molecular circuits, these will be investigated and used.

The power drain is a total of 250 watts which includes maximum power drain by the crystal oscillator ovens. With the present plan, the peak power requirements will not exceed 160 watts. Standby power will be a peak of 23 watts.

Table 7.3-7 is a weight breakdown of the individual components in the communication system.

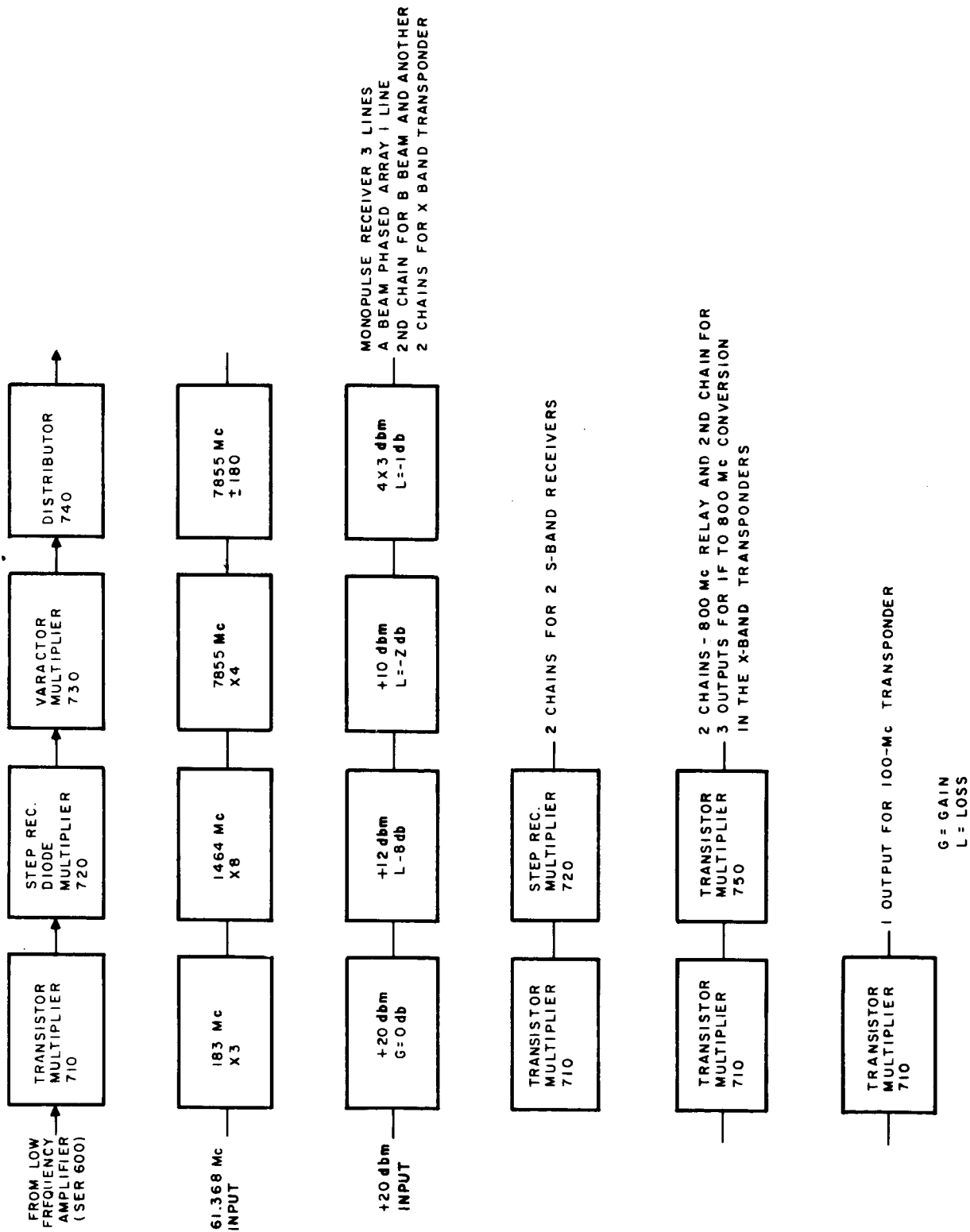


Figure 7.3-11 Multipliers in Frequency Generator, Representative Transfer Characteristics - Series 700

TABLE 7.3-7 COMMUNICATIONS EQUIPMENT WEIGHTS

	Weight (lbs)
X-Band down and up converters	2.50
100 MHz IF amplifiers	2.60
1.7 GHz Preamplifiers	0.37
Monopulse attitude error and detector	1.12
Identification signal	0.25
Modulator	0.25
Frequency generator	2.00
Stand down converter	1.00
800 MHz up converter	0.37
Signal processor & PSK mod.	0.50
2.3 GHz oscillator	3.00
100 MHz amplifiers	3.00
800 MHz amplifier with power converter	6.00
TWT with power supply	7.50
Channel separation filters and IF filters	2.00
Boxes, connectors, RF gasketing, cables, brackets, switches, etc.	7.54
Redundant Elements	15.00
	<hr/>
TOTAL	55.00

7.3.4 System Performance Summary

The system performance is described in the following design goals:

<u>Receivers</u>	7 units
	Monopulse Receiver, 3 channels
	A Beam, X-Band
	B Beam, X-Band
	S Band, two channels

<u>Transmitters</u>	6 units
	X-Band, Reflector
	X-Band, A Beam
	X-Band, B Beam
	S-Band
	UHF Band
	VHF Band

<u>Frequency Stability</u>	1 part in 10^6 long term, -20° to $+65^{\circ}$ C.
----------------------------	---

NOTE: A Beam and B Beam channels are not to be tuned to the same frequency.

Monopulse Receiver

Operating Frequency	7650 MHz to 8000 MHz
Error Channels	2 (Pitch & Roll)
Sensitivity	-120 dbm
Error Output Bandwidth	10 hertz
Signal-to-Noise Ratio (Sum Channel)	40 db min. for -120 dbm input
Error Sensitivity	.003 degrees max. at -120 dbm input
Saturated Error Output	1 volt

X-Band Receivers (Sum channel, A Beam, B Beam)

Operating Frequency	7650 MHz to 8000 MHz
---------------------	----------------------

IF Frequency	30 MHz
Bandwidth (IF)	1 db 5.25 MHz
	3db 5.55 MHz
Noise Figure	6 db
IF Output	0 dmb

S-Band Receivers

Operating Frequency	1. 1600 MHz to 1800 MHz
	2. 2000 MHz to 2200 MHz
Bandwidth (IF)	40 KHZ
(Baseband)	800 Hz
Noise Figure	4 db

X-Band Transmitters

Operating Frequency	7300 MHz to 7650 MHz
Bandwidth (IF)	40 KHz
Power Output	10 watts
Noise & spurious response	-50 dbm or better

S-Band Transmitter

Operating Frequency	2200 MHz to 2400 MHz
Bandwidth (IF)	8 KHz
Power Output	150 milliwatts
Noise and spurious response	-50 db or better

VHF Transmitter

Operating Frequency	95 MHz to 105 MHz
Bandwidth (IF)	165 KHz
Power Output	10 watts
Noise and spurious response	-50 db or better

APPENDIX 7A

FOUR PARABOLOID OFF-SET FEED CONFIGURATION

A square array of four paraboloids fed in an off-set arrangement was studied as an alternate to the conventional prime focus and Cassegrain configurations. The configuration is shown in Figure 7A-1. The principal advantage of the off-set configuration is that it has very little blockage because of the offset-position of the feed. Generally, this is not significant in a well designed conventional system because the blockage is small to begin with and any savings obtained in the offset configuration are usually balanced out by increased spillover losses. It is also difficult to achieve a symmetrical aperture distribution because most of the spillover occurs at the dish edge furthest from the feed. There is, however, an advantage in the present case where spacecraft design constraints result in a feed support mast which contributes a rather large amount of blockage loss. The difference in efficiency between the two systems is now approximately the feed mast contribution. The expected gain and efficiency of the off-set configuration is shown in Table 7A-1. Computations are based on the use of four 15 foot paraboloids, which provide the same radiating aperture as the single 30 foot paraboloid. Since the efficiency of the four dish configuration is greater, gain equivalency in the two systems requires 13 foot paraboloids, rather than 15 foot paraboloids. The expected gain and efficiency of the 100 MHz antenna is not shown in Table 7A-1 because it is impractical to feed the 4-paraboloid configuration with off-set feeds at 100 MHz. The reason for this is the extremely small electrical size of the paraboloids. The theoretical pattern of a 15 foot paraboloid with a 10 db tapered distribution is shown in Figure 7A-2. The polar angle includes a frequency variable which generalizes the pattern over the operating frequency bands. Figure 7A-3 is the radiation pattern of

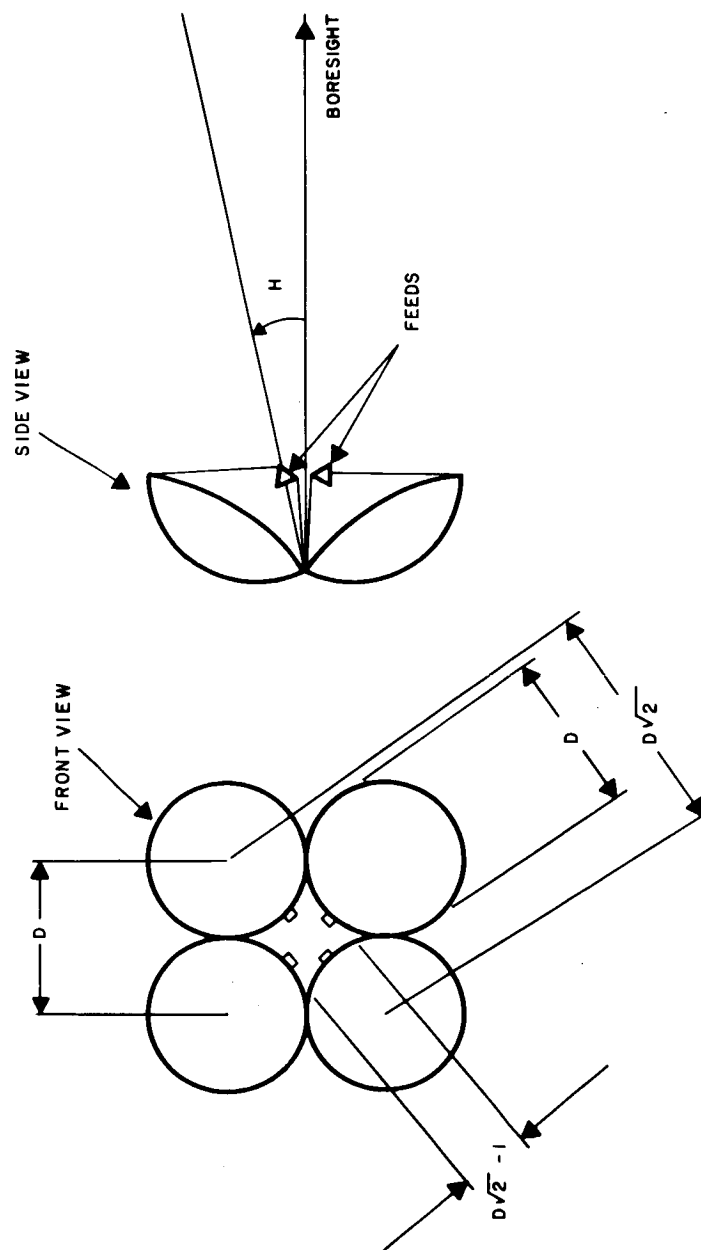


Figure 7.A-1 Four Paraboloid Offset Feed Configuration

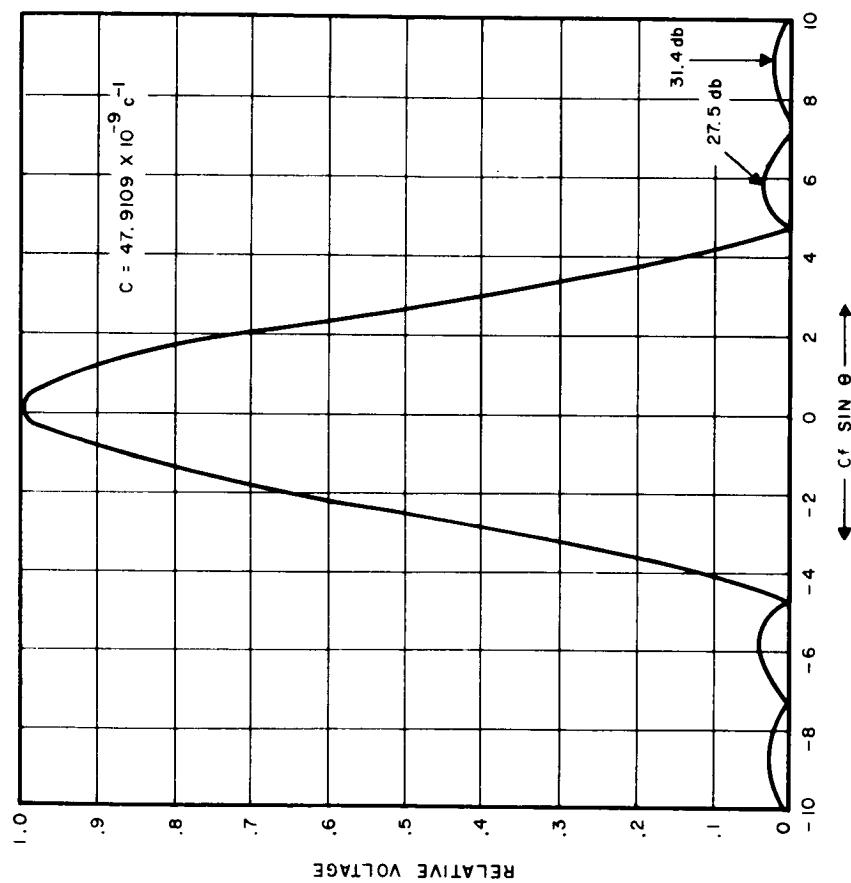


Figure 7.A-2 Radiation Pattern of a 15-Foot Paraboloid 10 db Tapered Distribution

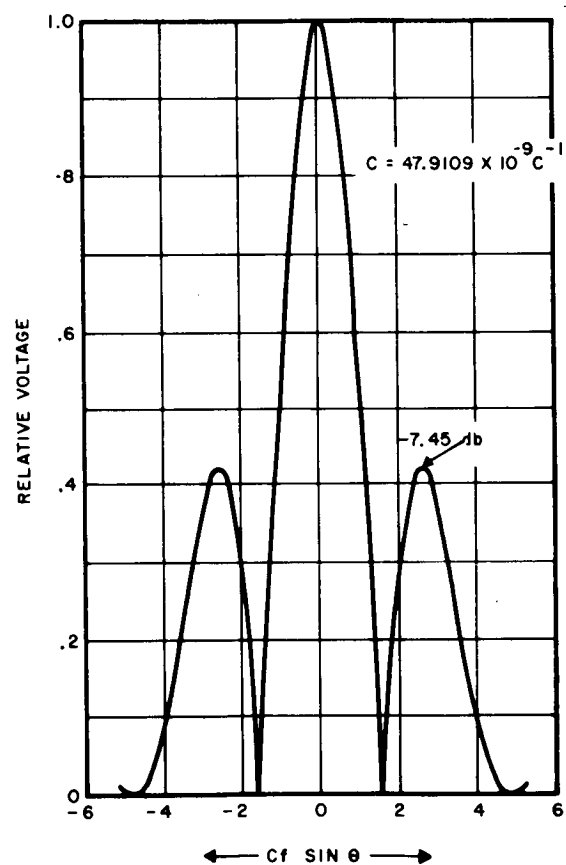


Figure 7.A-3 Radiation Pattern Four Paraboloid Array

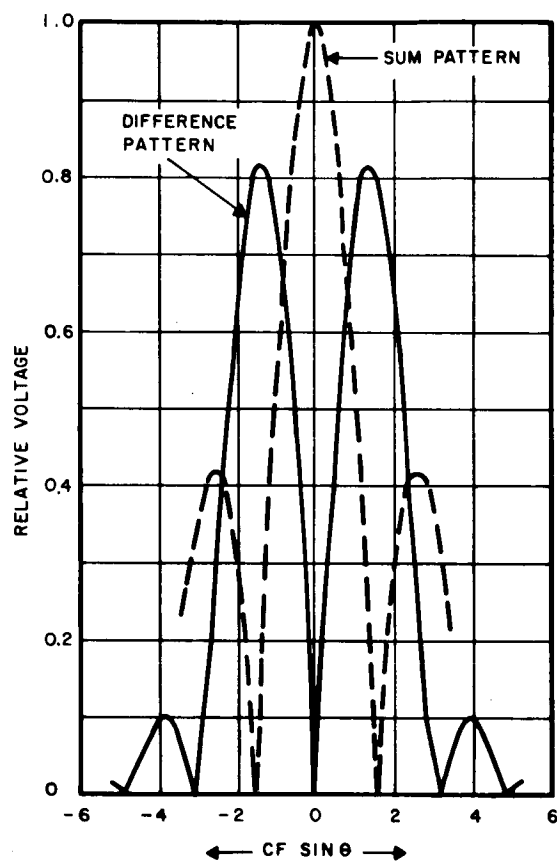
the 4-paraboloid array in the plane of minimum reflector separation. The extremely high sidelobe is a grating lobe resulting from too great a separation between the dishes. Although this pattern is not particularly attractive because of the high sidelobe, the monopulse pattern of the array is excellent; this is shown in Figure 7A-4. A 4-paraboloid configuration with log-periodic feeds has been designed by Radiation Systems, Inc. and is currently in use as a broadband telemetry antenna with a monopulse tracking capability.

The scanning performance of the 4-dish configuration, using array phasing techniques to scan the beam, was also studied. Figure 7A-5 indicates the loss of gain and the increase in sidelobe level as a function of beam scan. The sidelobe performance is especially poor with a level of only -3 db resulting from an extremely small scan of $1/2$ beamwidth. These results, however, are primarily caused by the high on-axis sidelobe level rather than the scanning function.

A reduction in gain occurs in the conventional configuration because of inaccuracies in the reflector surface and in the feed location. Since there are four small surfaces rather than a single large surface to consider, it appears as if the tolerance requirements of the 4-dish configuration are less stringent. This, however, is not true because the tolerances must be held over the entire configuration in order to maintain a uniform phase distribution for the combined aperture.

The cross polarization component of the single paraboloid is lower than that of the 4-reflector configuration because there is less cross polarization cancellation in the off-set configuration. In the single reflector, the cross polarization component appears as a lobe in the 45 degree plane of the radiation pattern. This is the so called Condon¹ lobe.

¹ Condon, E. W., 1941 "Theory of Radiation from Paraboloid Reflectors," Westinghouse Report No. 15, September 24, 1941



$$C = 47.9109 \times 10^{-9} \text{ c}^{-1}$$

Figure 7A-4
Monopulse Radiation Pattern of the Four Paraboloid Array

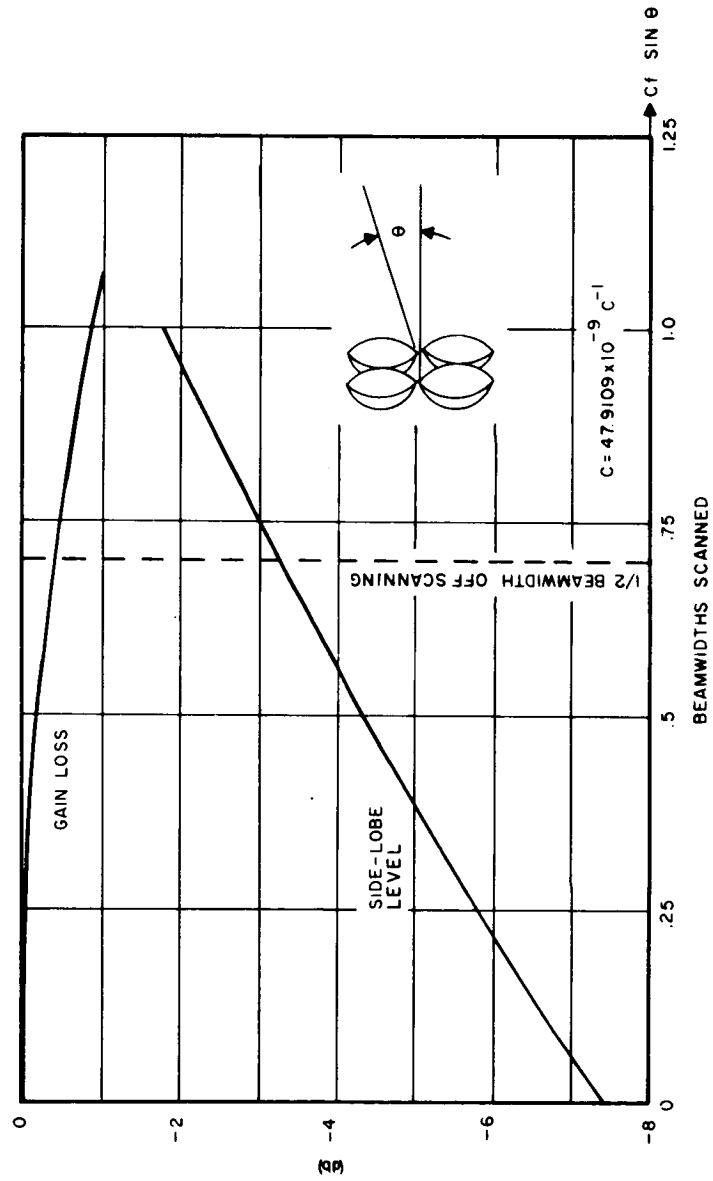


Figure 7A-5 Four Paraboloid Array Scanning Performance

TABLE 7A-1

FREQUENCY	GAIN (db)	EFFICIENCY
X-BAND	54.4	52%
S-BAND	43.5	57%
800 MHz	35.0	54%

APPENDIX 7B

IONOSPHERIC EFFECTS ON WAVE POLARIZATION

A change of wave polarization is produced by different indices of refraction (N) for the ordinary and extraordinary modes of propagation. In the case where the direction of propagation (Poynting vector) and the earth's magnetic field vector are parallel, propagation is called longitudinal; when the magnetic field vector and the Poynting vector are normal, propagation is called transverse. The characteristic polarization of the ordinary mode for longitudinal propagation is left-hand circular; for the extraordinary mode it is right-hand circular. The characteristic polarization of the ordinary mode for transverse propagation is linear with the electric field vector oriented parallel to the earth's magnetic field vector; for the extraordinary mode it is linear with the electric field vector oriented normal to the earth's field.

Polarization rotation (Faraday Rotation) occurs during longitudinal propagation of a linearly polarized wave because the left-hand and right-hand circularly polarized components, in which a linearly polarized wave can be decomposed, have different phase velocities. The polarization rotation which occurs during passage through a differential layer of the ionosphere is

$$d\Omega = \frac{K_o}{2} \left(N_o(z) - N_x(z) \right) dz \quad (1)$$

where K_o is the free space propagation constant and N_o , N_x are the indices of refraction of the ordinary and extraordinary modes. For a complete passage through the ionosphere the amount of rotation is given by

$$\Omega = \frac{K_o}{2} \int_{z_1}^{z_2} \left(N_o(z) - N_x(z) \right) dz \quad (2)$$

The indices of refraction are functions along the path z of the electron density and the magnetic field strength. Computations of Faraday rotation

based on (2) also require knowledge of the temporal variation of the electron density and magnetic field. The Appleton-Hartree dispersion equation¹ gives the indices of refraction as

$$N^2 = 1 - \frac{X}{(1 - jZ) - \frac{Y_T^2}{2(1 - X - jZ)} \pm \left[\frac{Y_T^4}{4(1 - X - jZ)^2} + Y_L^2 \right]^{1/2}} \quad (3)$$

with the (+) sign denoting N_o^2 and the (-) sign denoting N_x^2 . X , Z , Y_T and Y_L respectively involve ratios of the plasma, collision, transverse gyro and longitudinal gyro frequencies to the wave frequency. Since propagation will hardly ever be completely longitudinal or transverse the Hartree equation must be analyzed to determine the dominant effect. If for example Y_L dominates the Hartree equation propagation is termed quasi-longitudinal and if Y_T dominates propagation is termed quasi-transverse. Consider the square root term

$$\left[\frac{Y_T^4}{4(1 - X - jZ)^2} - Y_L^2 \right]^{1/2} \quad (4)$$

The transverse and longitudinal terms are equal when the following equation is satisfied

$$\frac{Y_T^4}{4} = Y_L^2 \quad (5)$$

with X , $Z \ll 1$.

In terms of the gyro frequency W_h , (5) becomes

¹ Kelso, J. M. 1964, "Radio Ray Propagation in the Ionosphere" McGraw Hill, PP. 128

$$\frac{1}{4} \left(\frac{W_h}{W} \sin \theta \right)^4 = \left(\frac{W_h}{W} \cos \theta \right)^2 \quad (6)$$

where θ is the angle between the Poynting vector and the earth's magnetic field. Typically W_h has a value of about 1.6 MHz⁽²⁾ so that for a wave frequency of 100 MHz the ratio $\frac{W_h}{W}$ is equal .016. The value of θ satisfying (6) is therefore 89.5°. Thus the transverse term will dominate only for angles between 89.5° and 90°. Since Y_L is clearly dominant in most cases it is now compared with the second power transverse term

$$\frac{Y_T^2}{2(1 - x - jZ)} \quad (7)$$

Following a similar procedure it is found that the longitudinal and transverse terms are again equal when θ equals 89.5°. For $\theta < 84.3^\circ$ Y_L is at least one order of magnitude greater than the second power transverse term and Y_L^2 is at least two orders of magnitude greater than the fourth power transverse term. Therefore, at the very least quasi-longitudinal propagation occurs for angles $\theta \leq 84.3^\circ$.

Assuming a dipole type distribution of magnetic field about the earth yields the following relationship⁽³⁾ between the latitude of a ground station (α) and the angle θ for propagation to and from an orbiting satellite.

$$\theta = \tan^{-1} \left[\frac{1}{\sin \alpha} \left(\cos \alpha - \frac{R}{R+h} \right) \right] \quad (8)$$

(2) ibid. pp. 145

(3) Microwave Journal Handbook, 1965, pp. 146

R is the radius from the center of the earth to the ionospheric layer and h is the altitude of the satellite above the layer. Considering the case of a synchronous orbit and a station located at $\alpha = 35^\circ$ N latitude (mid USA) the angle is found to be about 49° . For all the ground stations located in the USA propagation is clearly quasi-longitudinal because at the limit, $\theta = 84.3^\circ$, of the quasi-longitudinal approximation α equals 4.8° . Within this region, $\pm 4.8^\circ$ about the equator, propagation changes from longitudinal to transverse and the characteristic polarization changes from circular to linear.

Applying the quasi-longitudinal approximation to the Hartree equation yields

$$N^2 = 1 - \frac{X}{1 - jZ \pm Y_L} \quad (9)$$

Multiplying both the numerator and denominator of the second term by the complex conjugate of denominator and neglecting all squared and cross product terms results in

$$N_o^2 = 1 - \frac{X}{1 + 2Y_L} \quad (10a)$$

$$N_x^2 = 1 - \frac{X}{1 - 2Y_L} \quad (10b)$$

Using the first two terms in a binomial expansion to obtain the square root and then taking the difference between N_o and N_x results in

$$N_o - N_x = 2XY_L \quad (11)$$

Substitution of (11) in (5) gives the Faraday rotation as

$$\Omega_f = \frac{K_o}{2} \int_{z_1}^{z_2} 2X(z)Y_L(z) dz \quad (12)$$

Evaluation of (12) requires knowledge of the spatial and temporal behavior of X and Y_L ; time dependence in the equation is not explicitly indicated. J. M. Goodman ⁽⁴⁾ has developed an approximate expression for computing the Faraday rotation caused during passage through the ionosphere.

$$\Omega_{\ell} = \frac{10^4 X}{2} \quad (13)$$

Goodman assumes a magnetic field strength of 40 amp/m (equivalent to $Y_L = .014$ at 100 MHz) a Chapman electron distribution and an ionospheric thickness of 360 Km. Equation 13 is used to compute Faraday rotation as a function of frequency for quasi-longitudinal propagation (see Figure 7B-1). Two cases are given, one for a plasma frequency of 6 MHz corresponding to the typical value over the USA and the other for a plasma frequency of 14 MHz corresponding to a "worse case" situation. The plasma frequencies are obtained from CRPL maps of predicted maximum usable frequencies for September, 1964. The "worse case" frequency of 14 MHz has been scaled up slightly to take into account the approach of a sun spot maximum in the summer of 1968. Several measurements of Faraday rotation have been compared with the predicted values that are obtained from (13). Shuster and Levy ⁽⁵⁾ have measured the Faraday rotation at 2.3 GHz by reflecting radar signals from Venus. These results agree almost perfectly with the high frequency end of the "average" curve. Millman, Pineo and Hynck ⁽⁶⁾ used measurements of Faraday rotation to determine the electron density distribution over Bogata, Columbia. A one way Faraday

(5) Schuster D., Levy, G. S., "Faraday Rotation of Venus Radar Echoes" February, 1964, Astronomical Journal, Volume 69, No. 1, PP 42 - 48.

(6) Millman, Pineo, Hynck, "Ionospheric Investigations by Faraday Rotation of Back Scatter" October, 1964, Journal of Geophysical Research, PP 4051

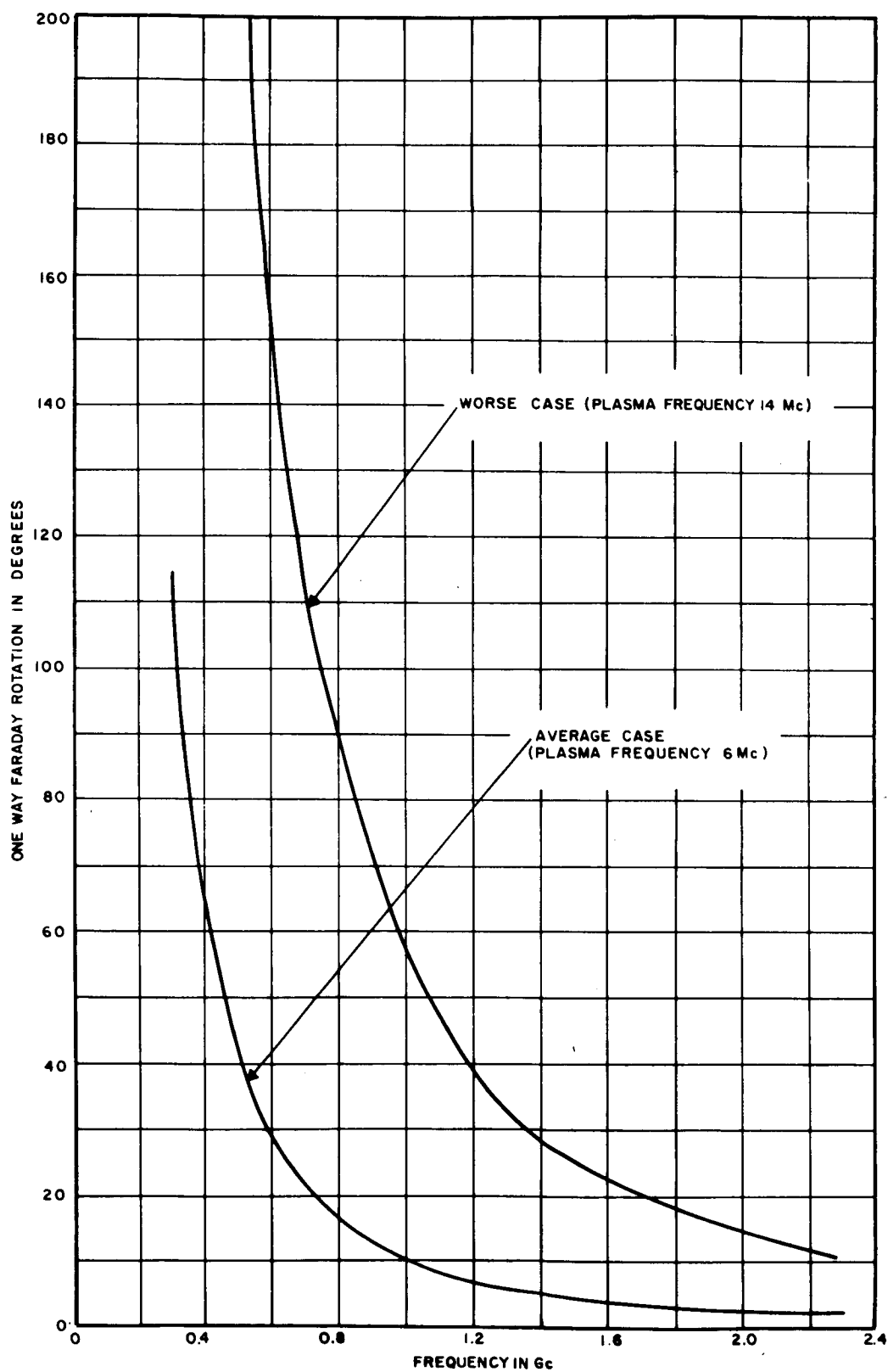


Figure 7B-1 Faraday Rotation as a Function of Frequency

rotation of 225° at 425 MHz was reported. This figure agrees quite well with the low frequency end of the "worse case" curve. Comparison is made with the worse case curve because the measurements were made at very low elevation angle (higher Y_L) and in the vicinity of the equator (higher X).

Quasi-transverse propagation takes place for angles of θ between 89.5° and 90° . At $\theta = 90^\circ$, Y_L vanishes and the Hartree equation becomes

$$N^2 = - \frac{X}{(1 - jZ) + \frac{(\pm Y_T^2 - Y_T^2)}{2(1 - X - jZ)}} \quad (14)$$

For the ordinary mode the (+) sign is used and results in

$$N_o^2 = 1 - \frac{X}{1 - jZ} \quad (15)$$

The ordinary mode is therefore unaffected by the earth's field and must be polarized such that the electric vector is parallel to the earth's field. The (-) sign is used for the extraordinary mode and results in

$$N_x^2 = 1 - \frac{X}{1 - jZ - \frac{Y_T^2}{1 - X - jZ}} \quad (16)$$

The extraordinary mode is affected by the earth's field and is therefore orthogonally polarized with respect to the ordinary mode. The rotation which now takes place is caused by the different phase velocities of the two linear components. Transverse propagation of both linear and circularly polarized waves will in general result in a conversion to elliptical polarization during passage through the ionosphere. This phenomenon is easily recognized by decomposing a linearly polarized wave into two orthogonally polarized linear waves with components parallel and perpendicular to the earth's field. Passage through the ionosphere will

result in some arbitrary time phase shift between the two components thus converting the wave to elliptical polarization. In the case of circular polarization the same analysis is applicable because the circular wave is itself composed of linear components. In the special case in which a phase shift of π occurs, a circularly polarized wave can be converted to its opposite "sense" of polarization. The magnitude of the transverse polarization effect can be estimated by using a procedure similar to that use for the longitudinal case. The difference in the indices of refraction is

$$N_o - N_x = \frac{X(X + Y_T^2)}{1 - 2(X + Y_T^2)} \quad (17)$$

The rotation equation therefore becomes

$$\Omega_t = \frac{K_o}{2} \int_{z_1}^{z_2} \frac{X(X + Y_T^2)}{1 - 2(X + Y_T^2)} dz \quad (18)$$

A comparison of the two rotation effects is obtained by taking the ratio of the integrand in (12) to that in (18). This ratio is

$$\frac{I_\ell}{I_t} = \frac{2XY(1 - 2[X + Y^2])}{X(X + Y^2)} = 8.4 \quad (19)$$

at 100 MHz. The factor 8.4 is now applied to (13) to obtain an estimate of the magnitude of the transverse-propagation polarization rotation

$$\Omega_t = \frac{10^4 X}{(2)(8.4)} \quad (20)$$

In the average case rotation is of the order of 2 radians. This effect is therefore significant enough at 100 MHz to limit the use of circular polarization as a method for reducing polarization "mismatch loss" between a synchronous satellite and ground stations very close to the equator. At 800 MHz the effect for the worst case estimated to be on the order of 6 degrees which is insignificant.

Polarization Mismatch Loss - - The power lost because of a polarization "mismatch" between two antennas is given by ⁽¹⁾

$$\frac{P_r}{P_o} = \frac{1}{2} \pm \frac{2 r_1^2 r_2^2}{(1 + r_1^2)(1 + r_2^2)} + \frac{(1 - r_1^2)(1 - r_2^2)}{2(1 + r_1^2)(1 + r_2^2)} \cos 2 \delta \quad (1)$$

where the (+) sign is used for antennas having the same "sense" of polarization and the (-) sign for antennas having the opposite sense. The axial ratios are given by r_1 and r_2 , and δ is the angle between the major axis of the polarization ellipses. For the case of two linearly polarized antennas the axial ratios are infinite and (1) becomes

$$\frac{P_r}{P_o} = \cos^2 \delta \quad (2)$$

The received power therefore varies as the cosine squared of the angle between the polarization vector's of the transmitting and receiving antennas. If propagation is taking place through the ionosphere and the two antennas are initially polarization matched, the angle δ is then equivalent to the Faraday rotation angle Ω and equation (2) will give the power lost. The same thing is true for the general equation (1) which will give the power lost because of Faraday rotation between two elliptically polarized antennas. Equation (1) is plotted in Figure 7B-2 with the axial ratios as parameters. Two special cases are considered: one is for antennas with identical axial ratios of the same sense and the other is for elliptical and circularly polarized antennas of the same sense. Equation (1) respectively becomes for these special cases

$$\frac{P_r}{P_o} = \frac{1}{2} + \frac{2r^2}{(1 + r^2)^2} + \frac{(1 - r^2)^2}{2(1 + r^2)^2} \cos 2 \delta \quad (3a)$$

(1) Matkin, Proc. IRE, December 1950, P. 1455

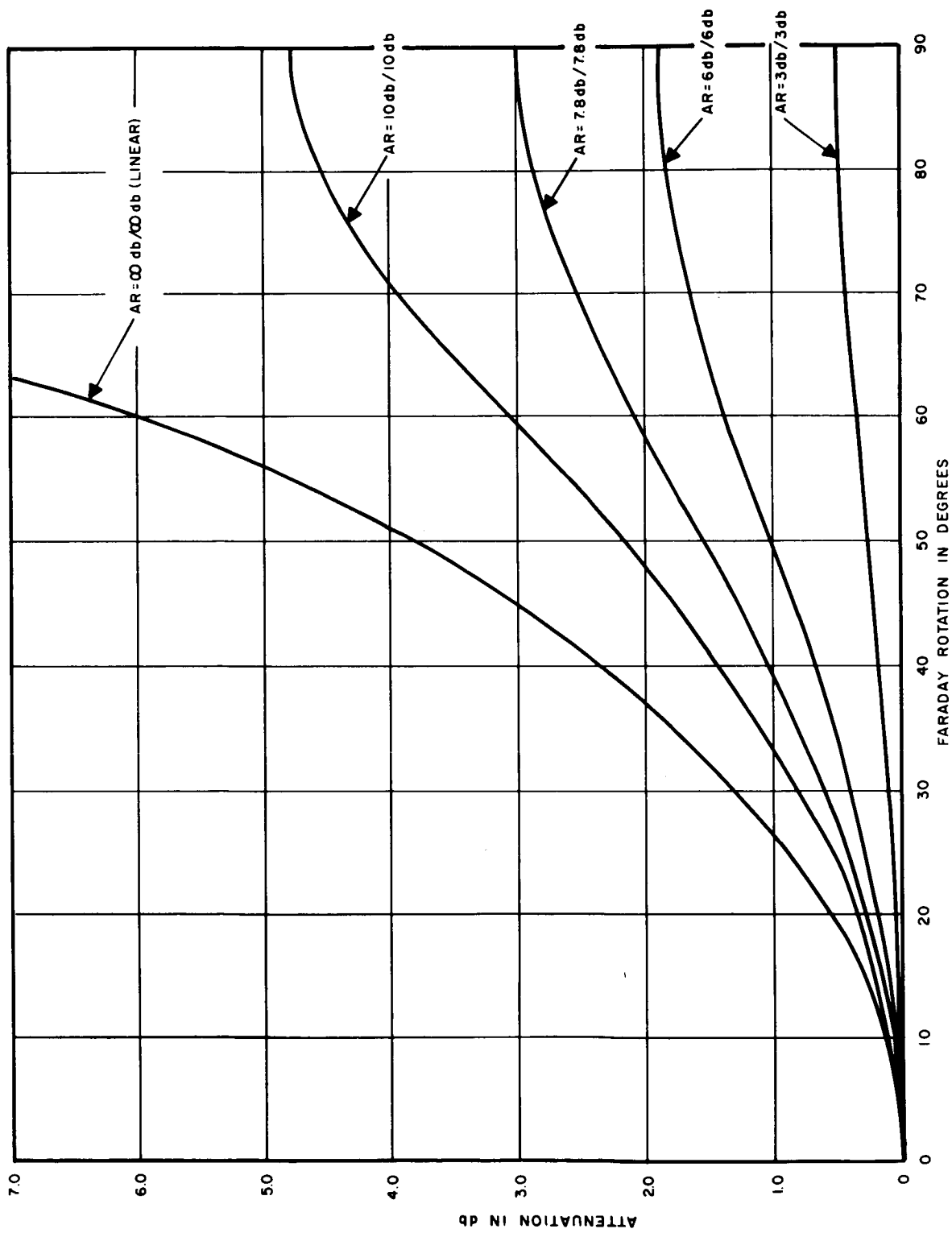


Figure 7B-2 Attenuation between Arbitrarily Polarized Antenna Caused by Faraday Rotation
AR = Axial Ratio

and

$$\frac{P_r}{P_o} = \frac{1}{2} + \frac{2r}{2(1+r^2)} \quad (3b)$$

Equation (3b) is independent of the angle δ and therefore for the special case of circular and elliptically polarized antennas no power is lost because of Faraday rotation. An expanded version of Figure 7B-2 (region $\theta \leq 30^\circ$) is shown in Figure 7B-3.

Polarization Study Conclusions

1. Polarization loss for longitudinal propagation caused by Faraday rotation is significant enough at 800 MHz and below to require the use of at least one circularly polarized antenna in each of the 100 MHz and 800 MHz links.
2. Use of circularly polarized antennas in the 100 MHz link will not guarantee freedom from severe polarization loss for ground stations located near the equator ($\pm 4.5^\circ$ latitude).
3. While Faraday rotation is insignificant above 1.7 GHz, improper polarization alignment of the ground station and spacecraft antennas will cause severe polarization loss. The use of at least one circularly polarized antenna in each of the 1.7, 2.1, 2.3, 7.3 and 8.3 GHz links will eliminate this problem.

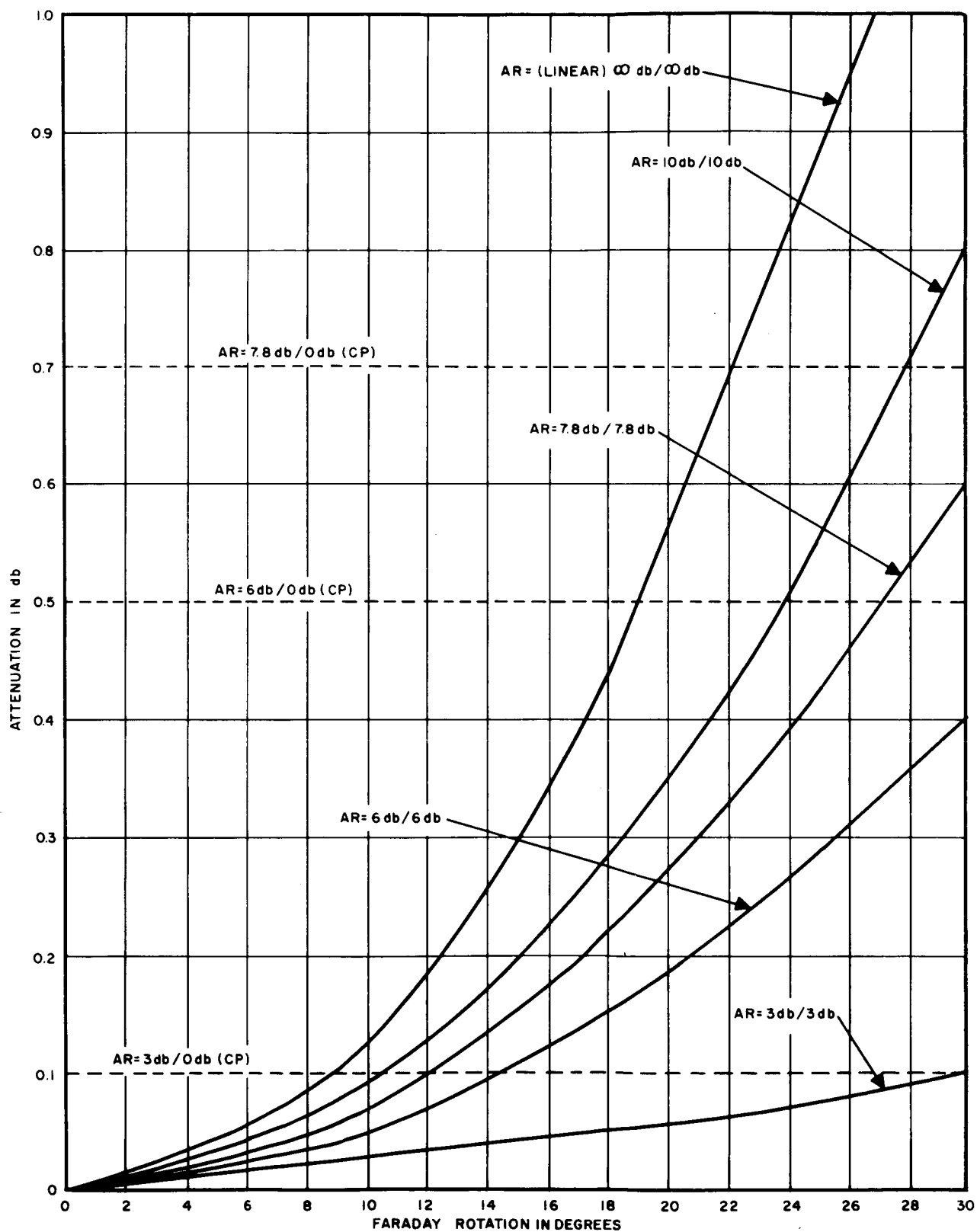


Figure 7B-3

Attenuation between Arbitrarily Polarized
Antennas Caused by Faraday Rotation AR = Axial Ratio

APPENDIX 7C SEPARATE 100 MHz ANTENNAS

The efficiency of a 30' parabolic antenna at 100 MHz is expected to be less than 30% because of its small electrical size ($D = 3.05 \lambda$). Separate antenna systems capable of providing equal or better performance at 100 MHz are single or small broadside arrays of end fire antennas. Helical or Yagi antennas are the preferred types of end fire antennas. In the most likely case where circular polarization is required the helix is to be preferred over the Yagi because it directly provides circular polarization. A crossed Yagi antenna can provide circular polarization, however, it is electrically more complex than the helix.

At 30% efficiency the expected gain of the paraboloid at 100 MHz is

$$G_p \cong .3 \left(\frac{\pi D}{\lambda} \right)^2 = 27.5 = 14.4 \text{ db} \quad (1)$$

where D is the diameter of the paraboloid. The gain of a single helix is approximately

$$G_h \cong 12 \left(\frac{\pi d}{\lambda} \right)^2 \left(\frac{ns}{\lambda} \right) \quad (2)$$

where d is the diameter of the helix, n is the number of turns and s is the spacing between turns. For axial mode operation (beam directed along the axis of the helix) it is required that

$$\frac{3}{4} < \frac{\pi d}{\lambda} < \frac{4}{3} \quad (3)$$

Setting $d = \frac{\lambda}{\pi}$ in eq. 2 results in

$$G_h = 12 \frac{ns}{\lambda} \quad (4)$$

Typically $S = .24 \lambda$ so that eq. 4 becomes

$$G_h = 2.88 n \quad (5)$$

To obtain a gain equivalent to that of the paraboloid (eq. 1) approximately 10 turns are therefore required. This results in an antenna which has an

electrical length of about 2.4λ , a physical length of about 23.6' and a physical diameter of about 3.13'. Equation 5 is plotted in Figure 7C-1. The abscissa has two base lines, one giving the number turns, and the second, the antenna length. The ordinate has three axes, one giving the antenna gain in db, another the gain as a number, and the third the equivalent paraboloid efficiency. As indicated in Figure 7C-1 an equivalent efficiency of 55% requires a 17 turn helix approximately 40' in length.

A small broadside array of short helices can be used to supply the same gain as the single long helix. Assuming no mutual coupling the total gain of an array is proportional to the number of elements (N) so that the gain (G_e) required of each antenna is

$$G_e = \frac{G}{N} \quad (6)$$

In the case where a gain of 50 (17 db) is required, the element gain for a four-element square array is

$$G_e = 50/4 = 12.5 \text{ (11 db)} \quad (7)$$

Figure 7C-1 can now be used to estimate the size of the helix. For a gain of 11 db the number of turns required is about 4.5 and the antenna length is about 10.6'. The spacing (h) between elements of the array is an important parameter; a spacing that is too large will cause the beamwidth to narrow and grating lobes to appear, a spacing that is too small will cause a loss in gain. In terms of an optimum, based on antenna gain, the approximate spacing should be such that the effective areas of adjacent elements just meet. In the case of the four element array of 11 db elements the effective area (A_e) of a single element is

$$A_e = \frac{G \lambda^2}{4 \pi} \quad (8)$$

The diameter (d_e) of the effective area circle is

$$d_e = \frac{\sqrt{G} \lambda}{\pi} = 1.13 \lambda \quad (9)$$

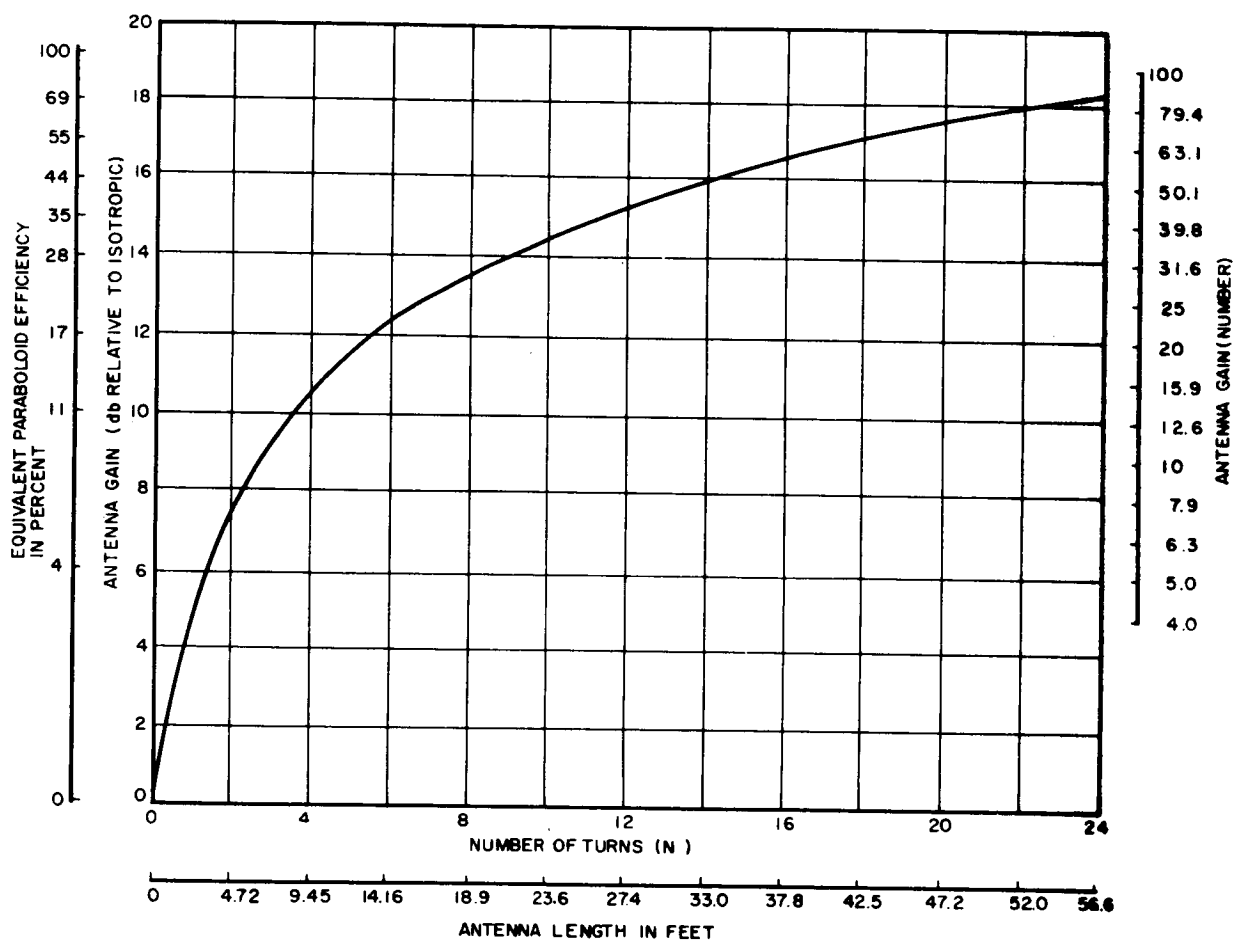


Figure 7C-1 Helical Antenna Gain as a Function of Antenna Length

and therefore the spacing (h) between elements in the array should be about 11.1' ($\lambda = 9.84'$). Although grating lobes appear for spacings greater than $.5 \lambda$ they should not be a problem because the first null appears at 26° off the array axis. This is well outside of the cone subtended by the earth's disk ($\cong \pm 9^\circ$). Figure 7C-2 is a plot of element spacing as a function of element gain for maximum array gain. The half power beamwidth of a helix is given by

$$\theta_n \cong \frac{52 \lambda}{\pi d} \sqrt{\frac{\lambda}{n s}} \quad (10)$$

Substitutions: $d = \lambda/\pi$, $s = .24 \lambda$, $n = 4.5$ and $\lambda = 9.84$ result in a beamwidth of 50° . The beamwidth of an array of isotropic radiators can be obtained from the normalized array factor

$$E(\chi) = \frac{2 \sin \frac{N \chi}{4}}{N \sin \frac{\chi}{2}} \quad (11)$$

where $\chi = \frac{2 \pi h}{\lambda} \sin \theta$.

Substitution of $N = 4$ and solving the equation

$$1.414 \sin \frac{\chi}{2} = \sin \chi \quad (12)$$

results in an "isotropic" array beamwidth (θ_i) of 25.6° . The approximate beamwidth (θ_a) of the 4 element array of helices is now obtained by using the parabolic approximation

$$\theta_a \sqrt{\frac{\theta_n^2 + \theta_i^2}{2}} = 22^\circ \quad (13)$$

The width is slightly larger than that required for earth disk coverage.

Helical antennas require ground plane reflectors the size of which depends to some degree upon the length of the helix. In general, reflectors should never be less than $\frac{\lambda}{2}$ in diameter. Most commercial helices will have ground plane diameters that vary between $\frac{\lambda}{2}$ and λ .

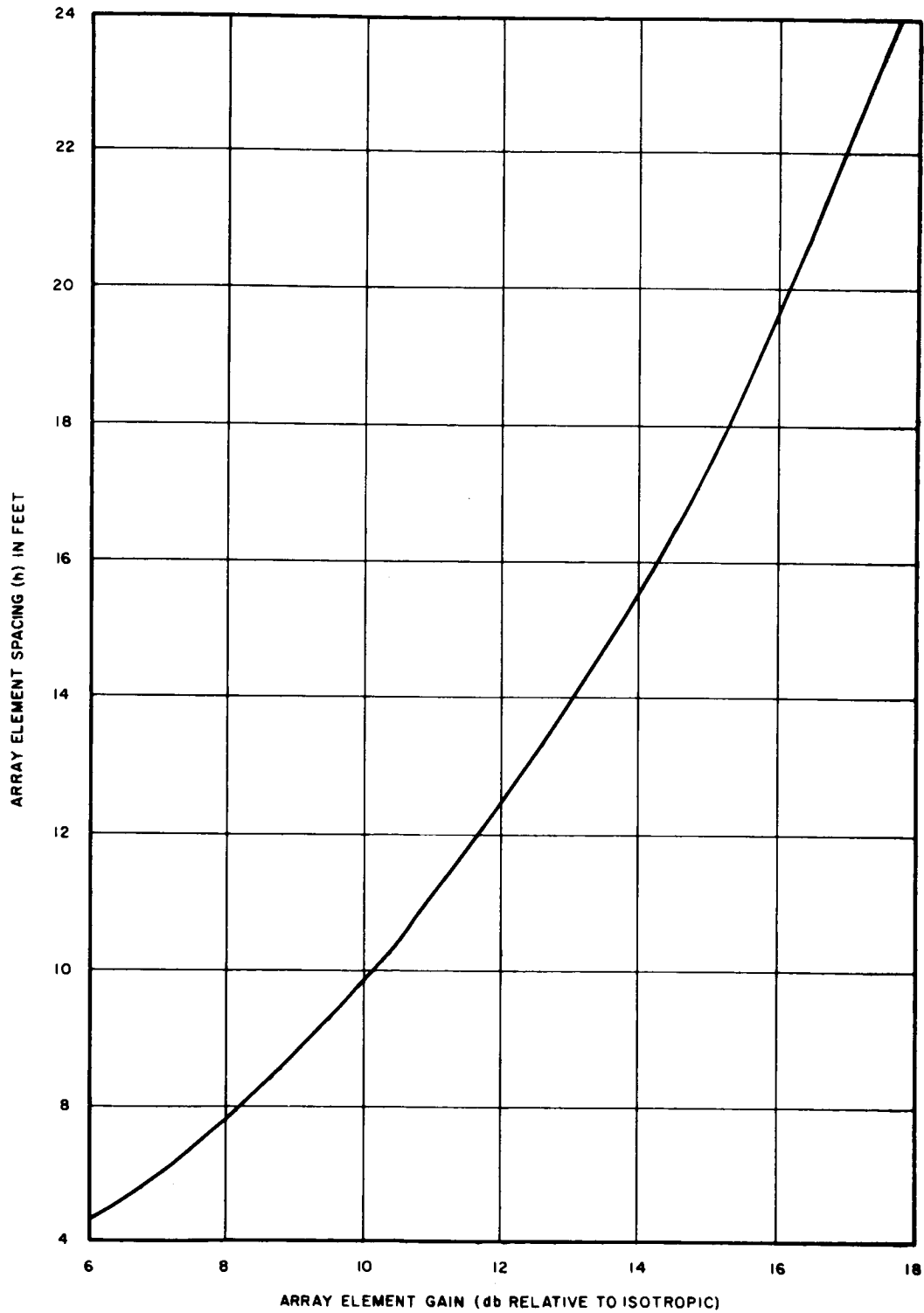


Figure 7C-2 Array Element Spacing as a Function of Array Element Gain

A comparison of the single long helix with the square array of shorter helices indicates that the space volume occupied by the two systems is about the same ($\cong 310 \text{ ft}^3$). From an electrical standpoint the single long helix is preferred over the array if the required gain is less than about 15 db_i . The long helix will produce a higher degree of circular polarization, a more symmetrical radiation pattern and be less complex. The axial ratio (degree of non-circularity) of a helix is given by

$$\text{AR} = \frac{2n + 1}{2n} \quad (14)$$

In the case of the long helix the ratio is about .1 db and for the array it is about .4 db. For gains greater than 15 db, antenna radiation losses which are not taken into account in eq. 2 will cause the curve in Figure 7C-2 to "flatten out" more than is shown. This means that a point of diminishing returns in the gain volume relationship is reached and a volumetric comparison will begin to favor the broadside array.

APPENDIX 7 D

COMMUNICATION COMPONENTS

This appendix describes the components used in the communication system. They are listed as a "Specification-Sheet" type of tabulation. The values given are typical for each of the units.

AMPLIFIERS

NAME: Tunnel Diode Preamplifier

SERIAL NO: 100

1. Function: to amplify the signal from the X-band antennas and provide an overall 6 db noise figure.
2. Center Frequency: 7.825 MC
3. Bandwidth (-1 db): 350 MC
4. Input Impedence: 50 OHMS
5. Output Impedence:
 1. 50 OHMS
 2. NA OHMS
 3. NA OHMS
6. Noise Figure: 6 db max.
7. Input Level: -50 dbm max.
8. Gain: 10 db
9. Saturated Output (1 db compression): -40 dbm
10. Gain Linearity to Saturation: ± 0.1 db max*
11. Phase Linearity: ± 2 degrees max*
12. Size: 4 cubic inches
13. Weight: .1 lbs.
14. Power Supply 6 volts and 0.005 amps.

* Gain and Phase tracking between amplifiers to be

$\pm 7^\circ$ or better

NA Not applicable

CONVERTERS

NAME: X-Band Mixer

SERIAL NO.: 110

1. Function: to convert X band signals to a 30 MC I.F.
2. Operating Frequency: Signal 1. From 7650 MC to 8000 MC
 L.O. 2. From 7680 MC to 8030 MC
 3. From
3. Bandwidth: 1. 350 MC
 2. NA MC
 3. NA MC
4. Input Impedence: 1. 50 Ohms
 2. 50 Ohms
5. Output Impedence: IF Part 3. 50 Ohms
6. Noise Figure: 8.5 db*
7. Signal Rejection, at IF Part -25 db min.
 Part 2 to 3:
8. Input Level: 30 dbm max. -120 dbm min.
9. Conversion Loss 0 dbm max. +3 dbm min.
 -6 db
10. Saturated Output -20 dbm min.
 (-1 db compression)
11. Conversion Linearity \pm 0.1 db**
12. Phase Linearity \pm 5 degrees max.**
13. Size 6 cubic inches
14. Weight 0.25 lbs.

* With Pre Amp Ser. # 120.

* When operating into an amplifier with 1.5 db noise figure.

** Phase and gain tracking between converters will be required to $\pm 7^\circ$.

NA Not applicable.

AMPLIFIERS

NAME: 30 MC IF Pre Amplifier

SERIAL NO.: 120

1. Function: to amplify the converted signal, provide a low noise figure at 30 MC.
2. Center Frequency: 30 MC
3. Bandwidth (-1 db): 15 MCmin.
4. Input Impedence: 50 Ohms
5. Output Impedence:
 1. 50 Ohms
 2. NA Ohms
 3. NA Ohms
6. Noise Figure: 1.5 db
7. Input Level: -46 dbm max. -130 dbm min
8. Gain: 16 db
9. Saturated Output (1 db compression): -20 dbm
10. Gain Linearity to Saturation: ± 0.1 db max.*
11. Phase Linearity: ± 5 degrees max.*
12. Size: 5 cubic inches
13. Weight: 0.15 lbs.
14. Power Supply 12 Volts and .014 Amps.

* Gain and Phase tracking between amplifiers to be $\pm 7^\circ$, or better

NA Not Applicable.

FILTERS

NAME: 30 MC IF Filter

SERIAL NO.: 130

1. Function: to confine the noise bandwidth, reject spurious signals and allow sufficient bandwidth for the color TV signal, plus frequency tolerance.
2. Center Frequency: (see figure 1) 30 MC
3. Bandwidth:
 - 1 db 5.25 MC
 - 3 db 5.55 MC
 - 30 db 7.2 MC
 - 60 db 14 MC
4. Input Impedence: 50 Ohms
5. Output Impedence: 50 Ohms
6. Input Level: +10 dbm max.
7. Insertion Loss: -8 db max.
8. Maximum Bandpass Ripple: \pm 0.1 db
9. Phase Linearity: \pm 5 degrees*
10. Spurious Response: -60 db min.
11. Size: 20 cubic inches
12. Weight: 0.6 lbs.

* Phase tracking between filters will be required to $\pm 7^\circ$.

NA Not applicable.

AMPLIFIERS

NAME: 30 MC IF Amplifier

SERIAL NO.: 140

1. Function: to amplify the 30 MC signal in the receiver and to provide AGC.
2. Center Frequency: 30 MC
3. Bandwidth (-1 db): 15 MC
4. Input Impedence: 50 Ohms
5. Output Impedence:
 1. 50 Ohms
 2. NA Ohms
 3. NA Ohms
6. Noise Figure: 10 db
7. Input Level: -60 dbm max. -120 dbm min.
8. Gain: +80 db
AGC, 60 db input 1 db output
9. Saturated Output (1 db compression): +10 dbm
+10 dbm
+10 Total + 14.5 dbm
10. Gain Linearity to Saturation: ± 0.1 db max.*
11. Phase Linearity: $\pm 10^\circ$ degrees max.*
12. Size: 10 cubic inches
13. Weight: .5 lbs.
14. Power Supply 12 Volts and .080 Amps.

* Gain and Phase tracking between amplifiers to be $\pm 7^\circ$.

NA Not Applicable.

FILTERS

NAME: Crystal Filter

SERIAL NO.: 150

1. Function: to reduce the noise bandwidth both for
monopulse and voice link.
2. Center Frequency: 30 MC
3. Bandwidth:

-1 db	40 KC	MC
-3 db	NA	MC
-30 db	NA	MC
-60 db	NA	MC
4. Input Impedence: 50 Ohms
5. Output Impedence: 50 Ohms
6. Input Level: -50 dbm max. +10 dbm min.
7. Insertion Loss: -8 db max.
8. Maximum Bandpass Ripple: \pm 0.1 db
9. Phase Linearity: \pm 2 degrees*
10. Spurious Response: -60 db min.
11. Size: 3 cubic inches
12. Weight: 0.2 lbs.

* Phase tracking between filters will be required to $\pm 7^\circ$.

NA Not applicable.

AMPLIFIERS

NAME: AGC Amplifier

SERIAL NO.: 160

1. Function: provide gain for AGC amplifier 30 MC signal for the product detector.
2. Center Frequency: 30 MC
3. Bandwidth (-1 db): 1 MC
4. Input Impedence: 50 Ohms
5. Output Impedence:
 1. 50 Ohms
 2. 50 Ohms
 3. NA Ohms
6. Noise Figure: NA db
7. Input Level: -25 dbm max. -40 dbm min.
8. Gain: +32 db
9. Saturated Output (1 db compression):
 - +8 dbm
 - +8 dbm
 - Total +11 dbm *
10. Gain Linearity to Saturation: \pm 0.1 db max. *
11. Phase Linearity: \pm 5 degrees max. *
12. Size: 8 cubic inches
13. Weight: .25 lbs.
14. Power Supply 12 Volts and .050 Amps.

* Gain and Phase tracking between amplifiers to be $\pm 7^\circ$.

NA Not Applicable.

NAME: Product Detector

SERIAL NO.: 170

1. Function: monopulse error detector.
2. Operating Frequency:
 - 1 30 MC
 - 2 30 MC
 - 3 DC
3. Bandwidth:
 - 1 40 KC
 - 2 40 KC
 - 3 100 CPS
4. Input Impedance:
 - 1 50 Ohms
 - 2 50 Ohms
 - 3 1000 Ohms
5. Output Impedance:
 - 3 1000 Ohms
6. Input Level:
 - 1 -50 dbm max. +10 dbm min.
 - 2 -50 dbm max. +10 dbm min.
7. Gain (Loss)
 - 0 db
8. Saturated Output:
(1 db compression)
 - +3 dbm
9. Gain Linearity
 - ± 0.1 db
10. Phase Linearity:
 - $\pm 5^\circ$
11. Size:
 - 10 cubic inches
12. Weight:
 - .3 lbs.
13. Power Supply:
 - 12 volts .015 amps.

NAME: Monopulse Error Output

SERIAL NO.:180

1. Function: a 10 cps filter and amplifier for the monopulse error output.
2. Operating Frequency: DC,
3. Bandwidth: (-3db) 10 cps
Attn at 6 db/octave)
4. Input Impedance: 1000 Ohms
5. Output Impedance: 1000 Ohms
6. Input Level: +3 dbm max. - 10 dbm min.
7. Gain (Loss): 0 db
8. Saturated Output
(1 db compression) +3 dbm
9. Gain Stability: ± 0.2 db
10. Phase Linearity: ± 1.0 degrees
11. Size: 6 cubic inches
12. Weight: .2 lbs.
13. Power Supply: 12 volts .020 amps.

FILTERS

NAME: FM Broadcast Filter

SERIAL NO.: 210

1. Function: to separate FM broadcast from all other signals and connect the signal to the 100 MC amplifier.
2. Center Frequency: (see figure 1) 30 MC
3. Bandwidth:

-1 db	.150 MC
-3 db	.165 MC
-30 db	NA MC
-60 db	.350 MC
4. Input Impedence: 50 Ohms
5. Output Impedence: 50 Ohms
6. Input Level: 0 dbm max. ~~+10 dbm~~-min.
7. Insertion Loss: -5 db max.
8. Maximum Bandpass Ripple: \pm 0.1 db
9. Phase Linearity: \pm 5 degrees*
10. Spurious Response: -60 db max.
11. Size: 3 cubic inches
12. Weight: 0.2 lbs.

* Phase tracking between filters will be required to $\pm 7^\circ$. or better

NA Not applicable.

CONVERTERS

NAME: 100 MC Up Converter

SERIAL NO.: 220

1. Function: to convert the 30 MC signal to 100 MC.

2. Operating Frequency:

1. 30 MC
2. 130 MC
3. 100 MC

3. Bandwidth:

1. 10 MC min.
2. 10 MC min.
3. 10 MC min.

4. Input Impedance:

1. 50 Ohms
2. 50 Ohms

5. Output Impedance:

3. 50 Ohms

6. Noise Figure:

10 db max.

7. Signal Rejection,
Part 2 to 3:

25 db

8. Input Level:

+3 dbm max.

9. Conversion Loss

+13 dbm max.
-10 db

10. Saturated Output
(-1 db compression)

-7 dbm min.

11. Conversion Linearity

\pm 1.0 db

12. Phase Linearity

\pm NA degrees max.

13. Size

3 cubic inches

14. Weight

.1 lbs.

NA Not applicable.

FILTERS

NAME: 100 MC Filter

SERIAL NO.: 230

1. Function: to reject spurious responses from 100 MC
upconverter (Ser. # 220)
2. Center Frequency: 100 MC
3. Bandwidth:

-1 db	20	MC
-3 db	21	MC
-30 db	34	MC
-60 db	60	MC
4. Input Impedence: 50 Ohms
5. Output Impedence: 50 Ohms
6. Input Level: 0 dbm max.
7. Insertion Loss: -5 db max.
8. Maximum Bandpass Ripple: \pm 0.1 db
9. Phase Linearity: \pm 20 degrees
10. Spurious Response: -60 db max.
11. Size: 15 cubic inches
12. Weight: .4 lbs.

NA Not applicable.

AMPLIFIERS

NAME: 100 MC Driver

SERIAL NO.: 240

1. Function: amplify the 100 MC signal to drive the power amplifier.
2. Center Frequency: 100 MC
3. Bandwidth (-1 db): 20 MC
4. Input Impedence: 50 Ohms
5. Output Impedence:
 1. 50 Ohms
 2. NA Ohms
 3. NA Ohms
6. Noise Figure: db
7. Input Level: -10 dbm max.
8. Gain: +33
9. Saturated Output (1 db compression): +23 dbm
10. Gain Linearity to Saturation: \pm NA db max.*
11. Phase Linearity: \pm NA degrees max.*
12. Size: 16 cubic inches
13. Weight: .5 lbs.
14. Power Supply 28 Volts and .040 Amps.

* Gain and Phase tracking between amplifiers to be $\pm 7^\circ$.

NA Not Applicable.

AMPLIFIERS

NAME: 100 MC Power Amplifier

SERIAL NO.: 250

- | | | | |
|--|---|--------------|---------------|
| 1. Function: | To amplify the 100 MC signal to 10 watts for re-transmission. | | |
| 2. Center Frequency: | 100 | MC | |
| 3. Bandwidth (-1 db): | 20 | MC | |
| 4. Input Impedence: | 50 | Ohms | |
| 5. Output Impedence: | 1. 50 | Ohms | |
| | 2. NA | Ohms | |
| | 3. NA | Ohms | |
| 6. Noise Figure: | -50 | db | |
| 7. Input Level: | +23 | dbm max. | +17 dbm min. |
| 8. Gain: | 20 | | |
| 9. Saturated Output
(1 db compression): | 42 | dbm | |
| 10. Gain Linearity to Saturation: | \pm | NA | db max.* |
| 11. Phase Linearity: | \pm | NA | degrees max.* |
| 12. Size: | 30 | cubic inches | |
| 13. Weight: | 1 | lbs. | |
| 14. Power Supply | 28 Volts and .600 Amps. | | |

* Gain and Phase tracking between amplifiers to be $\pm 7^\circ$.

NA Not Applicable.

CONVERTERS

NAME: 800 MC Up Converter

SERIAL NO.: 310

1. Function: to convert the 30 MC IF to 800 MC IF or for the 800 MC power amplifier.
2. Operating Frequency:
 1. From 30 MC
 - Input Signal Frequency
 2. From 30 MC
 - Local Oscillator Frequency
 3. From 800 MC
3. Bandwidth:
 1. 80 MC
 2. 0.5 MC
 3. 80 MC
4. Input Impedence:
 1. 50 Ohms
 2. 50 Ohms
 3. 50 Ohms
5. Output Impedence:
 3. 50 Ohms
6. Noise Figure: NA db*
7. Signal Rejection, Part 2 to 3: 25 db min.
8. Input Level: 0 dbm max.
9. Conversion Loss -10 dbm max. -6 dbm min.
10. Saturated Output (-1 db compression) +10 db
11. Conversion Linearity \pm -10 db**
12. Phase Linearity \pm NA degrees max.**
13. Size 2 cubic inches
14. Weight .1 lbs.

* When operating into an amplifier with 1.5 db noise figure.

** Phase and gain tracking between converters will be required to $\pm 7^\circ$.

NA Not applicable.

FILTERS

NAME: 800 MC Filter

SERIAL NO.: 320

1. Function: to reject spurious signals from the 800 MC upconverter.
2. Center Frequency: 800 MC
3. Bandwidth:

-1 db	NA	MC
-3 db	8	MC
-30 db	10	MC
-60 db	30	MC
4. Input Impedence: 50 Ohms
5. Output Impedence: 50 Ohms
6. Input Level: 0 dbm max.
7. Insertion Loss: 4 db max.
8. Maximum Bandpass Ripple: \pm 0.1 db
9. Phase Linearity: \pm 20 degrees*
10. Spurious Response: -60 db min.
11. Size: 10 cubic inches
12. Weight: .3 lbs.

* Phase tracking between filters will be required to $\pm 7^\circ$.

NA Not applicable.

AMPLIFIERS

NAME: 800 MC Amplifier

SERIAL NO.: 330

1. Function: to amplify the 800 MC TV signal to a drive level for the 800 MC linear amplifier.
2. Center Frequency: 800 MC
3. Bandwidth (-1 db): (-3 db) 6 MC
4. Input Impedence: 50 Ohms
5. Output Impedence:
 1. 50 Ohms
 2. NA Ohms
 3. NA Ohms
6. Noise Figure: NA db
7. Input Level: -30 dbm max. -36 dbm min.
8. Gain: +55
9. Saturated Output (1 db compression): +25 dbm
10. Gain Linearity to Saturation: \pm NA db max.*
11. Phase Linearity: \pm NA degrees max.*
12. Size: 30 cubic inches
13. Weight: 1 lbs.
14. Power Supply 28 Volts and .090Amps.

* Gain and Phase tracking between amplifiers to be $\pm 7^\circ$.

NA Not Applicable.

AMPLIFIERS

NAME: 800 MC Linear Amplifier

SERIAL NO.: 430

1. Function: to provide a 10 watt power output to the 800 MC TV Antenna.
2. Center Frequency: 800 MC
3. Bandwidth (-1 db): 6 MC
4. Input Impedence: 50 Ohms
5. Output Impedence:
 1. 50 Ohms
 2. NA Ohms
 3. NA Ohms
6. Noise Figure: NA db
7. Input Level: +25 dbm max. +20 dbm min.
8. Gain: +20
9. Saturated Output (1 db compression): +42 dbm
10. Intermodulation - 40 db max.*
11. Phase Linearity: \pm NA degrees max.*
12. Size: 60 cubic inches
13. Weight: 1.4 lbs.
14. Power Supply 28 Volts and 1.26 Amps.

* Gain and Phase tracking between amplifiers to be $\pm 7^\circ$.

NA Not Applicable.

NAME: 800 MC Hybrid

SERIAL NO.: 440

1. Function: to sum redundant 800 MC linear amplifier.
2. Operating Frequency: 800 MC
3. Bandwidth: 80 MC
4. Input Impedance:

1	50 Ohms
2	50 Ohms
5. Output Impedance: 50 Ohms
6. Input Level: 43 dbm
7. Gain (Loss) -.5 db max. at mid band
8. Size: 50 cubic inches
9. Weight: 1.2 lbs.

AMPLIFIERS

NAME: S Band Pre Amplifier

SERIAL NO.: 510 A & B

1. Function:	to amplify the low level received signal.		
	A	B	
2. Center Frequency:	1700 MC	2100	MC
3. Bandwidth (-1 db):	170 MC	210	MC
4. Input Impedence:		50	Ohms
5. Output Impedence:	1.	50	Ohms
	2.	NA	Ohms
	3.	NA	Ohms
6. Noise Figure:		4	db max.
7. Input Level:		-40	dbm max.-122 dbm min.
8. Gain:		+20	
9. Saturated Output (1 db compression):		-20	dbm
10. Gain Linearity to Saturation:	\pm	0.2	db max.*
11. Phase Linearity:	\pm	NA	degrees max.*
12. Size:		6	cubic inches
13. Weight:		.2	lbs.
14. Power Supply	12	Volts and .025 Amps.	

* Gain and Phase tracking between amplifiers to be $\pm 7^\circ$.

NA Not Applicable.

CONVERTERS

NAME: S Band Balanced Mixer

SERIAL NO.: 520

1. Function: to convert the S band signal to a 30 MC IF.
2. Operating Frequency:
 1. 1700 MC or 2100 MC
 2. 1730 MC or 2130 MC
 3. 30 MC and 30 MC
3. Bandwidth:
 1. 200 MC
 2. 200 MC
 3. 10 MC
4. Input Impedence:
 1. 50 Ohms
 2. 50 Ohms
5. Output Impedence:
 3. 50 Ohms
6. Noise Figure: 10 db* max.
7. Signal Rejection, Part 2 to 3: 25 db min.
8. Input Level: -20 dbm max. -100 dbm. min.
+6 dbm max. 0 dbm min.
9. Conversion Loss -10 db max.
10. Saturated Output (-1 db compression) -30 dbm min.
11. Conversion Linearity \pm 0.2 db**
12. Phase Linearity \pm NA degrees max.**
13. Size 8 cubic inches
14. Weight .2 lbs.

* When operating into an amplifier with 1.5 db noise figure.

** Phase and gain tracking between converters will be required to $\pm 7^\circ$.

NA Not applicable.

NAME: PSK Modulator

SERIAL NO.: 530

1. Function: to phase modulate the 2.3 GC signals with binary data.
2. Operating Frequency: 800 Bits/sec
3. Bandwidth: 10 KC
4. Input Impedance: 1000 Ohms
5. Output Impedance: 1000 Ohms
6. Noise: -50 db or less
7. Input Level: 0 dbm \pm 3 dbm
8. Phase Shift: $\pm 90^\circ$
9. Size: 10 cubic inches
10. Weight: .3 lbs.

OSCILLATORS

NAME: 2.3 GC Oscillator

SERIAL NO.: 540

1. Function: to provide the S band transmitting carrier.
2. Operating Frequency: 2200 to 2400 MC
3. Tuning Range or Resonator: Not less than 1.2 KC
4. Output Impedence: 50 Ohms
5. Output Level: +22 dbm min.
6. Noise & Spurious Output: -50 db
7. Long Term Stability
(24 hrs. & 20° C to +65° C): 5 PPM
8. Short Term Stability (1 hr.): 20 PPM
9. Size: 3 cubic inches
10. Weight: .1 lbs.
11. Power Supply: 28 Volts and .050 Amps.

NA Not Applicable

NAME: Isolator

SERIAL NO.: 550

1. Function: to isolate the oscillator output from the antenna.
2. Operating Frequency: 2.3 MC
3. Bandwidth: 230 MC
4. Input Impedance: 50 Ohms
5. Output Impedance: 50 Ohms
6. Isolation: 20 db min.
7. Input Level: 27 dbm max
8. Gain (Loss) -.2 db
9. Size: 18 cubic inches
10. Weight: .6 lbs.

CONVERTERS

NAME: Parametric up converter

SERIAL NO.: 340

1. Function: to convert the 800 MC signal to X-Band
at a high level.
2. Operating Frequency:
 1. 800 MC
 2. 6675 MC
 3. 7475 MC
3. Bandwidth:
 1. 10 MC
 2. 80 MC
 3. 80 MC
4. Input Impedence:
 1. 50 Ohms
 2. 50 Ohms
 3. 50 Ohms
5. Output Impedence
 3. 50 Ohms
6. Noise Figure: NA db*
7. Signal Rejection
Part 2 to 3: 25 db min.
8. Input Level: + 13 dbm max.
9. Conversion Loss: 0 db
10. Saturated Output:
(-1 db compression) +16 dbm min.
11. Conversion Linearity: ± 0.1 db**
12. Phase Linearity: \pm NA degrees max.**
13. Size: .6 cubic inches
14. Weight .3 lbx.

* When operating into an amplifier with 1.5 db noise figure.

** Phase and gain tracking between converters will be required to $\pm 7^\circ$.

NA Not applicable.

7-190

AMPLIFIERS

NAME: TWT Amplifier

SERIAL NO.: 370

1. Function: to amplify X-Band signals to 10 watts.
2. Center Frequency: 7475 GC
3. Bandwidth (-1 db): 350 MC min.
4. Input Impedence: 50 Ohms
5. Output Impedence:
 1. 50 Ohms
 2. NA Ohms
 3. NA Ohms
6. Noise Figure: db
7. Input Level: +17 dbm max.
8. Gain: Saturated 25 db nominal
9. Saturated Output
(1 db compression): +40 dbm min.
10. Gain Linearity to Saturation: \pm NA db max.*
11. Phase Linearity: \pm NA degrees max.*
12. Size: 220 cubic inches
13. Weight: 7 lbs.
14. Power Supply 28 Volts and 1.4 Amps.

* Gain and Phase tracking between amplifiers to be $\pm 7^\circ$.

NA Not Applicable.

NAME: Power Split

SERIAL NO.: 420

1. Function: to provide an even power split to two parts
with no loss of power.
2. Operating Frequency: 800 MC
3. Bandwidth: 6 MC
4. Input Impedance: 50 Ohms
5. Output Impedance (see note 1)

1	50 Ohms
2	50 Ohms
6. Input Level: + 25
7. Saturated Output: (1 db compression)

1	+25
2	+25
8. Size: 6 cubic inches
9. Weight: 0.2 lbs.
10. Power Supply: 28 volts .080 amps

Note 1: Isolated outputs such that a mismatch from short to open on one output will not effect the impedance of of the other output.

OSCILLATORS

NAME: Master Oscillator

SERIAL NO.: 610

1. Function: to provide a stable fundamental frequency
for the local oscillators in the system.
2. Operating Frequency: 57 MC \pm .0001%
3. Tuning Range NA
4. Output Impedence: 50 Ohms
5. Output Level: -10 dbm min.
6. Noise & Spurious Output: -60 db
7. Long Term Stability
(24 hrs. & 20° C to +65° C): 2.0 PPM
-20° to + 65° C
8. Short Term Stability (1 hr.): 1.0 PPM
-20° C to +65° C
9. Size: 8 cubic inches
10. Weight: 13 lbs.
11. Power Supply: 12 Volts and .005 Amps.
12 Volts and .9 Amps

NA Not Applicable

AMPLIFIERS

NAME: Buffer Amplifier

SERIAL NO.: 611

1. Function: to amplify the master oscillator signal and to isolate the oscillator from the modulator.
2. Center Frequency: 57 MC
3. Bandwidth (-1 db): 0.5 MC min
4. Input Impedence: 50 Ohms
5. Output Impedence:
 1. 50 Ohms
 2. NA Ohms
 3. NA Ohms
6. Noise Figure: NA db
7. Input Level: -10 dbm max.
8. Gain: 10 db
9. Saturated Output (1 db compression): +3 dbm
10. Output to input isolation: - 30 db min.
11. Phase Linearity: \pm NA degrees max.*
12. Size: 6 cubic inches
13. Weight: .25 lbs.
14. Power Supply 28 Volts and .010 Amps.

* Gain and Phase tracking between amplifiers to be $\pm 7^\circ$.

NA Not Applicable.

OSCILLATORS

NAME: Crystal Oscillator

SERIAL NO.: 612

1. Function: to provide a low frequency for the spectrum generator.
2. Operating Frequency: 78 MC \pm .0001%
3. Tuning Range NA
4. Output Impedence: 50 Ohms
5. Output Level: -10 dbm min.
6. Noise & Spurious Output: -60 db
7. Long Term Stability
(24 hrs. & 20° C to +65° C): 2.0 PPM
-20°C to +65°C
8. Short Term Stability (1 hr.): 1.0 PPM
-20°C to + 65° C
9. Size: 8 cubic inches
10. Weight: .3 lbs.
11. Power Supply: 12 Volts and .005 Amps.

NA Not Applicable

NAME: Pulse Forming Network

SERIAL NO.: 613 with 614

1. Function: To form a pulse for modulating the master oscillator signal and creating a spectrum of frequencies.
2. Repetition Rate; 78 KC \pm 00.01%
3. Output Pulse Duration: 0.1 useconds
(10 % to 90 %)
4. Input Impedance: 50 Ohms
5. Input Signal: Sine Wave
6. Input Level: -10 dbm
7. Output Impedance: 50 Ohms
8. Output level: 10 volts peak
9. Size: 20 cubic inches
10. Weight: .6 lbs.
11. Power Supply 28 volts 035 MA

FILTERS

NAME: Crystal Filter

SERIAL NO.: 617 A through I

1. Function: to pick out a particular frequency from the spectrum generator.

Operating 2. Center Frequency:	50 MC to 64	MC
	(exact frequency to be specified)	
3. Bandwidth:	-1 db NA MC	
	-3 db 8KC MC	
	-30 db NA MC	
	-60 db 70 KC MC	
4. Input Impedence:	50 Ohms	
5. Output Impedence:	50 Ohms	
6. Input Level:	0	dbm max.
7. Insertion Loss:	-10	db max.
8. Maximum Bandpass Ripple:	\pm 0.1	db
9. Phase Linearity:	\pm NA	degrees*
10. Spurious Response:	-60 db max.	db min.
11. Size:	8	cubic inches
12. Weight:	.3	lbs.

* Phase tracking between filters will be required to $\pm 7^\circ$.

NA Not applicable.

AMPLIFIERS

NAME: Amplifier

SERIAL NO.: 618

1. Function: to amplify the spectral frequency from the crystal filter.
2. Center Frequency: 57 MC
3. Bandwidth (-1 db): 15 MC
4. Input Impedence: 50 Ohms
5. Output Impedence:
 1. 50 Ohms
 2. NA Ohms
 3. NA Ohms
6. Noise Figure: NA db
7. Input Level: -40 dbm max.
8. Gain: 40 db
9. Saturated Output (1 db compression): +23 dbm
10. Gain Linearity to Saturation: \pm 0.5 db max.*
11. Phase Linearity: \pm NA degrees max.*
12. Size: 20 cubic inches
13. Weight: .6 lbs.
14. Power Supply 12 Volts and .035Amps.

* Gain and Phase tracking between amplifiers to be $\pm 7^\circ$.

NA Not Applicable.

CONVERTERS

NAME: High Frequency Mixer

SERIAL NO.: 619

1. Function: to mix the master oscillator signal with a variable frequency oscillator.
2. Operating Frequency:
 1. From 50 MC to 64 MC
 2. From 9.4 MC
 3. From 59.4 MC to 73.4 MC
3. Bandwidth:
 1. 15 MC
 2. 15 MC
 3. 15 MC
4. Input Impedence:
 1. 50 Ohms
 2. 50 Ohms
5. Output Impedence:
 3. 50 Ohms
6. Noise Figure: NA db*
7. Signal Rejection, Part 2 to 3: -25 db min.
8. Input Level:
 1. 0 dbm max.
 2. 0 dbm max.
9. Conversion Loss -10 db max.
10. Saturated Output (-1 db compression) -7 dbm min.
11. Conversion Linearity \pm NA db**
12. Phase Linearity \pm NA degrees max.**
13. Size 6 cubic inches
14. Weight 0.2 lbs.

* When operating into an amplifier with 1.5 db noise figure.

** Phase and gain tracking between converters will be required to $\pm 7^\circ$.

NA Not applicable.

OSCILLATORS

NAME: Variable Frequency Oscillator

SERIAL NO.: 620

1. Function: to provide tuning range for each of the local oscillator signals.
2. Operating Frequency: 9 to 10 MC
(exact frequency to be specified)
3. Tuning Range or Resonator: 3 MC max.
4. Output Impedence: 50 Ohms
5. Output Level: -10 dbm
6. Noise & Spurious Output: -60 db
7. Long Term Stability
(24 hrs. & 20° C to +65° C): 50 PPM
8. Short Term Stability (1 hr.): 25 PPM
9. Size: 6 cubic inches
10. Weight: .2 lbs.
11. Power Supply: 12 Volts and .010 Amps.

NA Not Applicable

AMPLIFIERS

NAME: High Frequency Driver

SERIAL NO.: 621

1. Function: to amplify the VFO signal to a suitable level for distribution.
2. Center Frequency: 9.5 MC
3. Bandwidth (-1 db): 4 MC
4. Input Impedence: 50 Ohms
5. Output Impedence:
 1. 50 Ohms
 2. NA Ohms
 3. NA Ohms
6. Noise Figure: NA db
7. Input Level: -10 dbm max.
8. Gain: 23.5 db
9. Saturated Output (1 db compression): +16.5 dbm
10. Gain Linearity \pm NA db max.*
11. Phase Linearity: \pm NA degrees max.*
12. Size: 10 cubic inches
13. Weight: .3 lbs.
14. Power Supply 28 Volts and 0.40 Amps.

* Gain and Phase tracking between amplifiers to be $\pm 7^\circ$.

NA Not Applicable.

NAME: High Frequency Distributor

SERIAL NO.: 622

1. Function: to distribute the VFO signal.
2. Operating Frequency: 9.5 MC
3. Bandwidth: 4⁺ MC
4. Input Impedance: 50 Ohms
5. Output Impedance:
 - 1 50 Ohms
 - 2 50 Ohms
 - 3 50 Ohms
 - 4 50 Ohms
6. Input Level: 23.5 dbm
7. Insertion Loss: -7.5 db
8. Output Level:
 - 1 0 dbm
 - 2 0 dbm
 - 3 0 dbm
 - 4 0 dbm
9. Size: 2 cubic inches
10. Weight: .1 lbs.

FILTERS

NAME: Filter

SERIAL NO.: 623

1. Function: to eliminate spurious responses and unwanted products from the mixer.
2. Center Frequency: 50 MC to 65 MC
(exact Frequency to be specified)
3. Bandwidth: -1 db NA MC
-3 db 3 MC
-20 db 4.5 MC
-30 db 7.5 MC
4. Input Impedence: 50 Ohms
5. Output Impedence: 50 Ohms
6. Input Level: -10 dbm max.
7. Insertion Loss: -5 db max.
8. Maximum Bandpass Ripple: ± 0.1 db
9. Phase Linearity: \pm NA degrees*
10. Spurious Response: -60 db min.
11. Size: 6 cubic inches
12. Weight: .2 lbs.

* Phase tracking between filters will be required to $\pm 7^\circ$.

NA Not applicable.

AMPLIFIERS

NAME: Amplifier

SERIAL NO.: 624

1. Function: to amplify the signal to a suitable level for the multipliers.
2. Center Frequency: 58 MC
3. Bandwidth (-1 db): 20 MC
4. Input Impedence: 50 Ohms
5. Output Impedence:
 1. 50 Ohms
 2. NA Ohms
 3. NA Ohms
6. Noise Figure: NA db
7. Input Level: -15 dbm max.
8. Gain: 35 db
9. Saturated Output (1 db compression): +23 dbm
10. Gain Linearity \pm NA db max.*
11. Phase Linearity: \pm NA degrees max.*
12. Size: 12 cubic inches
13. Weight: .35 lbs.
14. Power Supply 28 Volts and .050 Amps.

* Gain and Phase tracking between amplifiers to be $\pm 7^\circ$.

NA Not Applicable.

MULTIPLIERS

NAME: Transistor Frequency Multiplier

SERIAL NO.: 710

1. Function: to multiply the input frequency by 30.
2. Input Center Frequency: 57 MC
3. Input Tuning Range: 4 MC
4. Input Instantaneous Bandwidth: 3 MC
5. Output Center Frequency: 171 MC
6. Output Tuning Range: 11 MC
7. Output Instantaneous Bandwidth: 9 MC
8. Input Impedence: 50 Ohms
9. Output Impedence: 50 Ohms
10. Input Level: +20 dbm
11. Gain: 0 db min.
12. Output Level: +20 dbm
13. Harmonic & Spurious Suppression: -40 db
14. Size: 6 cubic inches
15. Weight: .1 lbs.
16. Power Supply : 28 Volts and 025 Amps.

NA Not Applicable.

MULTIPLIERS

NAME: Step Recovery Diode Multiplier

SERIAL NO.: 720

1. Function: to multiply a VHF to S-Band.
2. Input Center Frequency: 171 MC
(exact frequency to be specified)
3. Input Tuning Range: NA MC
4. Input Instantaneous Bandwidth: 11 MC
5. Output Center Frequency: S Band
6. Output Tuning Range: NA MC
7. Output Instantaneous Bandwidth: 87.5 MC
8. Input Impedence: 50 Ohms
9. Output Impedence: 50 Ohms
10. Input Level: +20 dbm
11. Loss: -8 db
12. Output Level: +12 dbm
13. Harmonic & Spurious Suppression: -40 db
14. Size: 8 cubic inches
15. Weight: .2 lbs.
16. Power Supply : 12 Volts and 025 Amps.

NA Not Applicable.

MULTIPLIERS

NAME: Varactor Multiplier

SERIAL NO.: 730

1. Function: to multiply the S-band signal to X-band.
2. Input Center Frequency: S-Band
3. Input Tuning Range: NA MC
4. Input Instantaneous Bandwidth: 87.5 MC
5. Output Center Frequency: X-Band
6. Output Tuning Range: NA MC
7. Output Instantaneous Bandwidth: 350 MC
8. Input Impedence: 50 Ohms
9. Output Impedence: 50 Ohms
10. Input Level: +12 dbm
11. Loss: -2 db
12. Output Level: +10 dbm
13. Harmonic & Spurious Suppression: -60 db min.
14. Size: 8 cubic inches
15. Weight: .2 lbs.
16. Power Supply : 12 Volts and 0 Amps.

NA Not Applicable.

NAME: X Band Distributor

SERIAL NO.: 740

1. Function: to distribute the local oscillator signal to the monopulse receiver mixers and the phased array A beam receiver mixer.
2. Center Frequency: 7855 MC
3. Bandwidth: 350 MC
4. Input Impedance: 50 Ohms
5. Output Impedance:
 - 1 50 Ohms
 - 2 50 Ohms
 - 3 50 Ohms
 - 4 50 Ohms
6. Input Level: 10 dbm
7. Insertion Loss: -1 db
8. Output Level:
 - 1 3 dbm
 - 2 3 dbm
 - 3 3 dbm
 - 4 3 dbm
9. Isolation Between any two output ports -40 db min.
10. Phase tracking between any two output ports $\pm 1^\circ$
11. Amplitude tracking between any two output ports ± 0.2 db
12. Size: 50 cubic inches
13. Weight: 1 lb.

MULTIPLIERS

NAME: 830 MC Multiplier

SERIAL NO.: 750

1. Function: to multiply by 4 for a 830 MC output.
2. Input Center Frequency: 206 MC
3. Input Tuning Range: 20 MC
4. Input Instantaneous Bandwidth: 5 MC
5. Output Center Frequency: 830 MC
6. Output Tuning Range: 80 MC
7. Output Instantaneous Bandwidth: 20 MC
8. Input Impedence: 50 Ohms
9. Output Impedence: 50 Ohms
10. Input Level: +20 dbm
11. Loss: 0 db
12. Output Level: +20 dbm
13. Harmonic & Spurious Suppression: -60 db min.
14. Size: 6 cubic inches
15. Weight: .1 lbs.
16. Power Supply: 28 volts & 025 amps.

NA Not Applicable.

